THE HONG KONG
POLYTECHNIC UNIVERSITY
香港理工大學
Pao Yue-kong Library
包玉剛圖書館

Copyright Undertaking

This thesis is protected by copyright, with all rights reserved.

By reading and using the thesis, the reader understands and agrees to the following terms:

1. The reader will abide by the rules and legal ordinances governing copyright regarding the use of the thesis.
2. The reader will use the thesis for the purpose of research or private study only and not for distribution or further reproduction or any other purpose.
3. The reader agrees to indemnify and hold the University harmless from and against any loss, damage, cost, liability or expenses arising from copyright infringement or unauthorized usage.

IMPORTANT

If you have reasons to believe that any materials in this thesis are deemed not suitable to be distributed in this form, or a copyright owner having difficulty with the material being included in our database, please contact lbsys@polyu.edu.hk providing details. The Library will look into your claim and consider taking remedial action upon receipt of the written requests.

Pao Yue-kong Library, The Hong Kong Polytechnic University, Hung Hom, Kowloon, Hong Kong

http://www.lib.polyu.edu.hk

BONE AND MUSCLE PROPERTIES IN INDIVIDUALS WITH CHRONIC STROKE

TIEV B. MILLER

PhD

The Hong Kong Polytechnic University

2021

The Hong Kong Polytechnic University

Department of Rehabilitation Sciences

Bone and Muscle Properties in Individuals with Chronic Stroke

Tiev B. Miller

A thesis submitted in partial fulfillment of the requirements for the degree of Doctor of Philosophy

September 2020

CERTIFICATE OF ORIGINALITY

I hereby declare that this thesis is my own work and that, to the best of my knowledge and belief, it reproduces no material previously published or written, nor material that has been accepted for the award of any other degree or diploma, except where due acknowledgement has been made in the text.

(Signed)

TIEV MILLER (Student Name)

Dedication

This thesis is dedicated to the study participants.

Abstract

Background: Bone health is often compromised after stroke with greater incidence of fracture on the paretic side. Unilateral alterations to paretic muscle are also a common sequela after stroke. Although the relationship between bone integrity and muscle strength post-stroke is well-established, the association between specific muscle material changes and the mechanical strength of bone is unknown. Moreover, alterations in bone tissue properties and their clinical correlates require further study. *Objectives:* The main objectives of this thesis project were (1) to investigate the impact of stroke on the bone properties of the distal radius and tibia using High Resolution – peripheral Quantitative Computed Tomography (HR-pQCT), and muscle properties of the biceps brachii and the medial gastrocnemius, and (2) to identify the correlates of mechanical bone strength and muscle tissue alterations in people with chronic stroke. *Methods:* This was a cross-sectional project involving 64 participants with chronic stroke (age: 60.8±7.7 years, stroke duration: 5.7±3.9 years) and 64 age- and sex-matched controls. Bilateral bone parameters of the distal radius and tibia were measured using HR-pQCT. Muscle architecture, stiffness and composition as well as brachial and popliteal artery vascular outcomes were evaluated using B-mode, elastography, pulse wave and color Doppler ultrasound. Other relevant clinical and functional outcomes were also assessed. A mixed design two-way repeated measures analysis of variance (ANOVA) was used to compare within and between group differences for all bilaterally assessed variables of the upper and lower limbs ($p \leq 0.05$). Post hoc analyses involved paired t-test for within-group differences and independent t-tests for between-group differences ($p \leq 0.017$). Pearson's correlations were used to determine associations between the side-to-side difference (%SSD) in all bilaterally assessed variables ($p \leq 0.05$). Lastly, multiple regression was used to determine significant predictors of percent side-to-side difference (%SSD) in estimated failure load of the distal radius and tibia for the stroke group. *Results:* There was a significant side by group interaction effect for estimated failure load and all volumetric density, trabecular, and cortical bone parameters ($p \leq 0.012$) of the distal radius, with the exception of intra-cortical porosity ($p=0.179$). Post hoc analyses showed percent side-to-side differences in these outcomes occurred only in the stroke group. Muscle echo intensity ($p=0.030$), Motor Activity Log (MAL) ($p=0.004$), and Fugl-Meyer Motor Assessment (FMA) scores ($p<0.001$) were significant determinants of the percent side-to-side difference in estimated failure load of the distal radius. For the distal tibia, a significant side by group interaction effect was observed for estimated failure load ($p \leq 0.001$), cortical area and thickness ($p \leq 0.001$), and all volumetric density parameters ($p \leq 0.009$). Post hoc analyses revealed significant side-to-side

differences in these parameters for the stroke group but not for controls. Multivariate regression analyses showed that the 10-meter walk test (p=0.043) and the ankle clonus score of the Composite Spasticity Scale (p=0.032) scores were significant predictors of %SSD in estimated failure load (R^2=0.213). *Conclusion:* This study showed that bone microstructure in the paretic upper limb and bone density and cortical macrostructure in the lower limb are significantly altered on the paretic side post-stroke. Muscle morphology, disuse, motor impairment, walking speed and spasticity are important correlates of distal radius and tibia bone strength and should be the potential targets for intervention to either maintain or improve bone health after stroke.

Publication List

Publications arising from this thesis

Journal Publications

Miller T, Ying MTC, & Pang MYC. (2021) Convergent validity and test-retest reliability of multimodal ultrasound and related measures in people with chronic stroke. Archives of Physical Medicine and Rehabilitation. November https://doi.org/10.1016/j.apmr.2021.09.015

Miller T, Qin L, Hung VWY, Ying MTC, Tsang CSL, Ouyang HX, Chung RCK, & Pang MYC. (2021) Gait speed and spasticity are independently associated with estimated failure load in the distal tibia after stroke: an HR-pQCT study. Osteoporosis International. October 12. https://doi.org/10.1007/s00198-021-06191-z

Miller T, Ying M, Tsang SL, Huang MZ, & Pang MYC. (2021) Reliability & validity of ultrasound elastography for musculoskeletal stiffness among neurological populations: a systematic review & meta-analysis. *Physical Therapy.* January, https://doi.org/10.1093/ptj/pzaa188

Miller T, Ying MTC, Hung VWY, Tsang CSL, Ouyang HX, Chung RCK, Qin L, & Pang MYC. (2021) Determinants of estimated failure load in the distal radius after stroke: an HR-pQCT study. *Bone.* March. https://doi.org/10.1016/j.bone.2020.115831

Conference Abstracts

Miller T, Huang MZ, Pang MYC, & Ying M. The validity and reliability of dynamic ultrasound elastography techniques in evaluating musculoskeletal stiffness: a systematic review. *World Confederation for Physical Therapy Congress*, 10-13 May 2019, Geneva, Switzerland. (Poster)

Miller T, Ouyang HX, Lau VLT, Huang MZ, Chan WT, Fung TS, Lau PY, Lee TY, Wong WL, Ying M, & Pang MYC. Muscle stiffness as a predictor of paretic upper limb functional use in individuals with chronic stroke. *Hong Kong Physiotherapy Association Conference*, 25 May 2019, Hong Kong. (Poster)

Miller T, Huang MZ, Ouyang HX, Tsang SL, Pang MYC, Ying M, Hung VWY & Qin L. Compromised cortical and trabecular bone density post-stroke are correlated with muscle stiffness. *Hong Kong Physiotherapy Association Conference*, 25 May 2019, Hong Kong. (Poster)

Miller T, Huang MZ, Tsang SL, Ouyang HX, Pang MYC & Ying M. Paretic upper limb stiffness and spasticity as predictors of motor activity in individuals with chronic stroke. *6th International Institute on the Model of Human Occupation Conference*, 27-29 September 2019 Chicago, USA. (Poster)

Miller T, Ying MTC & Pang MYC. Test-retest reliability and convergent validity of upper and lower extremity ultrasound elastography measures post-stroke. *11th World Congress for Neurorehabilitation*, 7-11 October, 2020 (ePoster)

Miller T, Huang MZ, Ying MTC & Pang MYC. Test-retest reliability of muscle architecture and echogenicity measures in the bilateral upper and lower extremities of individuals with chronic stroke using musculoskeletal ultrasound. *ESO-WSO Joint Stroke Virtual Conference*, 7-9 November 2020, Vienna, Austria (ePoster)

Miller T, Ying MTC, Qin L, & Pang MYC. Muscle morphology, function and disuse as failure load predictors in the paretic distal radius among individuals with chronic stroke. *ESO-WSO Joint Stroke Virtual Conference*, 7-9 November 2020, Vienna, Austria (ePoster)

Miller T, Tsang CSL, Hung VWY, Qin L, Ying MTC & Pang MYC. Gait speed and spasticity as predictors of estimated failure load in the distal tibia of individuals with chronic stroke. *World Confederation for Physical Therapy Congress*, April 8-10 2021, Dubai, U.A.E. (Platform Presentation)

Miller T, Ng J, Chung RCK, Ying MTC & Pang MYC. Altered muscle architecture is associated with paretic upper limb usage among individuals with chronic stroke: a path analysis. *World Confederation for Physical Therapy Congress*, April 8-10 2021, Dubai, U.A.E. (Platform Presentation)

Miller T, Ying MTC & Pang MYC. Regional muscle stiffness mapping and associations with upper extremity motor impairment in people with chronic stroke. *13th World Stroke Congress*, October 28-29 2021 (ePoster)

Miller T, Ying MTC & Pang MYC. Differences in resting intramuscular blood perfusion among individuals with chronic stroke. *13th World Stroke Congress*, October 28-29 2021 (ePoster)

Additional co-authored manuscripts and abstracts published while affiliated with Department of Rehabilitation Sciences of The Hong Kong Polytechnic University

Journal Publications

Bird ML, **Miller T**, Connell LA, & Eng JJ. (2019) Moving stroke rehabilitation evidence into practice: a systematic review of randomized controlled trials. *Clinical Rehabilitation*. April, 33(10), 1586-1595. https://doi.org/10.1177/0269215519847253

Huang MZ, **Miller T**, Ying M, & Pang, MYC. (2020) Whole-body vibration modulates leg muscle reflex and blood perfusion among people with chronic stroke: a randomized controlled crossover trial. *Scientific Reports*. January, 10(1), 1-11, 1473. https://doi.org/10.1038/s41598-020-58479-5

Bello UM, Chutiyami M, Salihu D, Abdu SI, Tafida BA, Jabbo AA, Gamawa A, Umar L, Lawan A, **Miller T**, & Winser SJ. (2020) Quality of life of stroke survivors in Africa: a systematic review and meta-analysis. *Quality of Life Research*. July 25: 1-9. https://doi.org/10.1007/s11136-020-02591-6

Yang ZH, **Miller T**, & Pang MYC. (2020) Relationship between bone strength index of the hemiparetic tibial diaphysis and muscle strength in stroke patients: influence of muscle contraction type and speed. *Osteoporosis International*. November 7: 1-9 https://doi.org/10.1007/s00198-020-05716-2

Yang ZH, **Miller T**, Xiang Z, & Pang MYC. (2021) Effects of different vibration frequencies on muscle strength, bone turnover and walking endurance in chronic stroke. *Scientific Reports*. January 8. https://doi.org/10.1038/s41598-020-80526-4

Yuen M, Ouyang HX, **Miller T**, & Pang MYC. (2021) Baduanjin Qigong improves balance, leg strength and mobility in individuals with chronic stroke: a randomized controlled study. *Neurorehabilitation and Neural Repair.* April. https://doi.org/10.1177/15459683211005020

Tsang CSL**,** Wong ST, **Miller T &** Pang MYC. (2021) Degree and pattern of dual-task interference during walking vary with component task type and complexity in people post-stroke: a systematic review and meta-analysis. *Journal of Physiotherapy.* December 23. https://doi.org/10.1016/j.jphys.2021.12.009

Conference Abstracts

Bird ML, **Miller T**, Connell LA, & Eng JJ. Systematic review of knowledge translation trials in stroke rehabilitation. *11th World Stroke Congress*, 17-20 October 2018, Montreal, Canada. (Poster)

Huang MZ, **Miller T**, Fu SN, & Pang MYC. Morphological and passive mechanical properties of the medial gastrocnemius muscle among individuals with chronic stroke. *Hong Kong Physiotherapy Association Conference*, 6 October 2018, Hong Kong. (Poster)

Gonzalez P, Fong K, **Miller T**, & Brown T. Examining the mental health crisis in doctoral students using the Model of Human Occupation: Evaluating occupational adaptation and participation in doctoral graduate students. *6th International Institute on the Model of Human Occupation Conference*, 27-29 September 2019 Chicago, USA. (Platform Presentation)

Bello UM, Chutiyami M, Salihu D, Abdu SI, Tafida BA, Jabbo AA, Gamawa A, Umar L, Lawan A, **Miller T**, & Winser SJ. Quality of life of stroke survivors in Africa: a systematic review and meta-analysis. *World Confederation for Physical Therapy Congress*, April 8-10 2021, Dubai, U.A.E. (ePoster)

Miller T, Bello UM, Tsang CSL, Winsor SJ, Ying MTC & Pang MYC. (2021) Conservative interventions for musculoskeletal stiffness: a systematic review and meta-analysis. *12th Pan-Pacific Conference on Rehabilitation*, November 27-28, 2021, Hong Kong (Poster)

The following manuscripts and abstracts have been submitted to peer-reviewed journals or conferences and are currently under or pending review

Journal Submissions

Huang M, **Miller T**, Fu SN, Ying MTC & Pang MYC. (2021) Structural and passive mechanical properties of the medial gastrocnemius muscle in ambulatory individuals with chronic stroke. *Medical Engineering and Physics*. (Under Review)

Miller T, Bello UM, Tsang CSL, Winsor SJ, Ying MTC & Pang MYC. (2021) Interventions for musculoskeletal stiffness: a systematic review and meta-analysis. *Journal of Sport and Health Science.* (Under Review)

Tsang CSL**, Miller T &** Pang MYC. (2021) Association between fall risk and assessments of single-task and dual-task walking among community-dwelling individuals with chronic stroke: A prospective cohort study. *Gait & Posture.* (Under Review)

Miller T, Chambara N, Ying MTC & Pang MYC. (2021) Angio PLanewave UltraSensitive Doppler Imaging for the assessment of intramuscular vascularity in older adults. *British Journal of Radiology.* (Pending Submission)

Conference Submissions

Miller T, Tsang CSL, Ouyang HX, Ying MTC, & Pang MYC. (2022) Associations between vascular function and upper limb motor impairment in individuals with chronic stroke. *World Physiotherapy Asia Western Pacific Regional Congress cum Hong Physiotherapy Association Conference*, June 18-20, 2022, Hong Kong, Hybrid Format. (Virtual Platform Presentation)

Bird ML, Stockley R, **Miller T**, & Ahuja KDK. Online resources and recommendations for the symptomatic management of fatigue after stroke: a scoping review. *World Physiotherapy Asia Western Pacific Regional Congress cum Hong Physiotherapy Association Conference*, June 18-20, 2022, Hong Kong, Hybrid Format. (ePoster)

Published acknowledgements for assistance with other studies while affiliated with the Department of Rehabilitation Sciences at The Hong Kong Polytechnic University

Gibbons TJ, Bird ML. (2018) Exercising on Different Unstable Surfaces Increases Core Abdominal Muscle Thickness: An Observational Study Using Real-Time Ultrasound. *Journal of Sport Rehabilitation*. November 1;28(8):803-8. http://doi.org/10.1123/jsr.2017-0385

Sánchez-Vidaña DI, Po KK, Fung TK, Chow JK, Lau WK, So PK, Lau BW, Tsang HW. (2019) Lavender essential oil ameliorates depression-like behavior and increases neurogenesis and dendritic complexity in rats. *Neuroscience Letters*. May 14;701:180-92. http://doi.org/10.1016/j.neulet.2019.02.042

Chambara N, Ying MTC. (2019) The Diagnostic Efficiency of Ultrasound Computer–Aided Diagnosis in Differentiating Thyroid Nodules: A Systematic Review and Narrative Synthesis. *Cancers*. November;11(11):1759. http://doi.org/10.3390/cancers11111759

The following abstracts were accepted to conferences that were later cancelled due to COVID-19 precautions

Miller T, Bello UM, Zhang J & Fong K. Therapeutic interventions for musculoskeletal stiffness: a systematic review and meta-analysis. *Singapore International Physiotherapy Congress*, June 19-22 2020, Singapore (Withdrawn)

Miller T, Bird ML, Huang MZ, Ying MTC & Pang, MYC. Test-retest reliability of muscle stiffness measures in the bilateral upper and lower extremities of individuals with chronic stroke using ultrasound elastography and myotonometry. *Smart Strokes 2020: Australasian Nursing and Allied Health Stroke Conference*, August 20-21 2020, Brisbane, Australia (Withdrawn)

Acknowledgements

This project was funded by a post-graduate research studentship through the Department of Rehabilitation Sciences at The Hong Kong Polytechnic University (Grant RL27). This study was also substantially supported by a research grant provided by the Research Grants Council (General Research Fund; 151031/18M).

First and foremost, I would like to acknowledge the influence of my wife, Jenny Kao, in making this all possible. Without her love, support and understanding throughout this difficult process, I would have surely given up during the first year of the program and went back into teaching in some capacity. Thanks for always listening to me and helping me laugh through the difficult times and challenges. I would also like to acknowledge the love and support of our parents, siblings and extended family members in Taiwan, South Korea, Canada and the United States. The challenges of living and working abroad were formidable and their presence and support has been absolutely essential.

I would like to express my deepest gratitude to my chief supervisor, Professor Marco Pang in the Department of Rehabilitation Sciences at The Hong Kong Polytechnic University. His guidance, insight and specialization have brought this innovative project to fruition. With patience and foresight, he has helped me to navigate my way through this degree program. I truly appreciate and cherish the opportunity to have lived in Hong Kong and be member of his research team.

I would also like to thank my co-supervisor, Dr. Michael Ying, Professor in the Department of Health Technology and Informatics at the Hong Kong Polytechnic University, for dedicating his time to my technical training and for providing me with resources and stringent deadlines which enabled me to complete the data collection. There were many students who were less fortunate during this difficult time at PolyU.

I would like to express my gratitude to Dr. Raymond Chung, Senior Scientific Officer in the Department of Rehabilitation Sciences at The Hong Kong Polytechnic University for his guidance in modifying the statistical analyses in order to address manuscript revisions requested by the editors and reviewers of Bone and Osteoporosis International.

I would also like to express my gratitude to Vivian Hung at the Bone Quality and Health Centre at Prince of Whales Hospital and Professor Ling Qin in the Department of Orthopaedics and Traumatology at The Chinese University of Hong Kong for their assistance with the data collection, manuscript revisions and technical support in generating representative figures using the FE solver software.

I would like to thank Dr. Marie-Louise Bird, Senior Lecturer in the School of Health Sciences at the University of Tasmania, and Professor Janice Eng, Dean of the Graduate School of Physical Therapy at the University of British Columbia. By allowing me to take part in your work, I was able to prepare myself for many of the challenges I've encountered during the course of this degree program.

I would like to thank my previous supervisors Professor Kent Adams, Chair of the Department of Kinesiology at California State University Monterey Bay, and Professor Ann Swank, Director of the Exercise Physiology Lab and Chair of the Department of Health & Sport Science at the University of Louisville. Your endorsement and continuous support over the years has been essential to my success as a researcher and instructor. I will always be appreciative of the kindness and compassion you showed me during my graduate program. I am also eternally grateful to you for giving me a strong foundation in Exercise Physiology.

I would also like to thank both Ah Man Cheung and Siu Sik Cheung in the Department of Rehabilitation Sciences at The Hong Kong Polytechnic University, for sharing their knowledge and skill sets in the both the design and application of the equipment and software programs used to complete this project.

I also have a tremendous amount of respect and gratitude for the administrative and procedural support provided by Dennis Mok and Alexandra Lo in the Department of Rehabilitation Sciences at The Hong Kong Polytechnic University. They are truly the glue that holds the department together and the lubricant that keeps its gears moving smoothly. Their work ethic, dedication and detailed guidance have been valuable assets and are deeply appreciated.

I would also like to acknowledge the assistance and competitive engagement provided by my fellow postgraduate research colleagues and teammates (Charlotte San Lau Tsang, Meizhen Huang, Echo Huixi Ouyang, Feigo Zhenhui Yang and Virginia Lok Tung Lau). It's been a challenging but rewarding experience. I am grateful for the opportunity to contribute to your research and proud of the work we've accomplished together under Marco's supervision. I would very much like to collaborate with you in future projects and I wish all of you the very best.

Last but not least, I would like thank the participants of the study for their willingness, commitment and courage. You have fought through bouts of chronic fatigue, pain, depression and disability and you refuse to relent. Your efforts are recognized and most appreciated.

Table of Contents

List of figures

List of abbreviations

6MWT = 6 Minute Walk Test

10MWT = 10 Meter Walk Test

%CV = percent coefficient of variance

%SSD = percent side-to-side difference

α = alpha level

β = Beta (standardized regression coefficient)

χ^2 = Chi-squared test

μFE = micro-finite element analysis

Ω = resistance to electrical current

AD = Arterial Diameter

ADM = Abductor Digiti Minimi

AM = Adductor Magnus

AMT = Abbreviated Mental Test

ANOVA = Analysis of Variance

ARFI = Acoustic Radiation Force Impulse

AT = Achilles Tendon

BB = Biceps Brachii

BIA = Bioelectrical Impedance Analysis

BMI = Body Mass Index

BMR = Basal Metabolic Rate

CI = Confidence Interval

CFI = Color Flow Imagining

cm = centimeters

CP = Cerebral Palsy

CSA = Cross Sectional Area

COSMIN = Consensus-based Standards for the Selection of Health Measurement Instruments

CSS = Composite Spasticity Scale

CUSE = Comb-Push Ultrasound Shear Elastography

d = Cohen's d (standardized mean difference)

DF = Dorsiflexion

DMD = Duchenne Muscular Dystrophy

DS = Dynamic Sonoelastography, Dynamic Stiffness

EMD = Electromechanical Delay

EMG = Electromyography

FAC = Functional Ambulation Category

FEA = Finite Element Analysis

FI = Functional Impairment

FL = Fascicle Length

FFM = Fat Free Mass

FM = Fat Mass

FMA = Fugl-Meyer Assessment

g = Hedges's g (bias adjusted standardized mean difference)

GM = Gluteus Maximus

GMFCS = Gross Motor Function Classification System

GMFM = Gross Motor Function Measure, NSAA = North Star Ambulatory Assessment

GRADE = Grading of Recommendations Assessment, Development and Evaluation

HA = Hydroxyapatite

HKD = Hong Kong Dollars

HR-pQCT = High Resolution peripheral Quantitative Computed Tomography

ICC = Intraclass Correlation Coefficient

IPT = Isometric Peak Torque

IQ = interquartile

kcal = kilocalorie

kg = kilograms

kPa = kilopascal

LE = Lower Extremity

LG = Lateral Gastrocnemius

LS = Lacunar Syndrome

m = meters

m/s = meters/ second

MAL = Motor Activity Log

MAS = Modified Ashworth Scale

MCSA = Muscle Cross Sectional Area

m/f = male/female

MG = Medial Gastrocnemius

mL/min = milliliters/ minute

mm = millimeters

mo = months

MRI = Magnetic Resonance Imaging

MSK = Musculoskeletal

MT = Muscle Thickness

N = Newton

N/A = Not applicable, not explicitly stated or undefined

N/m = Newton/ meters

PACS = Partial Anterior Circulation Syndrome

PASE = Physical Activity Scale for the Elderly

PCS = Posterior Circulation Syndrome

PD = Parkinson's Disease

PF = Plantarflexion

PICO = Population, Comparison, Intervention, Outcome

PMM = Predicted Muscle Mass

PPT = Pain Pressure Threshold

pQCT = peripheral Quantitative Computed Tomography

PSV = Peak Systolic Velocity

RF = Rectus Femoris

ROI = Region of Interest

RTS = Real Time Sonoelastography

SD = Standard Deviation

SE = Strain Elastography

SEM = Standard Error of Measurement

sEMG = Surface Electromyography

SM = Shear Modulus

SOL = Soleus

SR = Strain Ratio

SSI = SuperSonic Imagine

STREAM = Stroke Rehabilitation Assessment of Movement

STIR = Short-Tau Inversion Recovery

SWE = Shear Wave Elastography

SWV = Shear Wave Velocity

TA = Tibialis Anterior

TACS = Total Anterior Circulation Syndrome

TB = Triceps Brachii

Tm = Onset of Force Production/ Transmission Processes

TPT = Touch Pressure Threshold

TS = Tardieu Scale

TUG = Timed Up-&-Go

UE = Ultrasound Elastography, Upper Extremity

UPDRS = Unified Parkinson's Disease Rating Scale

vBMD = Volumetric Bone Mineral Density

Vflow = blood flow volume

VL = Vastus Lateralis

VM = Vastus Medialis

VTIQ = Virtual Touch Imaging Tissue Quantification Software

wk(s) = week(s)

y = years

Chapter 1. Introduction

1.1 Epidemiology of stroke

There is an increased societal burden of disease and disability which accompanies age-associated declines in physical and psychological function. In just over two decades time, the number of elderly aged 65 and above in Hong Kong doubled from half a million in 1988 to almost 1 million in 2008 [1]. By 2036 it is projected to more than double again (i.e., 2.3 million) [1]. Given this demographic shift, the prevalence of stroke among the elderly is a concern. Globally, stroke is a leading cause of neurologically-related disability [2]. The prevalence of stroke is rising in Hong Kong [1]. By 2030, it's estimated that the number of deaths due to stroke is expected to reach 8.2 million accounting for 12% of all deaths worldwide for that year. In Hong Kong, the number of community and institution-dwelling people aged 65 and above with stroke is projected to more than double between 2010 and 2036 from 61,000 to 162,000 accounting for more than 5% of the population [1]. Health care expenditures are also expected to rise. Approximately HKD$4,529 million will be spent on institutional care among people aged 65 and above with stroke in Hong Kong by 2036 [1]. Conventional stroke rehabilitation commonly involves strategies for improving motor function [3] and neuroplasticity [4], as stroke is commonly classified as neurological condition. The musculoskeletal system however, has received relatively little attention and is often granted lower priority during treatment [5]. A growing body of evidence suggests that both muscle and bone sustain considerable changes after stroke which may ultimately have substantial overall health implications [6].

1.2 Muscle properties and alterations after stroke

Muscle weakness is common after stroke [7]. Associated lesions in the brain after stroke interrupt the descending motor pathways and produce varying degrees of neuromuscular impairment in the upper and lower extremities [8]. Unilateral alterations in muscle structure [9], composition [10,11] and viscoelastic material characteristics [11] are often common corollaries resulting from neuromuscular impairment after stroke. These stroke-related structural and morphological muscle alterations may cause functional and strength declines [12]. In paretic muscles, physiological changes lead to diminished motor activation through the degeneration of high threshold motor units [13] and may reduce the overall

number of functional motor units resulting in shifts in fiber type expression [14]. Changes in muscle cross-sectional area caused by atrophy [12] and altered composition from increased intramuscular adiposity [15] have also been reported which may worsen functional disability [15]. Muscle spasticity is often evident post-stroke [16]. These functional declines may also lead to further physiological changes within muscle such as altered sarcomere twitch dynamics [17], muscle fascicle shortening [9] , and intramuscular collagen accumulation [18,19]. Altered structural parameters, such as muscle pennation, fiber length (i.e., fascicle length) and thickness, have also been shown to be correlated with measures of spasticity (i.e., Modified Ashworth Scale) among individuals with stroke [20]. Additionally, structural and physiological changes may also lead to the development of painful contractures [21], thus potentially resulting in further loss of function over time.

Muscle tissue stiffness is a biomechanical tissue property that may be an important determinant of stroke-related impairment [11]. As the use of diagnostic musculoskeletal ultrasound increases in prevalence among physical medicine training programs [22] and in clinical settings [23], ultrasound systems with advanced tissue imaging capabilities for measuring muscle biomechanical properties may be useful in assessing tissue alterations in people with chronic stroke and other populations with neurological conditions [24,25]. Until recently, in vivo assessment of muscle tissue stiffness was considered to be procedurally complex, ineffective in isolating specific tissue regions and may not be feasible across clinical settings [26,27].

Ultrasound elastography provides a direct, non-invasive quantification of biomechanical stiffness in real-time for individual muscle sites [28]. Elastography is a recently developed non-invasive ultrasound imaging modality used for in-vivo measurement of tissue biomechanical properties (i.e., stiffness) in human subjects [11,29,30]. The method of assessment involves the application of an acoustic radiation force impulses (AFRI) to induce shear waves in a tissue medium. Transverse and longitudinal particle motions are tracked in order to measure the shear wave propagation velocity and dispersion within the tissue. The resultant velocity can then be used to calculate a modulus or material stiffness value (i.e., shear modulus). Larger shear wave velocities and modulus values are generally representative of stiffer tissues. Shear wave elastography (SWE) and other ultrasound-based musculoskeletal elastography techniques have been used to examine populations with characteristic biomechanical tissue alterations such as individuals with cerebral palsy [31-37], Parkinson's disease [38,39], myopathy [40] and Duchenne muscular dystrophy [41,42]. To date, relatively few studies have involved the use of ultrasound elastography to measure muscle tissue stiffness in

people with stroke [10,11,43-47]. Subject samples (n=3-31) and stage of stroke recovery since onset varied across these studies. An important study by Lee et al. measuring upper extremity muscle stiffness in a group of individuals with chronic stroke (n=16) showed that the shear wave velocity was significantly greater for muscles of the stroke-affected compared to the non-affected side (69.5% bilateral difference) [11]. Wu et al. later confirmed these findings among patients with acute stroke (n=31) [43]. In a more recent study by Gao et al examining the stiffness of the biceps brachii muscle among participants with chronic stroke (n=24) and controls, the muscles of paretic sides showed significantly greater stiffness compared to the non-paretic sides and the bilateral limbs of healthy controls [10].

Several of the aforementioned studies also examined the association between muscle stiffness and clinical measures of function. A significant negative association between the side-to-side difference in muscle stiffness and Fugl-Meyer motor scores was identified, suggesting that paretic limb muscle stiffness may be closely related to functional deficits [11]. However, these results were based on a small sample of individuals with chronic stroke (n=16). With regards to spasticity, a significant negative correlation has been demonstrated between stiffness and passive range of motion ($R^2 = -0.88$, $p < 0.001$) in spastic upper limbs, as assessed with the Modified Ashworth and Tardieu Scales in people with chronic stroke. These findings elude to a potential relationship between stiffness and spasticity [10]. Again, these results were based on only a moderate sample size (n=12 participants without spasticity, n=12 participants with spasticity). Additionally, the muscles of the lower extremity were not assessed in these studies. Alterations in the mechanical properties of lower limb muscles may affect walking ability post-stroke [48]. Another study by Jakubowski et al showed that a similar pattern of unilateral muscle stiffness was evident for the paretic plantar and dorsiflexor muscles at varying ranges of motion and joint torque among individuals with chronic stroke (n=14) [45]. No study has yet to assess muscle biomechanical properties using SWE in both the upper and lower extremities concomitantly. This may provide important information, as the resultant clinical implications may differ for the upper and lower limbs.

1.3 Bone properties and alterations after stroke

Accessory to the aforementioned changes incurred by muscle, detrimental alterations to bone structural properties are also evident post stroke [49-56]. It is well know that the capacity of bone to fulfill its mechanical function is diminished in states of disease, such as osteoporosis [57]. Stroke-related impairment and consequent hemiosteoporosis of paretic limbs may also exacerbate diminution of bone tissue integrity and proclivity to fracture [58,59] which

can lead to serious health consequences [60,61]. Incident fractures are more likely occur in stroke survivors than age- and sex-matched individuals without a history of stroke [58]. The direction of falls [62] and the site of fracture[63] are more likely to occur on the stroke-affected side. Moreover, stroke-related changes to bone are often evident even within the first year following stroke onset [59] and may be independent of other factors effecting bone metabolism such as body composition and weight [64]. While disuse may be a main factor contributing to bone loss in the non-weight bearing paretic upper limb [54,65], abnormal gait patterns and differences in mechanical loading between the paretic and non-paretic sides appear to be important contributors to bone loss in the weight bearing lower limbs [66-68].

Studies of areal bone mineral density (aBMD) using dual-energy X-ray absorptiometry (DXA) have shown that loss of bone density is more pronounced on the paretic side for multiple bone sites (i.e., humerus, radius, femur, tibia) based on stroke duration, with presumably greater bilateral deficits in bone parameters at a given measurement site as time from stroke onset increases [69]. During the acute phase of stroke recovery (< 1 month) [65,66,70-77], little or no bilateral difference was observable. During the subacute phase (1-6 months) [59,64,67,78-83] bilateral differences were found between paretic and non-paretic sides in upper and lower limb bone sites. In cross-sectional studies involving patients in the chronic phase of stroke recovery (≥ 6 months) [49-51,54,68,84-89], a common finding for the upper limb was a lower aBMD on the paretic side relative to the non-paretic side at the site of the radius [82,83], humerus [59,82] and total arm [90,91]. Similar findings were reported for the lower limb at the sites of the femur[78,82] and calcaneus[82]. The results from longitudinal studies suggest that although the loss of bone density may be challenging to prevent [73], less bone loss was observed in patients following early motor recovery, mobilization, and weight-bearing[70,92].

Although the use of DXA is common in clinical settings, a significant limitation of this imaging modality may be the inability to assess additional factors related to bone loss other than quantity (i.e., aBMD) [93]. Methods used to assess bone geometry may be required for identifying patients most at risk of fracture [93]. Measures of bone geometry have been identified as important determinants of mechanical bone strength [94]. Peripheral quantitative computed tomography (pQCT) has been used to examine the impact of stroke on both volumetric bone density and bone geometry [49-56,89,95,96]. In studies involving people with chronic stroke, both bone mass and geometric properties were compromised in the paretic distal radius [49,52-54,96] and distal tibia [50,51,55,68,89,95,96] in comparison to the non-paretic side. These studies also showed lower bone strength indices in the paretic limbs.

According to a recent systematic review and meta-analysis on the impact of stroke on bone properties, the magnitude of bilateral difference in bone loss may be more pronounced for the upper limb compared to the lower limb [69]. Recovery of bone in the upper limb [56] is also less in comparison to the recovery of bone in the lower limb [97]. The systematic review also highlighted the lack of studies reporting changes in bone microstructure post-stroke.[69]

A significant limitation associated with previous studies involving the use of pQCT was the relatively low resolution of the scans (pixel size: 0.2-1.0mm) in comparison to high-resolution peripheral quantitative computed tomography (HR-pQCT) (pixel size: 41-246μm). Previously it was not possible to measure microstructural bone parameters (i.e., cortical porosity, trabecular number, trabecular thickness, trabecular separation), which are important factors in determining mechanical bone strength [98,99]. Another limitation of previous pQCT scanners is that they cannot be used for obtaining accurate measures of cortical thickness in people with stroke given the relatively thinner cortical shells of paretic sides despite no bilateral difference in total bone area [49]. Accurate measures of cortical thickness may be particularly important for assessing the upper limb when considering that the distal radius is a site where Colles-type fractures are likely to occur [99,100]. Additionally, deficits in microstructural bone parameters, such as intracortical porosity, have been shown to contribute to fracture in postmenopausal women [99]. Fewer trabecular number and greater separation between trabeculae at the distal radius has been observed for osteopenic women who sustained a fracture, while their counterparts without fracture exhibited an opposing trend for these microstructural bone parameters [101].

HR-pQCT provides reliable and valid measurements of macrostructural, microstructural and mechanical bone strength parameters at the distal radius and tibia. The estimation of bone strength is calculated by converting bone images into 3-dimensional voxel reconstructions of cubic hexahedral elements for further analysis (i.e., finite element analysis) [101-105]. The use of HR-pQCT for rendering mechanical strength estimates has been previously validated using experimental loading tests on cadaveric bones [100,106,107]. Microstructural parameters have demonstrated good correlation with bone stiffness and post-yield strength following mechanical testing [100,108]. HR-pQCT is considered to have greater sensitivity for discriminating fracture than DXA [102]. The microstructure of distal bone sites has been shown to discriminate incident fracture in postmenopausal women independently of aBMD values generated by DXA [98]. Microstructure has also been used to discriminate cases with prior fracture from controls without fracture history [109,110]. However, microstructure alone may lack the sensitivity and specificity to fully distinguish fracture risk [111]. Nevertheless, it

is an important predictor of mechanical bone strength and has clinical value in the assessment of stroke-related bone deficits. HR-pQCT has been used in large cohort trials involving a diverse range of populations [103-105,111-113] and for assessing the efficacy of intervention strategies [114]. To date, no study has sought to investigate changes in bone microstructure post-stroke.

1.4 The association between bone and muscle properties

The premise of Wolff's Law is that the ontogenous adaptation of bone tissue occurs in response to the stress stimulus, or external load enacted upon it [115]. The ability of muscle to produce force plays a prominent role in the remodeling and adaptation response of bone tissue that muscle is invested in [116]. Muscle structural parameters such as fiber pennation, fascicle length, and particularly volumetric parameters such as muscle cross-section area and thickness, have been shown to be important measures for predicting muscle force production capacity and muscle-bone strength index in animal models [116-118]. Hence, the source of mechanical strain imposed through muscular contractions may prompt consequent alterations in bone quantity (i.e., volumetric density) and bone structure (i.e., geometry). This suggests that muscle function and the integrity of bone tissue may be interrelated. However, Wolff's Law comprises both bone growth during modeling and the rate of turnover during remodeling which are subject to non-uniform, age-related influences, and should be considered as somewhat separate processes [115].

The "muscle-bone" unit, a theory promulgated by Eckhard Schoenau, considers muscle and bone as a functional conglomerate [119]. This concept, originally proposed in order to expound upon adolescent musculoskeletal development [119], has also been applied to the elderly [120,121], patients with impaired mobility [50,122], for discriminating between bone disorders across the lifespan [123], and for defining algorithms to assess bone health status among children with cerebral palsy [124]. In the elderly, a significant correlation has previously been demonstrated between concentric muscle power during leg extension and the mid-tibial shaft bone strength index [120]. Muscle cross-sectional area is also a strong predictor of tibial bone strength in adult and elderly males [121]. A growing body of evidence suggests there is a connection between muscle mass, muscle force generation capacity and the integrity of bone tissue in people with stroke [49-56,120,122]. This has been demonstrated in previous pQCT and DXA studies involving different bone sites such as the distal radius [49,85], the proximal femur [86,125] and the tibia post-stroke [122]. Muscle mass has been shown to be an important clinical correlate of the bone strength index of the distal tibial diaphysis in people

with chronic stroke [50]. The tibial diaphysis bone strength index was shown to be associated with lower leg muscle density in patients with subacute stroke as well [122]. However, the relationship between bone integrity and other factors affecting muscle function, such as muscle stiffness [11,45], echo intensity [11], fascicle length [9], fiber pennation angle and spasticity [46], have not been examined in both the upper and lower limbs concomitantly. As stroke-related alterations in muscle mechanical [10,11], volumetric (i.e., atrophy) [46,126], and structural properties [9,17] have been shown to contribute to both upper and lower limb functional impairment, these factors may also have a direct impact on bone health.

Although pQCT can be used to predict the biomechanical behavior of bone tissue and generate estimates of bone mechanical strength, it is not possible to estimate or predict muscle force generating capacity through any known diagnostic imaging tool [127] but rather with surrogate or proxy assessments used in conjunction [123]. Therefore, validation of the muscle-bone unit theory in stroke using a singular imaging modality may not be feasible. Another limitation of pQCT is the inability to assess specific structural characteristics of muscle. Using pQCT, only a gross anatomical cross-sectional area of muscle and bone is rendered for a particular scan region. Ultrasound maybe be useful in assessing architectural parameters (i.e., muscle fiber pennation angle, fascicle length, thickness, cross-sectional area) of individual muscles which have a more direct physiological bearing on muscle force production [127]. There is also evidence to support the use ultrasound for accurate measures of muscle volume, an important surrogate of force production capacity [128], in patients with acute [129] and subacute stroke [130].

1.5 Implications

While loss of bone density and muscle mass are expected with age, there is a significant disparity in the degree of loss between otherwise health elderly and those who have had a stroke [12,131,132]. A recent systematic review on post-stroke physical activity by Fini et al. estimates that individuals with stroke spend more than 78% of their time being inactive and sedentary, regardless of the amount of time since stroke onset [133]. These figures fall far short of the guideline recommendations for daily physical activity, placing individuals with stroke at even greater risk of developing additional health problems [134]. As previously stated, muscle contractions and weight-bearing exercises provide essential sources of mechanical and compression stress that are necessary for maintaining bone. A growing body of evidence suggests there is a close relationship between muscle strength and bone health, particularly in the peripheral musculature of the upper and lower extremities affected by stroke [49-51,66,85,86].

A greater emphasis on maintaining muscle strength, and perhaps bone integrity as a result, post-stroke could potentially have important implications for reducing the prevalence of falls and fractures.

Falling is common among community-dwelling individuals with chronic stroke. The proportion of fallers can range from 43% to 70% within the first year post-stroke [62,135,136]. The risk of repeated falls is more than 3 times higher four months post-stroke than for normal elderly [137]. Walking is the most common activity associated with falls post-stroke, and may be attributable to between 39% - 90% of falls [137-140]. Compared to normal elderly, the risk of fracture is 7 times higher 1 year post-stroke [63,141,142]. The hip is the most common fracture site post-stroke, accounting for 30% to 58% of all fractures [63,143,144]. The wrist is the second most common site, accounting for nearly 14% to 24% of all fractures [63,143]. Consequences of post-stroke fractures include an increased risk of mortality [61], decreased mobility and independence [61], increased hospital stay durations [60], and higher economic burden placed upon the healthcare system [145].

Community-dwelling stroke survivors play an essential role as research participants. Gaining a more thorough understanding of the changes incurred by the musculoskeletal system post-stroke will enable researchers and clinicians to develop intervention strategies that better assist patients in achieving their highest possible level of function. As patient education and information provision have been consistently identified as facilitators for physical activity reengagement post-stroke [146], the researchers hope that the findings of this project will provide important insights not only for clinicians, but for the study participants as well.

1.6 Project significance

The thesis project aimed to explicate stroke-related changes which may alter the normal biomechanical and structural properties of muscle and bone. Given that stroke is a heterogeneous condition with differing clinical presentations (e.g., severity of spasticity, motor impairment), it may be possible to identify functional impairments most associated or predictive of muscle and bone changes. Using ultrasound and computed tomography imaging, it is possible to examine (1) the viscoelastic, compositional, and architectural characteristics of muscle, (2) the structural, densiometric, geometric and strength parameters of bone, in addition to (3) the vascular function of the large peripheral arteries that supply these tissues. A comprehensive assessment of the upper and lower extremities provides novel insight as to the relationship between muscle alterations, the integrity of bone tissue after

stroke and their association with physical function and impairment.

1.7 Aims of the thesis and flow of studies

The primary aim of this project was to evaluate the impact of stroke on muscle and bone properties and the muscle-bone relationship. A secondary aim was to assess the degree of association between these properties and clinical measures of function and stroke-related impairment.

A series of interrelated studies were designed to achieve the aforementioned aims. A schematic diagram (Figure 1) is used to illustrate the flow of the studies comprising this thesis. First, it is important to review the literature to identify the knowns and unknowns surrounding the reliability and validity of the ultrasound elastography technique when used in people with neurological disorders. Therefore, in **Chapter 2** (*Reliability & validity of ultrasound elastography for evaluating muscle stiffness among neurological populations: a systematic review & meta-analysis),* a systematic review was undertaken to examine the psychometric properties of ultrasound elastography techniques in evaluating muscle stiffness among neurological populations.

Next, it is important to establish the reliability and validity of the ultrasound measures in individuals with chronic stroke, who are the main targets of our scientific investigations. **Chapter 3** (*Convergent validity and test-retest reliability of diagnostic ultrasound measures in the bilateral upper and lower extremities of individuals with chronic stroke using B-mode, elastography and Doppler)* described a study in which the convergent validity and test-retest reliability of various ultrasound measurement parameters involving the bilateral biceps brachii (BB), brachial artery, medial gastrocnemius (MG) and popliteal artery were assessed among a cohort of individuals with chronic stroke.

In **Chapter 4** (*Determinants of estimated failure load in the distal radius after stroke: an HR-pQCT study),* High-Resolution peripheral Quantitative Computed Tomography (HR-pQCT) was used to investigate the impact of stroke on the bone properties at the distal radius, and identify the relationship between the estimated failure load for the distal radius and muscle properties and other stroke-related impairments in individuals with chronic stroke.

The design of the study described in **Chapter 5** (*Gait speed and clonus as determinants of estimated failure load in the distal tibia after stroke)* was similar to that in Chapter 4. A cross-sectional study was undertaken to explore the influence of stroke on distal tibia bone properties and examine the association between estimated failure load and important clinical correlates among individuals with chronic stroke.

Finally, in **Chapter 6** (*Conclusion*), the results of each thesis chapter are summarized with concluding remarks and future implications for research.

Figure 1.1 Thesis flow diagram

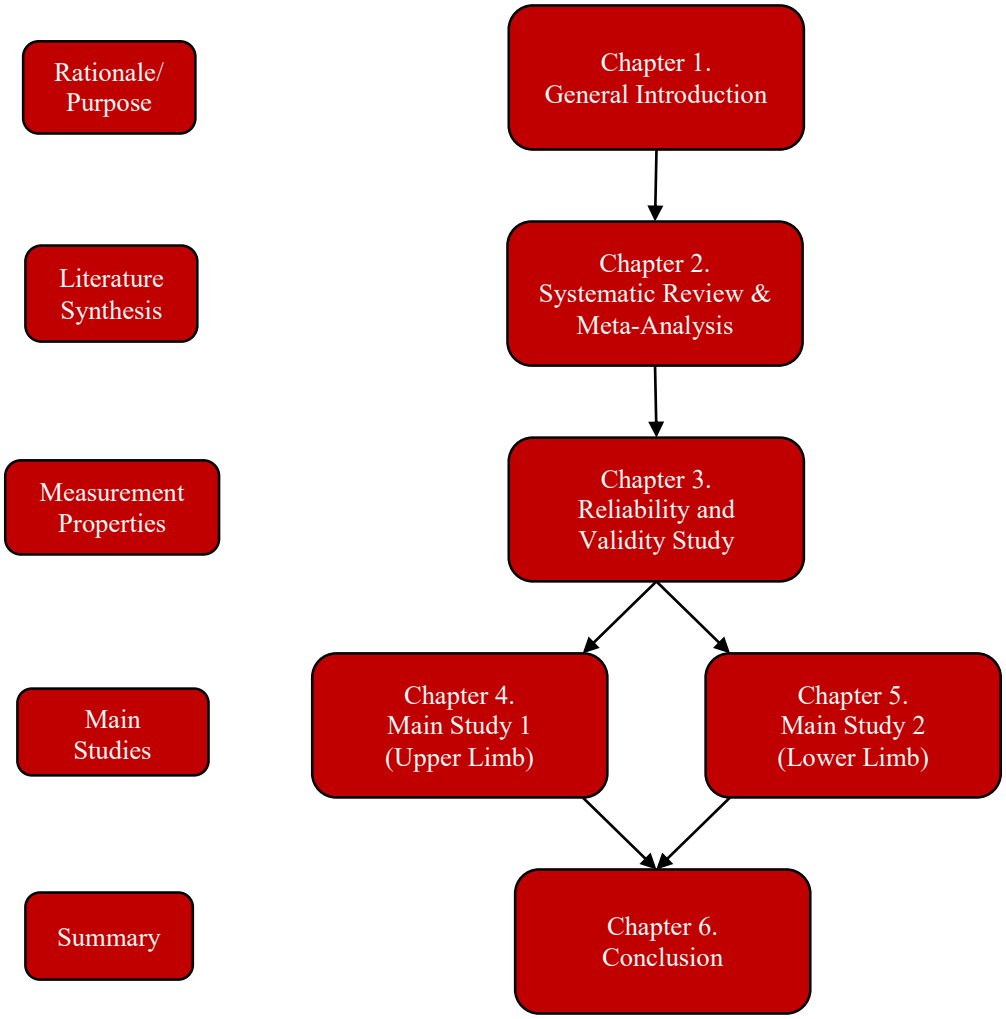

1.8 Study Objectives & Hypotheses

1.8.1 Chapter 2

Objective 1: To investigate the reliability and validity of ultrasound elastography for assessing muscle stiffness among populations with neurological conditions.

Hypothesis 1.1: Based on previous studies in healthy populations, it was hypothesized that ultrasound elastography would demonstrate good reliability for assessing muscle stiffness among neurological populations.

Hypothesis 1.2: Based on previous studies in populations with stroke, it was hypothesized that ultrasound elastography would show good concurrent and discriminative validity in

comparing muscle stiffness between groups and other clinically relevant assessments in populations with neurological conditions.

1.8.2 Chapter 3

Objective 2: To assess the convergent validity and test-retest reliability of multimodal ultrasound measures among individuals with chronic stroke.

Hypothesis 2.1: The multimodal ultrasound measures would demonstrate good correlation with other measures assessing similar or related constructs.

Hypothesis 2.2: By using acquisition procedures previously indicated for enhancing measurement reliability, it was hypothesized that the same measures obtained using B-Mode, elastography and Doppler ultrasound would demonstration moderate to good test-retest reliability.

1.8.3 Chapter 4

Objective 3: To assess the impact of stroke on muscle and bone properties and examine their relationship in the upper limb

Hypothesis 3.1: The bone parameters of the distal radius on the paretic side of participants with chronic stroke measured by HR-pQCT would show significant side-to-side differences that would be greater than those of age- and sex-matched controls.

Hypothesis 3.2: The biceps brachii muscle properties measured by ultrasound in participants with chronic stroke would demonstrate significant side-to-side differences that would be greater than those of age- and sex-matched controls.

Hypothesis 3.3: The vascular values of the brachial artery in participants with chronic stroke would demonstrate significant side-to-side differences that would be greater than those of age- and sex-matched controls.

Hypothesis 3.4: There would be a significant relationship between muscle measures of the biceps brachii and the estimated failure load of the distal radius for the stroke group.

1.8.4 Chapter 5

Objective 4: To assess the impact of stroke on muscle and bone properties and examine their relationship in the lower limb.

Hypothesis 4.1: The bone parameters of the distal tibia on the paretic side of participants with chronic stroke measured by HR-PQCT would show significant side-to-side differences that would be greater than those of age- and sex-matched controls.

Hypothesis 4.2: The medial gastrocnemius muscle properties measured by ultrasound in participants with chronic stroke would demonstrate significant side-to-side differences that would be greater than those of age- and sex-matched controls.

Hypothesis 4.3: The vascular values of the popliteal artery in participants with chronic stroke would demonstrate significant side-to-side differences that would be greater than those of age- and sex-matched controls.

Hypothesis 4.4: There would be a significant relationship between muscle measures of the medial gastrocnemius and the estimated failure load of the distal tibia for the stroke group.

Chapter 2. Reliability & validity of ultrasound elastography for evaluating muscle stiffness among populations with neurological conditions: a systematic review & meta-analysis

Abstract

Background: Ultrasound elastography is an emerging diagnostic technology used to investigate biomechanical properties of the musculoskeletal system. *Purpose:* To systematically review the psychometric properties of the ultrasound elastography techniques in evaluating muscle stiffness among populations with neurological conditions. *Data Sources:* A systematic search of MEDLINE, EMBASE, CINAHL and Cochrane Library databases was performed on January 31, 2020 in accordance with PRISMA guidelines. This review was prospectively registered (PROSPERO registration #: CRD42017076571). *Data Selection:* Using Covidence software, reviewers independently screened citations for inclusion. Peer-reviewed studies which evaluated in vivo muscle stiffness among populations with neurological conditions and reported relevant psychometric properties were considered for inclusion. *Data Extraction:* Twenty-one articles were included for final review. Data relevant to measurement technique, site and neurological condition were extracted. The Consensus-based Standards for the Selection of Health Measurement Instruments (COSMIN) checklist was used to rate methodological quality of included studies. Level of evidence for specific measurement outcomes was determined using a best-evidence synthesis approach. *Data Synthesis:* Reliability varied across populations, ultrasound systems and assessment conditions (i.e. joint/ body positions, active/ passive muscle, probe orientation) with most studies indicating moderate to good reliability (Intraclass Correlation Coefficient (ICC)=0.5-0.9, n=13). Meta-analysis results showed good overall correlation across studies (r=0.78, 95% Confidence Interval (CI)=0.64–0.86, $p \leq 0.00$) with no between-group difference based on population (Q=0.00, df=1, p=0.97). Convergent validity was demonstrated by strong correlations between stiffness values and measures of spasticity (n=5), functional motor recovery or impairment (n=5) and grey scale or color histogram pixel intensities (n=3). Discriminant or known-groups validity was also established for multiple studies indicating either significant between-group differences in stiffness values (n=12) or within-group differences between more- and less-affected limbs (n=6). Responsiveness was observed in all intervention studies reporting post-treatment stiffness changes (n=6). *Conclusions:* Overall, ultrasound elastography techniques show moderate reliability in evaluating in-vivo muscle

stiffness, good convergent validity with relevant clinical assessments, and good divergent validity in discriminating tissue changes within and between groups. *Impact Statement:* Ultrasound elastography will have clinical utility in assessing muscle stiffness, monitoring its temporal changes, and measuring the response to intervention in populations with neurological conditions.

2.1 Introduction

Altered muscle tissue mechanics and morphology are resultant corollaries among populations with neurological conditions and neuromuscular dysfunction [147,148]. Macro- and microstructural changes have been observed across various strata of muscle tissue in populations with common neurological conditions such as stroke and cerebral palsy (CP) [149-152]. Although the mechanism remains unclear, additional alterations in the biomechanical properties of muscle tissue may be a secondary sequela either associated with or resulting from underlying neurological etiologies (i.e., phasic hyperreflexia, hypertonia) [34,153]. Intramuscular collagen formation [154], extracellular matrix organization [155] and titin isoform diversity within fibers [156] are other factors thought to contribute to tissue alterations. The assessment of biomechanical properties, such as passive muscle stiffness, may have overt clinical value in determining tissue morphology and response to treatment or rehabilitation [157]. Subjective evaluation of altered muscle properties in populations with neurological conditions using qualitative clinical assessments such as manual palpation and muscle testing or modified Ashworth (MAS) and Tardieu scales are indirect and suboptimal [158,159]. Other quantitative assessments of these properties involving dynamometry and B-mode ultrasound can be procedurally complex, ineffective in isolating specific tissue regions and may not be feasible across clinical settings [26,27].

Alternatively, elastography provides a direct, non-invasive stiffness quantification of individual muscle structures in real-time [28]. As the use of diagnostic musculoskeletal ultrasound is becoming more prevalent in physical medicine and rehabilitation training programs [22] and in clinical physical therapy [23], ultrasound units with tissue imaging capabilities such as elastography may prove advantageous in monitoring transitory or progressive muscle changes associated with neurological conditions [24,25]. Elastography has also demonstrated utility in evaluating responsiveness to invasive [34,37,160-163] and non-invasive [164] clinical intervention strategies for reducing muscle stiffness and spasticity in populations with neurological conditions.

Ultrasound-based elastography methods developed as an outgrowth of tissue palpation and motion tracking techniques for identifying tissue masses harder and more resistant to displacement than surrounding reference tissues. Since the development of sonoelasticity imaging and static elastography in the early 1990's for quantifying the distribution of the elastic modulus in soft tissues [165,166], ultrasound elastography (UE) methods have continued to evolve [29]. Previous reviews have highlighted the utility of this technology for investigating the biomechanical properties of the musculoskeletal system [25,167-170]. There are several different UE techniques capable of providing either quantitative or qualitative measures of these properties [28], each differing in frequency, method of excitation and interface [171]. There is currently no consensus with regard to which method may be optimal for assessing muscle stiffness among populations with neurological conditions in vivo.

As the development and modification of elastography for measuring specific tissue types (e.g., thyroid, breast, muscle) remains on-going [172], a general knowledge of its underlying mechanisms, technical limitations, measurement attributes and an appraisal of its potential clinical application is warranted. Briefly, the estimation of stiffness using elastography requires measuring tissue displacements in response to the application of a stress generated via mechanical, acoustic radiation or internal endogenous forces [171]. Although UE systems demonstrate great potential in terms of clinical utility, their underlying accuracy is based upon non-biological material testing under absolute conditions [172,173]. Attempts have been made to investigate the limitation of material linearity when using UE to evaluate muscle properties among healthy populations and populations with neurological conditions [47,174,175]. However, differences in tissue type, geometry and activation remain confounding influences [176,177]. There are also operator-dependent sources of error as well as measurement range capabilities to be considered [178-180].

In the field of musculoskeletal elastography, a comprehensive review which systematically investigates the reliability and validity reported throughout the available literature is currently lacking. The primary objective of this review was to evaluate the evidence regarding the reliability and validity of UE for measuring muscle stiffness in populations with neurological conditions. Secondary objectives were to synthesize the information regarding measurement protocols, operators and equipment used for measuring muscle stiffness, and to assess study quality and level of evidence regarding stiffness measures. In healthy populations, UE has shown good reliability [30] and correlation with other measures assessing similar [181] or related physiological constructs [182,183] and measures

of physical function [184] and disability [185]. Therefore, it was hypothesized that overall measurement reliability and validity of UE for measuring muscle stiffness in populations with neurological conditions would be good.

2.2 Methods

2.2.1 Data sources & searches

A search was developed using the following concept domains as syntactic framework: (1) musculoskeletal stiffness, (2) ultrasound elastography and (3) validity and reliability. MEDLINE, EMBASE, CINAHL and Cochrane Library databases were searched. Paired and individual keywords, medical subject headings (MeSH), Embase subject headings (Emtree), field codes, boolean and proximity operators used in the search strategy syntax specific to each database are included in the supplementary appendices (Supplementary Appendix A). Results for each of the concept domains were combined to produce the final search results. In further refining the search, an additional filter was applied limiting the results to references with human subject populations published in English language journals between January 1990 and January 2020. References of articles selected for inclusion were reviewed to identify other relevant publications for inclusion. Reference lists from review articles discussing musculoskeletal elastography were also searched. A forward search was performed before the final synthesis and analysis to include studies published after the initial search and data extraction. This review was conducted in accordance with PRISMA guidelines [186] and prospectively registered with PROSPERO (registration #: CRD42017076571).

2.2.2 Study selection

Using Covidence online data extraction and screening software (Cochrane software Csr. Melbourne, Victoria, Australia: Veritas Health Innovation, p. Available at www.covidence.org), two reviewers (TM, MH) independently screened titles and abstracts to determine propriety for inclusion. Hand-searched publications from reference lists were then entered into the full-text screening. Two reviewers (TM, SLT) then extracted relevant data independently. All missing or omitted data were requested from authors of included studies. Data were included under the contingency authors replied within a timeframe of 10 working days. Conflicts arising between reviewers were resolved through discussion or by consulting a third reviewer (MP, MY) to reach consensus.

Selection of studies was based on the following criteria. *Inclusion criteria:* 1. peer reviewed articles published in English between 1990-2020, 2. human subjects studied in vivo, 3. studies investigated UE measurement properties for muscle, tendon, and/or fascia stiffness, 4. data collection took place in research settings or across all stages of the continuum of care, 5. subject populations with neurological conditions (i.e., stroke, spinal cord injury (SCI), CP, etc.), 6. muscle stiffness measured with UE was a primary or secondary diagnostic objective, 7. measurement validity and/or reliability of UE was also a primary or secondary outcome, 8. studies reported reliability, convergent, discriminant, known-groups, or criterion validity as determined with the use of a comparator (i.e., previously validated diagnostic methods for evaluating tissue stiffness such as magnetic resonance elastography, electronic palpation imaging, biopsies, and histopathological samples, gelatine-based phantoms, and/or tissue equivalent phantoms) 9. study design was either a case-controlled diagnostic, prospective or retrospective cohort, cross-sectional or longitudinal, pre-post intervention or randomized-controlled trial. *Exclusion criteria*: 1. published conference proceedings (i.e., presentations, posters, symposium, etc.) 2. book reports or chapters, 3. theses or dissertations, 4. unavailable in full text, 5. incorrect timeframe (i.e., before 1990), 6. involved animals or cadaver samples without comparative in vivo measures, 7. studies focused solely on the assessment of bone, cartilage, entheses, ligaments or joint capsules, 8. UE measured stiffness was not a primary or secondary outcome and 9. measurement properties were not a primary or secondary outcome.

2.2.3 Data extraction & quality assessment

The following items were extracted from included articles: 1. author information (i.e., names, title, year, location), 2. study design, 3. measurement reliability and validity, 4. diagnostic setting (i.e., inpatient, outpatient, laboratory), 5. ultrasound operator (i.e., technician, clinician, researcher), 6. ultrasound system and probe model, 6. probe alignment in relation to muscle fiber orientation (i.e., parallel, perpendicular or oblique), 7. muscle site, 8. body position and joint angle during testing, 9. subject demographics and characteristics, 10. measurement units (i.e., shear modulus (SM) in kilopascals (kPa) and/or shear wave velocity (SWV) in meters per second (m/s), strain ratio (SR), sonoelastographic index/score) and 11. details of image/data acquisition and processing (i.e., region of interest (ROI), number of trials, contact interface, software).

Rating of methodological quality for included studies was performed independently by two reviewers (TM, SLT) using the COnsensus-based Standards for the selection of health Measurement INstruments (COSMIN) Risk of Bias checklist (July 2018 version). Although

originally intended for health-related patient-reported outcomes [187], the checklist also facilitates the election of quality scores for studies in which measurement properties are based on operator or clinician-assessed outcomes of function [188] and disability [189] in populations with neurological conditions. Of the items encompassing the checklist, Boxes 6, 7, 8, 9a, 9b, 10a-10d were used to assess reliability, measurement error, criterion validity, convergent validity, discriminant or known-groups validity and responsiveness for each study, respectively. Other items contained within the checklist were omitted for the purposes of this review. The checklist uses a 4-point rating system in assigning ratings for each item. Ratings of 4, 3, 2 or 1 were deemed very good, adequate, doubtful or inadequate, respectively. In determining overall quality for each category, the lowest rating was used (i.e., worst score counts principle) [190,191]. A third reviewer (MP, MY) was consulted regarding any discrepancies. The level of evidence for measurement property results was determined using a best-evidence synthesis approach [192] described in a previous systematic review of reliability, validity, and responsiveness for physical capacity tasks that assessed functioning in patients with low back pain [193]. Criteria for strong, moderate, limited, unknown, or conflicting levels of evidence are also described in detail [193]. Briefly, a positive, indeterminate or negative rating was first assigned according to an established criterion for rating measurement properties reported by Prinsen et al [194]. Levels of evidence for measurement property ratings were then assigned according to measurement property rating consistency, combined sample size, and methodological quality for articles with similar or comparable outcome measures (i.e., quantitative or semi-quantitative estimates of muscle stiffness).

2.2.4 Data synthesis & analysis

A qualitative synthesis was conducted by tabulating data according to sample population, measurement site and UE technique. Comprehensive Meta-Analysis software (CMA version 3.0, Biostat Inc., Englewood, New Jersey, USA) was used for quantitative analyses. Subgroup analyses consisted of ≥3 homologous studies which assessed measurement reliability. Correlation coefficients (ICC) were transformed to Fisher's Z scale for analysis [195]. The software accommodates the combination of multiple outcomes (i.e., measurement sites, probe orientations or operators) which were pooled to calculate a single metric for analysis. Proportion of variance between studies was interpreted using Higgins' I^2 statistic and 95% prediction intervals (PI) were calculated to express absolute estimates of heterogeneity for each subgroup analysis [196]. A random effects model was chosen with the

assumption ICCs would vary between studies. Prior to subgroup analyses a univariate meta-regression was performed to determine the effect of independent factors related to study design (i.e., ICC model and form) on overall correlation estimates (i.e., dependent factor) [197].

2.3 Results

2.3.1 Screening

A flow diagram summarizing the screening process and results is provided in Figure 1. A total of 21 articles involving 326 individuals with neurological conditions and 177 control subjects met the criteria for final inclusion [10,11,24,31,34-36,38,39,41,43,45,46,153,160,161,163,164,198-200]. Excluded articles were either case studies [24,162] or did not report measurement validity or reliability [47].

2.3.2 Study characteristics

A summary of study characteristics and outcomes is provided in Table 2.1. Study designs varied in type and complexity. Most were observational studies of either cross-sectional or longitudinal design [10,11,31,35,36,38,39,41,43-46,153,161,199,200] with two measuring reliability as a primary outcome [43,46]. Six studies described the use of blinding procedures [39,43,160,163,198,200]. Measures were conducted by a radiologist, physician or physiatrist, others described as examiner, experimenter or investigator, or were not explicitly stated. Neurological conditions investigated were stroke, CP, Duchenne muscular dystrophy (DMD) and Parkinson's disease (PD). The medial gastrocnemius (MG), biceps brachii (BB) and tibialis anterior (TA) muscles were the most commonly assessed sites. Measures were collected during either passive or active muscle conditions with and without being concomitantly monitored by electromyography (EMG). One study used a constant-current stimulator to elicit contractions [199].

2.3.3 Ultrasound system

A summary of system specifications, settings, software, reported units and value ranges is provided in Table 2.2. UE systems varied across studies. All studies reported using linear array probes with frequencies ranging from 4-15MHz. Elastography methods involved either a dynamic time-course with an acoustic radiation force application, quasi-static time-course with a mechanical force application or dynamic with mechanical force. Commonly used system settings were either standard musculoskeletal presets or shear wave elastography

(SWE) mode. Units were reported as quantitative (SM, SWV) or semi-quantitative estimates of muscle stiffness (SR or elastographic index/scores with either grey scale or color histogram pixel intensity values).

2.3.4 Acquisition procedures

A summary of probe placement, fixation, applied compression, contact interface, processing software and other image and data acquisition methods are found in Table 2.2. For most studies, probe placement during image capture was performed in parallel alignment with fascicle orientation. Two studies investigated parallel and perpendicular alignments [43,46]. All studies used linear probes suitable for superficial structures. A transmission or stand-off gel couplant was used as the contact interface in several studies. The number of trials or single images captured for each muscle site ranged from 2-15. Selected ROIs ranged from 4.8mm in circular diameter to 30mm^2 in size and varied in placement depth, number and shape.

2.3.5 Reliability

A summary of reported ICCs and additional reliability information is provided in Table 2.3. According to the 95% CI of ICC estimations, reported values <0.5, between 0.5-0.75, between 0.75-0.9 and >0.90, were indicative of either poor, moderate, good, or excellent reliability, respectively. When considering all ICCs reported for studies, most demonstrated moderate to good reliability (ICC=0.5-0.9, n=13). However, two studies investigating reliability in patients with CP reported large variance in confidence intervals (95% CI = 0.33-0.84) [161,198]. Another study among patients with stroke demonstrated a substantial variance in the range of reported ICCs (ICC = 0.00-0.87) [46]. Of all the included studies, this was also the only study to report estimates of measurement error. Ranges for measurement error varied substantially based on differences in probe placement and muscles sites examined (SEM = 0.61-24.81) [46]. One other study also assessed measurement reliability using different probe placements among patients with stroke, reporting considerably less variance in the range of ICCs (ICC = 0.55-0.85) [43] in comparison to the former [46]. Comparative reliability of active versus passive muscle conditions could not be determined from the study which investigated these conditions concomitantly [153].

A graphical summary of subgroup analyses is provided in Figure 2. As the results of the meta-regression showed no significant influence of ICC model and form on overall correlation (Q=1.85, df=2, p=0.40), population-based subgroup analyses were conducted. The

overall correlation across subgroups was good (n=8, r=0.78, 95% CI=0.64–0.86, p≤0.00) with no significant difference between groups based on population (Q=0.00, df=1, p=0.97). For studies involving people with CP (n=4, r=0.78, 95% CI=0.58-0.89, p≤0.00) and with stroke (n=4, r=0.77, 95% CI=0.56-0.89, p≤0.00), the correlation was good. However, estimates of absolute heterogeneity indicated a wide dispersion in reliability across studies involving patients with CP (95% PI=0.02-0.97). Proportion of variance was mostly attributable to sampling error rather than true correlation (31.5%) (I^2=31.5, p=0.22). There was larger observed dispersion in estimates of absolute heterogeneity across studies involving patients with stroke suggesting greater variance in measures (95% PI=-0.52-0.99). Proportion of variance in true correlation was also larger (53.5%) with less attributed to error (46.5%) (I^2=53.5, p=0.09).

2.3.6 Convergent validity

A summary of convergent validity and study comparators is provided in Table 2.3. Several studies reported correlations between muscle stiffness and standardized assessments of spasticity and functional motor recovery or impairment. In two studies involving subjects with PD, Unified Parkinson's Disease Rating Scale (UPDRS) scores were positively correlated with SM values (r=0.65, p≤0.00) [38] and negatively correlated with SR (r=−0.78) [39]. For individuals with stroke, Fugl-Meyer assessment (FMA) scores were correlated with side-to-side difference (i.e., paretic and non-paretic) in SWV values (r^2=0.33, p=0.02) [11] and values for paretic sides alone (r=−0.58) [45]. Paretic side SWV values were positively correlated with MAS (r=0.66) and TS scores (r=0.54) and negatively correlated with Stroke Rehabilitation Assessment of Movement (STREAM) scores (r=-0.57) [43,153]. For individuals with CP, several studies reported significant correlations not only between stiffness values and functional scores [161-163,198] but also gray scale or color histogram pixel intensities [160,163] . Correlation between stiffness and echo intensity (i.e., grey scale value) was also observed among people with stroke (r^2=0.70, p≤0.00) [11].

2.3.7 Divergent validity

A summary of discriminant/known-groups validity is found in Table 2.3. In comparing people with CP to controls, stiffness was significantly greater for the CP group in several studies (p≤0.001) [35,36,160,198]. SWV values were also significantly higher in more-affected limbs (p≤0.024) [31]. However, when stratified according to motor function (i.e., GMFCS Levels I and II), there were no significant differences in SWV between groups [31].

In individuals with PD, stiffness was significantly greater compared to controls ($p \leq 0.05$) [38,39], with no difference between markedly and mildly symptomatic limbs ($p \leq 0.05$) [38]. Stiffness was significantly greater for people with DMD compared to controls across almost all muscle sites and conditions ($p \leq 0.005$) [41,199,200]. For individuals with stroke, findings varied by condition (i.e., spasticity, joint angle, muscle site, activation) with significantly greater stiffness in paretic versus non-paretic limbs ($p \leq 0.001$) [11,153] and controls during passive muscle states ($p \leq 0.001$) [153]. Differences in stiffness were also joint angle specific [10,43-45].

2.3.8 Responsiveness

A summary of responsiveness is found in Table 2.3. A total of five studies examined pre- to post-intervention changes in muscle stiffness [34,160,161,163,164]. Most examined changes following botulinum toxin injections in people with CP [34,160,161,163]. These studies reported significant reductions in stiffness values or scores/indices following treatment ($p \leq 0.05$). One study examined the effect of a robot-assisted stretching and joint mobility program in individuals with stroke and showed that SR values for the paretic Achilles tendon increased significantly from pre- to post-training ($p = .045$) [164]. Additionally, two longitudinal studies examining the effect of disease progression in people with DMD showed SM values significantly increased between 0 (pre) and 12 months (post) ($p < 0.001$) [41,199].

2.3.9 Quality assessment & level of evidence

A summary of the quality assessment, measurement property result ratings and level of evidence synthesis is provided in Table 2.4. Methodological quality ratings for reliability (Box 6) were adequate for most studies, with one study rated as doubtful due to an unclear description of testing conditions and time intervals between assessments [38]. Measurement error (Box 7) assessed for one study was adequate [46]. Criterion validity (Box 8) and responsiveness (Box 10a) using a criterion approach were not assessed due to a lack of concurrent comparators. Convergent validity (Box 9a) and discriminant/ known-groups validity (Box 9b) were very good or adequate for most studies. Two studies were rated as doubtful for convergent validity due to suboptimal analyses and inadequate reporting of outcomes [198,200]. Three studies were rated doubtful or inadequate for discriminant/ known-groups validity for inadequate reporting of relevant subgroup characteristics and suboptimal analyses [10,44,200]. Responsiveness using a construct approach for outcome (Box 10b),

between subgroups (Box 10c) or pre-to-post intervention comparisons (Box 10d) was very good for all studies.

Several studies stated a priori hypotheses [31,35,38,39,43,45,199,200]. When not explicitly stated, the authors expectations or assumptions were compared to reported outcomes (i.e., correlations, between-group differences, pre-to-post intervention values) in determining measurement property result ratings for validity and responsiveness. Results of the best-evidence synthesis suggest there is a moderate level of evidence for negative ratings of interrater reliability (ICC < 0.70) for stiffness estimates using quantitative UE methods. For intrarater reliability using quantitative methods, the level of evidence was moderate for positive ratings (ICC > 0.70). For semi-quantitative methods, the level of evidence for positive ratings was unknown for interrater reliability and limited for intrarater reliability due low total sample size (< 50). The level of evidence for an indeterminate rating of measurement error in one study using a quantitative method was unknown. For convergent validity (hypothesis testing) of quantitative methods, the level of evidence for positive ratings (i.e., mostly in accordance with hypotheses) was strong. The level of evidence for positive ratings was moderate for semi-quantitative methods due to sample size (< 100). For discriminant/ known-groups validity of quantitative methods, the level of evidence for positive ratings was strong. Limited level of evidence for positive ratings of semi-quantitative methods was also due to lower total sample size (< 50). The level of evidence for positive ratings of responsiveness of studies involving quantitative methods was limited. For semi-quantitative methods, the level of evidence for positive ratings was moderate due to higher sample size (> 25).

2.4 Discussion

2.4.1 Reliability

Studies reporting ICCs indicated mostly moderate to good measurement reliability overall. The methodological quality of most of these studies was also determined to be adequate. However, the results of the level of evidence synthesis suggest that evidence for intrarater reliability was stronger than interrater reliability for both quantitative and semi-quantitative methods. The evidence also ranged from moderate for quantitative estimates of stiffness, to unknown for semi-quantitative estimates. Furthermore, estimates of measurement error were not reported in most studies that assessed measurement reliability. This is an important metric not only for reliability, but for interpreting clinically meaningful changes in health-related outcomes [201]. Subgroup analyses demonstrated pooled estimates of reliability

were good overall with roughly equivocal correlations for CP and stroke subgroups. However, of the studies investigating reliability in people with stroke as a primary outcome [43,46], there was a large range in reported coefficients (ICC range=0.00-0.87). While the dispersion in estimates of heterogeneity were large for the CP subgroup (95% PI=0.02-0.97), the stroke subgroup was comparatively wider (95% PI=-0.52-0.99), suggesting the need for greater precision in measurement protocols. The variability in estimates may be attributable to differences in selected muscle sites, muscle activity, operator experience, probe alignment, ultrasound system and acquisition procedures used and subject age and gender.

In adult populations without neurological conditions, stiffness measures have been shown to vary by depth, activity and joint angle. Using a curvilinear probe in deep penetration mode, Blain et al demonstrated greater reliability for the superficial erector spinae than deeper multifidus muscles [202]. Alfuraih et al also reported better reliability for more superficial than comparatively deeper muscles [203]. Generally, the greater the depth of a given anatomical structure, the greater the attenuation effect on acoustic pulse transmission and wave tracking [171], which may affect reliability [203]. In isotropic tissues such as the thyroid, signal strength may diminish at depths between 4-6cm. In anisotropic tissues such as muscle, signal diminishment may occur at lesser depths [204]. It is unknown to what degree signal attenuation and probe type and measurement depth affect reliability in populations with neurological conditions. Stiffness has also been shown to have a linear relationship with joint torque in passive and active muscle [177]. The use of EMG may be particularly necessary in order to monitor muscle activation status when assessing patients with spasticity (i.e., stroke). Of the two studies investigating reliability in individuals with stroke as a primary outcome [43,46], only one involved the use of EMG during measures [43]. The other, where stiffness was measured at multiple muscle sites and probe orientations, demonstrated considerable variance in estimates of reliability and measurement error [46]. Although reliability was not a primary outcome, the study by Eby et al investigating muscle stiffness and torque response to passive elbow extension after stroke also incorporated the use of EMG and reported a comparatively smaller range of ICCs (ICC = 0.75-0.99) [44].

The influence of age on the reliability of stiffness measures is inconclusive. Only one study examined age-related differences in muscle stiffness showing that lower limb SM at different lengths was correlated with age in individuals with DMD ($r=0.55-0.74$, $p\leq0.05$) but not among controls ($r<0.43$) [41]. However, these findings do not suggest age has any substantive impact on reliability.

The amount of previous training or experience in musculoskeletal ultrasound and elastography also appears to influence measurement reliability. The range of reported reliability estimates was greater for studies with poorly defined operator experience (ICC range=0.00-0.94) than those with clearly defined experience (ICC range=0.65-0.92). Among these studies, operators were described as radiologists, physicians or physiatrists with 2-17 years of relevant experience.

There was also considerable variance among studies using multiple probe orientations. Mathevon et al demonstrated slightly greater variance for measures in perpendicular (ICC range=0.00-0.73) compared to parallel probe alignments (ICC range=0.27-0.87) [46]. Wu et al also showed greater intrarater and interrater reliability for parallel (ICC=0.85 and 0.76, respectively) compared to perpendicular alignments (ICC=0.71 and 0.55, respectively) [43]. As shear waves propagate longitudinally in alignment with muscle fiber direction, aligning the probe parallel to fibers may enhance measurement accuracy [205]. Perpendicular alignments, in contrast, have shown greater dispersion of shear waves [174,206].

Other aspects of measurement acquisition may also contribute to variability. ROI varied across most studies, which has been shown to influence values in regional tissue mapping studies [207]. Lack of contact interface standardization is another source of variability, as differences in the use of transmission gel have been shown to influence consistency [203]. Discrepancies in reported values between studies (i.e., kPa, m/s, etc.) is also problematic, as these values are related but separate phenomena [208]. Tissue stiffness estimations are predicated upon static deformation models of elastic materials and are described as stress (i.e., the force per unit in a given area) divided by strain (i.e., the expansion per unit of length), which is the equivalent of an elastic modulus value [172]. It is important to note that most UE systems operate under an assumption of material linearity wherein tissues are homogenous or structurally similar, isotropic (i.e., identical property values in all directions), and are non-viscous (i.e., identical fluid consistency) [171]. Examples which fit these assumptions in an absolute sense would be materials such as metal or glass. However, muscle tissues are heterogeneous, anisotropic and viscoelastic given the variation in their structural composition and fluid consistency [169]. For SWE systems, SWV is likely to be the most appropriate unit for interpretability across studies as this is a measure of shear wave propagation velocity [169]. While the SM (i.e., stiffness estimation under the assumption of an absolute elasticity model) may be appropriate for isotropic tissues like the liver [209], muscle tissues are largely anisotropic due to fascicle order and orientation [210].

Intersystem differences may also contribute to variance across studies. UE systems use their own unique algorithms for capturing images and calculating stiffness values and can be generally categorized by either quasi-static or dynamic means of excitation [171,211]. Dynamic methods are complex involving a varying time-course force application in the form of vibration or an acoustic force pulse with a specific frequency (50 to 500 Hz) and often use ultrafast imaging of induced displacements or deformations [29,212]. These deformation forces are sent through tissues as either compression waves with high propagation speeds (approx. 1500 m/s) or shear waves with low propagation speeds (approx. 1—50 m/s) [213]. Tissue displacements and wave velocities are then tracked and tissue stiffness estimations are generated based on tissue motion, frequency shifts or velocity changes [214]. While static and dynamic methods are similar in that both use an external stress and follow changes in strain, the stress applied in dynamic methods is definable and less operator-dependent, thus holding to the proportionality of Hooke's Law in the estimation of Young's modulus and provide a more quantitative measure [213,215]. Static methods provide semi-quantitative strain ratio based estimations through manual application of multi-compression cycles. However, long acquisition times and difficulties in producing artifact-free compression cycles are inherent technical challenges [206,215]. In studies exploring intersystem comparisons using dynamic and static methods in tissue mimicking phantoms or muscle in vivo, dynamic methods have demonstrated slightly greater measurement reliability [178,179,216,217]. In this review, fewer studies used systems requiring mechanical force application (i.e., tissue compression). Although these systems are associated with greater operator-dependent error, Wu et al and Mathevon et al reported the largest variance in reliability using SWE systems (ICC range=0.55-0.85 and 0.00-0.87, respectively) [43,46]. Moreover, Gao et al reported good interrater (ICC=0.84) and intrarater reliability (ICC=0.88) using a strain system [39]. Good intrarater reliability was also reported by Park et al (ICC=0.85, 0.87) and Kwon et al (ICC=0.81, 0.88) using sonoelastography systems [36,163]. Furthermore, the operators in both of these studies were described as physiatrists with 16 to 17 years of experience in using musculoskeletal ultrasound [36,163]. In comparison, Wu et al described the operator as a physiatrist with 2 years of experience in musculoskeletal ultrasound [43]. The operator in the Mathevon et al study was described as an investigator with no mention of additional experience or training outside of the measures collected for the study [46]. Although the risk of committing operator-related errors may be reduced with dynamic systems, it is reasonable to assume that acceptable levels of measurement reliability can be achieved with relevant training and experience in the use of other systems.

Taken together, the current evidence suggests UE has moderate reliability when used among populations with neurological conditions. Care should be taken to ensure measurement acquisition protocols are standardized. Reliability appears to be more difficult to achieve with multiple operators than in instances with a single operator. The use of EMG rather than visual confirmation of muscle activity status may also be an important consideration in assessing patients with characteristic spasticity or hypertonia.

2.4.2 Validity

As expected, convergent validity was observed in studies with strong correlations between stiffness and reduced functional motor recovery or increased impairment and spasticity. Additionally, strong correlations between stiffness and grey scale or color histogram pixel intensities were also observed. Higher echo intensity in musculoskeletal ultrasound is generally indicative of greater organizational density of collagen rather than the presence of fluid within tissues [218]. For subjects with neurological conditions, this may represent changes in composition, fiber type distribution and intrinsic mechanical properties resulting from alterations in muscle tissue innervation [131,151]. Tissue composition alterations were also evident in one study involving people with DMD which showed fatty replacement and patchy edema on muscle MRI scans in addition to increased SM values [200]. However, there was no significant correlation between these parameters, perhaps due to the small cohort size. The SWE method used was also not found to have any clear diagnostic advantage or greater sensitivity in detecting early changes to muscle in comparison to MRI [200].

Discriminant or known-groups validity was observed in more than half of included studies suggesting that UE may be useful in monitoring muscle pathology over time. The high degree of responsiveness observed across intervention studies also suggests that UE may be useful in evaluating responsiveness to treatment. However, there is no gold standard method for assessing muscle stiffness. While concurrent methods (i.e., echo intensity, spasticity and motor function scales) showed strong correlations with stiffness, they are separate constructs. Other methods such as myotonometry and portable hardness meters may be useful comparators and have been used to examine stiffness after stroke [219] and in patients with PD [220]. Few studies have examined the validity of using myotonometry and UE concurrently [221].

2.4.3 Limitations of the studies reviewed

Many studies did not clearly define operator experience which may influence measurement consistency. Of the included studies reporting estimates of reliability, most did not provide estimates for measurement error. Another limitation was the lack of concurrent comparators necessary for establishing criterion validity. Future research endeavors should explore the concomitant use of existing technologies (i.e., magnetic resonance elastography, myotonometry) in elucidating the validity of UE among populations with neurological conditions. Additionally, the concomitant use of EMG may be important not only for reliability, as previous described, but also measurement validity. Although there were strong correlations between clinical assessments of spasticity (i.e., FMA, MAS) and muscle stiffness measures [11,43,45,153], these assessments are limited in their ability to distinguish between active reflex or neurogenic components of stiffness and passive non-reflex mediated components [222]. It is also unknown whether degenerative within-subject factors such as bilateral differences in motor-unit threshold and denervation of affected limbs [13] also contribute to muscle stiffness. When paired with UE, electrophysiological evaluation may be of value in this regard.

2.4.4 Limitations of this systematic review

As overall estimates of reliability were similar for CP and stroke subgroups, differences in measurement protocols may have contributed substantially to the observed heterogeneity between subgroups. These methodological differences negatively influence the interpretability of the review findings. Although the number of studies involving people with stroke and CP were sufficient for conducting subgroup analyses, the number of studies assessing reliability among other populations with neurological conditions (i.e., PD, DMD) were limited. To the knowledge of the authors, there is currently no research examining the use of UE in populations with other neurological conditions (i.e., SCI) not described in this review. This will require future investigation. There was also a paucity of studies examining UE responsiveness following non-invasive treatments for individuals with neurological conditions. This may be an important, yet unaddressed, aspect of the technology which translates to routine clinical application. Studies which assess pre- to -post changes in muscle stiffness following common non-invasive therapeutic modalities are needed moving forward. Lastly, only peer-reviewed articles published in English language journals were considered for inclusion. This may have introduced language bias and limited the number of potentially relevant studies for consideration.

2.5 Conclusion

Overall, UE demonstrates moderate reliability in evaluating in-vivo muscle stiffness across a range of populations with neurological conditions. This method also demonstrates strong convergent validity with relevant clinical assessments, and strong divergent validity in discriminating tissue changes within and between groups. However, further investigation regarding UE systems, image acquisition procedures and the use of concurrent assessments may be warranted to standardize measurement protocols and potentially enhance reliability and validity.

Figure 2.1 Flow diagram

Flow diagram illustrating article screening and selection in accordance with PRISMA guidelines [186]. A total of 21 articles were included in the final review.

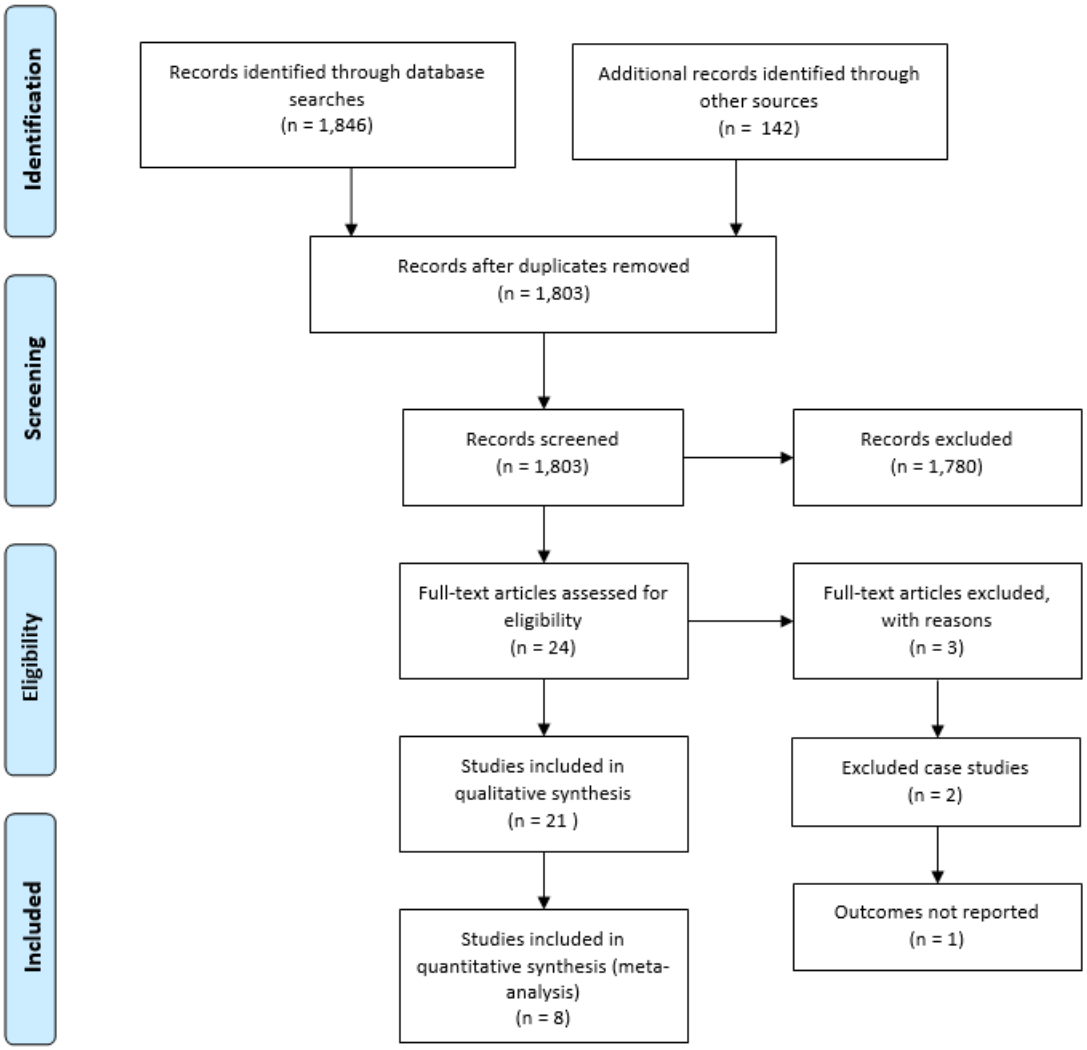

Figure 2.2 Forest plot

Graphical summary of subgroup analyses for studies involving patients with CP or stroke. Correlation coefficients were transformed to Fisher's Z scale for analysis. Overall correlation across subgroups was r=0.78 (95% CI=0.64–0.86, p≤0.00).

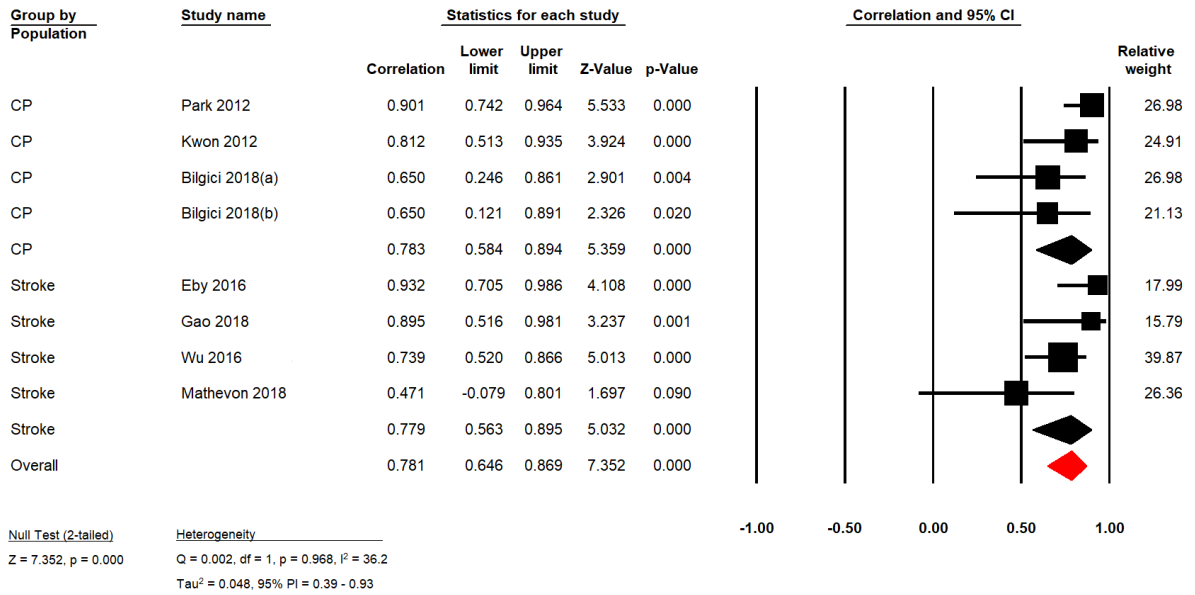

Table 2.1 Study characteristics

Study	Sample Characteristics		Measurement			
	Neurological Group	Control Group	Muscle Site(s)	Passive/ Active	Body Position/ Joint Angle	Assessor/ Blinding
Bilgici 2018(a) - Cross sectional - (Turkey)	17 patients w/ CP (32 legs) 2 = hemiplegic MAS 1 = 3 (1.72 (0.35)), MAS 2 = 8 (2.79 (0.61)), MAS 3 = 17 (3.31 (0.50)), MAS 4 = 4 (4.37 (0.19)) m/f = 9/8 age: 9.25 (2.68)y, range: 6–14y weight: 24.53 (7.77)kg, range: 17–45kg	25 controls (50 legs) children of similar age w/o systemic/ neurological disease visiting hospital for other reasons m/f = 10/15 age: 10.40 (2.76)y, range: 7-15y weight: 36.48 (13.42)kg, range: 20-63kg	MG	Passive, no EMG	Prone position w/ feet in neutral position (0°) over the edge of the examination table	**Assessor:** Radiologist w/ 4ys of UE experience **Blinding:** Blinded to patient MAS scores
Bilgici 2018(b) – Pre-post intervention - (Turkey)	12 patients w/ CP (24 legs) m/f = 6/6 age: 8.58 (2.48)y, range: 6–14y weight: 21.83 (5.13)kg	N/A	MG	Passive, no EMG	Prone position w/ feet in neutral position (0°) over the edge of the examination table	**Assessor:** Radiologist w/ 4ys of UE experience **Blinding:** Blinded to patient MAS scores
Boyaci 2014 – Pre-post intervention - (Turkey)	16 CP children (25 legs) 9 = diplegic, 7 = hemiplegic m/f = 11/5 age: 48.87 (16.47)mo weight: 15.87 ± 3.55kg	17 children w/o neurological history (34 legs) age: 45.52 (20.13)mo weight: 17.29 (5.92)kg	MG, LG, SOL	Passive, no EMG	Prone position w/ feet over the edge of the examination couch	**Assessor:** Radiologist w/ 6ys of ultrasound experience **Blinding:** Not explicitly stated
Brandenburg 2018 - Prospective longitudinal cohort (intervention) - (USA)	9 children w/ spastic CP bilateral = 5, unilateral = 4 GMFCS: level I = 4, level II = 3, level III = 2 m/f = 5/4 median age: 60 (35-92)mo, age range: 25-105mo median BMI: 16.7 (15.9-17.9), BMI range: 15.3–18.6	N/A	LG (most affected leg)	Passive w/ sEMG (U-Control; Thought Technology Ltd.) set at lowest scale range (X1, upper threshold 3.0)	Prone position w/ feet over the edge of the examination table	**Assessor:** Not stated, assumed to be the researcher **Blinding:** No explicitly stated
Brandenburg 2016 – Cross sectional - (USA)	13 children w/ CP m/f = 7/6 median age: 5y 1m, IQ range: 4y 4m-7y 8m	13 typically developing children m/f = 7/6 median age: 5y 3m, IQ range: 4y 4m - 9y 4m	LG (most affected leg)	Passive w/ sEMG (U-Control; Thought Technology Ltd.) set at lowest scale range (X1, upper threshold 3.0)	Prone position w/ feet over the edge of the examination table	**Assessor:** Not stated, assumed to be the researcher **Blinding:** Not explicitly stated
Du 2016 – Cross sectional - (China)	46 patients w/ PD (British Brain Bank clinical criteria) m/f = 27/19 age: 47.9 (2.8)y	31 healthy controls m/f = 18/13 age: 46.7 (3.2)y	BB	Passive, no EMG	Supine position w/ limbs kept in full relaxation	**Assessor:** Not stated, assumed to be 2 researchers **Blinding:** Not explicitly stated
Eby 2016 – Cross sectional - (USA)	9 subjects w/ chronic stroke m/f = 7/2 age: 58.3y, range: 41-79y	4 healthy controls m/f = 2/2 age: 56y, range: 42-70y	BB (long head)	Passive w/ sEMG (MA-300, Motion Lab Systems) and a dynamometer	80° and 150° elbow flexion/extension and at 3 preselected joint angles ranging btw 85° and 150°	**Assessor:** Not stated, assumed to be the same rater/ researcher **Blinding:** Not explicitly stated
Gao 2018 - Cross sectional - (USA)	8 patients w/ stroke m/f = 5/3 age: 59y, range: 34-72y	8 healthy controls m/f = 4/4 age: 49y, range: 40-56y	BB	Passive, w/ the use of VTIQ quality map to monitor patient or probe motion during image capture, no EMG	Supine position w/ arm relaxed and forearm supinated	**Assessor:** A single observer (J.G.) acquired VTIQ SWV images **Blinding:** Not explicitly stated
Gao 2016 - Cross sectional - (USA)	14 patients w/ PD disease duration: 78 (13)mo, range: 6-134mo muscle rigidity scores: high (UPDRS III–IV) = 3, low (UPDRS I–II) = 11 m/f = 8/6 age: 61 (10)y, range = 41-78y	10 healthy controls m/f = 5/5 age: 60 ± 11y, range: 54-82y	BB	Passive, probe and subject arms were held stable by the researchers to minimize movement during compression cycles, no EMG	Supine position w/ arm relaxed, elbow extended and the forearm supinated (forearm elevated 15° from the bed)	**Assessor:** Physician w/ experience in MSK ultrasound. For reliability measures, 2 observers assessed 10 healthy controls **Blinding:** Blinded to UPDRS motor score and disease duration, aware of symptomatic patients w/ PD
Jakubowski 2017 - Cross sectional - (USA)	14 subjects w/ chronic stroke stroke duration: 10.6 (7.3)y, range: 4.3-29.3y FMA: 19.1 (6.1), range: 8-28	N/A	MG, TA	Passive, w/ EMG (Bagnoli, Delsys Inc.)	Seated w/ foot secured to a dynamometer (Biodex Medical systems Inc.) and knee in extension, bilateral ankle moved passively by the experimenter in 6 positions: neutral 90°, 15° PF, max DF, max PF, and 2	**Assessor:** Described as an experimenter **Blinding:** Not explicitly stated

	m/f = 6/8 age: 60.1 (5.9)y, range: 46–68y height: 1.7 (0.1)m, range: 1.5-1.8m body mass: 77.6 (12.5)kg, range = 58.0–96.4kg				intermediate angles where the torque on the paretic side was btw max DF and neutral or max PF and neutral, respectively	
Kwon 2012 - Cross sectional - (South Korea)	15 children w/ spastic CP (27 legs) diplegia = 12, hemiplegia = 3 m/f = 10/5 age: 58.7 (20.6)mo	13 children w/o neurological or MSK disability (26 legs) m/f = 4/9 age: 46.9 (20.2)mo	MG, SOL	Passive, no EMG	Prone w/ feet hanging from the edge of an examination plinth	**Assessor:** Physiatrist (G.Y.P.) w/ 16ys of MSK ultrasound and 3ys of UE experience **Blinding:** Not explicitly stated
Lacourpaille 2017 – Longitudinal - (France)	10 patients w/ DMD (genetically confirmed) age: 13.6 (6.3)y, range: 7-23y	9 age matched healthy controls	MG, TA, VL, BB, TB, and ADM	Passive for stiffness measures and active for EMD measures, a constant-current stimulator (Digitimer DS7A, Digitimer) was used to elicit contractions	Seated. MG: knee flexed at 90° (shortened) or fully extended (stretched) w/ ankle in neutral, TA: knee extended fully w/ ankle in neutral or 20° PF, VL: knee fully extended or flexed at 90°, BB: elbow flexed at 90° or overextended w/ hand in neutral, TB: arm extended or abducted and flexed at 90°, ADM: hand in pronation w/ 5th finger in maximal abduction or in alignment w/ 5th metacarpal	**Assessor:** Not stated, assumed to be the researcher. **Blinding:** Not explicitly stated
Lacourpaille 2015 - Cross sectional - (France)	14 patients w/ DMD age: 13.3 (5.9)y, range 5–22y	13 age-matched healthy controls age: 12.8 (5.5)y, range 6-24y	MG, TA, VL, BB, TB, and ADM	Passive, no EMG	Lying on a plinth. MG: knee flexed at 90° (shortened) or fully extended (stretched) w/ ankle in neutral, TA: knee extended fully w/ ankle in neutral or 20° PF, VL: knee fully extended or flexed at 90°, BB: elbow flexed at 90° or overextended w/ hand in neutral, TB: arm extended or abducted and flexed at 90°, ADM: hand in pronation w/ 5th finger in maximal abduction or in alignment w/ 5th metacarpal	**Assessor:** Described as an examiner, assumed to be the researcher **Blinding:** Not explicitly stated
Lee 2018 - Cross sectional - (USA)	14 subjects w/ chronic stroke stroke duration: 10.2 (8.4)y, range: 2.1-27.3y FMA: 19.6 (15.0), range: 4-48 MAS range: 0-3 TS: 1–3 muscle quality, 62°-145° catch angle for 3 speeds m/f = 5/9 age: 58.9 (7.4)y height: 1.68 (0.10)m body mass: 85.5 (18.2)kg	8 age- and sex-matched controls w/o neurological or muscular disorders m/f = 4/4 age: 57.4 (7.4)y height: 1.68 (0.11)m body mass: 75.0 (12.0)kg	BB	Active and Passive w/ sEMG (Bagnoli Delsys, Inc.)	Seated in a dynamometer (Biodex Medical Systems Inc.), upper arm resting on a plastic support, forearm secured in a fiberglass cast w/ wrist and forearm in neutral position and placed in a ring-mount interface mounted on the table, shoulder positioned w/ humerus abducted 45° and elbow at 90° of flexion	**Assessor:** Not clearly stated, assumed to be the researcher. **Blinding:** Not explicitly stated
Lee 2016 - Cross sectional - (USA)	8 subjects w/ spastic hemiplegic CP GMFCS: level I = 3, level II = 5 m/f = 5/3 age: 9.4 (3.7)y height: 1.31 (0.17)m body mass: 33.3 (12.8)kg	N/A	MG and TA	Passive w/ EMG	Seated in an IntelliStretch rotary actuator (IntelliStretch Rehabilitation Robot, Rehabtek LLC) to monitor ankle angle and torque continuously, knee placed in max extension w/ foot strapped to the device, MG and TA measures taken in 5 ankle positions (neutral, maximum DF, maximum PF, and 2 intermediary angles)	**Assessor:** Not clearly stated, assumed to be the researcher. **Blinding:** Not explicitly stated
Lee 2015 - Cross sectional - (USA)	16 subjects w/ chronic stroke stroke duration: 11.6 (11.4)y, range: 1.9–42.2y FMA: 19 (15), range: 4-48 MAS range: 0-3 TS: 1-3 muscle quality, 62°-145° catch angle for 3 speeds m/f = 6/10 age: 60.7 (8.0)y height: 1.71 (0.15)m body mass: 85.5 (18.2)kg	N/A	BB	Passive w/ sEMG	Seated in a dynamometer (Biodex Medical Systems Inc.), upper arm resting on a plastic support, forearm secured in a fiberglass cast w/ wrist and forearm in neutral position and placed in a ring-mount interface mounted on the table, shoulder positioned w/ humerus abducted 45° and elbow at 90° of flexion	**Assessor:** Not clearly stated, assumed to be the researcher. **Blinding:** Not explicitly stated
Mathevon 2018 – Observational/ Reliability - (France)	14 subjects w/ stroke stroke duration: 39mo, range: 6-255mo paretic side left/right: 6/8 m/f = 10/4 age: 56.9 (10.8)y height: 170.9 (8.9)cm weight: 80.9 (13.2)kg	N/A	MG and TA	Passive and during DF, no EMG	TA at rest and max DF: Supine. MG at rest: prone w/ feet below the table and no hip rotation at maximum passive-ankle DF w/ full knee extension. Stretching was performed manually by a second investigator (L.F.A.) in all trials.	**Assessor:** Described as an experimental investigator, assessed each patient twice at an interval of 1 week at the same time of the day **Blinding:** Not explicitly stated
Park 2012 – Pre-post intervention - (South Korea)	17 children w/ CP diplegia = 12, hemiplegia = 5 m/f = 10/7	N/A	MG	Passive, no EMG	Prone w/ feet hanging from the edge of an examination table	**Assessor:** Physiatrist w/ 17ys of MSK ultrasound and 4ys of RTS experience

	age: 57 (22)mo, range: 26-110mo weight: 12.5kg, range: 11-15kg					**Blinding:** image analysis conducted by another physiatrist
Pichiecchio 2018 - Cross sectional - (Italy)	5 children w/ DMD (clinical and molecular diagnosis of dystrophinopathy) m/f = 5/0 median age: 48mo, range 38-59mo BMI <30	5 age-matched healthy controls m/f = 4/1 median age: 39mo, range: 39-47mo BMI <30	GM, RF, VM, VL, AM, TA, and MG	Passive, no EMG	Supine on an examination bed (or in their mother's arms) and then in prone position	**SWE Assessors:** 2 radiologists (C.B., F.C.), w/ 5y of MSK ultrasound experience **Blinding:** blinded to subject characteristics **MRI Assessors:** 2 radiologists (A.P., F.A.), one w/ considerable expertise in neuromuscular disorders and the other, a resident, w/ 4ys of MRI experience
Shao 2019 - Pre-post intervention (China)	24 patients w/ mild hemiplegic stroke and impaired plantar flexion (MAS ≥ 2) stroke duration: 10.1 (3.7)mo m/f = 14/10 age: 60.7 (8.8)y, range: 41–75y	N/A	AT	Passive, no EMG	Prone w/ feet hanging from the edge of an examination table	**Assessor:** MSK radiologist w/ > 6y of MSK ultrasound imaging experience **Blinding:** Not explicitly stated
Wu 2016 - Cross sectional - (Taiwan)	31 patients w/ acute stroke stroke duration < 3m in 29 patients stroke duration: 8.4 (7.6)wks infarct = 19, hemorrhage = 12 paretic right/left = 11/20 m/f = 21/10 age: 60.3 (13.0)y height: 164.7 (6.9)m weight: 63.4 (12.3)kg	21 healthy controls m/f = 14/7 age: 31.2 (7.9)y height: 168.5 (7.1)m weight: 168.5 (7.1)kg	BB	Passive w/ sEMG used to monitor muscle activity	Supine on an examination bed w/ shoulders and elbows in a relaxed neutral position. SWV obtained at 0° (full extension) and 90° of elbow flexion using an custom elbow stabilizer	**Assessor:** Physiatrist w/ 2ys of MSK ultrasound experience (> 1000 cases), familiarized w/ the study protocol for optimization of SWV measures by examining 15 unimpaired subjects not included in the study (preliminary test) **Blinding:** Physical appearance of patients and controls prevented blinding of the rater to paretic limbs

Table 2.2 System specifications and acquisition procedures

Study	System Specifications					Acquisition Method				
	System	Probe	Settings/ Software	Units Reported	Probe Alignment	ROI	Number of Trials	Transducer Pressure/ Placement	Contact Interface	Image Acquisition/ Processing
Bilgici 2018(a)	Acuson S2000 US system (Siemens Medical)	linear array (9L4)	N/A	SWV (m/s) (range of 0-9)	parallel	ROI box 0.5 cm^2 in size placed in the mid-section of the MG corresponding to the largest circumference	5 measures for each muscle w/ the mean value used for analysis	minimal compression applied w/ the probe weight	N/A	Value ''x.xx'' displayed in case of faulty measures, repeated until valid values were obtained
Bilgici 2018(b)	Acuson S2000 US system (Siemens Medical)	linear array (9L4)	VTIQ software	SWV (m/s) (range of 0-9)	parallel	ROI box 0.5 cm^2 in size placed in the mid-section of the MG corresponding to the largest circumference	5 measures for each muscle w/ the mean value used for analysis	minimal compression applied w/ the probe weight	N/A	Value ''x.xx'' displayed in case of faulty measures, repeated until valid values were obtained, VTIQ software
Boyaci 2014	Mylab Twice US system w/ sonoelastography and Doppler (Esaote)	broadband linear array (12MHz)	N/A	ELX 2/1 Index and color pattern pixel intensities	parallel	ROI of 7.5×7.5 mm^2 in size, ELX 2/1 index calculated as a ratio of the elastic properties of the MG, LG and SOL w/in the ROI	N/A	N/A	N/A	Pixel color pattern in 0 to 255 range, w/ median blue, green, and red pixel histogram intensities analyzed w/ ImageJ software (National Institutes of Health)
Brandenburg 2018	Aixplorer US scanner (SuperSonic Imagine)	linear array (SL15-4; SuperSonic Imagine)	MSK preset	SM (kPa)	parallel	circular ROI w/ mean diameter of 4.8–5.0mm w/in the elastogram	measures at 3 foot positions and repeated twice, average of 3 measures used for analysis	minimal pressure on skin by one of the examiners	N/A	Open-source imaging plug-in for the DICOM reader (OsiriX Imaging Software) used to measure modulus values w/in the ROI
Brandenburg 2016	Aixplorer US scanner (version 4.0; SuperSonic Imagine)	linear array (SL15–4; SuperSonic Imagine)	MSK preset, SWE Optimization: Standard, HD/ Frame Rate: Balanced, Zoom: 120%, Smoothing: 5, Persistence: High	SM (kPa)	parallel	circular ROI w/ mean diameter of 4.8–5.0mm w/in the elastogram	measures at 3 foot positions and repeated twice, average of 3 measures used for analysis	minimal pressure on skin by one of the examiners	N/A	Open-source imaging plug-in for the DICOM reader (OsiriX Imaging Software) used to measure modulus values w/in the ROI
Du 2016	Aixplorer US scanner (SuperSonic Imagine)	linear array (4–15 MHz)	MSK setting, Q-Box software	SM (kPa)	parallel	5mm diameter circle in the ROI center w/ homogeneous color distribution for a 3 seconds minimum	3 measures per muscle and side w/ the average 3 measures used for analysis	gently placed on skin w/o compression	N/A	Q-Box software
Eby 2016	Verasonics US scanner (Verasonics Inc.)	linear array (L7-4, Philips Healthcare)	CUSE and SWE settings	SM (kPa) w/ color bar range 0-16 (m/s)	assumed to be parallel	approx. 160 mm^2 ROI using CUSE	3 measures at 80° and 150° elbow angles	custom holder securely fixed to the arm maintaining continuous contact pressure	transmission gel couplant applied	Shear wave motion recorded using a high frame rate technique and calculated from image data based on one-dimensional autocorrelation
Gao 2018	Acuson S3000 HELX (Siemens Medical)	linear array (9L4)	pre-locked settings w/ mechanical index 1.1, depth 4cm, scanning frequency 7 MHz, Map D/Space time (0), total gain 0dB, dynamic range 70dB, single focus, harmonic imaging kept constant, VTIQ software	SWV (m/s)	parallel	ROI of 1.5 × 1.5 mm, 1-3 cm depth from the skin w/in a color coded SWV map	10 trials w/ 5 ROIs of 1.5cm depth and 5 ROIs of 2.0cm depth from skin surface at both 90° passive elbow flexion and max passive elbow extension (up to 180°)	N/A	transmission gel couplant applied	VTIQ software
Gao 2016	Logic E9 US scanner (General Electric)	linear array (L9-3)	grayscale imaging settings for SE optimized for speckle tracking, high frame rate (N40 frames per second), single focus, turn off speckle reduction, low scanning frequency (6 MHz)	SR	parallel	Reference strain standardized to 5mm axial region in subcutaneous tissue (distance from skin to muscle)	3 compression cycles w/ 2 minute time interval btw trials	sand bag (1.5 kg) tied to probe for constant compression, 5 second compression cycles used to during tissue deformation sequence	transmission gel couplant applied	Strain of target muscle and reference tissues estimated w/ 2-D speckle tracking software (EchoInsight, Epsilon Imaging)
Jakubowski 2017	Aixplorer US system (SuperSonic Imagine)	linear array (4–15 MHz, Super Linear 15-4)	N/A	SWV (m/s)	parallel	ROI of 30mm width w/ depth set to muscle thickness	3 trials per ankle position	custom neoprene sleeve used to minimize probe movement	N/A	images manually cropped and exported for off-line processing using custom-written program in Matlab (Mathworks)

Kwon 2012	Acuson S2000 US system w/ B-mode and DS (Siemens Medical)	multi frequency linear (4–9 MHz)	N/A	SWV (m/s), SR, DS score and color pixel intensity	parallel	ROI of 5 x 5 mm^2 for SWV acquisition, ROI for pixel analysis set to cover entire muscle, excluding hyperechoic epimysium	2 trials w/ 2 representative images taken during each	compression adjusted according to quality factor display, factor ≥ 60 indicated optimal compression	N/A	color pattern (0 to 255 pixel range) of images analyzed w/ Image J software (National Institutes of Health), median blue and red pixel intensities obtained w/ color histogram
Lacourpaille 2017	Aixplorer US scanner (version 7, SuperSonic Imagine)	linear array (4–15 MHz)	SWE and research mode to acquire raw radio-frequency signals at 4 kHz, force and US data synchronized w/ transistor to transistor logic pulses	SM (kPa)	parallel	ROI corresponded to the largest muscular region w/o fascia	10 trails for each muscle and position, then averaged to obtain representative values	probe placed on thickest part of muscle belly	N/A	SSI recordings exported from system software (Version 7.0, SuperSonic Imagine) as mp4 and sequenced in jpeg format w/ custom program in Matlab (version 10.0, Mathworks Inc.), color maps were converted to SM
Lacourpaille 2015	Aixplorer US scanner (SuperSonic Imagine)	linear array (4–15 MHz)	SWE mode	SM (kPa)	not stated, not inferable due to lack of images and figures depicting alignment	N/A	10 trails for each muscle and position, then averaged to obtain representative values	probe placed on thickest part of muscle belly	N/A	N/A
Lee 2018	Aixplorer US system (SuperSonic Imagine)	Not explicitly stated	N/A	SWV (range 0-16 m/s)	parallel	circular region w/ varying diameters w/in an ROI of 12 x 12mm btw superficial and deep aponeuroses	3 trials per % max voluntary contraction	custom neoprene sleeve used to minimize probe movement	N/A	images cropped and muscle area w/in the ROI analysed w/ a custom program in Matlab (Mathworks Inc.)
Lee 2016	Aixplorer US system (SuperSonic Imagine)	linear array (4–15 MHz, Super Linear 15-4)	SSI software (Q Box)	SWV (m/s)	parallel	circular region w/ varying diameters w/in an ROI of 12 x 12mm, all manually cropped areas w/in the muscle used to calculate SWV spatial averages	60 trials (2 legs, 2 muscles, 15 trials per muscle)	custom neoprene sleeve used to minimize probe movement, placed over muscle belly mid-region	N/A	image were analysed w/ custom program in Matlab (Mathworks Inc.), Q Box software used to generate SWV values w/ a quality factor > 0.8.
Lee 2015	Aixplorer US system (SuperSonic Imagine)	linear array (4–15 MHz, SuperLinear 15–4)	SSI software (Q Box)	SWV (m/s)	parallel	ROI of 12 x 12mm placed in the mid-section btw superficial and deep aponeuroses	N/A	custom neoprene sleeve used to minimize probe movement	N/A	SWV and quality factor values in the ROI extracted and analysed w/ custom program in Matlab (Mathworks)
Mathevon 2018	Aixplorer US scanner (version 6.1.1, SuperSonic Imagine)	linear array (4–15 MHZ, SuperLinear 15–4)	2D muscle measures w/ B-mode US, data processed w/ SSI software (Q-Box)	SM (kPa)	parallel (sagittal) and perpendicular (axial)	3 circular ROI (Q-boxes) positioned over the largest contiguous area possible	mean value of 5 measures over 5 seconds used for analysis	compression limited by a thick layer of gel and the support of the examin table	transmission gel couplant applied	data processed w/ system software (Q-Box)
Park 2012	Antares US system w/ B-mode and RTS (Siemens Medical)	multi frequency linear (5-13 MHz)	image color pattern analyzed w/ Image J software (National Institutes of Health)	RTS score	parallel	ROI set to cover the entire muscle, excluding hyperechoic perimysium	N/A	manually adjusted compression, perimysium appeared yellow to red on RTS, w/ standardized color scale encoding	N/A	image color pattern analyzed w/ ImageJ software (National Institutes of Health), RTS score graded semi-quantitatively as follows: 1 (purple to green: soft), 2 (green to yellow), 3 (yellow to red), and 4 (red: hard)
Pichiecchio 2018	Toshiba Aplio 500 SWE US scanner (Toshiba Medical)	multi frequency linear array (4-15 MHz)	shear wave module (Toshiba Medical)	SM (kPa)	Assumed to be parallel	Circular ROI of 5mm w/ homogeneous stiffness values w/in an area void of tendon, fascial tissue	N/A	probe placed in a fixed position	transmission gel couplant applied	N/A
Shao 2019	Acuson S2000 US system (Siemens Medical)	linear array (5–14 MHz, Siemens)	elastographic unit w/ strain quality indicator (proprietary software, Siemens)	SR and elasticity score	parallel	Depth 3x AT thickness, SR ROI 2cm above insertion w/ corresponding deep fat reference area	3 trials to calculate SR	appropriate pressure applied	10mm gel pad (SONAR-AID)	Score/ grade calculated accordingly: SR=B/A (fat-to-tendon SR), elasticity: 3=red (soft), 2=green/ yellow (medium), 1=blue (hard)
Wu 2016	Acuson S2000 US system (Siemens Medical)	linear array (7-9 MHz, 9L4, Siemens)	Virtual Touch Quantification Technology (VTQ) (Siemens)	SWV (m/s)	parallel (longitudinal) and perpendicular (transverse)	ROI of 0.5 x 0.5cm in the mid-muscle belly	5 trials per arm in each elbow posture and averaged for analysis	probe held stationary during acquisition	transmission gel couplant applied	N/A

Table 2.3 Reliability and validity summary

Study	Reliability	Validity			
		Convergent/ Concurrent	Discriminant/ Known Groups	Responsiveness	Comparator(s)
Bilgici 2018(a)	**Interrater Reliability:** ICC=.65 (agreement, 95% CI=.33–.84, p=.001)	**Convergent Validity:** SWV values of MG correlated w/ ankle spasticity MAS scores (p=.001)	**Known Groups Validity:** Mean SWV values for the MG in patients w/ CP (3.17±.81, min–max 1.291-4.540) were significantly higher than controls (1.45±.25, min–max .938–2.080, p=.001)	N/A	Controls and MAS
Bilgici 2018(b)	**Interrater Reliability:** ICC=.65 (agreement, 95% CI=.33–.84, p=.001)	**Convergent Validity:** SWV values positively correlated w/ MAS score (q=.578, p=0.003)	N/A	**Responsiveness:** Significant difference in mean SWV values pre-BTA (3.20±.14) and post-BTA (2.45±.21, p=.001)	SWV and MAS measured pre-BTA and 1 mo post
Boyaci 2014	N/A	**Convergent Validity:** ELX 2/1 index was correlated w/ median red pixel intensity in the CP group (r=.516, p=.008). Mean MAS for the ankle decreased, from 3.4 to 2.6 (p<.05). Mean MAS scores decreased significantly from pre- (3.44±.58) to post-trial (2.60±.64, p<.001), while mean GMFM scores increased significantly from pre- (54.28±19.19) to post-trial (59.03±16.49, p=.001)	**Known Groups Validity:** ELX 2/1 indices of the CP group (MG=2.27±.88, LG=1.84±.85) were significantly higher than controls (MG=1.12±.27, LG=1.17±.39, p<.05)	**Responsiveness:** ELX 2/1 indices in the GM and GL muscles in the CP group decreased significantly post-treatment (p<.05)	Controls, pixel intensity, ELX 2/1 index, MAS and GMFM scores measured pre-procedure and 1 month post
Brandenburg 2018	N/A	**Convergent Validity:** Spearman rank correlations used to explore the relationship btw SM and continuous variables (BoNT-A dose, and ankle DF passive ROM). However, no outcomes were reported	N/A	**Responsiveness:** Despite no significant change in ankle ROM or spasticity, there was a significant difference in LG SM after BoNT-A injections	MAS, max ankle DF ROM, GMFCS
Brandenburg 2016	N/A	**Convergent Validity:** No correlation btw SM values and GMFCS level, MAS grade, or history of calf muscle botulinum toxin injection. There was a significant difference in median ankle ROM btw the CP group (-12° to 20°) and controls (5° to 31°)	**Known Groups Validity:** SM at all 3 foot positions were significantly greater for CP children (20° PF = 15.0 (11.6, 17.5),10° PF = 19.1 (15.0, 23.6), 0° PF = 28.9 (24.6, 44.2)) than controls (20° PF = 7.8 (6.1, 11.0),10° PF = 9.6 (7.3, 15.6), 0° PF = 14.9 (10.9, 20.9)). CP children had greater variability in SM, indicated by larger SD for measures at all ankle positions	N/A	Healthy controls (age- and gender-matched typically developing children), MAS, maximal ankle DF ROM, GMFCS
Du 2016	(9 control subjects only) **Interrater Reliability:** ICC(3,2)=.74 (95% CI=.68–.78) **Intrarater Reliability:** ICC(3,1)=.78 (95% CI=.75–.82)	**Convergent Validity:** Positive linear correlation found btw SM values and UPDRS motion scores in patients w/ PD (r=.646, p=.000)	**Known Groups Validity:** Significant difference in SM of the BB btw PD (54.94±20.91) and controls (24.44±5.09, p<.05) **Discriminant Validity:** No significant difference btw remarkably (54.94±20.91) and mildly symptomatic arms (47.77±24.00, p<.05)	N/A	Remarkably and mildly symptomatic arms in patients w/ PD, btw patients and controls, and btw SM and UPDRS
Eby 2016	**Intrarater Reliability:** ICC(1,1) range=.76-.99 at both 80° and 150° for all subjects ICC(1,1) range=.75-.97 for 3 preselected joint angles (ICCs indicated consistent stiffness throughout testing for dominant sides of controls, but largely inconsistent stiffness for other study conditions)	**Convergent Validity:** No association was found btw stroke mechanism, location, or hemisphere and MAS or FMA scores. SM values and torque during all 40°/sec trials: A= controls, w/ minimal torque and SM responses; y=17.394x + 7.898, R^2=.103. B= S1, w/ strong torque and SM responses to passive extension; y=36.856x + 18.197, R^2=.829, and C= S6, S3, S7, w/ strong torque response and minimal SM responses; y=2.712x + 6.676, R^2=.181.	**Known Groups Validity:** Torque and passive stiffness increased minimally for controls and was most pronounced in contralateral limbs of subjects w/ stroke. Several patterns of SM and torque responses to passive elbow extension were identified, w/ a subset of several subjects displaying very strong torque response w/ minimal stiffness response	N/A	Healthy controls and velocity dependent torque
Gao 2018	**Intrarater Reliability:** ICC=.94 (agreement, p<.001) for non-spastic BB ICC=.82 (agreement, p<.01) for spastic BB **Software Usage:** VTIQ indicates SWV quality and reliability w/ homogeneous green color scale throughout image maps	**Convergent Validity:** A strong negative correlation was found btw SWV and passive ROM (R^2=−.88, p<.0001) in spastic upper limbs. The correlation btw mean SWV and other MAS and TS parameters was weak (p>.05).	**Known Groups Validity:** At 90°, there was no significant difference in SWV btw controls and spastic BB or btw non-spastic and spastic BB. However, there was a significant difference btw controls and non-spastic BB based on Bonferroni correction. At max elbow extension, the difference in SWV btw healthy and spastic BB, and btw non-spastic and spastic BB, was significant (all values p<.01), but not significant btw controls and non-spastic BB (p>.05)	N/A	Controls (btw subjects), non-paretic arm (w/in subjects), SWV, ROM, MAS, TS and echogenicity across 3 groups (healthy, non-spastic and spastic BB muscles)
Gao 2016	**Intrarater Reliability:** ICC=.88 **Interrater Reliability:** ICC=.84	**Convergent Validity:** A negative correlation was found btw SR values and UPDRS scores (r=−.78)	**Known Groups Validity:** There was a significant difference in SR btw patients w/ PD (2.65±.36) and controls (3.30±.27). There was also no significant gender or side-to-side difference in SR among controls	N/A	Controls and UPDRS for muscle rigidity
Jakubowski 2017	N/A	**Convergent Validity:** Weak correlations were found btw MG SWV and joint stiffness for non-paretic (r=.384, p=.001) and paretic sides (r=.363, p=.002). Ankle angle, joint torque, and fascicle strain were significantly correlated w/ MG and TA SWV. (SWV vs ankle angle: MG=.705, TA=−.574, p<.001), (SWV vs joint torque GM=.626, TA=−.475, p<.001), (SWV vs fascicle strain: MG=.665, TA=.397, p<.001). FMA score was correlated	**Discriminant Validity:** There were significant increases of 27.7% and 26.9% in SWV for the paretic compared to the non-paretic MG at 90° (p=.033) and 15° PF (p=.001). However, no significant difference was found btw-sides for the TA. Paretic MG and TA SWV at torque-matched position btw max PF and neutral was 18.7% (p=.109) greater and 14.7% (p=.109) less than non-paretic sides. SWV of paretic MG and TA at torque-	N/A	Joint torque, ankle angle, fascicle strain, and estimates of clinical measures (FMA, passive/ active ROM), joint stiffness, muscle architecture (thickness, fascicle length, pennation

		w/ SWV for the paretic TA at 15° PF (r=−.586, p=.035). No correlations were found for the MG at any ankle angle. As muscle thickness increased, SWV decreased for both non-paretic (r=−.565, p=.035) and paretic MG (r=−.648, p=.012) at 90°	matched position btw neutral and max DF were 16.8% (p=.033) greater and 16.3% (p=.109) less than non-paretic sides. Stiffness estimates of paretic TA from torque and angle measures were significantly greater by 23.1% (p=.033) than non-paretic TA. No significant difference for MG		angle) and stiffness on each leg and muscle independently
Kwon 2012	**Intrarater Reliability:** ICC=.812 (repeated measures, CP group DS scores) ICC=.886 (repeated measures, control group DS scores)	**Convergent Validity:** MAS score was positively correlated w/ the DS score (r=.712) and SWV (r=.710) and negatively correlated w/ SR (r=-0.766, p=.001)	**Known Groups Validity:** MG DS score was significantly higher for the CP group than controls (2.5±.5 vs 1.1±.3, p=.01). MG SWV was also significantly higher for the CP group than controls (2.5±.7 vs 1.3±.4). SR was significantly lower for the CP group than that controls (.5±.4 vs 1.3±.8, p=.01)	N/A	Controls, MAS, SR (MG to SOL muscles), and DS score interpreted as: 1 (purple/ green =soft), 2 (green/ yellow= mostly soft), 3 (yellow/ red= mostly hard), 4 (red= hard)
Lacourpaille 2017	N/A	**Convergent Validity:** For controls, evoked max torque increased at T+12mo (+11.2±7.6%, d=2.1, p<.001) but Tm (p=.382) and EMD (p=.999) did not change. In contrast, DMD children showed no change in evoked max torque (p=.222) but both EMD (+12.9±11.3%, d=2.5, p<.001) and Tm (+10.1±21.6%, d=1.27, p=.003) were significantly longer at T+12 than T0.	**Known Groups Validity:** Muscle stiffness increased at T+12mo in DMD children for the TA (+75.1±93.5%, p=.043), MG (+144.8±180.6%, p=.050) and TB (+35.5±32.2%, p=.005). Analysis of SM maps for MG (stretched position) and TA (shortened position) and group (DMD, controls) showed significant time × group interaction for TA (p=.043) and TB (p=.005) and a significant time × length × group interaction for MG SM (p=.050).	**Responsiveness:** TA (+75.1±93.5%, d=1.04, p=.009) and TB SM (+35.5±32.2%, d=.29, p<.001) were significantly higher at T+12 than T0 in DMD children, regardless of the muscle length, w/ no change for controls (all p>.369). Also a significant increase in GM SM (lengthened) at T+12 (p<.001) compared to T0 (+123.6±180.2%, d=1.05; in DMD but not controls (p>.715)	Controls, electromechanical delay (EMD) and electrically induced maximal torque (elbow flexion)
Lacourpaille 2015	N/A	**Convergent Validity:** SM of the MG at both muscle lengths correlated w/ age in patients w/ DMD (lengthened: r=.74, p=.005 shortened: r=.55, p=.050). No significant correlation was found for controls (r<.43 in all cases). SM of GM at both lengths correlated w/ age in patients w/ DMD (long: r=.74, p=.005, short: r=.55, p=.050) No significant correlation was found for healthy participants (r<.43 in all cases).	**Known Groups Validity:** SM was significantly higher in patients w/ DMD compared to controls for all muscles (main effect for group, p<.033 in all cases), except for ADM (p=.394). For lengthened muscle, SM of the TA (p=.005) and BB (p=.017) were significantly higher in patients w/ DMD than controls, but no difference btw groups for short TA (p=.991) and BB (p=.999). A significant group x muscle length interaction was found for TA (p=.026) and BB (p=.048).	**Responsiveness:** Effect of DMD on changes in SM from T0 to T+12mo was moderate to large for all muscles (Cohen's d range=.48-.99) except the ADM (d=.33)	Controls, muscle length and age
Lee 2018	No ICC reported for this study **Preliminary Reliability Assessment:** Repeatability and reliability of SWV was previously tested among 3 controls and 3 subjects w/ stroke twice on separate days. ICC=.932, CV=4.5% (controls) ICC=.821, CV=6.5% (non-paretic side) ICC=.715, CV=9.2% (paretic side)	**Convergent Validity:** As voluntary activation increased, SWV increased non-linearly, w/ an average power fit of R^2=.83±.09 for the non-paretic side, R^2=.61±.24 for the paretic side, and R^2=.24±.15 for controls. Passive SWV on the paretic side was correlated w/ MAS scores for the elbow extensors (p=.044)	**Known Groups Validity:** Mean passive SWV across all subjects were significantly different btw the non-paretic (2.34±.41) and paretic sides (3.30±1.20, p<.001) and btw paretic sides and controls (2.24±.18, p<.001). There was no significant difference in SWV btw-sides or controls in active muscles (10, 25, 50, 75, 100% max voluntary contraction). **Discriminant Validity:** Non-paretic arms showed significantly greater passive and active elbow ROM than paretic arms (non-paretic: active=180±5° to 44±11°, passive=182±4° to 37±6°), (paretic: active= 145±27° to 59±10°, passive=175±8° to 45±7°), (active: p=.006), (passive: p=.001)	N/A	Voluntary muscle activation (active muscle condition only), MAS and ROM
Lee 2016	No ICC reported for this study **Preliminary Reliability Assessment:** Repeatability and reliability of SWV was previously tested among 3 unimpaired subjects twice on separate days. ICC=.932, CV=4.5%	**Convergent Validity:** MG and TA muscle thickness and fascicle length w/ the ankle at 90°, were significantly reduced on the more-affected side. There was no significant correlation btw SWV of the MG or TA and ankle ROM as indicated by max DF angle	**Known-Groups Validity:** There was no significant difference in SWV btw CP children w/ GMFCS Levels I and II. **Discriminant Validity:** MG and TA SWV was significantly higher in the more- than less-affected limb (MG: S1, S3, S5–S8, TA: S3–S8) at 90° in 6/8 subjects. Average difference was 14% (MG) and 20% (TA) greater in the more- than less-effected limbs, (more-affected MG=5.05±.55), (less-affected MG=4.46±.57, p=.024), (more-affected TA=3.86±.79) and (less-affected TA=3.22±.40, p=.03)	N/A	SWV, muscle thickness, fascicle strain, torque, and ankle angle and clinical assessments (ankle ROM and GMFCS Levels I and II)
Lee 2015	No ICC reported for this study **Preliminary Reliability Assessment:** Repeatability and reliability was previously tested among 3 unimpaired subjects twice on separate days. ICC=.932, CV=4.5% (SWV) ICC=.882, CV=4.2% (Echo Intensity) **Software Usage:** Each value was accompanied by a "quality factor" indicating SWV reliability	**Convergent Validity:** Btw-sides differences in SWV and echo intensity were strongly correlated (R^2=.703, p=.002). A significant linear relationship was observed for the btw-sides difference in SWV and stroke duration (R^2=.301, p=.03) as well as a linear relationship btw SWV and elapsed time since stroke onset. Btw-sides difference in SWV was significantly correlated w/ FMA score (R^2=.327, p=.02)	**Discriminant Validity:** Measures of SWV were 69.5 % greater in paretic (3.67±1.28) than non-paretic BB (2.23±.40, p=.001). Echo intensity was 15.5% greater in paretic (109.48±21.90) than non-paretic BB (83.03±28.96, p=.004).	N/A	Btw-sides comparison, FMA score, echo intensity

Mathevon 2018	**Intrarater Reliability:** **Axial (rest)**: (CV= 53.91, SEM=20.02, ICC=.00, paretic MG), (CV=42.15, SEM=9.29, ICC=.73, non-paretic MG), (CV=40.74, SEM=22.25, ICC=.64, paretic TA), (CV=37.00, SEM=24.81, ICC=.51, non-paretic TA) **Sagittal (rest)**: (CV= 9.86, SEM=0.61, ICC=.87, paretic MG), (CV=17.64, SEM=1.70, ICC=.36, non-paretic MG), (CV=15.60, SEM=2.09, ICC=.43, paretic TA), (CV=18.50, SEM=4.35, ICC=.27, non-paretic TA) **Sagittal (max passive DF):** (CV=40.58, SEM=18.21, ICC=.11, paretic MG), (CV=24.05, SEM=8.32, ICC=.30, non-paretic MG) **Other:** CV for MG thickness and pennation angle were acceptable at rest and in DF on both sides. CV for TA thickness were acceptable for both sides, but not pennation angle on either side	N/A	N/A	N/A	Muscle thickness and pennation angle
Park 2012	**Intrarater Reliability** (pre-intervention, repeated measures): ICC=.855 (RTS scores) ICC=.906 (red pixel intensity) ICC=.915 (blue pixel intensity) **Intrarater Reliability** (post-intervention, repeated measures): ICC=.878 (RTS scores) ICC=.912 (red pixel intensity) ICC=.926 (blue pixel intensity)	**Convergent Validity:** RTS score was positively correlated w/ mean red pixel intensity in the MG (r=.756) and negatively correlated w/ mean blue pixel intensity (r=-.605). MAS score was positively correlated w/ RTS score (r=.778). There was no correlation btw RTS and GMFM scores.	N/A	**Responsiveness:** Mean RTS score of the MG before and at 4 weeks after intervention decreased significantly from 3.4 to 1.5 (p=.05).	Color pixel intensity, MAS and GMFM scores
Pichiecchio 2018	N/A, no values from the statistical analyses were reported	**Convergent Validity:** DMD children showed fatty replacement and patchy edema on muscle MRI and increased stiffness on SWE. However, there was no significant correlation btw stiffness values and MRI scores. Muscle MRI T1-w images showed fatty replacement in 3/5 children in the GM, w/ thigh and leg muscles affected in 2/5 children. Hyperintensity of STIR was identified in 4/5 children	**Known Groups Validity:** Stiffness was moderately higher in DMD children compared to controls in the RF, VL, AM and GM muscles	N/A	Controls, MRI and NSAA
Shao 2019	N/A	**Convergent Validity**: positive correlation btw SR and 10MWT (r=.83, p=.009), and TUG scores (r=.87, p=.012), and moderately positive correlation btw elasticity score and 10MWT (r=.58, p=.048), and TUG scores (r=.62, p=.011)	N/A	**Responsiveness:** pre-training, SR were significantly lower for impaired (2.92±.83) than healthy AT (3.50±.64) (p=.009). Post-training, SR of impaired AT increased significantly by 9 wks (3.39±.75) compared to pre-training (2.92±.83) (p=.045)	10MWT, TUG, AT length and thickness
Wu 2016	**Intrarater Reliability:** ICC=.852 (95% CI=.565– .955, longitudinal axis) ICC=.711 (95% CI=.260–.907, transverse axis) **Interrater Reliability** ICC=.768 (95% CI=.373–.927, longitudinal axis) ICC=.552 (95% CI=.002–.846, transverse axis)	**Convergent Validity:** At 90°, paretic side SWV correlated positively w/ post stroke duration (r=.467, p=.008), MAS (r=.662, p=.001)and TS (r=.536, p=.002) and negatively w/ STREAM score (r=-.572, p=.001)	**Known Groups Validity:** SWV was significantly greater on the paretic side than the non-paretic side at both 90° (2.23±.15 vs. 1.88±.08, p=.036) and 0° (3.28±.11 vs. 2.93±.06, p=.002). For controls, SWV did not significantly differ btw-sides at 0° (p=.311) or 90° (p=.436) or btw males and females at 0° (2.94±.03 vs 2.96±.07, p=.831) or 90° (1.92±.06 vs 1.73±.06, p=.063). For the subgroup analysis conducted among 9 patients w/ no change in muscle tone (MAS score=0), SWV was significantly lower on the paretic than non-paretic sides at 90° (1.49±.06 vs 1.76±.16, p=.046), but not at 0° (2.90±.14 vs 2.98±.11, p=.529)	N/A	Controls, Subgroup analysis for differences in SWV btw spastic and non-spastic patients w/ stroke (MAS score=0), Stroke duration, MAS, MTS, and STREAM

Table 2.4 Quality assessment and level of evidence synthesis

UE Method	Outcome Measure(s)	Study	Sample Size (Patients/Controls)	Quality Rating (COSMIN)[187]	Results Rating[194]	Level of Evidence[192]
Reliability						
Quantitative	SWV (m/s)	Bilgici 2018(a)	17/25	Adequate	Interrater (-)	Total N = 60/55, Interrater, Moderate (-); Total N = 63/46, Intrarater, Moderate (+)
	SWV (m/s)	Bilgici 2018(b)	12/0	Adequate	Interrater (-)	
	SM (kPa)	Du 2016	0/9	Doubtful	Interrater (+), Intrarater (+)	
	SM (kPa)	Eby 2016	9/4	Adequate	Intrarater (+)	
	SWV (m/s)	Gao 2018	8/8	Adequate	Intrarater (+)	
	SWV (m/s)	Kwon 2012	15/13	Adequate	Intrarater (+)	
	SM (kPa)	Mathoven 2018	14/0	Adequate	Intrarater (-)	
	SWV (m/s)	Wu 2016	31/21	Adequate	Interrater (-), Intrarater (+)	
Semi-Quantitative	SR	Gao 2016	14/10	Adequate	Interrater (+), Intrarater (+)	Total N = 14/0, Interrater, Unknown (+); Total N = 46/23, Intrarater, Limited (+)
	SR, DS score, color pixel intensity	Kwon 2012	15/13	Adequate	Intrarater (+)	
	RTS score	Park 2012	17/0	Adequate	Intrarater (+)	
Measurement Error						
Quantitative	SM (kPa)	Mathoven 2018	14/0	Adequate	(?)	Total N = 14/0, Unknown (?)
Hypothesis Testing (Convergent Validity)[a1]						
Quantitative	SWV (m/s)	Bilgici 2018(a)	17/25	Doubtful	(+)	Total N = 197/97, Strong (+)
	SWV (m/s)	Bilgici 2018(b)	12/0	Very good	(+)	
	SM (kPa)	Brandenburg 2018	9/0	Adequate	(-)	
	SM (kPa)	Brandenburg 2016	13/13	Adequate	(-)	
	SM (kPa)	Du 2016	46/31	Adequate	(+)	
	SM (kPa)	Eby 2016	9/4	Adequate	(+)	
	SWV (m/s)	Gao 2018	8/8	Adequate	(+)	
	SWV (m/s)	Jakubowski 2017	14/0	Very good	(+)	
	SWV (m/s)	Kwon 2012	15/13	Adequate	(+)	
	SM (kPa)	Lacourpaille 2017	10/9	Very good	(+)	
	SM (kPa)	Lacourpaille 2015	14/3	Adequate	(+)	
	SWV (m/s)	Lee 2018	14/8	Adequate	(+)	
	SWV (m/s)	Lee 2016	8/0	Very good	(+)	
	SWV (m/s)	Lee 2015	16/0	Adequate	(+)	
	SM (kPa)	Pichiecchio 2018	5/5	Doubtful	(-)	
	SWV (m/s)	Wu 2016	31/21	Very good	(+)	
Semi-Quantitative	ELX 2/1 Index, color pixel intensity	Boyaci 2014	16/17	Adequate	(+)	Total N = 86/40, Moderate (+)
	SR	Gao 2016	14/10	Adequate	(+)	
	SR, DS score, color pixel intensity	Kwon 2012	15/13	Adequate	(+)	
	RTS score	Park 2012	17/0	Very good	(+)	
	SR, elasticity score	Shao 2019	24/0	Very good	(+)	
Hypothesis Testing (Discriminative/ Known-Groups Validity)[a2]						
Quantitative	SWV (m/s)	Bilgici 2018(a)	17/25	Very good	(+)	Total N = 198/123, Strong (+)
	SM (kPa)	Brandenburg 2016	13/13	Very good	(+)	
	SM (kPa)	Du 2016	46/31	Very good	(+)	
	SM (kPa)	Eby 2016	9/4	Doubtful	(+)	
	SWV (m/s)	Gao 2018	8/8	Doubtful	(+)	

	SWV (m/s)	Jakubowski 2017	14/0	Very good	(+)	
	SWV (m/s)	Kwon 2012	15/13	Very good	(+)	
	SM (kPa)	Lacourpaille 2017	10/9	Very good	(+)	
	SM (kPa)	Lacourpaille 2015	14/3	Adequate	(+)	
	SWV (m/s)	Lee 2018	14/8	Very good	(+)	
	SWV (m/s)	Lee 2016	8/0	Very good	(+)	
	SWV (m/s)	Lee 2015	16/0	Very good	(+)	
	SM (kPa)	Pichiecchio 2018	5/5	Inadequate	(-)	
	SWV (m/s)	Wu 2016	31/21	Very good	(+)	
Semi-Quantitative	ELX 2/1 Index, color pixel intensity	Boyaci 2014	16/17	Very good	(+)	Total N = 45/40, Limited (+)
	SR	Gao 2016	14/10	Very good	(+)	
	SR, DS score, color pixel intensity	Kwon 2012	15/13	Adequate	(+)	
Responsiveness						
Quantitative	SWV (m/s)	Bilgici 2018(b)	12/0	Very good[d]	(+)	Total N = 36/22, Limited (+)
	SM (kPa)	Brandenburg 2018	9/0	Adequate[d]	(-)	
	SM (kPa)	Lacourpaille 2017	10/9	Very good[c]	(+)	
	SM (kPa)	Lacourpaille 2015	14/13	Very good[c]	(+)	
Semi-Quantitative	ELX 2/1 Index, color pixel intensity	Boyaci 2014	16/17	Very good[b,d]	(+)	Total N = 57/17, Moderate (+)
	RTS score	Park 2012	17/0	Very good[b,d]	(+)	
	SR, elasticity score	Shao 2019	24/0	Very good[b,d]	(+)	

[a1]COSMIN Box 9a - Comparison with other outcome measures (Convergent validity)

[a2]COSMIN Box 9b - Comparison between subgroups (Discriminative or known-groups validity)

[b]COSMIN Box 10b - Responsiveness (Construct approach - comparisons with other outcome measures)

[c]COSMIN Box 10c - Responsiveness (Construct approach - comparisons between subgroups)

[d]COSMIN Box 10d - Responsiveness (Construct approach - pre-to-post intervention)

Results Rating: (+) = Positive, (?) = Indeterminate, (-) = Negative

Supplementary Appendix A. Database Search Syntax

(MEDLINE - Ovid)
Domain Concept: Musculoskeletal Stiffness
1. Musculoskeletal Diseases/ or Musculoskeletal System/
2. ((musc* or tendon* or fascia*) adj3 (stiff* or hard* or rigid* or propert* or mechani* or biomechani*)).ti,ab.
3. (stiff* adj3 passive).ti,ab.
4. muscle stiffness.ti,ab.
5. tendon stiffness.ti,ab.
6. fascia stiffness.ti,ab.
7. 1 or 2 or 3 or 4 or 5 or 6 [muscle stiffness]
Domain Concept: Ultrasound Elastography
8. Ultrasonography/ or Image Interpretation Computer-Assisted/
9. ((ultrasound* or ultrasonograph*) adj2 (elastograph*)).ti,ab.
10. ((imag*) adj2 (displacement or strain)).ti,ab.
11. ((shear wave) adj2 (speed* or modul* or measur* or imag*)).ti,ab.
12. acoustic radiation force impulse imag*.ti,ab.
13. shear wave elasticity imag*.ti,ab.
14. supersonic shear imag*.ti,ab.
15. shearwave dispersion ultrasound vibrometry.ti,ab.
16. harmonic motion imag*.ti,ab.
17. 8 or 9 or 10 or 11 or 12 or 13 or 14 or 15 or 16 [ultrasound elastography]
Domain Concept: Validity & Reliability
18. Diagnosis/ or Diagnosis, Computer-Assisted/ or Reproducibility of Results/
19. ((diagnos* or measur*) adj3 (accura* or reproducib* or reliab* or valid*)).ti,ab.
20. ((inter-operator* or intra-operator*) adj2 (reliab* or reproducib*)).ti,ab.
21. reliability.ti,ab.
22. validity.ti,ab.
23. 18 or 19 or 20 or 21 or 22 [validity & reliability]
Results:
24. 7 and 17 and 23 ([muscle stiffness] and [ultrasound elastography] and [validity & reliability])
25. limit 24 to ([English language] and [human subjects] and [year 1990-current])

(EMBASE - Elsevier)
Domain Concept: Musculoskeletal Stiffness
1. (musculoskeletal AND 'disease'/exp OR musculoskeletal) AND system (76,899)
2. ('musc*' OR 'tendon*' OR 'fascia*') NEAR/3 ('stiff*' OR 'hard*' OR 'rigid*' OR 'propert*' OR 'mechani*' OR 'biomechani*')
3. 'stiff*' NEAR/3 ('passive')
4. 'muscle stiffness':ab,ti
5. 'tendon stiffness':ab,ti
6. 'fascia stiffness':ab,ti
7. 1 OR 2 OR 3 OR 4 OR 5 OR 6 [muscle stiffness]
Domain Concept: Ultrasound Elastography
8. 'ultrasound'/exp OR 'echography'/exp
9. ('ultrasound*' OR 'ultrasonograph*' OR 'echograph*') NEAR/2 ('elastograph*)
10. 'imag*' NEAR/2 ('displacement' OR 'strain')
11. 'shear wave' NEAR/2 ('speed*' OR 'modul*' OR 'measur*' OR 'imag*')
12. 'acoustic radiation force impulse imag*':ab,ti
13. 'shear wave elasticity imag*':ab,ti
14. 'supersonic shear imag*':ab,ti
15. 'shearwave dispersion ultrasound vibrometry':ab,ti
16. 'harmonic motion imag*':ab,ti
17. 8 OR 9 OR 10 OR 11 OR 12 OR 13 OR 14 OR 15 OR 16 [ultrasound elastography]
Domain Concept: Validity & Reliability
18. ('computer'/exp OR computer) AND assisted AND 'diagnosis'/exp OR 'reproducibility'/exp
19. ('diagnos*' OR 'measur*') NEAR/3 ('accura*' OR 'reproducib*' OR 'reliab*' OR 'valid*')
20. ('inter-operator*' OR 'intra-operator*') NEAR/2 ('reliab*' OR 'reproducib*')
21. 'reliability':ab,ti
22. 'validity':ab,ti

23. 18 OR 19 OR 20 OR 21 OR 22 [validity & reliability]
Results:
24. 7 AND 17 AND 23 ([muscle stiffness] and [ultrasound elastography] and [validity & reliability])
25. limit 24 to ([English language] and [human subjects] and [year 1990-current])

(CINAHL - Ebsco)
Domain Concept: Musculoskeletal Stiffness
1. MH Musculoskeletal Diseases+ OR MH Musculoskeletal System+
2. TI ((musc* or tendon* or fascia*) N3 (stiff* or hard* or rigid* or propert* or mechani* or biomechani*)) OR AB ((musc* or tendon* or fascia*) N3 (stiff* or hard* or rigid* or propert* or mechani* or biomechani*))
3. TI (stiff* N3 passive) OR AB (stiff* N3 passive)
4. TI muscle stiffness OR AB muscle stiffness
5. TI tendon stiffness OR AB tendon stiffness
6. TI fascia stiffness OR AB fascia stiffness
7. 1 or 2 or 3 or 4 or 5 or 6 [muscle stiffness]
Domain Concept: Ultrasound Elastography
8. MH Ultrasonography+
9. TI ((ultrasound* or ultrasonograph*) N2 (elastograph*)) OR AB ((ultrasound* or ultrasonograph*) N2 (elastograph*))
10. TI ((imag*) N2 (displacement or strain)) OR AB ((imag*) N2 (displacement or strain))
11. TI ((shear wave) N2 (speed* or modul* or measur* or imag*)) OR AB ((shear wave) N2 (speed* or modul* or measur* or imag*))
12. TI acoustic radiation force impulse imag* OR AB acoustic radiation force impulse imag*
13. TI shear wave elasticity imag* OR AB shear wave elasticity imag*
14. TI supersonic shear imag* OR AB supersonic shear imag*
15. TI shear wave dispersion ultrasound vibrometry OR AB shear wave dispersion ultrasound vibrometry
16. TI harmonic motion imag* OR AB harmonic motion imag*
17. 8 or 9 or 10 or 11 or 12 or 13 or 14 or 15 or 16 [ultrasound elastography]
Domain Concept: Validity & Reliability
18. MH Reproducibility of Results+
19. TI ((diagnos* or measur*) N3 (accura* or reproducib* or reliab* or valid*)) OR AB ((diagnos* or measur*) N3 (accura* or reproducib* or reliab* or valid*))
20. TI ((inter-operator* or intra-operator*) N2 (reliab* or reproducib*)) OR AB ((inter-operator* or intra-operator*) N2 (reliab* or reproducib*))
21. TI reliability OR AB reliability
22. TI validity OR AB validity
23. 18 or 19 or 20 or 21 or 22 [validity & reliability]
Results:
24. 7 and 17 and 23 ([muscle stiffness] and [ultrasound elastography] and [validity & reliability])
25. limit 24 to ([English language] and [human subjects] and [year 1990-current])

(Cochrane Library - Wiley)
Domain Concept: Musculoskeletal Stiffness
1. [mh musculoskeletal diseases]
2. [mh musculoskeletal system]
3. 1 or 2
4. (musc* or tendon* or fascia*) near/3 (stiff* or hard* or rigid* or propert* or mechani* or biomechani*):ti,ab
5. stiff* near/3 (passive):ti,ab
6. muscle stiffness:ti,ab
7. tendon stiffness:ti,ab
8. fascia stiffness:ti,ab
9. 3 or 4 or 5 or 6 or 7 or 8 [muscle stiffness]
Domain Concept: Ultrasound Elastography
10. [mh ultrasonography]
11. (ultrasound* or ultrasonograph*) NEAR/2 (elastograph*):ti,ab
12. imag* near/2 (displacement or strain)
13. shear wave near/2 (speed* or modul* or measur* or imag*)
14. acoustic radiation force impulse imag*:ab,ti
15. shear wave elasticity imag*:ab,ti
16. supersonic shear imag*:ab,ti

17. shearwave dispersion ultrasound vibrometry:ab,ti
18. harmonic motion imag*:ab,ti
19. 10 or 11 or 12 or 13 or 14 or 15 or 16 or 17 or 18 [ultrasound elastography]
Domain Concept: Validity & Reliability
20. [mh reproducibility of results]
21. (diagnos* or measur*) near/3 (accura* or reproducib* or reliab* or valid*):ti,ab
22. (inter-operator* or intra-operator*) near/2 (reliab* or reproducib*):ti,ab
23. reliability:ti,ab
24. validity:ti,ab
25. 20 or 21 or 22 or 23 or 24 [validity & reliability] (30,026)
Results:
26. 9 and 19 and 25 ([muscle stiffness] and [ultrasound elastography] and [validity & reliability])
27. limit 26 to [year 1990-current]

Chapter 3. Convergent validity and test-retest reliability of skeletal muscle measures among individuals with chronic stroke using B-mode, elastography and Doppler ultrasound

Abstract

Background: The large variability in musculoskeletal presentations between individuals with chronic stroke highlights the need for measurement precision when using diagnostic ultrasound to evaluate structural, material and vascular alterations. *Purpose:* To assess the test-retest reliability and convergent validity of various ultrasound measurement parameters involving the bilateral biceps brachii (BB), brachial artery, medial gastrocnemius (MG) and popliteal artery among chronic stroke survivors. *Methods:* A two-way mixed effects intraclass correlation coefficient (ICC) model was used for determining consistency between intersession measures performed by a single operator among 20 participants with chronic stroke (age: 58.1±7.1 years, post-stroke duration: 4.9±3.2 years). Greyscale, elastography, pulse wave and color Doppler ultrasound modes were used during acquisition. Convergent validity was assessed by examining the associations between ultrasound measures and assessments of related constructs. *Results:* ICC estimates ranged from moderate to excellent for mechanical (ICC=0.69–0.93), architectural (ICC=0.84–0.99) and vascular measures (ICC=0.62–0.95). There was a significant association between myotonometry and elastography measures of the paretic (r=0.750–0.843, p≤0.001) and non-paretic MG muscles (r=0.533–0.690, p≤0.015). Paretic BB elastography measures were correlated with scores of spasticity (Composite Spasticity Score: r=0.521–0.639, p≤0.018). *Conclusions:* The results indicate an acceptable level of intersession reliability is achievable for muscle and vascular measures using multimodal ultrasound among individuals with chronic stroke. Moderate correlations with myotonometry and spasticity were also observed, thus demonstrating convergent validity for ultrasound elastography measures.

3.1 Introduction

Unilateral alterations in muscle structure [9], composition [10,11], viscoelastic material characteristics [11] and microvasculature [223] are evident during the chronic stages of stroke recovery. Neurogenically modulated changes in paretic muscle tissue after stroke are mechanistically complex and often inconsistent with alterations typically ensuing disuse, over-stimulation or aging alone [131,147]. Stroke produces segmental sarcomere abnormality

[17], reduced sarcomere serial number [224] diminished motor activation through the degeneration of high threshold motor units [13] and potential disruptions to normal intramuscular collagen formation and organization [154], extracellular matrix remodeling [225] and titin isoform expression [156]. The use of assessment scales and clinical gradation of axiomatic neuromuscular dysfunction (i.e., spasticity severity and mechanical resistance to passive extensibility) are anchoring approaches that are diagnostically insufficient for evaluating variegated morphological phenomena in musculature among individuals with stroke.

Prevalence in the use of diagnostic ultrasound systems with advanced tissue and blood flow imagining modalities is increasing among clinicians in physical medicine and rehabilitation [22,23]. However, the applicability of these systems for identifying tissue pathology after stroke in conjunction with conventional assessments of spasticity, motor impairment and physical function remains relatively understudied. Moreover, our understanding of their psychometric properties, optimal measurement protocols and which auxiliary clinical assessments are ultimately most reflective of ultrasound findings, currently lacks uniformity [11,43] and is often based on compartmentalized findings involving relatively small subject samples (n=9)[44] (n=12)[10].

To date, few studies have assessed the reliability of musculoskeletal ultrasound elastography as a primary outcome in individuals with stroke [43,46]. Although multiple measurement sites were assessed, these were either exclusively upper [43] or lower limb muscles [46] and thus have differing clinical implications. In studies assessing muscle architecture post-stroke, the number which have examined muscles of the lower limb [45,46,126,226-228] are disproportionately greater than those for upper limb muscles [9,224]. Perhaps of even greater paucity, are studies designed to comprehensively examine measurement reliability in both the upper and lower bilateral limbs of individuals with chronic stroke [129], none of which have done so with multiple ultrasound modalities. Furthermore, studies assessing ultrasound measurement reliability in populations with neurological conditions seldom report estimates of measurement error or relative dispersion in standard deviation [229], which are important for interpreting changes in measurement outcomes [201].

In terms of validating measures obtained using ultrasound, a number of viable assessments exist which may be useful in ascertaining related clinical information. Although ultrasound elastography is an objective means of quantifying musculoskeletal stiffness, the limited portability and high cost of scanner systems make ultrasound-based measures difficult to administer in a variety of clinical settings. Several studies have investigated the use of

myotonometers to assess muscle stiffness in patients with stroke [219,230-232]. While similar studies have examined the relationship between stiffness measures obtained using both ultrasound elastography and either hand-held durometers [233] or myotonometers [181,221] in healthy individuals, there is a lack of research validating the concurrent use of these devices among populations with neuromuscular dysfunction (i.e., stroke, Parkinson's Disease, muscular dystrophy). Evidence suggests that alterations in muscle tissue composition may also reflect viscoelastic material changes. Both body mass index (BMI) and echo intensity have been shown to be significantly correlated with elastography measures [10,11,234]. However, more information is needed regarding the use of comprehensive body composition testing in conjunction with ultrasound elastography and echo intensity measures among individuals with chronic stroke.

Muscle architecture, particularly muscle thickness, pennation angle and cross sectional area, are important correlates of peak muscle force production capability [128,235]. While cross sectional area measures in the upper [236] and lower limbs [237] using panoramic or extended field-of-view (EFOV) ultrasound have been shown to be reproducible in healthy individuals, there are no studies examining the use of this technique in conjunction with measures strength after stroke. Although EFOV has also been used to assess muscle fascicle length in the upper limb after stroke [9,224], test-retest reliability and correlation with joint-angle specific measures of peak force in this population are not well-established.

Diminished cardiorespiratory fitness [238] and consequently adverse peripheral vascular adaptations in paretic limbs (i.e., reduced arterial diameter and blood flow volume)[239,240] are also acknowledge sequela resulting from inactivity after stroke. However, little is known about the reliability of vascular ultrasound measures and their correlation with common clinical indices of peripheral vascular disease [241,242].

3.1.1 Objectives

Given the aforementioned limitations and nescience in this area of research, the current study aimed to assess the test-retest reliability of ultrasound measurement parameters involving the muscles of the bilateral upper and lower limbs, as well as the peripheral arteries within relative proximity that supply them, among a group of chronic stroke survivors. The association between these measures and other clinical tests evaluating similar or related physical outcomes was also assessed.

3.2 Methods

3.2.1 Participants

A total of 20 community-dwelling individuals with chronic stroke were recruited through convenience sampling between April and December 2018. Prior to data collection, participants were screened by phone for possible inclusion. Informed consent was obtained on the day of the initial functional assessment. The study was approved by the Human Subjects Ethics Sub-committee of the University (reference number HSEARS20171212003 on January 2, 2018) and the Clinical Research Ethics Committee of the hospital (Joint Chinese University of Hong Kong-New Territories East Cluster Clinical Research Ethics Committee, CREC reference number 2017-711 on April 10, 2018). All procedures were conducted in accordance with the Helsinki Declaration for human experiments. The inclusion criteria were as follows: (1) history of chronic stroke (onset > 6 months), (2) > 18 years of age, (3) community-dwelling, (4) able to achieve 60° of passive elbow flexion and 0° of passive ankle plantar-dorsiflexion, and (5) an Abbreviated Mental Test (AMT) score ≥ 6 [243]. The exclusion criteria were as follows: (1) diagnoses of other neurological conditions, (2) any serious musculoskeletal dysfunctions, disorders or conditions (e.g. amputations, joint replacements, etc.), (3) severe contractures prohibiting passive elbow flexion or ankle plantar-dorsiflexion in the desired testing range, (4) other serious contraindications for study participation.

3.2.2 Procedures

Ultrasound measures were conducted in the university imaging laboratory. Measures for the second session (T2) were obtained between 7-14 days after the first session (T1). All other physical assessments and the collection of demographic information, medical history, and stroke-specific measures of spasticity and motor recovery were performed by a physical therapist one day prior to the first ultrasound assessment (T1). Each ultrasound measurement session was approximately 2 hours in duration, conducted at the same time of day, within the same room kept at an average temperature of 25°C. Measures were performed by a single operator with three years of experience in musculoskeletal, elastography and vascular ultrasound (TM). The assessment sequence for each session (i.e., paretic versus non-paretic side, upper versus lower limb) was randomized to minimize the order effect. Participants were instructed to remain relaxed during ultrasound assessments. Surface electromyography (sEMG) (Bagnoli EMG system, Delsys Inc, Natick, Massachusetts, USA) was used to

confirm passive muscle status. Using LabVIEW software (National Instruments Co., Austin, Texas, USA), a low-pass filter (<10Hz) was applied for wave rectification of signals and a notch filter was applied (50, 100, 150Hz) to maintain signal strength and reduce noise during assessments. After preparing the skin (i.e., shaving, abrading, sterilization and applying transmission gel), a sensor (SX230, Biometrics Ltd, Gwent, UK) was affixed to the surface with die cut medical adhesive tape. During ultrasound assessments, sEMG signals were simultaneously monitored to confirm the absence of muscle contractions. In the event of contracture or spastic responses, images or recordings were discarded and retaken.

An AixPlorer ultrasound unit (AixPlorer, Supersonic Imagine, Aix en-Provence, France), coupled with a linear transducer array (4–15 MHz, SuperLinear, 15-4, Vermon, France) was used to measure muscle stiffness, architecture, echo intensity and arterial blood flow of the upper limb (biceps brachii (BB) muscle, brachial artery) and lower limb (medial gastrocnemius (MG), popliteal artery) on both the paretic and non-paretic sides. Super-compound and high penetration modes were set at a medium frame rate to optimize image resolution and visualization of anatomical boarders. To facilitate transmission and reduce probe compression during measures, a 2mm thick gel couplant layer served as the interface between the skin and probe. Measurements were performed while participants were lying in either a supine position for upper limb assessments or prone position for the lower limb assessments. The ankle joint was maintained in a neutral plantar-dorsiflexion (0º) fixed by an anchored device with restricted eversion, inversion and rotation and the elbow joint was maintained in 60° of flexion with the shoulder abducted in 45° using a custom arm immobilization device. The proximal one third (i.e., 33%) of the total tibial length measured from the base of the distal Achilles tendon, at the level of the inferior boarder of the lateral malleolus up to the midline of the popliteal crease, served as the measurement site for the MG [46]. The site for the BB muscle was the distal third (i.e., 66%) of the total humeral length between the coracoid process of the scapula and the crease of cubital fossa on the radial side [43]. With the exception of intramuscular blood perfusion, all vascular measures were taken at the popliteal artery on the fossa near the popliteal crease or at the brachial artery on the medial aspect of the upper arm at the level of the BB measurement site. The average of 3 trials for each parameter measured was used for the analysis.

3.2.3 Muscle stiffness (elastography)

Muscle stiffness was measured in elastography mode with shear wave velocity (m/s) and shear modulus (kPa) values generated using a Q-box trace function (Supersonic Imagine,

Aix en-Provence, France). Assuming linearity in the material behavior of tissues (i.e., isotropic, linear and homogenous), the shear modulus values are directly related to orthogonal shear wave propagation velocities [244]. The conversion from shear wave velocity to modulus is performed using the following equation (E=3 p V^2_s). E is the Young's modulus, which is set equal to 3 as a constant representing Poisson's ratio for strain. p represents an assumed tissue density of approximately 1 g/cm^3 (1000 kg/m^{-3} for muscle density) under an assumption of elastic linearity and constant muscle mass density. V^2_s represents the propagation velocity of shear waves generated by the transducer [172,203]. The region of interest (ROI) was a rectangular area of 1.89cm^2 and 1.23cm^2 for BB and MG measures, respectively. Each image was captured after a consistent and stable color distribution was observed. As stiffness values vary substantially depending on probe orientation [205,245], each elastogram was captured with the probe aligned parallel to the muscle fiber orientation and after a consistent, stable color distribution was observed.

3.2.4 Echo intensity (B-mode ultrasound)

Echo intensity was measured using B-mode with a standardized gain of 50% in the same orientation and ROI used to capture each elastogram for the BB (1.89 cm^2) and MG muscles (1.23cm^2). To ensure the ultrasound beam was aligned with minimum anisotropy, the probe was angled cranially and caudally within the scan plane until a maximal echo intensity (i.e., brightness) was observed. Gray-scale pixel values were calculated with an impixel function in Matlab (version R2018a, Mathworks, Natick, Massachusetts, USA). Darkest and lightest pixels were represented by upper and lower value limits of 0 and 255, respectively. Moderate to good test-retest reliability has been reported for single transverse image echo intensity measures of the BB ((ICC 2,1 = 0.82) [236] and gastrocnemius muscles ((ICC 2,1 = 0.76) [246] among healthy individuals.

3.2.5 Muscle architecture (B-mode ultrasound)

Measures of muscle thickness (cm), cross-sectional area (cm^2), and fascicle length (cm) for the BB and MG were obtained using B-mode. The muscle fascicle pennation angle (n°) of the MG, defined as the angle of fascicle insertion into the deep aponeurosis [247], was also measured using the hip angle function (Supersonic Imagine, Aix en-Provence, France). As the BB is categorized as a fusiform muscle and has minimal structural pennation [248], pennation angle was only measured for the MG. Measures of pennation angle and muscle thickness were single transverse images. The MG muscle thickness was the vertical distance

between the superficial and deep aponeurosis in the scan plane center, excluding the encapsulating fascia, [249,250] using a distance/ length function (Supersonic Imagine, Aix en-Provence, France). The muscle thickness of the most anterior portion of the elbow flexors (BB and brachialis) was the vertical distance between the adipose tissue to muscle interface and the muscle to humerus bone interface [236]. MG fascicle length measures were obtained using the distance/ length function by selecting an intact muscle fiber with full visual continuity from the superficial aponeurosis and deep aponeurosis at the center of the image pane. The fascicle length can also be estimated using the following equation: fascicle length = muscle thickness - (sin pennation angle)$^{-1}$ [251]. The fascicle length of the BB long head were measured according to the protocol described in studies by Nelson et al [9,252]. A panoramic image capture function (Supersonic Imagine, Aix en-Provence, France) was used while continuously scanning the length of the muscle head from proximal to distal attachments. The probe was maintained in a longitudinal direction with a parallel alignment to the fascicle orientation. Muscle cross sectional area of the BB and MG was also measured using panoramic image capture. For the BB, a foam padded adhesive probe support was placed in line with the muscle circumference (i.e., axis of the upper arm at the distal 66% of the total humeral length) in order to maintain probe perpendicularity, reduce translation and ensure clarity during panoramic image capture. The probe was moved from the medial to lateral aspect while continuously scanning the muscle in alignment with the probe support. Using the polygon/ perimeter trace function (Supersonic Imagine, Aix en-Provence, France), the area within fascial border of the BB muscle was manually selected. Similar to the cross sectional area measurement protocol for the MG described by Rosenburg et al [237], an adhesive probe support was placed in line with the muscle circumference (i.e., axis of the lower leg at the proximal 33% of the total tibial length) and continuous scanning was performed from the medial (tibia) to lateral side (border of the lateral gastrocnemius and peroneal muscle). The area within fascial border of the MG was then traced.

3.2.6 Vascular measures (Doppler ultrasound)

For the brachial artery (at the anatomical site previously specified), peak systolic velocity (cm/s) was measured with pulse wave Doppler ultrasound. The probe was initially placed transversely along the medial aspect of the upper arm. For measuring the peak systolic velocity of the popliteal artery (site previously specified), the probe was placed in a sagittal orientation on the popliteal fossa at the approximate level of the popliteal crease. After visual confirmation of the artery was confirmed with color Doppler in the transverse image plane,

the probe was then rotated sagittally and tilted to visualize the artery longitudinally. Then an electronic calliper was positioned in the center of the artery. The sample volume was standardized at 0.5mm for the brachial artery and 1.0mm for the popliteal artery. Doppler steering and fine angle correction were adjusted to optimize angle-to-flow at an insonation ≤ 60°. The auto-trace function was applied in estimating the full range of positive and negative flow. Three consistent spectral waveform cycle readings were used to calculate measures.

Blood flow volume (mL/min) for the brachial and popliteal arteries were derived from peak systolic velocity estimates. Within the same image, arterial diameter (AD) (cm) was measured by placing the calipers at each end of the superior and inferior borders of the endothelial wall. Using the system tools, the arterial blood flow volume was calculated (Supersonic Imagine, Aix en-Provence, France).

The vascular index was used to estimate intramuscular blood perfusion. The measurement was first proposed as qualitative grading scale for measuring exercise-induced changes in muscle blow flow using power Doppler by Newman et al [(253)] and was later adapted and refined as a semi-quantitative approach for estimating thyroid vascularity by Ying et al [(254)]. The later method, involves calculation of vascular index as a ratio of color pixels to the number of total pixels within a given ROI. The semi-quantitative approach has shown a strong correlation with the previous qualitative grading method when measuring the same construct in plantar fascia ($r = 0.70$, $p = 0.001$) as well as good intrarater (ICC = 0.88) and moderate interrater (ICC = 0.61) reliability [(255)]. The method used in the current study was adapted from the protocol described in detail by Huang et al [(223)]. The probe was placed on the BB or MG muscle belly in a transverse orientation (site previously specified for B-mode and elastography measures). Using the color flow imaging mode (CFI) to map Doppler signal strength from flow movement rather than frequency shifts, the rectangular ROI was placed within the fascial borders of the muscle and standardized according to a frame rate of 11 Hz, a 50% gray-scale gain, and a color gain range of 70 - 85%. Standardization was based upon a preliminary trial cohort of 10 subjects with chronic stroke that did not participate in the reliability study. For each participant, color gain was increased to 85% and gradually reduced until color noise was either not discernible or reached the lower gain limit (70%). Color gain was then kept the same for the opposing limb. Image and data processing were performed using custom scripts in Matlab (version R2018a, Mathworks, Natick, Massachusetts, USA). Doppler recordings were exported in .avi format and sequenced as individual frames in .png format to reduce the influence of file compression on image quality. Frames captured at the upper range of the color flow spectrum (i.e., 2.0 cm/s) were then

selected and the ROI manually trimmed. The ratio of color to total pixels within the ROI was calculated [254]. The highest vascular index from each of the three recorded trials was identified and used to calculate the mean for further analysis.

3.2.7 Dyanmic muscle stiffness (myotonometry)

Dynamic stiffness (N/m) was also measured using a MyotonPRO device (Myoton AS, Tallinn, Estonia). Durometry and myotonometry are superficial administered mechanical deformation techniques which provide an additional quantification of muscle tissue stiffness. Measures were performed by placing the probe applicator at center point of the ultrasound probe site. The device has demonstrated excellent within-session reliability for testing the BB muscle ((ICC 3,2) = 0.97 – 0.99) in healthy subjects [256] and excellent intra-rater reliability for the MG muscle in patients with spinal cord injury (ICC 3,1) = 0.88 – 0.97) [257].

3.2.8 Muscle strength (dynamometry)

Isometric peak torque (N/m) of the ankle plantar-flexors and elbow flexors was measured bilaterally using a dynamometer system (Humac Norm Systems, Stoughton, Massachusetts, USA) and defined as the maximal sustained torque for 250 milliseconds [258]. Three trials were performed for each limb with a 1-minute rest interval between each. The isometric peak torque was tested in 0° (neutral position) of ankle plantar-dorsiflexion and 60° of elbow flexion with 45° of shoulder abduction. Isometric strength testing conditions have previously demonstrated a relatively smaller degree of measurement error in comparison to isokinetic strength testing [259]. Elbow flexion torque has been shown to be greatest in 56° for healthy individuals [260] and 60° for paretic arms in individuals with stroke [261]. The ankle angle was selected based on anatomical models accounting for force-length properties at joint positions predicted to be optimal for isometric force production, and clinic relevance when performing manual muscle testing [262]. Elbow and ankle angles also corresponded to the joint fixation positions assumed during ultrasound assessments.

3.2.10 Ankle-brachial index

The ankle-brachial index (ABI) is a ratio of the ankle systolic pressure over the brachial systolic pressure and is often used as an indicator of peripheral vascular disease, atherosclerosis, and functional impairment [242]. ABI was assessed using an IntelliSense Omron HEM 907XL oscillometric blood pressure monitor (Omron Healthcare, Kyoto, Japan). Following a 10-minute rest period, during which patients assumed a supine position,

blood pressure measurements for the brachial artery at the upper arm and the dorsalis pedis and posterior tibial arteries at the ankle were taken on the paretic and non-paretic sides. For ankle measures, the cuff was placed superior to the medial and lateral malleoli for ankle measures and at the mid-portion of the upper arm for arm measures. Blood pressures were measured twice on each side. A third confirmatory measure was taken in the event that systolic measures differed by more than 10 mmHg [(263)]. If the two initial measures were consistent (≤ 10 mmHg), the higher of the two systolic arm and ankle measurements were used to calculate the ABI for each leg (i.e., systolic pressure of the ankle divided by the systolic pressure of the arm) [(264)].

3.2.13 Stroke-related impairments

Demographic information was collected during the initial session. Stroke characteristics were classified by type (ischemic vs hemorrhagic) and location according to the Oxfordshire Community Stroke Project Classification (OCSP): (1) total anterior circulation syndrome, (2) partial anterior circulation syndrome, (3) lacunar syndrome, or (4) posterior circulation syndrome. [(265)]. The Fugl-Meyer motor assessment (FMA) was used to determine the degree of motor impairment in the paretic upper and lower extremities. Motor scores ranged from 0-66 and 0-34 for the upper and lower extremities, respectively. Higher scores were indicative of greater motor impairment [(266)]. Spasticity of the paretic elbow flexors and ankle plantar-flexors was measured using the Composite Spasticity Scale (CSS) [(267)]. The CSS is scored on an ordinal scale from 0-16, with higher scores indicting greater spasticity. The scale is comprised of three components (1) biceps/ Achilles tendon jerk (score range of 0-4, 5-point scale), (2) resistance to full range of passive joint displacement for elbow flexion/ ankle dorsiflexion (score range of 0-8, 5-point scale doubly weighted), and (3) the duration and amount of wrist/ ankle clonus elicited (score range of 1-4, 4-point scale) [(268)]. The Motor Activity Log (MAL) was used to determine perceived frequency and quality of paretic arm usage during 30 functional activities of daily living [(4)]. Mean scores from the Amount of Use (AOU) and Quality of Movement (QOM) scales were used for analysis. Lower scores indicate greater perceived impairment.

3.2.14 Statistical analysis

All analyses were conducted using SPSS (version 23.0, SPSS Inc., Chicago, Illinois, USA). A two-way mixed effects intraclass correlation coefficient (ICC) model was used for determining consistency between intersession measures performed by a single rater among a

random sample of 20 subjects. Ratings of reliability were based on ICC estimates with a 95% confident interval, standard error in measurement (SEM) and coefficient of variation (%CV). ICC values of less than 0.5, between 0.5 and 0.75, between 0.75 and 0.9, and greater than 0.90 indicate poor, moderate, good, and excellent reliability, respectively [269]. A value of 10% was used as the upper limit of acceptability for %CV [229]. Normality and homogeneity of variance were tested with Shapiro-Wilks and Levene's tests, respectively. Paired t-tests were used to compare mean differences between limbs and Pearson's correlations were used to assess the relationship between ultrasound measures and other assessments for evaluating similar or related measurement constructs (i.e., dynamic stiffness using myotonometry, spasticity with the CSS and systemic vascular function with the ABI) at a significance level of $p \leq 0.05$. In the event that either the assumptions of normality or variance were not met, a non-parametric equivalent was used (i.e. Wilcoxon Signed-Rank, Spearman's Rho).

3.3 Results

3.3.1 Participant characteristics

A total of 20 participants with chronic stroke completed all assessments. A summary containing demographic, medical and stroke-specific characteristics is provided in Table 3.1. The number of participants presenting with right or left side hemiparesis was equivalent. Just over half had a hemorrhagic stroke (n = 11). Of the participants with an ischemic stroke (n = 9), the majority were classified as partial anterior circulation syndrome (PACS) (n = 8). Average FMA upper (38.4 ± 18) and lower extremity (26.2 ± 5.5) scores suggest moderate motor impairment [8] with mild spasticity [270] based on CSS upper (9.3 ± 2.7) and lower limb (7.7 ± 2.3) scores. Average ratings of perceived paretic arm usage frequency was minimal (MAL - AOU = 1.3 ± 1.4) and movement quality was low (MAL - QOM = 1.4 ± 1.5).

3.3.2 Muscle stiffness and echo intensity

A summary of within-subject comparisons and reliability analysis results for muscle stiffness and echo intensity is shown in Table 3.2. For the lower limb at T1 and T2, significant between-sides differences were observed for the shear modulus, shear wave velocity and echo intensity of the MG muscles. For the upper limb at T1 and T2, between-sides differences were also significant for dynamic stiffness and echo intensity of the BB muscles. The SEM was consistently below the standard deviation for all measures. The ICCs ranged from moderate to excellent (ICC = 0.69 – 0.93) with acceptable %CV for all shear

wave velocity and echo intensity measures. Several %CV were > 10% suggesting temporal reliability for shear modulus and dynamic stiffness in paretic and non-paretic limbs was suboptimal.

3.3.3 Muscle architecture

The results of within-subject comparisons and reliability for muscle architecture are provided in Table 3.3. Significant between-sides differences were found for MG and BB muscle size (i.e., muscle thickness, cross sectional area) at both T1 and T2. Bilateral differences in fascicle length and pennation angle of the MG muscle were seen only at T2 and T1, respectively. Between-sides difference in fascicle length of the BB muscle was only observed at T1. SEM was consistently lower than standard deviations with acceptable %CV for all measures. ICC values were good to excellent (ICC = 0.84 – 0.99).

3.3.4 Vascular measures

Table 3.4 shows the within-subject comparisons and reliability results for vascular measures. Significant between-sides differences at both T1 and T2 were observed for the arterial diameter and vascular index of the brachial and popliteal arteries. Significant differences in blood flow volume of the brachial artery were only at found at T2. The ICC estimates were moderate to excellent (ICC = 0.62 – 0.95). The SEM was consistently lower than standard deviations with acceptable %CV across all peak systolic velocity and arterial diameter measures. For all blood flow volume and most vascular index measures, %CV surpassed the acceptable upper limit. The %CV for the non-paretic muscle vascular index was comparably lower than that of the paretic muscle. The opposite was observed for blood flow volume, indicating poorer temporal reliability for the arterial blood flow volume on the non-paretic side.

3.3.5 Correlations

Mostly consistent correlations found at both time points (i.e., T1 and T2) between ultrasound measures and other assessment variables are presented in this section. A summary of all correlations with significant results is provided in Tables 3.5-3.7. There was a significant association between elastography measures and dynamic stiffness in the paretic ($r = 0.750 – 0.843$, $p \leq 0.001$) and non-paretic GM muscles ($r = 0.533 – 0.690$, $p \leq 0.015$) at

both T1 and T2 (Table 3.6). The dynamic stiffness was also correlated with shear wave velocity of paretic BB muscles at T2 only ($r = 0.452$, $p = 0.045$) (Table 3.5).

Additionally, scores of upper limb spasticity (CSS – Upper Limb Total: $r = 0.625 – 0.639$, $p \leq 0.003$; CSS – Resistance to Displacement: $r = 0.521 – 0.603$, $p \leq 0.018$) were correlated with elastography measures of paretic BB muscles at T1 and T2 (Table 3.5). The isometric peak torque of the elbow flexors was significantly correlated with the muscle thickness ($r = 0.550 – 0.756$, $p \leq 0.024$) and cross sectional area ($r = 0.498 – 0.867$, $p \leq 0.025$) of the paretic and non-paretic BB at T1 and T2. Correlations between elbow flexor peak torque and fascicle length ($r = 0.453 – 0.651$, $p \leq 0.045$) were only observed for the non-paretic BB at both T1 and T2 (Table 3.5). Ankle plantarflexor isometric peak torque was also correlated with the muscle thickness of the paretic and non-paretic MG ($r = 0.481 – 0.579$, $p \leq 0.032$) and fascicle length of the paretic MG ($r = 0.458 – 0.570$, $p \leq 0.042$) at both time points (Table 3.6).

Correlations between ultrasound measures and the ABI (of paretic and non-paretic sides) were largely inconsistent across sites and sessions. Of the vascular measures taken, ABI was only found to be correlated with the vascular index of paretic MG muscles at T1 ($r = 0.690$, $p = 0.001$) and non-paretic brachial artery blood flow volume at T1 ($r = 0.539$, $p = 0.014$) (Table 3.7).

3.4 Discussion

3.4.1 Test-retest reliability

The results of this study indicate acceptable test-retest reliability for most measures in the bilateral upper and lower limbs assessed. ICC estimates ranged from moderate to excellent for muscle stiffness and echo intensity (ICC = 0.69 - 0.93), muscle architecture (ICC = 0.84 - 0.99) and vascular measures (ICC = 0.62 - 0.95). The shear modulus (%CV = 6.30 - 15.11), dynamic stiffness (%CV = 9.68 - 14.69), vascular index (%CV = 9.73 - 20.25) and blood flow volume (%CV = 13.33 - 22.57) parameters had the largest estimates of relative variance across all measures. The ICC estimate for shear wave velocity of the paretic BB in this study (ICC = 0.80, 95% CI: 0.50 - 0.92) was comparable to the estimate for intrarater reliability reported by Wu et al for the same longitudinal (i.e., sagittal) probe orientation (ICC = 0.85, 95% CI: 0.57 - 0.96) [43]. For the shear modulus of the paretic MG, our estimate (ICC = 0.81, 95%CI: 0.52 - 0.92) was also comparable to a previously reported estimate by Mathevon et al for measures at rest (ICC = 0.87) [46]. Measures of muscle

thickness have been shown to be a reliable method of assessing muscle size across several sites after stroke [46,129]. The reliability of paretic MG pennation angle measures in the current study (ICC = 0.88, 95% CI: 0.70 – 0.95) was comparable to a previously reported estimate by Mathevon et al (ICC = 0.94) [46].

Reliability estimates obtained for cross sectional area and fascicle length measures using the panoramic image capture modality and vascular measures obtained using pulse wave Doppler (i.e., peak systolic velocity, blood flow volume, arterial diameter) were presumably novel features of the current study. Panoramic cross sectional area measures have demonstrated good to excellent reliability for BB [46] and MG [237] muscles among healthy subjects but the reliability of this measure in individuals with stroke has not been assessed previously. Additionally, panoramic or EFOV techniques have been used for obtaining bilateral fascicle length measures of the BB after stroke [9]. However, measurement reliability was not reported. The ICC estimates obtained for vascular index measures of the upper and lower limb muscles in the current study (ICC = 0.73 – 0.88) were lower than the pilot trial results of intersession reliability for the paretic MG reported by Huang et al (ICC = 0.93, 95% CI: 0.89 - 0.96) [223] and comparable to the intrarater reliability for plantar fascia measures reported by Chen et al (ICC = 0.88) [255].

3.4.2 Convergent validity

Although consistent correlations were only observed between CSS (i.e., upper limb total score) and elastography measures of the paretic upper limb in the current study, pennation angle and muscle thickness have also been shown to be positively correlated and fascicle length negatively correlated with other measures of spasticity (i.e., Modified Ashworth Scale) post-stroke [20]. Of the spasticity subscales comprising the CSS, resistance to displacement (i.e., passive extensibility) was the only consistent correlate of elastography measures. This may indicate a relationship between mechanical resistance and viscoelastic material alterations in the paretic upper limb.

Given that no gold standard method exists for assessing muscle stiffness, dynamic stiffness using myotonometry offers a similar measurement construct related to elastography which is also non-invasive and clinically feasible. Our findings suggest a moderate correlation between these measures in the bilateral lower limb but not the upper limb. Previous studies examining the association between elastography measures and dynamic stiffness in several muscle regions and different contractile intensities ($r = 0.23 - 0.71$, $p < 0.05$) by Kelly et al [181] and the gastrocnemius muscle and Achilles tendon ($r = 0.46 - 0.54$, p

< 0.05) by Feng et al [221] have also demonstrated moderate to strong correlations. Other commercial durometer devices have shown considerably weaker correlation with elastography measures (r=0.085-0.208, p=0.115-0.694) [233]. There was no significant correlation observed between myotonometry and echo intensity of the upper and lower limb muscles perhaps suggesting that dynamic stiffness measures may reflect a closer relationship with paretic tissue compliance and extensibility rather than compositional change.

As expected [128], volumetric architectural measures (i.e., muscle thickness, cross sectional area) were consistent correlates of isometric strength. However, other architectural parameters such as fascicle length and pennation angle, were not as consistently correlated across sites and time points. Shorter fascicles in paretic BB [9] and MG muscles [271] have been shown to be associated with higher levels of motor impairment which may impact muscle force-generating capacity after stroke. Studies reporting comparatively lower resting pennation angle measures of paretic MG muscles suggest this structural parameter may also influence impairment [46,126]. However, the degree to which pennation angle contributes to strength or functional impairment after stroke is not conclusive [45,228,271] and may be secondary to the role of shorter fascicle length and reductions in muscle volume. Our findings appear to reflect this to some extent as well.

Although there were significant intra-limb differences observed for arterial diameter and vascular index ($p \leq 0.05$), correlations between vascular measures and ABI were largely inconsistent across measurement sites and time points. However, this may have been due to the average ABI of this group of subjects (paretic side = 1.11 ± 0.09, non-paretic side = 1.17 ± 0.06), which was within a normal range (0.90 to ≤ 1.40) and not indicative of peripheral artery disease or systemic dysfunction (< 0.40) [241]. As overall cardiovascular fitness decreases after stroke, comparatively lower metabolic demand of paretic muscles results in unilateral vascular remodeling and reductions in flow volume [240,272]. Consequently, the results of the current study suggest that reduced intramuscular blood perfusion in paretic limbs may be influenced by both localized and systemic changes in metabolic demand.

3.4.3 Limitations

While the sample recruited for this study (n=20) was larger than in previous studies examining measurement reliability as a primary outcome by Mathevon et al (n=14) [46] and Wu et al (n=12) [43], it was still relatively small compared to recommended sample sizes for ICC estimates (n=30) [269], as well as SEM and %CV (n=50) [229]. The number of measurement sessions was also limited considering that multiple follow-ups are common

when monitoring temporal muscle tissue changes. Measuring the response to intervention in populations with stroke or other neurological conditions may warrant multiple follow-up sessions [34,164]. Interrater reliability was also not assessed. Although follow-up sessions may be conducted by the same clinician or operator, variance in measures among multiple operators is justification for further examination in future studies. Finally, with regards to measurement acquisition procedures, there is tremendous variability throughout the available literature [203]. The authors attempted to incorporate procedural aspects that would enhance reliability (i.e., standardized probe orientation, gel layer, ROI size and depth).

3.5 Conclusion

The results indicate an acceptable level of intersession reliability is achievable for muscle and vascular measures in paretic and non-paretic limbs using several diagnostic ultrasound modalities among individuals with chronic stroke. Ultrasound measures also demonstrated moderate correlation with similar measurement constructs using clinically viable assessments of tissue stiffness, composition, and vascular function as possible comparators.

Table 3.1 Participant Characteristics

		N=20
Demographic Information & Functional Impairment	Sex (men/women), n	12/8
	Age, years	58.1 ± 7.1
	Hand dominance (Left/ Right/ Equivalent), n	1/19/0
	Leg dominance (Left/ Right/ Equivalent), n	3/16/1
	BMI (kg/m^2)	23.2 ± 2.3
	ABI (Paretic/ Non-Paretic)	1.11 ± 0.09/1.17 ± 0.06*
	IPT – Elbow (Paretic/ Non-Paretic)	18.34 ± 7.12/ 29.51 ± 10.58*
	IPT – Ankle (Paretic/ Non-Paretic)	40.26 ± 18.26/ 67.60 ± 27.88*
	AMT (out of 10)	9.2 ± 1.3
	FAC (out of 6)	5.8 ± 0.5
	PASE	98.6 ± 76.2
	10MWT	0.89 ± 0.33
Comorbidity	Total number of comorbidities per person	1.2 ± 1.5
	Hypertension, n	8
	Hyperlipidemia, n	4
	Cardiac arrhythmia, n	1
	Diabetes mellitus, n	2
	Ischemic heart disease, n	1
Medications	Total number of medications per person	3.7 ± 2.2
	Antihypertensive agents, n	12
	Hypolipidemic agents, n	11
	Hypoglycemic agents, n	2
	Anticoagulants, n	4
Stroke Characteristics	Paretic Side (Left/ Right), n	10/10
	Stroke Type (Ischemic/ Hemorrhagic), n	9/11
	Stroke Duration, years	4.8 ± 3.2
	Stroke Location (TACS/ PACS/ LS/ PCS/ Hemorrhagic)	1/ 8/ 0/ 0/ 11
	CSS - Upper Limb (1-16)	9.3 ± 2.7
	CSS - Lower Limb (1-16)	7.7 ± 2.3
	FMA - Upper Extremity (0-66)	38.4 ± 18.0
	FMA - Lower Extremity (0-34)	26.2 ± 5.5
	MAL - Amount of Use	1.29 ± 1.38
	MAL – Quality of Movement	1.35 ± 1.45
Body Composition	Body Fat (%)	26.44 ± 7.95
	Basil Metabolic Rate (kcal)	1236.81 ± 172.37
	Fat Mass (kg)	15.58 ± 6.10
	Fat Free Mass (kg)	44.34 ± 6.99
	Total Body Water (kg)	31.14 ± 4.54
	Visceral Fat Rating	9.75 ± 3.02
	Impedance (Ω)	650.40 ± 68.33

*Significant at $p \leqslant 0.05$ (Paired t-test)

Abbreviations: Ω = unit of resistance to electrical current, BMI = Body Mass Index, AMT = Abbreviated Mental Test, ABI = Ankle-Brachial Index, IPT = Isometric Peak Torque, TACS = Total Anterior Circulation Syndrome, PACS = Partial Anterior Circulation Syndrome, LS = Lacunar Syndrome, PCS = Posterior Circulation Syndrome, CSS = Composite Spasticity Scale, FMA = Fugl-Meyer Assessment, MAL = Motor Activity Log

Table 3.2 Muscle stiffness and echo intensity

Measure	Side	Site	T1 Mean	T1 SD	T2 Mean	T2 SD	ICC (95% CI)	%CV	SEM
SM (kPa)	NP	BB	29.17	16.90	25.11	15.72	0.81 (0.53, 0.93)	14.25	4.99
	P	BB	32.72	15.15	30.88	16.75	0.78 (0.45, 0.91)	15.11	5.28
	NP	MG	46.06	16.18	53.71	13.75	0.71 (0.26, 0.89)	10.19	5.73
	P	MG	75.93‡	59.56	84.12‡	78.85	0.81 (0.52, 0.92)	6.30†	16.24
SWV (m/s)	NP	BB	2.91	0.84	2.73	0.72	0.80 (0.51, 0.92)	7.02†	0.25
	P	BB	3.15	0.76	3.05	0.84	0.80 (0.50, 0.92)	7.54†	0.25
	NP	MG	3.79	0.76	4.13	0.54	0.69 (0.21, 0.88)	5.74†	0.26
	P	MG	4.75‡	1.48	4.76‡	1.36	0.93 (0.84, 0.97)	3.27†	0.20
DS (N/m)	NP	BB	202.15	19.06	206.75	20.54	0.77 (0.42, 0.91)	9.68†	6.69
	P	BB	222.15*	29.78	231.50*	35.22	0.84 (0.59, 0.94)	14.31	9.34
	NP	MG	309.80	36.64	322.35	46.85	0.82 (0.55, 0.93)	13.18	12.58
	P	MG	331.60	56.99	324.05	39.54	0.74 (0.35, 0.90)	14.69	17.65
EI	NP	BB	104.63	10.81	104.19	11.45	0.84 (0.59, 0.94)	5.89†	3.16
	P	BB	112.35*	10.36	109.75‡	10.68	0.84 (0.60, 0.94)	5.07†	2.98
	NP	MG	77.03	22.50	78.09	22.37	0.88 (0.70, 0.95)	8.00†	5.52
	P	MG	95.24*	22.60	95.24*	17.43	0.89 (0.73, 0.96)	4.23†	4.71

*Significant at $p \leq 0.05$ (Paired t-test)
‡Significant at $p \leq 0.05$ (Wilcoxon test)
†Coefficient of variance (%CV) ≤ 10%
SM = Shear Modulus, m/s = meters/ second, SWV = Shear Wave Velocity, kPa = kilopascals, NP = Non-Paretic, P = Paretic, Biceps Brachii = BB, Medial Gastrocnemius = MG, DS = Dynamic Stiffness, N/m = Newton/ meters, EI = Echo Intensity

Table 3.3 Muscle architecture

Measure	Side	Site	T1 Mean	T1 SD	T2 Mean	T2 SD	ICC (95% CI)	%CV	SEM
MT (cm)	NP	BB	2.72*	0.39	2.72*	0.33	0.98 (0.96, 0.99)	1.69†	0.03
	P	BB	2.54	0.43	2.54	0.44	0.99 (0.97, 1.00)	1.40†	0.03
	NP	MG	1.74*	0.25	1.73*	0.25	0.99 (0.97, 1.00)	1.53†	0.02
	P	MG	1.50	0.23	1.50	0.21	0.99 (0.98, 1.00)	1.67†	0.02
CSA (cm^2)	NP	BB	9.45*	2.29	9.70*	2.41	0.98 (0.94, 0.99)	2.61†	0.25
	P	BB	7.63	2.04	7.75	2.05	0.95 (0.88, 0.98)	3.04†	0.31
	NP	MG	9.86*	2.50	9.72*	2.55	0.98 (0.96, 0.99)	1.99†	0.23
	P	MG	7.98	2.03	8.05	1.96	0.98 (0.94, 0.99)	2.37†	0.22
FL (cm)	NP	BB	11.48*	1.28	11.82	1.39	0.92 (0.78, 0.97)	2.47†	0.26
	P	BB	10.37	1.64	11.28	1.84	0.90 (0.09, 0.97)	2.64†	0.40
	NP	MG	4.85	0.47	5.00*	0.45	0.84 (0.59, 0.94)	3.05†	0.13
	P	MG	4.63	0.75	4.71	0.57	0.89 (0.73, 0.96)	3.92†	0.15
PA	NP	MG	20.18*	2.32	18.97	2.44	0.92 (0.79, 0.97)	3.62†	0.49
	P	MG	18.68	2.24	18.08	2.34	0.88 (0.70, 0.95)	4.60†	0.56

*Significant at $p \leq 0.05$ (Paired t-test)
‡Significant at $p \leq 0.05$ (Wilcoxon test)
†Coefficient of variance (%CV) ≤ 10%
MT = Muscle Thickness, CSA = Cross Sectional Area, cm = centimeters, FL = Fascicle Length, PA = Pennation Angle

Table 3.4 Vascular measures

Measure	Side	Site	T1 Mean	T1 SD	T2 Mean	T2 SD	ICC (95% CI)	%CV	SEM
PSV (cm/s)	NP	BB	73.72	14.84	74.62	18.42	0.83 (0.56, 0.93)	3.24†	4.95
	P	BB	74.37	16.33	73.99	14.15	0.76 (0.40, 0.91)	4.18†	5.27
	NP	MG	45.57	16.55	43.11	11.07	0.87 (0.68, 0.95)	3.81†	3.55
	P	MG	45.51	15.63	46.29	11.94	0.85 (0.62, 0.94)	5.03†	3.82
Vflow (mL/min)	NP	BB	41.90	20.32	43.65*	21.47	0.77 (0.41, 0.91)	15.41	7.17
	P	BB	37.25	21.63	32.10	15.36	0.67 (0.17, 0.87)	13.33	7.60
	NP	MG	34.57	25.34	32.12	21.55	0.92 (0.80, 0.97)	22.57	4.68
	P	MG	29.67	15.49	33.03	13.46	0.62 (0.06, 0.85)	20.15	6.29
AD (cm)	NP	BB	0.36*	0.06	0.36*	0.06	0.92 (0.79, 0.97)	2.94†	0.01
	P	BB	0.32	0.05	0.31	0.05	0.89 (0.72, 0.96)	3.51†	0.01
	NP	MG	0.56*	0.11	0.54‡	0.12	0.90 (0.75, 0.96)	3.32†	0.03
	P	MG	0.52	0.11	0.52	0.10	0.95 (0.87, 0.98)	3.79†	0.02
VI	NP	BB	0.71*	0.37	0.70‡	0.29	0.73 (0.31, 0.89)	12.67	0.12
	P	BB	0.33	0.16	0.35	0.21	0.74 (0.35, 0.90)	20.25	0.07
	NP	MG	1.40‡	0.59	1.46‡	0.48	0.88 (0.70, 0.95)	9.73†	0.13
	P	MG	0.63	0.43	0.73	0.41	0.85 (0.63, 0.94)	18.10	0.11

*Significant at $p \leq 0.05$ (Paired t-test)
‡Significant at $p \leq 0.05$ (Wilcoxon test)
†Coefficient of variance (%CV) ≤ 10%
PSV = Peak Systolic Velocity, cm/s = centimeters/ second, Vflow = Blood Flow Volume, mL/min = milliliters/ minute, AD = Arterial Diameter, VI = Vascular Index

Table 3.5 Correlations for upper limb muscle measures

			Paretic Side			Non-Paretic Side		
Variable	**Session**	**Site**	**Measure**	**r**	**p**	**Measure**	**r**	**p**
Myotonometry (Upper Limb)								
	T2	BB	SWV	0.452	0.045*			
Spasticity (Upper Limb)								
CSS - UL - RTD								
	T1	BB	SM	0.521	0.018*	-	-	-
			SWV	0.540	0.014*	-	-	-
	T2	BB	SM	0.603	0.005**	-	-	-
			SWV	0.579	0.007**	-	-	-
CSS - UL - Total								
	T1	BB	SM	0.639	0.002**	-	-	-
			SWV	0.633	0.003**	-	-	-
	T2	BB	SM	0.637	0.003**	-	-	-
			SWV	0.625	0.003**	-	-	-
IPT (Upper Limb)								
	T1	BB	MT	0.550	0.012*	MT	0.736	0.000**
			CSA	0.498	0.025*	CSA	0.867	0.000**
						FL	0.651	0.002**
	T2	BB	MT	0.618	0.024*	MT	0.756	0.000**
			CSA	0.622	0.003**	CSA	0.815	0.000**
						FL	0.453	0.045*

* Correlation significant at $p < 0.05$
** Correlation significant at $p < 0.01$
Biceps Brachii = BB, Medial Gastrocnemius = MG, T1 = Session 1, T2 = Session 2
SM = Shear Modulus, SWV = Shear Wave Velocity, MT = Muscle Thickness, FL = Fascicle Length, CSA = Cross Sectional Area, IPT = Isometric Peak Torque, CSS - UL - RTD = Composite Spasticity Scale - Upper Limb - Resistance to Displacement, CSS - UL - Total = Composite Spasticity Scale - Upper Limb - Total

Table 3.6 Correlations for lower limb muscle measures

Variable	Session	Site	Paretic Side Measure	r	p	Non-Paretic Side Measure	r	p
Myotonometry (Lower Limb)								
	T1	MG	SM	0.762	0.000**	SM	0.574	0.008**
			SWV	0.798	0.000**	SWV	0.533	0.015*
	T2	MG	SM	0.843	0.000**	SM	0.690	0.001**
			SWV	0.750	0.000**	SWV	0.688	0.001**
IPT (Lower Limb)								
	T1	MG	MT	0.496	0.026*	MT	0.481	0.032*
			CSA	0.503	0.024*	CSA	0.458	0.042*
			FL	0.570	0.009**			
	T2	MG	MT	0.556	0.011*	MT	0.579	0.007**
			FL	0.458	0.042*	CSA	0.532	0.016*

* Correlation significant at $p < 0.05$
** Correlation significant at $p < 0.01$
Biceps Brachii = BB, Medial Gastrocnemius = MG, T1 = Session 1, T2 = Session 2
SM = Shear Modulus, SWV = Shear Wave Velocity, MT = Muscle Thickness, FL = Fascicle Length, CSA = Cross Sectional Area, IPT = Isometric Peak Torque

Table 3.7 Correlations for vascular measures

			Paretic Side			Non-Paretic Side		
Variable	**Session**	**Site**	**Measure**	**r**	**p**	**Measure**	**r**	**p**
ABI (Upper Limb)	T1	BB				Vflow	0.539	0.014*
ABI (Lower Limb)	T1	MG	VI	0.690	0.001**			

* Correlation significant at $p < 0.05$
** Correlation significant at $p < 0.01$
Biceps Brachii = BB, Medial Gastrocnemius = MG, T1 = Session 1, T2 = Session 2
ABI = Ankle – Brachial Index, Vflow = Blood Flow Velocity, VI = Vascular Index

Chapter 4. Determinants of estimated failure load in the distal radius after stroke: an HR-pQCT study

Abstract

Bone health is often compromised after stroke and the distal radius is a common site of fragility fractures. The macro- and mircoproperties of bone tissue after stroke and their clinical correlates are understudied. The objectives of the study were to use High-Resolution peripheral Quantitative Computed Tomography (HR-pQCT) to investigate the impact of stroke on the bone properties at the distal radius, and to identify the correlates of the estimated failure load for the distal radius in people with chronic stroke. This was a cross-sectional study of 64 participants with chronic stroke (age: 60.8±7.7 years, stroke duration: 5.7±3.9 years) and 64 age- and sex-matched controls. Bilateral bone structural, densiometric, geometric and strength parameters of the distal radius were measured using HR-pQCT. The architecture, stiffness and echo intensity of the bilateral biceps brachii muscle and brachial artery blood flow were evaluated using diagnostic ultrasound. Other outcomes included the Fugl-Meyer Motor Assessment (FMA), Motor Activity Log (MAL), and Composite Spasticity Scale. The results revealed a significant side (paretic vs non-dominant, non-paretic vs dominant) by group (stroke vs control) interaction effect for estimated failure load and all volumetric density, trabecular, and cortical bone parameters ($p \leq 0.012$) with the exception of intra-cortical porosity ($p=0.179$). Post hoc analysis showed percent side-to-side differences in these outcomes occurred only in the stroke group. Muscle echo intensity ($p=0.030$), MAL ($p=0.004$), and FMA scores ($p<0.001$) were significant determinants of the percent side-to-side difference in estimated failure load of the distal radius. This was the first study to show bone microstructure is altered in upper limb post-stroke. We found that the paretic distal radius had compromised bone structural properties and lower estimated failure load compared to the non-paretic side. Muscle morphology, disuse, and motor impairment are important correlates of distal radius bone strength and should be the potential targets for intervention to improve bone health post-stroke.

4.1 Introduction

The economic implications of stroke are large, with long-term and indirect expenditures increasing for stroke-related health care [273]. The musculoskeletal system has been shown to undergo substantial change after stroke [6], with bone loss prevention often

being under prioritized during recovery [5]. Reduced bone mass and altered geometry, which compromise bone strength, are among the more serious complications after stroke [49,274]. Along with advanced age and female sex, reduced bone strength is an important factor related to upper limb fragility fractures after stroke [58]. While dual-energy x-ray absorptiometry (DXA) is often used in the clinical assessment of total and site-specific areal bone mineral density (aBMD) post-stroke [59,80], peripheral quantitative computed tomography (pQCT) can be used to examine compartmentalized volumetric density and geometry of both trabecular and cortical bone at peripheral skeletal sites [52,80,275]. It has also been used in research investigating specific musculoskeletal conditions such as adolescent idiopathic scoliosis, psoriatic arthritis and hip fracture [276-278]. As DXA lacks the ability to assess bone loss factors beyond bone quantity (i.e. aBMD), other methods used to assess bone architecture are needed for effectively identifying patient groups at risk of fracture [93].

Several studies have used pQCT to examine bone properties of the upper limb post-stroke [49,52,54,80,96,279]. At the distal radius site (i.e., epiphysis), a consistent finding was a lower BMD on the paretic side, with no significant side-to-side difference in total area [52,54]. Previously, it was not possible to evaluate bone microstructure (e.g., cortical porosity, trabecular number, thickness and separation) using pQCT [49]. Bone microstructure is another important factor determining bone fragility [98,99,101]. Among large prospective cohort studies, microstructure is consistently shown to be a predictor of fracture risk estimation in other populations [103-105]. Thus, examining bone microstructure using high-resolution peripheral quantitative computed tomography (HR-pQCT) should be of value in the study of bone health among individuals with stroke. Measures of bone density, architecture and mechanical properties using HR-pQCT have also demonstrated moderate to good correlation with those of DXA (R^2=0.69-0.80) and micro-computed tomography (R^2=0.59-0.96) [280].

Previous studies have shown that neuromuscular and vascular factors have either been moderately associated with (ρ=0.569-620, $p \leq 0.009$) or predictive of (β=364, p=0.002) compressive bone strength indices (cBSI) among patients with stroke using pQCT [52,54]. It is unknown whether these factors are also correlated with bone microstructure and mechanical properties measured with HR-pQCT. The aims of this study were to investigate the impact of stroke on bone properties of the distal radius and to examine the association between the estimated failure load and common clinical indicators of physical function during the chronic stage of recovery. The wrist region is the second most frequent site of fragility fractures post-stroke [58]. As changes in peripheral bone sites have been shown to be more pronounced in the upper limb than lower limb following stroke [96], the distal radius was examined in this study.

4.2 Methods

4.2.1 Participants

Individuals with chronic stroke and age- and sex-matched controls without prior stroke history were recruited from the general public, community self-help groups and an existing patient database. Relevant medical history and demographic data were obtained by phone interviews. Recruitment of participants commenced April 11, 2018 and ended February 28, 2019. A total of 67 stroke and 66 control participants were screened prior to data collection which was conducted from June 1, 2018 to March 30, 2019. From the stroke group, one person was excluded due to a congenital bone deformation in the tibia and two others withdrew from the study before all of the assessments were conducted. From the control group, one person was excluded due to a previous Achilles tendon repair surgery and another person was excluded due to an essential tremor. Study approval was granted by the Human Subjects Ethics Sub-committee of the University (reference number HSEARS20171212003 on January 2, 2018) and the Clinical Research Ethics Committee of the hospital (Joint Chinese University of Hong Kong-New Territories East Cluster Clinical Research Ethics Committee, CREC reference number 2017-711 on April 10, 2018). Informed consent was obtained for all participants prior to data collection. All procedures were conducted in accordance with the Helsinki Declaration for human experiments.

For between-group comparisons of bone variables, a priori power analysis was done using GPower 3.1 software (Heinrich Heine Universitat Dusseldorf, Germany) [281]. Based on a previous pQCT study by Pang et al. [52], the side × group interaction effect for the bone strength index of the radius yielded an effect size of f=0.25. Assuming the same effect size, an alpha of 0.05, and a power of 0.8, a minimum of 49 participants per group were required. For the hierarchical regression analysis in predicting %SSD of estimated failure load among individuals with stroke, a separate power analysis was done using the Free Statistics Calculators version 4.0 (https://www.danielsoper.com/statcalc/calculator.aspx?id=16). A previous pQCT study found that various stroke impairment variables (e.g., motor impairment, strength, paretic upper limb usage, spasticity) were associated with the side-to-side difference in cortical thickness and bone mineral content of the radius (R^2 change = 0.20-0.26, equivalent to effect sizes f^2= 0.25-0.35) [49]. Therefore, assuming an effect size of f^2=0.25, an alpha of 0.05, and a power of 0.8, a minimum sample size of 61 individuals with chronic stroke would be required to detect a significant effect of 5 impairment variables (e.g., muscle

parameters measured by ultrasound, spasticity, etc.), after accounting for the effect of age, sex, post-stroke duration and body mass index (BMI).

After considering the two power analyses above, we aimed to recruit a minimum of 61 individuals with stroke, and 61 control participants.

4.2.2 Inclusion & exclusion criteria

The inclusion criteria for the stroke group were: (1) history of chronic stroke (onset>6 months), (2) age>18, (3) community-dwelling, (4) able to reach 60° of passive elbow flexion, (5) Abbreviated Mental Test (AMT) score ≥6 [243]. The exclusion criteria were: (1) diagnoses of other neurological conditions, (2) significant musculoskeletal conditions (e.g. amputations), (3) metal implants in distal radius, (4) upper extremity fracture within the past 12 months, (5) diagnosis of osteoporosis, (6) severe contractures prohibiting the individual from reaching 60° of passive elbow flexion, (7) other serious illnesses that precluded participation in the study. The control group had the same eligibility criteria with the exception of prior stroke history.

4.2.3 Measurement procedures

HR-pQCT

Bone imaging was conducted at a bone imaging center in a local hospital by an experienced technician (VWYH, LQ). HR-pQCT (XtremeCT II, Scanco Medical AG, Brüttisellen, Switzerland) was used to measure bone properties of the bilateral distal radius. A summary description of all HR-pQCT variables collected is provided in the supplementary appendices (Supplemental Table 4.1). The scan region was fixed at 9.0 mm (distal radius) proximal from the mid-joint line. Length of the scan region spanned 10.2 mm proximally (i.e., 168 slices stacked). A fixed rather than relative offset distance (i.e., %-length method) was used as the relative method entails accurate limb length measurement prior to scanning, and assumes proportionality between limb length and bone regions of the epiphysis, metaphysis and diaphysis [282]. Standard analysis of 3D bone volumetric density, geometry, trabecular microarchitecture and cortical parameters was conducted using Image Processing Language software (IPL v5.08b, Scanco Medical AG, Brüttisellen, Switzerland). The forearm, wrist and hand were immobilized prior to placement within the scanner gantry using a formable padded cast provided by the manufacturer in order to standardize anatomical orientation and minimize motion during acquisition. To confirm image quality, motion grading guidelines were followed [283]. Scans with a motion artefact score of 5 were excluded

[282]. The second generation scanner (XtremeCT II) has demonstrated excellent reproducibility [284]. In the current study, the root mean squared percent coefficient of variation ($CV\%_{RMS}$) of short term precision for the radius among a cohort of 30 healthy individuals were 0.21-0.94% for geometric measures. The corresponding values for density and microstructural parameters were 0.29-0.95% and 0.52-3.36%, respectively. This scanner has comparatively higher resolution (isotropic voxel size of 61 μm for XtremeCT II and 82 μm for XtremeCT I) and has demonstrated excellent agreement with the previous-generation scanner for most densitometric measures [285].

Estimated Failure Load

All micro-finite element (μFE) analyses were performed using the FE-solver provided by the manufacturer. CT images were segmented using a dual-threshold technique and converted into an FE mesh. A voxel-by-voxel conversion approach was used to convert each voxel into a cubic hexahedral finite element for analysis. Boundary conditions of the uniaxial compression test were applied to all elements with a Young's modulus of 10 GPa and a Poisson's ratio of 0.3 assigned [100]. Pistoia's criterion was adopted and the estimated failure load (N) was expected when >2% of the elements were strained beyond a critical limit of 7000 microstrain [100]. These settings were selected based on several validation studies using experimental loading tests on cadaveric bones [100,106,107]. Similar settings have been applied in previous clinical studies to predict fracture risk [278].

Ultrasound

To measure various aspects of muscle properties (stiffness, echo intensity, cross-sectional area, circulation), ultrasound imaging was conducted in a muscle imaging lab of the University by an operator with 3 years of relevant experience (TM). An Aixplorer ultrasound scanner (Aixplorer, SuperSonic Imagine, Aix en-Provence, France) coupled with a linear array probe (4-15 MHz, SuperLinear, 15-4, Vermon, France) was used. For each parameter, the average of 3 measures was used for the analysis. A standoff gel couplant layer of approximately 2mm thickness served as the interface between the probe and skin surface to minimize probe compression on muscle during measurements. Surface electromyography (sEMG) (Bagnoli EMG system, Delsys Inc, Natick, Massachusetts, USA) was used concomitantly to confirm muscle relaxation. In the event of contracture or spastic response, images were retaken. A low-pass filter <10Hz was applied for wave rectification of all real-time sEMG signal data using LabVIEW software (National Instruments Co., Austin, Texas,

USA). A notch filter was also applied at 50, 100 and 150Hz frequencies to preserve sEMG signal integrity and suppress powerline and harmonic noise during image capture. Following skin preparation (i.e., shaving, abrading, sterilization and conductive gel), a sensor (SX230, Biometrics Ltd, Gwent, UK) was placed on the skin surface of the muscle and affixed using a die cut medical grade adhesive tape. A bilateral comparison of muscle parameters is shown in Supplemental Figure 1.

Muscle stiffness: The shear modulus (kPa) and shear wave velocity (m/s) of the biceps brachii muscles were measured using a standard musculoskeletal imaging preset in shear wave elastography mode. Shear wave velocity is a measure of shear wave dispersion through tissue and is used to calculate modulus values (i.e., ratio of stress to strain) as an estimate of stiffness [(172)]. While both these measures are directly related to biomechanical tissue properties, discrepancies in the interpretability of reported values between studies have been identified as problematic and should therefore not be used interchangeably [(208)]. To aid in the interpretation and comparison of results across studies, both values were collected and used for analysis. During image acquisition, participants were placed in a supine position with the shoulder abducted 45° and elbow joint immobilized at 60° of flexion using an external fixation device. Measurement sites were standardized at the lower third of the humerus (approximately 66% of the total length) according to an adapted procedure used by Wu et al [(43)]. The probe was placed in parallel alignment to the muscle fascicle direction. The region of interest (ROI) was standardized for all measures (1.89 cm^2 area with an approximate depth of 1 cm below the subcutaneous tissue layer). Individual images were captured after a consistent and stable color distribution was observed. All values were generated using a Q-box Trace function (Supersonic Imagine, Aix en-Provence, France) during image processing.

Echo intensity: Muscle echo intensity was measured using B-mode ultrasound. For each measurement, the probe was angled cranially and caudally until maximal echo intensity was observed in the scanning plane. Gray-scale analysis was conducted with an impixel calculation function using a customized program written in Matlab (version R2018a, Mathworks, Natick, Massachusetts, USA). The ROI (1.89 cm^2 area) was the same as each elastogram captured [(11)]. Gray-scale values were standardized at a gain of 50% for all measures, with darkest and lightest pixels represented by values of 0 and 255, respectively.

Muscle cross-sectional area: Muscle cross-sectional area (MCSA) (in cm^2) of the biceps brachii was measured using a panoramic image capture function in B-mode ultrasound at the measurement site previously specified for muscle stiffness measures. A foam padded adhesive probe support was placed in line with the muscle circumference to reduce probe translation and ensure clarity during image capture. Using the perimeter trace function (Supersonic Imagine, Aix en-Provence, France), a muscle region from the medial to lateral borders was manually selected.

Vascular measures: Vascular parameters were also measured as previous work has indicated that the influence of these factors on bone strength are regional and more pronounced in the epiphysis than diaphysis [51,55]. Peak systolic velocity (cm/s) of the brachial artery was measured using pulse wave Doppler ultrasound by initially placing the probe transversely along the medial aspect of the upper arm (measurement site previously stated). The probe was then rotated sagittally and tilted to visualize the artery longitudinally. An electronic calliper was then placed in the artery center, and the sample volume was standardized at 0.5mm. Angle correction and steering were adjusted to optimize angle-to-flow ($\leq 60°$ insonation). Spectral waveform cycles with 3 consistent readings were used to calculate each measurement trial. Blood flow volume (mL/min) for the brachial artery was derived from peak systolic velocity. Within the same image pane, arterial diameter (cm) was measured by placing the calipers at each end of the superior and inferior borders of the endothelial wall. Flow volume was then calculated using the system tools (Supersonic Imagine, Aix en-Provence, France).

Functional assessment procedures

Measures of functional and stroke-specific impairments were conducted in a university laboratory by a physical therapist. For muscle strength and touch pressure threshold parameters, the average of 3 trials were used for the analysis. Functional assessments were conducted on a separate day prior to ultrasound assessments to minimize the influence of strength testing on muscle, vascular and elastography outcomes. All functional assessments were obtained for both control and stroke groups (i.e., physical activity level, muscle strength, touch pressure threshold) with the exception of spasticity, motor impairment and paretic limb usage. These stroke-specific assessments were only conducted among participants with stroke.

Spasticity: The composite spasticity scale (CSS) was used to measure elbow flexor spasticity (score range: 1-16). The CSS has shown high test-retest reliability in previous studies examining spasticity among patients with stroke (ICC=0.97) [268,270].

Upper limb motor impairment: The Fugl-Meyer Motor Assessment (FMA) is a stroke-specific assessment used to evaluate the motor impairment of the paretic arm for reflex, neuromuscular coordination and volitional movement with and without accompanying synergies (score range: 0-66). FMA has demonstrated high inter-rater reliability (ICC=0.97) in patients with stroke [286].

Paretic limb use: The Motor Activity Log (MAL) questionnaire served as a subjective appraisal of paretic arm usage frequency during 30 functional activities according to the Amount of Use (AOU) scale. Mean scores from the 30-item scale were used for analysis. Among patients with stroke, the MAL-AOU scale has shown high internal consistency (Cronbach's α=0.88) [4].

Physical activity level: An adapted version of the 12-item Physical Activity Scale for the Elderly (PASE) was used to evaluate general physical activity level. Scores are calculated by weights and frequency values which correspond to each activity type assessed, with higher scores indicating higher activity level. This version has been previously validated in elderly Chinese populations and has demonstrated good test-retest reliability (ICC = 0.81) and fair to moderate association with other clinically relevant measures of function [287].

Muscle strength: Isometric peak torque (N/m) of the elbow flexors was assessed using a dynamometer (Humac Norm Systems, Stoughton, Massachusetts, USA) in 60° of elbow flexion and 45° of shoulder abduction. Measurement error has been shown to be smaller for isometric than isokinetic testing conditions [259]. A 60° angle was used for testing based on evidence suggesting elbow flexion torque is greatest in 56° for healthy individuals [260] and 60° for paretic arms in participants with stroke [261]. Wrists were used as the contact interface between participants and the dynamometer handle due to impairments in grip strength or dexterity of paretic hands. The wrist was held in place by elastic straps. A triangular support cushion was also placed in the lower-axilla region to maintain a 45° angle of shoulder abduction.

4.2.4 Statistical analysis

The following analyses were performed using SPSS (version 23.0, SPSS Inc., Chicago, Illinois, USA) at a significance level of 0.05 (two-tailed). Independent t, Mann-Whitney U and χ^2 tests were used for comparing baseline between-group differences for participant characteristics according to continuous, ordinal and nominal levels of data, respectively. A two-way factorial repeated measures analysis of variance (ANOVA) [within-subject factor: side (paretic vs non-paretic for stroke group or dominant vs non-dominant for control group), between-subject factor: group (stroke vs control)] was performed for HR-pQCT, ultrasound and isometric peak torque variables that were assessed bilaterally. A significant F-ratio for the ANOVA results represents a difference between at least two of the means (i.e., largest vs smallest). For an $F > 4.3$ (i.e., critical value), the between-sides or between-group effect was significant at $p<0.05$, with larger F values representing greater difference within (i.e., side) or between group means. Following the ANOVA, post hoc paired t-tests were used to compare between the two sides. Post hoc independent t-tests were also used to compare the percent (%) side-to-side difference (%SSD) between the stroke and control groups. A more stringent significance level of 0.017 (Bonferroni's correction: 0.05/3) was used for post hoc tests to adjust for multiple comparisons. The following formula was used in calculating %SSD:

$$\frac{\text{Non-paretic or Dominant side} - \text{Paretic or Non-dominant side}}{\text{Non-paretic or Dominant side}} \times 100$$

Pearson's r was used to determine the bivariate correlation between the side-to-side difference (%SSD) in estimated failure load of the distal radius and the %SSD of other variables. Relationships between variables were defined as having minimal or no correlation (r=0.00-0.25), fair (r=0.25-0.50), moderate to strong (r=0.50-0.75) or very strong correlation ($r > 0.75$) [288]. As %SSD calculations were not suitable for stroke-specific assessment outcomes with only measurements on the paretic side (i.e., CSS, FMA and MAL-AOU), raw values were used to assess their correlation with the %SSD in estimated failure load. Correlations were also used to examine the association between all bone parameters and other continuous variables (e.g., stroke onset duration, physical activity level and BMI). Mann-Whitney U tests were used to determine differences in the %SSD in estimated failure load for stroke participant subgroups categorized according to alcohol, tobacco and supplement usage.

A subgroup analysis was conducted using dichotomous grouping based on average stroke duration (i.e., below or above 5.8 ± 4.0 years) and using tertiles of comparable subject groupings according to stroke onset chronology (i.e., </= 3 years (n=19), 4-5 years (n=21), and >/= 6 years (n=24)). Between-group differences in all bone parameters were assessed with independent t-tests for dichotomous grouping and one-way ANOVA for tertiles.

Hierarchical multiple regression analysis was used to identify significant determinants of the %SSD in estimated failure load (dependent variable) for the stroke group. The choice of independent variables was based on both physiological relevance and results of the bivariate correlation analysis. Prior to the regression analysis, separate bivariate correlation analyses were performed to assess the degree of association among the independent variables (e.g., ultrasound and clinical outcomes). Variables with a correlation >0.6 were used in separate regression models to avoid multicollinearity [52]. Variables that were significantly associated with the %SSD in estimated failure load in the bivariate correlation analysis ($p<0.05$), along with sex, age and post-stroke duration, were forced into each regression model using the enter method. Failure load is considered a material parameter accounting for material behavior (yield, post-yield) and loading (magnitude of applied force) required to strain bone tissue beyond a critical limit [100]. Estimated failure load has been shown to be a better predictor of incident fracture than volumetric density [109] and bone morphometry measures alone [100]. The identification of failure load thresholds suggestive of higher fracture risk have been described in a multicenter prospective study involving large cohorts of elderly men and women [113]. This study showed estimated failure load to be the strongest correlate with incident fracture [113]. Stroke-related impairment and consequent hemiosteoporosis of paretic limbs may also exacerbate proclivity to fracture [58]. Although estimated failure load is essentially a material parameter and not a direct determinant of fracture risk, the amount of bilateral difference in estimated failure load among individuals with stroke, in comparison to that of age and gender-matched controls, may provide a meaningful comparison of hemiparetic bone status which differs from previous estimates of bone strength (e.g., compressive bone strength index, polar stress-strain index) [49,52,54,96].

4.3 Results

4.3.1 Participant characteristics

A summary of participant characteristics is provided in Table 4.1. A total of 64 participants with stroke and 64 healthy controls completed all the assessments. No significant differences were found for sex (p=0.858), age (p=0.306) or limb dominance (p=0.319)

between stroke and control groups. There was also no significant difference in alcohol (p=0.276), tobacco (p=0.428) or supplement usage (vitamin D: p=1.000; calcium: p=0.188) between groups. For female participants, there was no significant difference between groups for time since menopause onset (p=0.787). For the stroke group, the mean scores for the CSS (8.6±2.5), FMA (35.9±18.9) and MAL-AOU (1.3±1.3) indicated mild spasticity, a moderate degree of motor impairment, and minimal perceived usage frequency of the paretic arm, respectively. A significant between-group differences in the total number of comorbidities and medications were also observed (p<0.001).

4.3.2 HR-pQCT variables

There was a significant significant side × group interaction effect for estimated failure load (F=80.0, p<0.001). A significant interaction effect was also observed for all volumetric density (F=55.7-100.1, p<0.001), macrostructural (F=7.06-50.6, p≤0.009), and microstructural parameters (F=6.44-15.6, p≤0.012) with the exception of intracortical porosity (F=1.82, p=0.179) (Table 4.2). Post hoc paired t-tests showed significant differences in cortical area, trabecular area, number and separation, and estimated failure load parameters between the two sides in both the stroke and control groups (p≤0.017). In addition, all volumetric density parameters and cortical thickness demonstrated significant side-to-side differences in the stroke group (p≤0.017), but not in controls. On the other hand, the cortical perimeter showed a side-to-side difference in the control group (p≤0.017), but not the stroke group. With the exception of intracortical porosity and trabecular thickness, post hoc analyses showed significant differences in %SSD of all bone parameters between the stroke and control groups (p≤0.017) (Table 4.2). The HR-pQCT images obtained from a representative participant with stroke and gender matched control participant are displayed in Figure 4.1.

4.3.3 Other variables

For other bilaterally measured ultrasound and functional variables, there was a significant side × group interaction effect for MCSA (F=25.5, p≤0.001), echo intensity (F=17.8, p≤0.001), peak systolic velocity (F=5.0, p≤0.027) and isometric strength (F=69.7, p≤0.001). Shear modulus (F=1.5, p=0.214), shear wave velocity (F=1.5, p=0.223), and blood flow volume (F=0.98, p=0.324) showed no significant interaction effects (Table 4.3). Post hoc paired t-tests showed significant side-to-side differences for MCSA, echo intensity and isometric strength in the stroke group (p≤0.017), but not controls. Post hoc independent t-tests also showed significant between-group differences in %SSD for MCSA, echo intensity,

and isometric strength, ($p \leq 0.017$) (Table 4.3). Bilateral ultrasound images obtained from a representative participant with stroke are displayed in Figure 4.2.

4.3.4 Subgroups

There was also no association between stroke duration and all other bone parameters ($r = -0.214 – 0.218$, $p \leq 0.893$) (Supplemental Table 4.4). When participants were grouped dichotomously according to below or above average stroke duration, independent t-test showed no significant differences in all bone variables between groups (Supplemental Table 4.2). For tertile subdivision of comparable group numbers (i.e., </= 3 years (n=19), 4-5 years (n=21), and >/= 6 years (n=24)), one-way ANOVA results showed no significant between-groups difference for all bone variables (Supplemental Table 4.3).

4.3.5 Relationship to %SSD of estimated failure load and regression analysis

For the bivariate correlation analyses (Table 4.4) the %SSD in estimated failure load showed a fair correlation with CSS ($r = 0.295$, $p = 0.018$) and moderate correlation with FMA ($r = -0.541$, $p < 0.001$) and MAL-AOU ($r = -0.453$, $p < 0.001$). There was also minimal to fair correlation between the %SSD in estimated failure load and shear modulus, shear wave velocity, echo intensity, ($r = -0.247$ - -0.296, $p \leq 0.049$) and blood flow volume ($r = 0.249$, $p \leq 0.047$). There were no correlations between the %SSD in estimated failure load and stroke onset duration, BMI or PASE ($r = -0.130 – 0.017$, $p \leq 0.898$). There were no differences in the %SSD in estimated failure load for subgroups categorized according to alcohol, tobacco, and supplement usage (Supplemental Table 4.5).

Among the independent variables considered for the regression analysis, there was a moderate to strong association of FMA with MAL-AOU ($r > 0.7$, $p < 0.001$) and CSS ($r > -0.6$, $p < 0.001$) (Table 4.5). Hence, separate regression models were used to avoid multicollinearity. After accounting for sex, age, stroke duration and BMI, MAL-AOU ($\beta = -0.400$, $p = 0.004$) and echo intensity ($\beta = -0.251$, $p = 0.033$) (model 1) and FMA-UL ($\beta = -0.524$, $p < 0.001$) (model 2) remained independently associated with the %SSD in estimated failure load measured at the distal radius. Overall, the two models explained approximately 31.2-37.6% of the variance in the %SSD in estimated failure load (Table 4.6).

4.4 Discussion

All HR-pQCT variables, except intracortical porosity, demonstrated significant interaction effects, indicating that stroke had a substantial impact on bone density,

macrostructure and most microstructure variables. Among the various potential clinical correlates, differences in muscle morphology (echo intensity), motor impairment severity (FMA), and perceived usage frequency (MAL-AOU) emerged as the predominant determinants of the %SSD in estimated failure load at the distal radius.

4.4.1 Side-to-side differences in HR-pQCT variables

Side-to-side differences in volumetric density parameters (4.6%-23.1%, $p \leq 0.017$) (i.e., lower cortical, trabecular and total vBMD in paretic limbs) are largely consistent with previous pQCT studies in populations with stroke [52,80,96]. Previously it has been problematic to measure cortical area and thickness parameters at the distal radius due to thin cortical shells on the paretic side and the lower resolution of previous pQCT scanners [52]. In the present study using HR-pQCT, these parameters were significantly diminished on the paretic side (14.4%-15.1%, $p \leq 0.017$). The detrimental impact of stroke on geometric and structural bone parameters of the radius have also been reported previously [49].

In terms of bone microstructure, the deficits on the paretic side were more evident in trabecular number (12.3%, $p \leq 0.017$) and separation (24.3%, $p \leq 0.017$) than other trabecular parameters (i.e., trabecular thickness and intracortical porosity). Significantly lower number and greater average distance between trabeculae may indicate substantial loss of trabeculae on paretic sides and reduced connectivity with greater heterogeneous distribution of trabecular bone. When assessed collectively, trabecular vBMD and separation appear to show the largest %SSD (>20%) relative to other parameters measured, and may contribute more to the large %SSD in estimated failure load of the radius (stroke: 23.8% vs controls: 2.9%). Similar changes in these parameters have been observed when comparing premenopausal and postmenopausal osteopenic or osteoporotic women ($p<0.01$), with significantly greater loss and more heterogenous distribution of trabeculae for the radius among fractured osteopenic women compared to unfractured women ($p<0.02$) despite similar spine and hip bone density [101]. Low trabecular number in the radius has also been shown to be highly associated with increased osteoporotic, vertebral and non-vertebral fracture risk (Hazard Ratio=1.46-1.80 per SD, $p \leq 0.01$) in a large prospective trial of elderly men [111]. In recent meta-analyses, trabecular vBMD in particular, as well as the ratio of trabecular to total bone volume (i.e., trabecular bone volume fraction (BV/TV)), was strongly associated with fracture [109,110]. However, trabecular microstructure alone may lack the sensitivity and specificity to fully distinguish fracture risk [111]. Though not exclusively for the identification of Colles-type fractures of the radius, material bone parameters derived from the μFE analysis have been

suggested to be superior to vBMD and microstructure for separating fragility fracture cases from controls at multiple bone sites [289]. However, the degree to which compromised microstructural properties contribute to fracture risk in individuals with stroke remains unaddressed by the current study.

4.4.2 Echo intensity

Echo intensity is a sonographic measure of grayscale pixel intensity (i.e., ratio of dark to light pixels) often used for assessing muscle mechanical properties and morphological differences relative to a reference tissue. Higher echo intensity (i.e. hyperechoic or brighter image) represents compositional changes in fluid content, intramuscular fat accumulation, fibrous connective tissue (i.e., collagen density) [290] and possible alterations in fiber type distribution and innervation (i.e., denervation) [48]. In the present study, paretic biceps brachii muscles had significantly higher echo intensity than non-paretic muscles and the bilateral muscles of controls. Similar findings have been reported in previous studies on lower and upper limb muscles post-stroke. Barenpas et al showed that higher echo intensity of the paretic medial gastrocnemius muscle was fairly correlated with reduced gait speed ($r=-0.40$, $p=0.04$) and moderately correlated with stroke onset duration ($r=0.57$, $p<0.01$) [48]. In another study by Lee et al, muscle echo intensity was strongly correlated with passive muscle stiffness of the paretic biceps brachii post-stroke ($R^2=0.703$, $p=0.002$) [11]. The identification of muscle echo intensity as a significant predictor of the estimated failure load ($R^2=0.374$, $p=0.050$) is a potentially distinguishing element of the current study. Although the magnitude of the bivariate correlation with the %SSD in estimated failure load ($r=-0.296$, $p=0.017$) was only fair and also comparatively lower than that of FMA ($r=-0.541$, $p<0.001$) and MAL-AOU ($r=-0.453$, $p<0.001$), it suggests that stroke-related changes in the biomechanical properties of muscle and bone may be somewhat interrelated. A possible conjecture of this finding is that interventions which modify muscle echo intensity, and perhaps muscle stiffness, may be useful for improving bone strength in individuals with stroke. Some preliminary research in this area is emerging. Implanted peroneal functional electrical stimulation (FES) has been shown to be effective in reducing paretic tibialis anterior muscle echo intensity of people with chronic stroke exhibiting foot drop [291]. Whether the same technique can modify the echo intensity of the paretic upper limb muscles will require further study. There is also a need to search for other therapeutic interventions that are effective in modulating the mechanical properties of the muscle and consequently improving bone strength in the paretic upper limb.

4.4.3 Upper limb motor recovery

FMA score was also moderately associated with the %SSD in estimated failure load (β=-0.524, p<0.001), possibly suggesting that better motor recovery, as indicated by higher FMA scores, was associated with less compromised bone strength on the paretic side (i.e., lower %SSD in estimated failure load). A previous study reported only fair association between Wolf Motor Function Test scores and %SSD in cortical bone mineral content (BMC) (r=-0.415, p<0.005), cortical thickness (r=-0.415, p<0.005) and no association with the %SSD in polar stress-strain index p-SSI (r=-0.150) of the radius diaphysis [49]. Another study showed only fair association between FMA scores and the stress-strain index of the paretic radius midshaft (R^2=0.38, p=0.04) [279]. Whether or not rehabilitation interventions with motor training components can potentially influence bone strength after stroke is difficult to determine based on the inconsistencies in reported associations. However, a study involving a 6-month comprehensive motor exercise program was shown to be effective in increasing trabecular bone content (p=0.048) and cortical bone thickness (p=0.026) of the paretic tibia in people with chronic stroke [3]. A similar program targeting the neuromotor system which can enhance bone strength in upper limb sites, awaits further study.

4.4.4 Perceived paretic upper limb use

Lower MAL scores, indicative of greater perceived paretic arm disuse, demonstrated a fair association with higher %SSD in estimated failure load (β=-0.400, p=0.004). As stated previously, paretic arm motor impairment, of which disuse is a major component, has been identified as a correlate of BMC loss in the paretic distal radius (r=-0.415, p<0.005) and reduced bone stress-strain index in the midshaft of the paretic radius (R^2=0.38, p=0.04) [49,279]. This suggests that more frequent paretic arm usage during daily activities may be an important prescriptive element. During acute and subacute stages of stroke recovery, failed attempts to use the paretic arm in daily activities reinforce psychological patterns of disuse often termed the “learned non-use” phenomenon. Constraint-induced movement therapy, although commonly used to overcome non-use [4], has not been explored as a potential intervention for improving bone strength post-stroke.

4.4.5 Other variables

Previous pQCT studies in populations with stroke have shown a fair association between bone strength and vascular elasticity indices (large arteries: r=0.332, p=0.007; small arteries: r=0.517, p<0.001) in the paretic radius [52], and also a fair to moderate association

between the bone strength index of the paretic tibia and peak oxygen consumption (VO^2) (r=0.454-0.596, p≤0.012) [50] (r=0.615, p<0.05) [51]. However, blood flow volume was not determined to be a significant predictor of estimated failure load in the current study. One rather perplexing result of the current study was the lack of correlation between elbow flexion strength and %SSD in estimated failure load. Muscle strength has consistently proven to be a strong correlate and predictor of bone geometry, density and strength in the paretic radius [49,52,85]. This is perhaps explained by the different muscle groups tested. In the present study, mean peak torque during elbow flexion was the only measure of paretic arm strength. As the biceps brachii and the brachial artery were the main muscle and vascular structures measured during ultrasound assessments, we felt the measurement of elbow flexor strength was appropriate. Previous research showed that the degree of strength impairment in elbow flexion (25.6% of normal) was similar to that in more proximal (shoulder abduction; 23.6% of normal) and distal (wrist extension; 25.6% of normal) muscle actions. However, in our study, the %SSD in elbow flexion strength reported here (31.6%±49.7%) was less pronounced than that of the composite muscle strength (inclusive of grip strength) (38.5%±35.2%) previously reported [49]. This may partly explain why we were unable to identify a significant relationship between elbow flexion strength and %SSD in estimated failure load.

The effect of spasticity on estimated failure load was diminished in the multivariate regression. Previous studies examining the impact of spasticity and bone properties post-stroke have produced mixed results [49,52,55,80,85]. There were also methodological differences between spasticity measures in the present study (i.e., CSS) compared to previous studies (i.e., Modified Ashworth Scale) in which spasticity was a significant correlate of bone density and geometry [49]. The Modified Ashworth Scale is only used to evaluate resistance to passive movement whereas the CSS is a more comprehensive multi-component scale for assessing additional neurogenic aspects of spasticity (i.e., tendon jerk and wrist clonus).

4.4.6 Limitations

In this study, the standard μFE analysis with the same linear elastic modulus assignment was used for all participants. Other studies have used non-linear approaches (i.e., models using asymmetric, bilinear yield strain criteria) with higher and lower modulus values for cortical and trabecular bone elements, respectively [107,292,293]. Although the elastic modulus of cortical and trabecular tissues have been shown to differ based on modulus direction [294], there appears to be support for the use of linear μFE analysis for estimating

bone strength in specific instances where moduli of homogeneous tissue and scaled CT-attenuation models were compared using both non-linear and linear analyses [107]. Although more computationally intensive, non-linear μFE analysis may offer a more direct estimate of bone mechanical strength properties. Therefore, given the anticipated low volumetric bone density of the paretic side [52,54,80,96], particularly for cortical bone [52,54], the use of a non-linear and/or density-dependent modulus in the μFE analysis of bone strength properties among stroke groups may warrant future investigation. Limb length differences between subjects and groups is also a potential confounding element associated with the fixed offset distance scanning protocol used in this study [282]. Although several studies to date have used a fixed offset approach to standardize measures [99,104,105,111,276-278], it may be important to consider the limitations associated with both fixed and relative offset methods based on factors influencing limb length for a given subject sample [282]. There are also a number of confounding factors influencing bone status and metabolism (e.g., associated comorbidities, medication, BMI, physical activity level) which were not accounted for in the regression models given the limited sample size. The number of predictors was restricted to six in each model allowing for approximately 10 observations per variable [295] assuming low variance ($n \geq 8$, with additional degrees of freedom for covariates) [296]. Future studies with a larger sample size are needed. Furthermore, participants from the stroke and control groups were only recruited through a non-probability sampling method and results may not be generalizable to individuals with diverse clinical presentations. Finally, this cross-sectional study cannot prove a causal relationship between stroke-related impairment and distal radius fracture. The relationship between estimated failure load and incident fracture in people with stroke will require further investigation.

4.5 Conclusion

This study showed that bone density, macrostructure and microstructure of the paretic distal radius were compromised in individuals with chronic stroke. There was a substantially lower estimated failure load for the paretic compared to the non-paretic side. The degree of motor recovery, perceived frequency of paretic arm use, and muscle morphology were emergent correlates of estimated failure load in the distal radius. The clinical relevance of these factors for improving bone strength after stroke remains unaddressed and will require further study.

Table 4.1 Characteristics of participants

		Stroke (n=64)	Control (n=64)	p
Demographics	Sex (men/women), n	38/26	39/25	0.858
	Age, years	60.8 ± 7.7	59.4 ± 7.8	0.306
	Menopause (women), years	12.4 ± 13.1	11.5 ± 9.9	0.787
	Education, years	9.8 ± 3.7	11.8 ± 3.7	0.002[b]
	Hand dominance (Left/Right/Equivalent), n	1/62/1	2/62/0	0.319
	Body mass index (kg/m^2)	24.3 ± 3.1	23.4± 2.8	0.081
	AMT (out of 10)	9.3 ± 1.1	9.9 ± 0.4	<0.001[b]
	PASE	114.7 ± 87.4	142.2 ± 79.4	0.065
Stroke Characteristics	Paretic Side (Left/Right), n	36/28	-	-
	Type of Stroke (Ischemic/Hemorrhagic), n	41/23	-	-
	Stroke duration, years	5.8 ± 4.0	-	-
	CSS (1-16)	8.6 ± 2.5	-	-
	FMA (0-66)	35.9 ± 18.9	-	-
	MAL-AOU (0-5)	1.3 ± 1.3	-	-
Comorbidity	Total number of comorbidities per person	1.3 ± 1.3	0.6 ± 0.9	<0.001[b]
	Hypertension, n	37	22	0.006[b]
	Hyperlipidemia, n	21	4	<0.001[b]
	Cardiac arrhythmia, n	1	0	0.315
	Diabetes mellitus, n	14	8	0.150
	Ischemic heart disease, n	1	0	0.315
Medications	Total number of medications per person	4.5 ± 3.1	0.9 ± 1.2	<0.001[b]
	Antihypertensive agents, n	42	16	<0.001[b]
	Hypolipidemic agents, n	41	10	<0.001[b]
	Hypoglycemic agents, n	10	6	0.259
	Anticoagulants, n	23	3	<0.001[b]
	Antispasmodic agents, n	6	0	0.011[a]
	PPI/ Gastric agents, n	25	2	<0.001[b]
	SSRI/ Antidepressants, n	8	1	0.016[a]
Other	Alcohol history (yes/no), n	14/50	24/40	0.053
	Alcohol consumption (drinks/day)	0.2 ± 0.3	0.1 ± 0.3	0.276
	Smoking history (yes/no), n	15/49	14/50	0.833
	Tobacco use (packs/day)	0.7 ± 0.4	0.6 ± 0.3	0.428
	Daily Vitamin D supplementation (yes/no), n	4/60	4/60	1.000
	Daily Calcium supplementation (yes/no), n	3/61	7/57	0.188

[a] $p \leq 0.05$ Statistically significant
[b] $p \leq 0.01$ Statistically significant
AMT = Abbreviated Mental Test, PASE = Physical Activity Scale for the Elderly, PPI = Proton Pump Inhibitor, SSRI = Selective Serotonin Reuptake Inhibitor, CSS = Composite Spasticity Scale, FMA = Fugl-Meyer Assessment, MAL = Motor Activity Log (Amount of Use)

Table 4.2 Comparison of HR-pQCT variables

	Stroke Group (n=64)			Control Group (n=64)			Main Effect: Side (Within)		Main Effect: Group (Between)		Side × Group Interaction Effect	
Parameter	Paretic	Non-Paretic	SSD (%)	Non-Dominant	Dominant	SSD (%)	F	p	F	p	F	p
Density	Total vBMD (mg HA/cm^3)											
	292.0 ± 83.5	352.8 ± 62.8[a]	18.1 ± 13.7[b]	339.4 ± 60.0	337.9 ± 62.3	-0.84 ± 6.83	91.5	<0.001[c]	1.97	0.163	100.1	<0.001[c]
	Cortical vBMD (mg HA/cm^3)											
	871.1 ± 75.2	912.0 ± 53.0[a]	4.6 ± 4.7[b]	914.9 ± 55.4	913.0 ± 51.5	-0.21 ± 2.36	46.3	<0.001[c]	4.89	0.029[c]	55.7	<0.001[c]
	Trabecular vBMD (mg HA/cm^3)											
	116.3 ± 49.3	147.0 ± 36.1[a]	23.1 ± 21.7[b]	137.3 ± 38.5	139.5 ± 39.6	0.74 ± 10.24	75.9	<0.001[c]	0.92	0.339	57.4	<0.001[c]
Macrostructure	Cortical Area (mm^2)											
	56.7 ± 15.6	66.3 ± 13.7[a]	15.1 ± 12.4[b]	65.6 ± 12.6	67.3 ± 14.2[a]	1.89 ± 6.85	97.4	<0.001[c]	4.34	0.039[c]	47.9	<0.001[c]
	Cortical Perimeter (mm)											
	66.2 ± 8.4	66.2 ± 8.3	0.04 ± 3.84[b]	66.9 ± 8.5	68.1 ± 7.7[a]	1.85 ± 3.26	8.53	0.004[c]	0.76	0.385	7.06	0.009[c]
	Cortical Thickness (mm)											
	1.04 ± 0.26	1.21 ± 0.20[a]	14.4 ± 13.3[b]	1.18 ± 0.18	1.19 ± 0.20	-0.04 ± 8.3	60.3	<0.001[c]	3.09	0.081	50.6	<0.001[c]
Microstructure	Trabecular Area (mm^2)											
	194.1 ± 51.8[a]	187.9 ± 53.3	-4.25 ± 10.5[b]	194.8 ± 56.6	199.9 ± 50.6[a]	3.1 ± 7.7	0.14	0.708	0.47	0.494	13.3	<0.001[c]
	Trabecular Number (1/mm)											
	1.08 ± 0.28	1.23 ± 0.20[a]	12.3 ± 16.5[b]	1.20 ± 0.19	1.24 ± 0.19[a]	2.75 ± 9.19	44.7	<0.001[c]	3.23	0.075	15.6	<0.001[c]
	Trabecular Thickness (mm)											
	0.22 ± 0.02	0.23 ± 0.02	0.50 ± 6.29	0.23 ±0.02[a]	0.22 ± 0.02	-1.03 ± 3.77	0.001	0.981	0.09	0.765	6.44	0.012[c]
	Trabecular Separation (mm)											
	0.98 ± 0.47[a]	0.78 ± 0.20	-24.3 ± 36.0[b]	0.80 ± 0.17	0.77 ± 0.20[a]	-4.3 ± 15.2	25.5	<0.001[c]	4.63	0.033[c]	13.8	<0.001[c]
	Intra-cortical Porosity (%)											
	0.010 ± 0.0064	0.011 ± 0.0069	3.13 ± 50.7	0.0095 ± 0.0064	0.0093 ± 0.0059	7.03 ± 41.7	0.62	0.432	1.05	0.308	1.82	0.179
μFE	Estimated failure Load (N)											
	2980 ± 1066	3865 ± 949[a]	23.8 ± 15.1[b]	3738 ± 983	3868 ± 1033[a]	2.9 ± 8.5	144.4	<0.001[c]	4.81	0.030[c]	80.0	<0.001[c]

Value expressed as mean ± SD unless otherwise indicated

[a]$p \leq 0.017$ Statistically significant between-sides difference (post hoc paired t-test)

[b]$p \leq 0.017$ Statistically significant side-to-side difference between two groups (post hoc independent t-test)

[c]$p \leq 0.05$ Statistically significant results (two-way repeated measures ANOVA)

vBMD = Volumetric Bone Mineral Density, HA = Hydroxyapatite, N = Newtons, μFE = Finite Element Analysis

Table 4.3 Comparison of ultrasound and functional impairment variables

		Stroke Group (n=64)			Control Group (n=64)			Main Effect: Side (Within)		Main Effect: Group (Between)		Side × Group Interaction Effect	
Measures		Paretic	Non-Paretic	STSD (%)	Non-Dominant	Dominant	STSD (%)	F	p	F	p	F	p
Ultrasound	Cross-Sectional Area (cm^2)	7.60 ± 2.18	8.93 ± 2.38[a]	13.7 ± 16.1[b]	8.32 ± 2.72	8.55 ± 2.73	2.28 ± 10.1	50.4	<0.001[c]	0.15	0.695	25.5	<0.001[c]
	Shear Modulus (kPa)	37.6 ± 22.2	32.2 ± 20.0	-44.5 ± 104.7	26.9 ± 15.1	25.9 ± 16.0	-29.1 ± 98.9	3.39	0.068	13.0	0.003[c]	1.5	0.214
	Shear Wave Velocity (m/s)	3.34 ± 0.97	3.06 ± 0.92	-15.1 ± 38.6	2.83 ± 0.77	2.76 ± 0.83	-8.7 ± 36.5	4.64	0.033[c]	9.73	0.002[c]	1.5	0.223
	Echo Intensity	113.4 ± 12.7[a]	104.8 ± 12.4	-9.18 ± 13.9[b]	96.5 ± 14.0	98.6 ± 15.2	0.86 ± 15.8	6.42	0.013[c]	32.3	<0.001[c]	17.8	<0.001[c]
	Peak Systolic Velocity (cm/s)	77.4 ± 15.4	76.8 ± 15.1	-2.65 ± 19.9	73.7 ± 17.4	78.3 ± 15.2[a]	5.35 ± 16.3	2.95	0.088	0.19	0.663	5.0	0.027[c]
	Blood Flow Volume (mL/min)	42.5 ± 23.2	49.7 ± 23.3	-2.78 ± 88.5	30.6 ± 19.8	41.8 ± 22.6[a]	11.6 ± 61.7	19.9	<0.001[c]	8.75	0.004[c]	0.98	0.324
IPT	Isometric Peak Torque (N/m)	18.4 ± 9.3	29.6 ± 11.2[a]	31.6 ± 49.7[b]	26.5 ± 10.3	27.0 ± 11.1	-0.14 ± 11.6	84.0	<0.001[c]	2.48	0.118	69.7	<0.001[c]

Value expressed as mean ± SD unless otherwise indicated
[a]$p \leq 0.017$ Statistically significant between-sides difference (post hoc paired t-test)
[b]$p \leq 0.017$ Statistically significant side-to-side difference between two groups (post hoc independent t-test)
[c]$p \leq 0.05$ Statistically significant results (two-way repeated measures ANOVA)
kPa = Kilopascals

Table 4.4 Correlates of side-to-side difference in estimated failure load

	Variables	r	p
Stroke Impairment	Stroke duration	-0.130	0.306
	CSS	0.295	0.018*
	FMA	-0.541	0.000**
	MAL - AOU	-0.453	0.000**
Other	Isometric Peak Torque (%SSD)	0.171	0.176
	BMI	0.017	0.893
	PASE	0.016	0.898
	Total Comorbidities	-0.102	0.422
	Total Medications	-0.160	0.206
	Alcohol Consumption	0.030	0.920
	Tobacco Usage	-0.105	0.709
Ultrasound	Cross-Sectional Area (%SSD)	0.074	0.559
	Echo Intensity (%SSD)	-0.296	0.017*
	Peak Systolic Velocity (%SSD)	0.056	0.660
	Blood Flow Volume (%SSD)	0.249	0.047*
	Shear Wave Velocity (%SSD)	-0.274	0.029*
	Shear Modulus (%SSD)	-0.247	0.049*

*Significant correlation at the 0.05 level (2-tailed)
**Significant correlation at the 0.01 level (2-tailed)
%SSD= percent side-to-side difference, CSS = Composite Spasticity Scale, FMA = Fugl-Meyer Assessment-Upper Limb, MAL-AOU = Motor Activity Log-Amount of Use

Table 4.5 Correlation among predictor variables

	CSS	FMA	MAL-AOU	EI	Vflow	SWV	SM
CSS	-	-	-	-	-	-	-
FMA	-0.670**	-	-	-	-	-	-
MAL-AOU	-0.526**	0.780**	-	-	-	-	-
EI	-0.053	0.126	0.064	-	-	-	-
Vflow	0.079	-0.130	-0.199	-0.116	-	-	-
SWV	-0.370**	0.305*	0.136	0.244	-0.162	-	-
SM	-0.381**	0.299*	0.135	0.227	-0.126	0.977**	-

*Significant correlation at the 0.05 level (2-tailed)
**Significant correlation at the 0.01 level (2-tailed)
CSS = Composite Spasticity Scale, FMA = Fugl-Meyer Assessment, MAL-AOU = Motor Activity Log-Amount of Use, EI = Echo Intensity, Vflow = Blood Flow Volume, SWV = Shear Wave Velocity, SM = Shear Modulus

Table 4.6 Regression models for predicting percent side-to-side difference in estimated failure load

Predictor	F Change	R^2	B	95%CI	Beta	p
Model 1						
Sex (Men=0, Women=1)			2.484	-4.545, 9.514	0.081	0.482
Age		0.037	0.040	-0.433, 0.513	0.020	0.866
Post-Stroke Duration			-0.652	-1.559, 0.255	-0.171	0.155
BMI	7.466		-0.042	-1.215, 1.131	-0.008	0.943
Motor Activity Log			-4.640	-7.726, -1.555	-0.400	0.004[b]
Echo Intensity (%SSD)		0.312	-0.273	-0.523, -0.024	-0.251	0.033[a]
Composite Spasticity Scale			0.546	-1.157, 2.249	0.089	0.523
Model 2						
Sex (Men=0, Women=1)			3.362	-3.092, 10.025	0.110	0.305
Age		0.037	0.055	-0.380, 0.475	0.028	0.795
Post-Stroke Duration			-0.565	-1.360, 0.345	-0.148	0.167
BMI	15.535		-0.257	-1.368, 0.855	-0.052	0.646
Echo Intensity (%SSD)			-0.239	-0.476, 0.003	-0.220	0.047[a]
Fugl-Meyer Assessment		0.376	-0.419	-0.592, -0.246	-0.524	<0.001[b]

[a]$p \leq 0.05$ Statistically significant
[b]$p \leq 0.01$ Statistically significant
B = Unstandardized regression coefficient, Beta = Standardized regression coefficient, 95%CI = 95% confidence interval

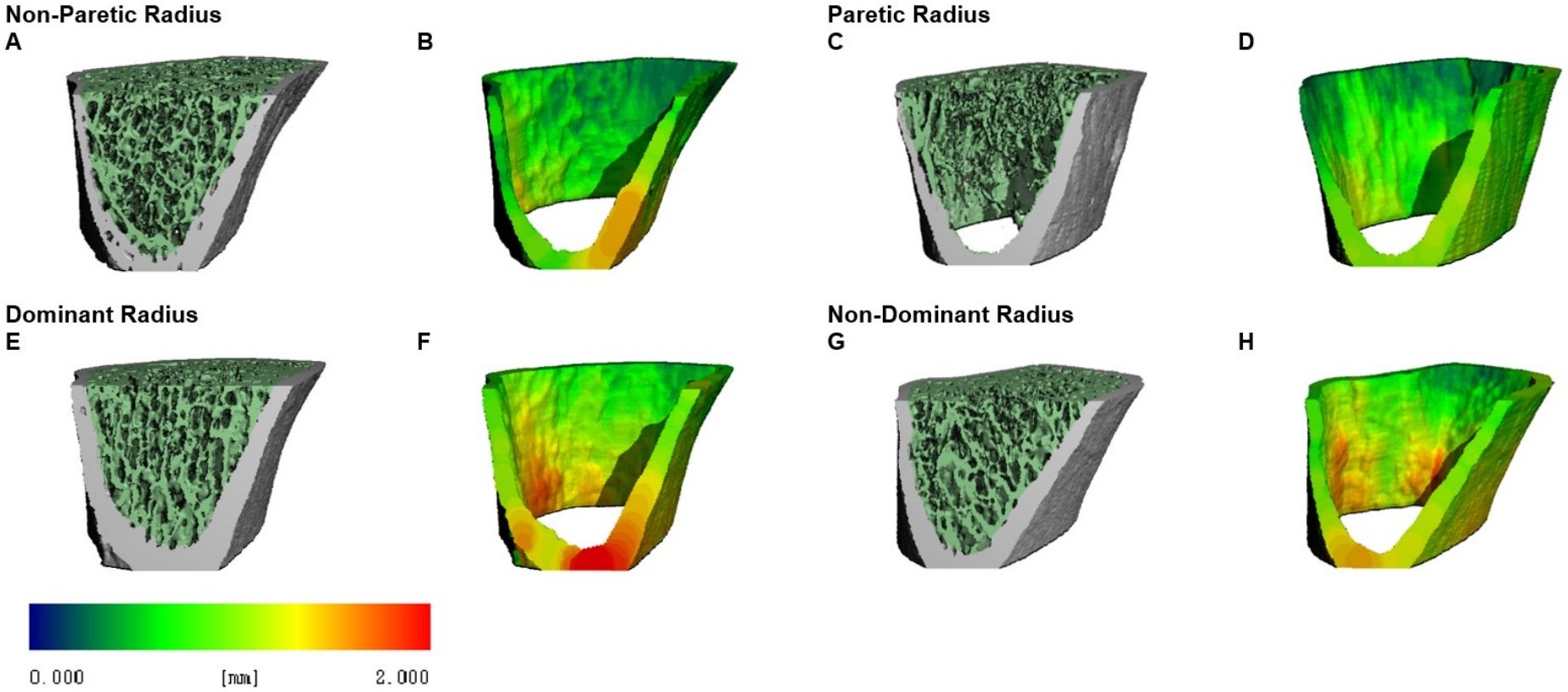

Figure 4.1 Bilateral comparison of bone parameters

HR-pQCT generated 3D rendering of the distal radius bone for a representative female participant with flaccid left arm hemiparesis (upper panel) and a healthy female control participant (lower panel). The sagittal cut plane was standardized at a depth of 30% with the wider epiphyseal portion of the radius oriented superiorly and the diaphyseal portions inferiorly. There are comparatively fewer trabeculae with reduced density and network connectivity on the paretic side. Thinning of the cortical shell is also more pronounced on the paretic side as indicated by a darker spectral color gradient. The upper panel shows a bilateral view of the (A) trabecular segment and (B) cortical thickness of the non-paretic radius compared to the (C) trabecular segment and (D) cortical thickness of the paretic radius and the lower panel shows the (E) trabecular segment and (F) cortical thickness of the dominant radius relative to the (G) trabecular segment and (H) cortical thickness of the non-dominant radius.

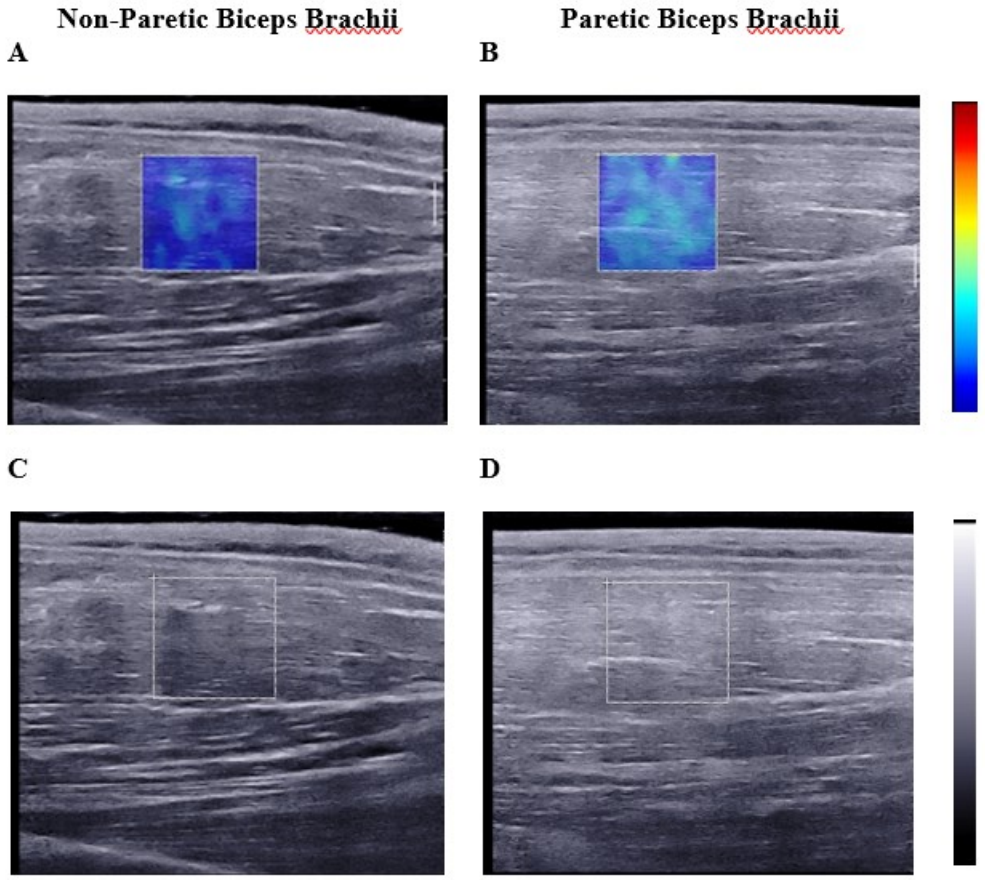

Figure 4.2 Bilateral comparison of muscle parameters

Ultrasound generated images of the BB muscles for a representative male participant with left arm hemiparesis. There are comparatively greater compositional tissue changes and stiffness for the paretic BB muscle. The upper panel shows the ROI (1.89cm^2) used to calculate SWV (0-11.2 m/s) and SM values (0-350 kPa). Highest and lowest stiffness values are represented by red and blue pixels, respectively. Non-paretic muscle (A) was less stiff than paretic (B). The lower panel shows the same ROI was used to calculate EI values (0-255). Highest and lowest grayscale pixel intensities are represented by white and black pixels, respectively. Similar to stiffness, non-paretic muscle (C) showed comparatively lower EI than paretic (D).

Supplemental Table 4.1 HR-pQCT variable summary

Category	Parameter	Description
Density	Total volumetric bone mineral density (Tt.vBMD), mg HA/cm3	Mean bone density of the total bone segment
	Cortical volumetric bone mineral density (Ct.vBMD), mg HA/cm^3	Mean density of the cortical bone compartment
	Trabecular volumetric bone mineral density (Tb.vBMD), mg HA/cm^3	Mean density of the trabecular bone compartment
Microstructure	Trabecular number (Tb.N), 1/mm	Mean number of trabeculae per unit of length
	Trabecular thickness (Tb.Th), mm	Mean thickness of trabeculae
	Trabecular separation (Tb.Sp), mm	Mean distance between trabeculae
	Intracortical porosity (Ct.Po), %	Percentage of bone mineral content within a 1mm cortical area slice (voxel-based method)
Macrostructure	Trabecular area (Tb.Ar), mm^2	Cross-sectional measure of the trabecular bone area
	Cortical area (Ct.Ar), mm^2	Cross-sectional measure of the cortical bone area
	Cortical perimeter (Ct. Pm), mm	Periosteal perimeter of cortical bone
	Cortical thickness (Ct.Th), mm	Mean thickness of the cortical area, irrespective of intracortical pore topography (direct method)
µFE	Failure load (FL), N	Failure occurs when 2% of the bone tissue under strain exceeds the critical limit (7000 mstrain)

Supplemental Table 4.2 Between-group differences for %SSD bone parameters based on stroke duration

	Parameter	Below Average N=40 Mean ± SD	Above Average N=24 Mean ± SD	Sig	95% CI Lower	95% CI Upper
%SSD Density	Total vBMD	18.70 ± 14.31	17.17 ± 12.99	0.669	-5.61	8.68
	Cortical vBMD	4.52 ± 4.50	4.65 ± 5.10	0.918	-2.57	2.32
	Trabecular vBMD	22.68 ± 21.70	23.80 ± 22.20	0.845	-12.41	10.19
%SSD Macrostructure	Cortical Area	14.81 ± 13.09	15.48 ± 11.32	0.834	-7.11	5.76
	Cortical Perimeter	-0.02 ± 4.05	0.15 ± 3.54	0.868	-2.17	1.83
	Cortical Thickness	14.40 ± 13.76	14.39 ± 12.79	0.997	-6.91	6.93
%SSD Microstructure	Trabecular Area	-5.01 ± 10.51	-2.98 ± 10.63	0.459	-7.48	3.42
	Trabecular Number	11.02 ± 16.31	14.35 ± 16.96	0.438	-11.88	5.21
	Trabecular Thickness	1.46 ± 5.64	-1.09 ± 7.09	0.117	-0.66	5.76
	Trabecular Separation	-22.46 ± 38.10	-27.35 ± 32.67	0.602	-13.78	23.56
	Intracortical Porosity	2.92 ± 46.21	3.47 ± 58.36	0.967	-26.91	25.79
%SSD µFE	Failure Load	24.47 ± 16.08	22.53 ± 13.56	0.622	-5.90	9.78

p < 0.05 Statistically significant difference between subgroups (independent t-test)
%SSD= percent side-to-side difference, Below Average = ≤ 5 years since stroke onset, Above Average = > 5 years since stroke onset

Supplemental 4.3 Between-group difference tertile stroke duration subgroups

	Perimeter	Group 1 Mean ± SD (N=19)	Group 2 Mean ± SD (N=21)	Group 3 Mean ± SD (N=24)	F	Sig
%SSD Density	Total vBMD	17.71 ± 15.08	19.61 ± 13.89	17.17 ± 12.99	0.184	0.832
	Cortical vBMD	3.13 ± 4.10	5.78 ± 4.57	4.65 ± 5.10	1.629	0.204
	Trabecular vBMD	21.97 ± 22.25	23.33 ± 21.72	23.80 ± 22.20	0.038	0.963
%SSD Macrostructure	Cortical Area	12.48 ± 11.01	16.92 ± 14.68	15.48 ± 11.32	0.657	0.522
	Cortical Perimeter	0.84 ± 3.82	-0.80 ± 4.19	0.15 ± 3.54	0.923	0.403
	Cortical Thickness	11.53 ± 13.38	17.00 ± 13.91	14.39 ± 12.79	0.840	0.437
%SSD Microstructure	Trabecular Area	-5.75 ± 12.26	-4.34 ± 8.89	-2.98 ± 10.63	0.361	0.698
	Trabecular Number	8.54 ± 15.89	13.25 ± 16.74	14.35 ± 16.96	0.707	0.497
	Trabecular Thickness	1.79 ± 5.99	1.16 ± 5.43	-1.09 ± 7.09	1.297	0.281
	Trabecular Separation	-16.76 ± 26.69	-27.61 ± 46.16	-27.35 ± 32.67	0.585	0.560
	Intracortical Porosity	-5.26 ± 49.71	10.32 ± 42.65	3.47 ± 58.36	0.465	0.630
%SSD µFE	Failure Load	24.37 ± 14.49	24.57 ± 17.75	22.53 ± 13.56	0.121	0.886

$p < 0.05$ Statistically significant difference between subgroups (one-way ANOVA)
Group 1 = ≤ 3 years since stroke onset, Group 2 = 4-5 years since stroke onset, Group 3 = ≥ 6 years since stroke onset

Supplemental Table 4.4 Correlates of stroke duration

	Parameter	r	Sig
%SSD Density	Total vBMD	-0.130	0.304
	Cortical vBMD	0.145	0.253
	Trabecular vBMD	-0.017	0.893
%SSD Macrostructure	Cortical Area	0.048	0.709
	Cortical Perimeter	0.019	0.880
	Cortical Thickness	0.031	0.805
%SSD Microstructure	Trabecular Area	0.218	0.083
	Trabecular Number	0.101	0.426
	Trabecular Thickness	-0.214	0.089
	Trabecular Separation	-0.096	0.449
	Intracortical Porosity	0.060	0.639
%SSD μFE	Failure Load	-0.130	0.306

Significant correlation at the 0.05 level (2-tailed)
%SSD = percent side-to-side difference

Supplemental 4.5 Differences in %SSD in estimated failure load for subgroups according to alcohol, tobacco and supplement usage (participants with stroke)

	N	Mean Ranks	Sum of Ranks	p
Non-drinker	50	33.10	1655.00	0.626
Drinker	14	30.36	425.00	
Non-smoker	49	33.20	1627.00	0.585
Smoker	15	30.20	453.00	
No supplement usage	61	32.31	1971.00	0.742
Calcium (daily)	3	36.33	109.00	
No supplement usage	60	32.38	1943.00	0.862
Vitamin D (daily)	4	34.25	137.00	

Significant correlation at the 0.05 level (2-tailed)
%SSD = percent side-to-side difference

Chapter 5. Gait speed and spasticity as determinants of estimated failure load in the distal tibia after stroke

Abstract

Background: Lower extremity bone health is often compromised after stroke. Altered macro- and microstructural properties of bone tissue may have important neuromuscular and functional correlates. *Purpose:* (1) To explore the influence of stroke on distal tibia bone properties and, (2) examine the association between estimated failure load and important clinical correlates in people with chronic stroke. *Methods:* 64 individuals with stroke (age: 60.8±7.7 years, stroke duration: 5.7±3.9 years) and 64 age- and sex-matched controls were recruited for this cross sectional study. Bone parameters of the distal tibia were measured bilaterally using High Resolution peripheral Quantitative Computed Tomography (HR-pQCT). Muscle architecture, stiffness and echo intensity of the medial gastrocnemius muscle and blood flow of tibial artery were assessed with ultrasound. Clinically relevant measures of function were assessed using the 10 meter walk test (10MWT), Fugl-Meyer Motor Assessment (FMA), Brief BESTest and Composite Spasticity Scale (CSS). *Results:* A significant side-group interaction effect was observed for estimated failure load ($p \leq 0.001$), cortical area and thickness ($p \leq 0.001$), and all volumetric density parameters ($p \leq 0.009$). Post hoc analyses of side-to-side differences in these parameters were also significant for the stroke group but not for controls. The 10MWT ($p=0.043$), and CSS scores for ankle clonus ($p=0.032$) were significant predictors of percent side-to-side difference in estimated failure load. *Conclusion:* The paretic distal tibia showed compromised bone density and cortical macrostructure, contributing to a comparatively lower estimated failure load than that of the non-paretic tibia. Gait speed and spasticity appear to be strong correlates of bone strength in the distal tibia. Future intervention strategies with the aim of preserving or improving bone strength should incorporate elements which target these functional limitations.

5.1 Introduction

The musculoskeletal system endures considerable change after stroke [6]. The relationship between muscle function and bone integrity post-stroke is evident [50,51,122], with declines in bone strength identified as a major risk factor for fracture [297]. Although fracture risk has been shown to increase after stroke [143,298], preventative measures for reducing bone loss in the chronic stages of stroke are often under underemphasized during recovery [5].

Moreover, both fall proclivity[62] and incidence of fracture[63] are more likely to occur on the paretic side highlighting the deleterious nature of progressive unilateral bone loss after stroke. Fractures occurring in the lower limb after stroke, especially the hip [5,274], often result in protracted hospitalization [297] loss of mobility, [299] and death [61]. Thus, factors influencing bone loss, and consequently bone strength, are of particular relevance for individuals with chronic stroke [6].

Previous studies have examined paretic lower limb bone status using either peripheral quantitative computed tomography (pQCT) or dual-energy X-ray absorptiometry (DXA) [3,50,51,55,56,80,95,96]. A consistent finding is lower cortical bone mineral density and compromised bone geometry of the paretic tibia. DXA provides clinically relevant assessment of areal bone mineral density (aBMD) post-stroke [59,80], but lacks the sensitivity to evaluate compartmental bone segments independently [93]. Although more often used for research purposes, pQCT scans not only provide estimates of bone density and but also geometry[50,51], an important determinant of bone strength [93]. A limitation of previous pQCT studies was the inability to examine bone microstructure, which is relevant to the investigation of bone fragility [101]. Microstructure [104,105,111,300] and estimated failure load [105,300,301] of the tibia have been shown to important determinants of incident fracture in large prospective trials.

Bone microstructure and estimated failure load can be assessed using high-resolution peripheral quantitative computed tomography (HR-pQCT). To the knowledge of the authors, there are currently no studies which have utilized HR-pQCT to examine the bone properties of the lower limb among individuals with chronic stroke. Additionally, in previous studies using pQCT, neuromuscular and vascular factors have been identified as important clinical correlates of the bone strength index in people with stroke [52,54]. The association between HR-pQCT bone measures of the tibia and clinically relevant measures of dysfunction and impairment after stroke are unknown.

The objective of this study was to examine the impact of stroke on the bone properties of the distal tibia and the association between estimated failure load and important clinical correlates in people with chronic stroke. It was hypothesized that compromised bone status would be more evident on the paretic side in comparison to the non-paretic side and matched controls. It was also hypothesized that the side-to-side difference in estimated bone failure load would be strongly correlated with neuromuscular factors and stroke-related lower limb impairment.

5.2 Methods

5.2.1 Participants

Individuals with chronic stroke and age- and sex-matched controls without prior stroke history were recruited through convenience sampling. Recruitment occurred between April 11, 2018 and February 28, 2019. prior to data collection, 67 individuals with stroke and 66 healthy controls were screened by phone between June 1, 2018 to March 30, 2019. Demographic and medical data were also collected during the initial screening. Among the participants with stroke, an individual was excluded due to a congenital tibial bone deformation and two others withdrew of their own volition prior to completing all assessments. Among the healthy controls, an individual was excluded for an Achilles tendon repair and another for an essential tremor. The study was approved by the Human Subjects Ethics Sub-committee of the University (reference number HSEARS20171212003 on January 2, 2018) and the Clinical Research Ethics Committee of the hospital (Joint Chinese University of Hong Kong-New Territories East Cluster Clinical Research Ethics Committee, CREC reference number 2017-711 on April 10, 2018). Prior to data collection, informed consent was obtained for all participants. Assessment procedures were conducted according to the Helsinki Declaration for human experiments.

5.2.2 Inclusion & exclusion criteria

Stroke group inclusion criteria: (1) history of chronic stroke (onset > 6 months), (2) > 18 years of age, (3) residing within the local community, (4) able to achieve 0° of passive ankle plantar-dorsiflexion required for conducting ultrasound and isometric strength assessments, (5) Abbreviated Mental Test (AMT) score ≥6 [(243)]. Stroke group exclusion criteria: (1) diagnoses of other neurological conditions, (2) musculoskeletal conditions, disorders or dysfunctions (e.g. limb amputation), (3) metal implants in the distal tibia, (4) lower extremity fracture within the previous 12 months, (5) prior diagnosis of osteoporosis, (6) other serious illnesses that precluded study participation. The control group eligibility criteria were the same with the exception of previous stroke history.

5.2.3 Procedures

HR-pQCT

Bone imaging was conducted at a bone imaging center in a local hospital by an experienced technician (VWYH, LQ). High Resolution peripheral Quantitative Computed Tomography (HR-pQCT) (XtremeCT II, Scanco Medical AG, Brüttisellen, Switzerland) was

used to measure bone properties of the bilateral distal tibia. The scan region was fixed at 22 mm proximal from the mid-joint line. Length of the scan region spanned 10.2 mm proximally (i.e., 168 stacked slices). Standard 3D analysis of all bone parameters was performed with the Image Processing Language software (IPL v5.08b, Scanco Medical AG, Brüttisellen, Switzerland). Cortical porosity was calculated by a relative void-voxel based method and cortical thickness was calculated using a direct method [302]. The root mean squared percent coefficient of variation ($CV\%_{RMS}$) of short term precision for the distal tibia among a cohort of 30 healthy individuals were 0.21-0.75% for cortical and trabecular bone morphometry, 0.30-0.74% for volumetric density, 7.82%-23.88% for cortical porosity and 0.56-2.18% for trabecular microarchitecture parameters.

Finite Element Analysis

All micro-finite element (μFE) analyses were performed using the FE-solver provided by the manufacturer (Scanco Medical AG, Brüttisellen, Switzerland). CT images were segmented using a dual-threshold technique and converted into an FE mesh. A voxel-by-voxel conversion approach was used to convert each voxel into a cubic hexahedral finite element for analysis. Boundary conditions of the uniaxial compression test were applied to all elements with a Young's modulus of 10 GPa and a Poisson's ratio of 0.3 assigned [100]. Pistoia's criterion was adopted and the estimated failure load (N) was expected when >2% of the elements were strained beyond a critical limit of 7000 microstrain [100]. These settings were selected based on several validation studies using experimental loading tests on cadaveric bones [100,106,107]. Similar settings were applied in previous clinical studies to predict fracture risk [278].

Ultrasound measures

An AixPlorer ultrasound unit (AixPlorer, Supersonic Imagine, Aix en-Provence, France), set the standard musculoskeletal preset, with a linear transducer array (4–15 MHz, SuperLinear, 15-4, Vermon, France) was used to measure medial gastrocnemius muscle architecture, stiffness, echo intensity and blood flow of the popliteal artery on both the paretic and non-paretic sides. Measures were conducted at the same imaging lab of the university by a single operator with three years of relevant experience in musculoskeletal, elastography and Doppler ultrasound techniques (TM). Musculoskeletal ultrasound settings were standardized to include supercompound and high penetration modes at a medium frame rate in order to enhance visualization of structural boarders and optimize image resolution. To minimize

probe compression on the muscle during measures, a 2mm thick gel couplant layer served as the interface between the probe and skin. All measures were assessed with participants lying in a prone position. For muscle stiffness, echo intensity and architecture measures using B-mode or elastography, the probe was placed on the medial gastrocnemius muscle in a sagittal orientation at the proximal one third (i.e., 33%) of the total tibial length as measured from the base of the distal Achilles tendon, at the level of the inferior boarder of the lateral malleolus up to the midline of the popliteal crease. For blood flow measures of the popliteal artery using pulse wave Doppler mode, the ultrasound probe was placed in a sagittal orientation on the popliteal fossa, at the approximate level of the popliteal crease. For all measures, the ankle was maintained in a neutral dorsiflexion/ plantarflexion (90^{o}) fixed by an anchored foot board device with restricted eversion, inversion and rotation. Surface electromyography (sEMG) (Bagnoli EMG system, Delsys In, Massachusetts, USA) readings were taken during ultrasound measures in order to confirm the absence of muscle contractions. In the event of contraction, images were discarded and retaken. The average of three measures was used in the analysis of all muscle and vascular measures.

Muscle stiffness: Muscle stiffness was assessed using elastography mode. The shear wave velocity (m/s) and shear modulus (kPa) values were generated using a Q-box trace function (Supersonic software, Aix en-Provence, France). The region of interest (ROI) for each elastogram was a standardized area of 1.23 cm^2 at an approximate depth of 1cm below the subcutaneous skin layer. Each elastogram was captured when a stable color distribution was observed.

Echo intensity: Echo intensity (EI) of the medial gastrocnemius was determined using B-mode ultrasound and a post-processing function with a customized program written in Matlab (version R2018a, Mathworks, Natick, Massachusetts, USA). The acquisition and analysis of the ultrasound images were adapted from the protocol described by Lee et al, in that the ROI was the same as each elastogram captured [(11)]. A standardized grey scale gain of 50% was used for all measurements. Darkest pixels have a value of 0 and brightest pixels have a value of 255 (black = 0, white = 255), respectively. To ensure the ultrasound beam was aligned with minimum anisotropy, the transducer was angled cranially and caudally until a scan plane with maximal EI of the muscle was obtained.

Muscle architecture: Fascicle length (FL) and pennation angle (PA) for the medial gastrocnemius were obtained using B-mode ultrasound. The muscle fascicle length (FL) (cm) was measured using a distance/ length function (Supersonic software). An intact muscle fiber with full visual continuity from the superficial aponeurosis and deep aponeurosis at the center of the image pane was selected. Muscle pennation angle (PA) (°) was measured using the hip angle function (Supersonic software). The degree of pennation is defined as the angle of the muscle fascicle insertion into the deep aponeurosis [(247)].

Blood flow: In assessing popliteal artery peak systolic velocity (PSV) (cm/s), the probe was placed in a sagittal orientation on the popliteal fossa, approximately at the level of the popliteal crease. The probe was then rotated and tilted for optimal visualization of the artery. A low wall filter was applied and the pulse repetition frequency (PRF) scale was adjusted to avoid aliasing and artifact. The electronic caliper was placed in the center of the artery. Then fine angle correction and steering adjustments were applied to optimize the degree of angle-to-flow (≤ 60º angle of insonation) in order to reduce measurement error. The inversion function (Supersonic software) was used when necessary for producing a positive Doppler shift. The auto-trace function (Supersonic software) was applied for the full range of positive and negative flow. Visual confirmation of spectral wave forms with 3 consistent readings were selected for calculating each measure. Blood flow volume (mL/min) for the popliteal artery was derived from PSV and arterial diameter (cm) measures. Arterial diameter was measured by placing each end of the electronic calipers at the superior and inferior boarders of the endothelial walls of the artery. All stroke-specific and functional impairment measures were conducted in a separate laboratory of the university by a physical therapist and are described below.

Stroke-Specific Assessments

Stroke characteristics: Demographic information was collected during the initial screening. Lower limb dominance was determined using a ball kicking task [(303)]. Information regarding stroke type, location, and duration since onset, was obtained from medical records and brain scan findings (e.g., CT, MRI). Stroke type was classified by subgroup (ischemic vs hemorrhagic) and location according to the Oxfordshire Community Stroke Project Classification (OCSP): (1) total anterior circulation syndrome, (2) partial anterior circulation syndrome, (3) lacunar syndrome, or (4) posterior circulation syndrome. Despite previously observed limitations in differentiating small cortical and subcortical infarcts [(304)], the OCSP

has been shown to be useful as a common clinical classification tool in predicting stroke size and site [265].

Motor function recovery: The Fugl-Meyer motor assessment (FMA) was used to determine the degree of motor impairment in the paretic lower limb. The motor scores for the lower limb ranged from 0-34. The FMA has demonstrated high inter-rater reliability (ICC=0.92-0.99) [286,305] and test-retest reliability (ICC=0.97) [266].

Spasticity: Spasticity of the ankle plantar-flexors was measured using the Composite Spasticity Scale (CSS) (score range: 1-16) developed by Chan [267]. The CSS is an ordinal scale comprising three clinical components (1) Achilles tendon jerk (score range of 0-4, 5-point scale), (2) resistance to full range of passive joint displacement for ankle dorsiflexion (score range of 0-8, 5-point scale doubly weighted), and (3) the duration and amount of ankle clonus elicited (score range of 1-4, 4-point scale). The CSS has previously demonstrated good to excellent reliability (ICC = 0.80 – 0.97) [268].

Other Measures

Cognition: An adapted version of the 10-item Abbreviated Mental Test (AMT) was used in determining the level of cognitive impairment for each participant. This version has been previously validated among geriatric patients [306] and elderly individuals in residential care homes in Hong Kong [243] and has demonstrated excellent test-retest and inter-rater reliability (ICC = 0.99) [243].

Physical activity level: An adapted Chinese version of the 12-item Physical Activity Scale for the Elderly (PASE-C) was used to assess general physical activity level. Higher scores indicated higher activity level. The original version of the scale has been previously validated using accelerometry [307] and actigraph monitoring data [308]. The version of the PASE used in this study has been previously validated in elderly Chinese populations [287] and has demonstrated good test-retest reliability (ICC = 0.81) and fair to moderate association with other clinically relevant measures of physical function [287].

Walking status: The 10 meter walk test (10MWT) at a safe maximal speed was used to assess walking velocity [309]. The average duration for completing the 10MWT varies. Normative data reported by Severinsen et al [310] suggests an average score of 0.84 ± 0.3 m/s for

populations with stroke. Clinical assessment of walking status has been shown to have excellent test-retest reliability for both comfortable (ICC=0.94) and fast gait speeds (ICC=0.97) in people with stroke [309].

The Functional Ambulation Category (FAC) is a subjective 6-level visual measurement of general walking ability based upon patient walking independence or the amount of assistance required. The FAC has demonstrated excellent reliability (Cohen's k = 0.950 for test-retest reliability and k = 0.905 inter-rater reliability), and good responsiveness (100% sensitivity, 78% specificity) among populations with stroke. [311] FAC scores have also been shown to have good concurrent (Spearman's rho = 0.901 - 0.952, respectively) and predictive validity and are correlated with walking velocity (i.e., gait speed, and stride length) as measured by the 10MWT [311,312].

Balance: Functional balance was measured using the 6-item Brief-BESTest. Each item is rated on a 3-point ordinal scale. The total score ranges between 0 and 28, with higher scores indicating better balance ability. The Brief-BESTest has shown high interrater reliability (ICC = 0.82-0.88) and the ability to differentiate fall status (sensitivity = 81%, specificity = 73%) among patients with COPD when compared to the BESTest, Mini-BESTest and Berg Balance Scale [313]. The Brief-BESTest has demonstrated comparable reliability to the BESTest ($r=0.95$, $p<0.001$) and Mini-BESTest ($r=0.94$, $p<0.001$) and moderately high predictive ability (sensitivity=0.76, specificity=0.84) in determining falls among patients with Parkinson's disease [314]. The Brief-best test has also demonstrated good intra-rater ($ICC_{2,1}$ = 0.974) and inter-rater ($ICC_{2,1}$ = 0.980) reliability and internal consistency (Cronbach's alpha = 0.818), as well as moderate to very strong correlation with other clinical measures of physical function ($r = 0.547– 0.911$, $p < 0.001$) among individuals with chronic stroke [315].

Muscle strength: To assess muscle strength, isometric peak torque during maximal voluntary contraction of the ankle plantar-flexors was measured bilaterally using a dynamometer system (Humac Norm Systems, Stoughton, Massachusetts, USA). Peak torque was defined as the maximum sustained torque value for a period of 250 milliseconds [258]. During testing, participants were instructed to perform an isometric contraction to maximal volition. Verbal encouragement from the assessor was provided in order to elicit maximal effort. A total of 3 trials was conducted for each limb with a 1-minute rest period between trials to minimize fatigue. Peak torque was tested in 0° (neutral position) of ankle plantar-dorsiflexion. Joint angle and contraction type have been shown to contribute to the activation and peak force

production of plantar flexor muscles during both isokinetic and isometric contractions after stroke [316]. Consequently, muscle length may influence the capacity to generate maximal isometric contraction, as shorter muscle length has been associated with reduced isometric force production post-stroke [7,261,317,318]. This angle was chosen according to objective anatomical models accounting for force-length properties at joint positions that were predicted to be optimal for isometric torque production, clinic relevance in manual muscle testing [262] and to match the fixed joint angle used during the ultrasound measures. Smaller relative measurement errors have also been reported for isometric testing when compared with isokinetic testing conditions [259]. As safety was a concern associated with maximal voluntary strength testing, participants were instructed to avoid performing the Valsalva maneuver during testing. This was a necessary precaution as systemic arterial blood pressure is known to be higher for resistance exercises performed in supine positions [319]. Isokinetic dynamometer strength testing among people with chronic stroke has demonstrated good inter-rater reliability for ankle plantarflexion assessments (ICC = 0.85) [320].

Sensory function: Hemiplegic pain in the upper and lower limb is a common sequela post stroke [321,322] and may be the result of central neuropathic pain without any obvious nociceptive or neurogenic origin [323,324]. Loss of motor function has been shown to be predictive of pain post-stroke [325]. This suggests a potential link between pain, sensation, and function as impairment to cutaneous sensation is known to be associated with motor dysfunction[326]. In animal limb suspension models, electrical stimulation of the dorsal root ganglion was shown to prevent bone loss during prolonged unloading of the tibia [327]. The extent to which pain and sensory threshold influence bone integrity post-stroke is unknown.

Touch pressure threshold (TPT) was assessed using Semmes-Weinstein monofilaments (Homecraft Rolyan, Patterson Medical Co., Sutton-in-Ashfield, UK) on the plantar surface of the hallux. This is an important area to examine sensory deficit, as a lack of sensation and functional strength in the hallux may greatly impair balance [328,329]. During testing, participants were blindfolded and placed in a comfortable supine lying position. A monofilament of medium diameter was applied perpendicular to the skin surface of the tested area. Participants were instructed to give a verbal indication of when the monofilament was first felt making contact with the skin in the region tested. If touch pressure sensation was consistently reported, a monofilament with the next smaller diameter was used for testing. This process continued until participants no longer consistently reported the sensation of

touch pressure. If touch pressure was not reported despite the monofilament making contact with the skin, a monofilament with the next greater diameter was used.

To evaluate pain pressure threshold (PPT), a handheld Baseline dolorimeter device (Baseline Evaluation Instruments, PTS, Italy) with a 10kg (22lb) maximum resistance was used. The PPT was defined as "the minimal pressure that causes a change in sensation from pressure to pain" [330]. The point of interface between the device and skin surface was a flat circular probe with a standardized circumference of (1.52 cm^2) covered by a rubber applicator. The probe was placed perpendicular to the surface the skin at the tender point and pushed until subjective pain threshold was reached. The tender point site for the lower limb was located at the mid-tibial shaft, as measured by the distance between the lateral malleolus and fibular head. The applicator was placed in between the tibialis anterior muscle and the palpable spine of tibia bone [331]. Participants assumed a supine position with legs fully extended and supported by the examination table. To ensure perpendicular application of the device interface to the tender point site, a bubble level was mounted to the device and the direction of force was adjusted accordingly. Operator force pressure rate was also kept constant. Mechanical force pressure rate was defined as each kilogram per 1 cm^2 (kg/cm^2) in the region of application (i.e., anatomical tender point) at a 90° vertical angle. Previous evidence suggests that the rate at which manual force is applied must be consistent in order to achieve optimal measurement reliability [332]. Therefore, pressure was applied gradually at a rate of approximately 1 kg/sec (2.2lb/sec) [330,333]. Participants were instructed to give verbal indication of when the sensation changed from pressure to pain. Three measurement trials were performed with a rest interval of 30 seconds between each trial and the average was used for analysis. Handheld dolorimetery and algometry have demonstrated excellent construct validity when correlated with force plate readings ($r = 0.90\text{-}0.99$) [332]. Although values vary based upon the influence of gender and the site being tested [330,333], good internal consistency has been reported for PPT assessments among patients with stroke (Cronbach's $\alpha > 0.929 - 0.957$) [330].

5.2.4 Statistical analysis

For between-group comparisons of bone variables, a priori power analysis was conducted using the GPower software (GPower version 3.1, Heinrich Heine Universitat Dusseldorf, Germany) [281]. Based on a study by Pang et al [55] using pQCT to assess the compressive bone strength index (cBSI) of the distal tibia epiphysis, the side-group interaction effect for the cBSI produced an effect size of f=0.297. A minimum of 70 (i.e., 35

participants per group) was required assuming the same effect size, a power of 0.80, and an alpha level of 0.05. For the regression analysis in predicting the %SSD in estimated failure load, a separate power analysis was done using the Free Statistics Calculators software (version 4.0) (https://www.danielsoper.com/statcalc/calculator.aspx?id=16). A previous pQCT study in people with chronic stroke by Pang et al. found that gait velocity was significantly associated with the bone strength index of the distal tibia (with effect size f^2=0.24), after accounting for other relevant variables. Assuming an effect size of f^2=0.24 attributable to the stroke impairment variables, a power of 0.8 and an alpha of 0.05, a minimum sample size of 64 people with stroke would be required to detect significant effects of 5 stroke impairment variables (e.g., muscle parameters measured by ultrasound, spasticity, gait velocity, etc.), after accounting for the effects of age, sex, post-stroke duration, physical activity (PASE) and BMI.

After considering the two power analyses above, a minimum of 64 individuals with stroke, and 64 control participants would be recruited.

SPSS (version 23.0, SPSS Inc., Chicago, Illinois, USA) was used for the following analyses (two-tailed). Independent t, Mann-Whitney U and χ^2 tests were used for comparing baseline between-group differences for participant characteristics according to continuous, ordinal and nominal levels of data, respectively. A mixed design two-way repeated measures analysis of variance (ANOVA) [within-subject factor: side (paretic (stroke group) or non-dominant (control group) side vs non-paretic (stroke group) or dominant (control group) side), between-subject factor: group (stroke vs control)] was performed for all HR-pQCT, ultrasound and functional outcomes measured bilaterally at a significance level of 0.05. Post hoc paired t-tests were used to compare between sides (paretic vs non-paretic, non-dominant vs dominant) and post hoc independent t-tests were used to compare the percent side-to-side difference (%SSD) between groups at a more stringent alpha level ($p \leq 0.01$). Correlation analyses (Pearson's r) were used to determine the association between the %SSD in estimated failure load of the distal tibia and %SSD or raw values (i.e., CSS, FMA, Brief-BESTest and 10MWT) of all other parameters. To calculate %SSD for each parameter measured bilaterally, the following formula was used:

$$\frac{\text{Non-paretic or Dominant side} - \text{Paretic or Non-dominant side}}{\text{Non-paretic or Dominant side}} \times 100$$

Hierarchical multiple regression analysis was then used to determine the strongest predictors of the dependent variable (%SSD in estimated failure load). Sex, age, post-stroke duration and physical activity level (PASE) were added using the enter method because of their physiological relevance. The predictors that showed significant associations with the dependent variable in the bivariate correlation analysis were then added using the stepwise method. A separate set of correlations were performed prior to the regression analysis to test the association among predictors (independent variables). To avoid multicollinearity, highly correlated predictors (i.e., > 0.6) were placed in separate models [52].

5.3 Results

5.3.1 Participant characteristics

A total of 128 participants (64 stroke, 64 control) were assessed. These were the same participants described in Chapter 4. Participant characteristics are summarized in Table 5.1. Significant between-group differences were observed for level of education, cognition, balance scores, walking velocity, walking aids or orthoses used, total number of falls within the previous year, total number of comorbidities and medications ($p \leq 0.01$). There were also no significant differences in alcohol ($p=0.276$), tobacco ($p=0.428$) or supplement usage (vitamin D: $p=1.000$; calcium: $p=0.188$) between groups. For female participants, there was also no significant difference between groups for time since menopause onset ($p=0.787$). Mean scores for the FMA (26.70 ± 4.40) and CSS (7.08 ± 2.55) suggest that, on average, participants in the stroke group exhibited a moderate degree of motor impairment [8] and mild spasticity [270], respectively. Significant between-group differences in the total number of comorbidities and medications were also observed ($p<0.001$).

5.3.2 HR-pQCT

A significant side-group interaction effect was observed for estimated failure load ($p\leq0.001$), cortical area and thickness ($p\leq0.001$), and all volumetric density parameters ($p\leq0.009$) (Table 5.2). Post hoc paired t-tests showed significant between-sides differences in these same parameters for the stroke group ($p\leq0.01$). Post hoc independent t-tests also showed significant side-to-side differences between groups for the same parameters and intracortical porosity ($p\leq0.01$). A summary of the analysis results for HR-pQCT parameters is provided in Table 5.2. Bilateral comparisons of trabecular and cortical segments of the distal tibia for a representative participant with chronic stroke and an age- and sex-matched control subject are provided in Figure 1.

5.3.3 Other measures

A significant side-group interaction effect was observed for muscle echo intensity ($p \leq 0.001$), fascicle length ($p=0.022$), shear modulus ($p=0.046$), shear wave velocity ($p=0.040$), and arterial diameter ($p=0.017$). Pennation angle and other vascular parameters showed no significant interaction effects (Table 5.3). Significant side-group interaction effects were also observed for touch pressure threshold ($p=0.006$) and isometric peak torque ($p \leq 0.001$) but not pain pressure threshold. Post hoc paired t-tests showed significant between-sides differences for fascicle length, echo intensity, arterial diameter, isometric peak torque and touch pressure threshold in the stroke group ($p \leq 0.01$), but not in controls. Only the between-sides difference in pennation angle was significant for the control group and not for the stroke group. Post hoc independent t-tests also showed a significantly greater between-group difference in %SSD for echo intensity, and isometric peak torque parameters in the stroke group ($p \leq 0.01$). A summary of the analysis results for ultrasound, and functional impairment parameters are provided in Table 5.3.

5.3.4 Correlation

The correlation analysis showed that CSS - ankle clonus ($p=0.019$), FMA ($p=0.048$), Brief-BESTest ($p<0.001$), and 10MWT ($p<0.001$) were significantly correlated with the %SSD in estimated failure load. There were also significant associations between the %SSD in estimated failure load and %SSD in isometric peak torque ($p<0.001$), fascicle length ($p=0.003$) and echo intensity measures ($p=0.003$) (Table 5.4). There were no differences in the %SSD in estimated failure load for subgroups categorized according to alcohol, tobacco, and supplement usage (Supplemental Table 5.1).

5.3.5 Regression

Of the independent variables considered for inclusion in the regression, there was a strong correlation observed between 10MWT and Brief-BESTest ($r=0.683$, $p<0.01$) (Table 5.5). Initially, these predictors were entered in separate models to avoid multicollinearity. After accounting for sex, age, stroke duration, physical activity level (PASE) and Body mass index (BMI) (model 1), CSS - ankle clonus (models 2 and 3) and 10MWT (model 3) were independently associated with the dependent variable (%SSD in estimated failure load) ($p<0.05$). The %SSD in fascicle length, %SSD in echo intensity, %SSD in isometric peak torque, FMA-LE and Brief-BESTest were eliminated as predictive factors in the stepwise

model. Overall, the final model (model 3) explained approximately 23% of the variance in the %SSD in estimated failure load (Table 5.6).

5.4 Discussion

The study results support the stated hypotheses. The side by group interaction effects indicate reduced bone density, cortical area, thickness and lower estimated failure load for the distal tibia on the paretic side when compared to the non-paretic side and the bilateral limbs of controls. The side by group interaction effects observed for ultrasound and functional measures also indicate lower values in muscle architecture, mechanical properties (i.e., stiffness and echo intensity), isometric strength and sensation of the paretic side compared to the non-paretic side and controls. Of the significant correlations found between the %SSD in estimated failure load and all other measures, spasticity (i.e., more sustained clonus of the ankle) and gait speed (i.e., 10MWT) emerged as the predominant predictors in the regression analysis.

5.4.1 Comparisons of HR-pQCT parameters

The bilateral disparity in volumetric density parameters observed in the present study are in line with findings from previous pQCT studies of the distal radius [52,80,96] and distal tibia [51,55,96] among individuals with stroke. Additionally, bilateral differences in cortical area and thickness were also apparent. Previously it was difficult to measure cortical macrostructure due to thin paretic cortical bone and the low resolution of previous pQCT scanners [52].

Lower cortical bone area on the paretic side without a side-to-side difference in total area contributed to a larger marrow cavity area on the paretic side. These findings may reflect those of previous pQCT studies involving individuals with stroke with suspected endosteal resorption [50,55]. These studies found that greater %SSD in cortical area without concomitant changes in total bone area contribute to larger marrow cavity area in the paretic tibial diaphysis.

Interestingly, bone microstructure (i.e., trabecular number, thickness, separation and intracortical porosity) showed little difference between sides and groups compared to the bilateral difference observed for other parameters. The findings of the present study are also largely in contrast to those put forth by HR-pQCT studies in other clinical and elderly populations [101,112]. Among postmenopausal women, trabecular number for both the distal radius and distal tibia was shown to be significantly lower in comparison to premenopausal

women ($p \leq 0.001$) [101]. Age-related deficits in other microstructural parameters such as cortical porosity, have been observed for both the radius ($\rho=0.7$, $p<0.001$) and tibia ($\rho=0.5$, $p<0.001$) among males and females [112].

The within-group and between-group comparisons of HR-pQCT parameters suggested that the largest contributors of the %SSD in estimated failure load of distal tibia may be volumetric density and macrostructure rather than microstructure. Taken altogether, volumetric density (4%-8%) and cortical macrostructure (0.3%-11%) showed the largest side-to-side differences relative to other bone parameters measured. In contrast, the findings of the upper limb study (Chapter 4) conducted among the same sample of participants suggest that bilateral differences in bone microstructure (i.e., %SSD in trabecular number: 12.3%, $p \leq 0.017$; %SSD in trabecular separation: 24.3%, $p \leq 0.017$) were more likely to be significant contributors of the %SSD in estimated failure load than cortical macrostructure, possibly indicating a more substantial loss and reduced connectivity of trabeculae in the distal radius. Of all the parameters assessed, trabecular vBMD and trabecular separation showed the largest %SSD (>20%) relative to other parameters measured, and were determined to contribute most to the between-group difference in %SSD of estimated failure load for the distal radius (stroke: 23.8% vs controls: 2.9%). This was approximately double the between-group difference in %SSD of the estimated failure load for the distal tibia observed in the present study (stroke: 10.3% vs controls: 0.5%).

A previous pQCT study described a somewhat similar discrepancy between upper and lower limb bone loss after stroke [96]. The non-weight bearing distal radius (11.31%) has been shown to have a %SSD of 11.3% in trabecular vBMD, which is approximately 2-3 times the relative bilateral difference observed for the distal tibia (3.2%) among individuals with stroke [96].

Although the present study does not attempt to examine the association between specific bone parameters and fracture, the findings suggest that microstructural bone may contribute less to the mechanical strength of paretic distal tibia than volumetric density and cortical macrostructure post-stroke.

5.4.2 Comparisons of ultrasound parameters

The findings suggested that stroke had a significant impact on architecture (i.e., fascicle length) and tissue mechanical properties of the medial gastrocnemius muscle (i.e., shear modulus, shear wave velocity and echo intensity as indicated by significant side by group interaction effects). With relation to the upper limb (Chapter 4), these findings are

consistent with interaction effects observed for some ultrasound parameters measured for the biceps brachii (i.e., echo intensity) but not others (i.e., shear modulus, shear wave velocity). The bilateral differences in echo intensity were relatively larger for the medial gastrocnemius (stroke: 25.6% vs controls: 1.3%) when compared to the biceps brachii (stroke: 9.2% vs controls: 0.9%), perhaps suggesting that the magnitude of stroke-related mechanical tissue alteration is more pronounced in the weight bearing lower extremities.

Significant bilateral differences in tissue mechanical properties (i.e., shear modulus, shear wave velocity, echo intensity) have been reported in studies exclusively focused on muscles of the upper limb [10,11,43,153] or lower limbs [45] after stroke. To date, there are no studies which have examined the relative differences between upper and lower limbs in the same group of individuals with chronic stroke.

5.4.3 Gait speed as a determinant of estimated failure load

In the present study, slower gait speed was independently associated with greater %SSD in estimated failure load (Model 3: β=-0.297, p=0.030), suggesting that more impaired walking speed in ambulating individuals with chronic stroke was related to more compromised bone strength on the paretic side. Though not entirely analogous, this finding is somewhat reflective of results from a previous study in which gait velocity was independently associated with the tibial bone strength index of the paretic side (β=-0.379, p=0.001) [51]. A study assessing ambulatory function post-stroke showed that slower daily gait speeds were predictive of lower daily ambulatory activity [334]. In addition, gait speed has also been shown to affect the magnitude of leg loading during walking in people with stroke, with significantly less leg loading on the paretic side observed for individuals with stroke (i.e., home and limited community ambulators) compared to controls during slower walking speeds [335]. The amount of weight borne by the paretic leg has been suggested to be a contributing factor related to bone loss post-stroke [66-68]. Another study found that a higher daily frequency of loading during standing and upright activity was associated with slower bone turnover rate between the time of onset and six months post-stroke [70]. Therefore, for those who had relatively slower walking speeds, lower ambulatory activity and less leg loading during their gait cycle (i.e., pattern of asymmetrical weight-bearing), these factors may combine to adversely affect bone quality in the lower limbs, particularly on the paretic side.

Early ambulation and structured group exercise interventions may play an important role in maintaining bone strength and reducing fracture risk after stroke [6,336]. Treadmill

walking interventions have been shown to produce modest improvement in tibial bone geometry among people with stroke [95]. Comprehensive, multicomponent community-based fitness and mobility programs have also been shown to increase bone mineral density and cortical thickness after stroke [3,91]. The dosage of gait and mobility training at different stages of stroke recovery remain the subject of further study.

5.4.4 Spasticity as a determinant of estimated failure load

The CSS subscale score for sustained ankle clonus was independently associated with the %SSD in estimated failure load in the regression models (Model 2: β=0.291, p=0.021; Model 3: β=0.248 p=0.044). This perhaps suggests that neurogenic aspects of spasticity had a predominant influence over other non-neurogenic scale components (i.e., resistance to passive movement) in regards to their association with the %SSD in estimated failure load. However, a general consensus regarding the impact of spasticity on post-stroke bone status for both upper and lower limbs is currently lacking as reported correlations between these parameters have been inconsistent across studies [49-52,55,80,85].

The ability to assess diverse presentations of spasticity may be a methodological limitation of previous studies. The Modified Ashworth Scale is only used to evaluate resistance to joint displacement during passive elbow extension or ankle dorsiflexion. By contrast, the CSS is a multi-component scale offering a more comprehensive evaluation of spasticity post-stroke. A previous study showed spasticity (measured by the Modified Ashworth Scale) was moderately correlated with cortical bone mineral content (r=0.457, p<0.05) and cortical thickness (r=0.476, p<0.05) of the paretic distal radius in bivariate analyses and independently associated with %SSD in cortical thickness in regression analyses (β=0.497, p=0.001) [49]. In a study of the lower limb, spasticity was significantly associated with multiple bone parameters (i.e., total bone mineral content, total density, trabecular density and bone strength index) ($p < 0.05$) and moderate to severe spasticity was independently associated with the bone strength index (β=-0.235, p=0.028) [51] in multiple regression models. Yet in another lower limb study, spasticity and bone strength index have shown no significant correlation (males: r=-0.167, females: r=-0.014) suggesting that hypertonic muscle activity may have conferred a somewhat protective effect on bone [50]. For investigating the impact of spasticity on tibial bone parameters, future studies should consider the precision of the assessment used. Categorization of patient subgroups should also be based on the severity and clinical presentation of spasticity.

5.4.5 Other factors

Although there was a mild correlation observed between %SSD in isometric peak toque and %SSD in estimated failure load in the bivariate analysis ($r=0.386$, $p<0.001$), the influence of plantarflexor muscle strength was diminished in the regression analysis. This is in contrast to previous studies citing the apparent relationship between muscle weakness and bone strength in paretic limbs post-stroke [52,53,96]. The association between muscle weakness and bone strength is also evident in previous pQCT and DXA studies involving the distal radius [49,85], the proximal femur [86,125] and the tibia post-stroke [122]. Intervention studies also showed that comprehensive exercise programs which incorporate an element of resistance training may improve bone status post-stroke [3,91]. However, in the present study, muscle weakness was not a significant determinant of bone strength. One potential explanation for the lack of association observed in the regression analysis is the measurement of peak torque produced during isometric contractions (i.e., static) rather than during dynamic contractions. In studies using animal models, dynamic contractions were shown to be more effective for increasing bone formation than static contractions [337,338]. Yet another possible explanation was the measurement of strength involving the plantar flexors for performing a singular joint movement. Composite muscle strength scores involving multiple muscle groups and joint actions (i.e., knee and hip flexion/extension) may be more representative of total limb strength [49].

In the bivariate analysis, the %SSD in echo intensity showed a mild negative correlation with %SSD in estimated failure load ($r=-0.259$, $p=0.003$) in the stroke group. Although other measures of mechanical tissue properties such as shear wave velocity and shear modulus have demonstrated moderate correlation with echo intensity in previous studies [10,11], echo intensity emerged as a comparatively a stronger correlate of the estimated failure load of the distal tibia in this study. The %SSD in fascicle length also demonstrated a mild correlation with %SSD in estimated failure load ($r=0.261$, $p=0.003$). This is understandable, given the previously observed relationship between stroke-related motor impairment and muscle architecture in the upper and lower limbs [9,17]. Better motor control has been shown to be associated with greater bone preservation in the lower limb within the first 6 months of stroke recovery [70]. However, the effects of both the %SSD in fascicle length and %SSD in echo intensity were diminished in the multivariate regression analysis. This is in contrast to our findings for the distal radius (Chapter 4), where %SSD in echo intensity was a significant determinant of the estimated failure load. This is despite the %SSD in echo intensity found in the distal radius (9.2%) being relatively smaller than the distal tibia

(25.6%) identified here, as noted previously. Perhaps the estimated failure load of the weight bearing tibia was more influenced by the amount of loading during impact activities such as walking (i.e., influenced by gait speed), rather than compositional change to the muscle itself.

There was also no apparent association between %SSD in estimated failure load and any vascular parameters measured. Reduced blood flow volume, arterial diameter and unilateral vascular remodeling [240,241,272,339,340] are resultant adaptations of reduced metabolic demand of paretic muscles and diminished cardiovascular fitness after stroke. These factors are thought play an important role in bone metabolism [75,341,342]. Changes in peripheral microvasculature are also evident after stroke, with lower intramuscular blood perfusion of paretic lower limb muscles [223]. Cardiovascular fitness level has been identified as a modifiable risk factor in the prevention of both cardiovascular diseases such as atherosclerosis and bone loss during osteoporosis [343] given their close biological linkage [344,345]. The inner arterial wall and the osteon of cortical bone are both lined with an endothelial lumen [344]. In addition to the endothelial interface shared between bone and systemic vessels, highly vascular inner trabecular bone is also known to have a rich blood supply from its interface with bone marrow endothelial tissue [345]. Although no association between vascular parameters and bone strength were observed in the present study, previous studies in populations with stroke have found a relationship between the vascular compliance of both large [52] and small peripheral arteries [52,53] and bone strength index of the distal radius. In addition to bone porosity [341], the contractile function of skeletal muscle is known to impact the delivery of blood through microvascular capillary networks within Haversian and Volkman canals of bone, thus indirectly influencing nutrient exchange and bone metabolism [342]. It is unclear as to why no association was observed for any vascular measures as the sample size recruited was comparable to previous studies [52,53]. One possible explanation may be the difference in measures used between studies. Blood flow volume in particular is perhaps more reflective of overall cardiac output capacity [346], while vascular elasticity measured in previous studies [52,53] is representative of peripheral vascular adaptation (i.e. arterial compliance to flow volume and endothelial function). Peak systolic velocity is considered be a robust measure of systemic vascular function [347,348] demonstrating good association with other angiographic measures of arterial compliance and stenosis [349] and may thus be a more useful comparator to methods used previously for assessing the relationship between cardiovascular parameters and bone strength [52,53].

In the present study, a significant side by group interaction effect was found for touch pressure threshold ($F=7.89$, $p<0.006$). However, it was not significantly associated with

the %SSD in estimated failure load. Peripheral sensory deficits are common post-stroke but the role of sensation in bone health outcomes remains unknown. Electrical stimulation of afferent sensory relay in the dorsal root ganglion has been shown to prevent disuse-related bone loss in animal limb suspension models [327]. A similar phenomenon of bone density loss reversal has been observed in the distal femoral epiphysis of patients with spinal cord injury following high volume functional electrical stimulation (FES) cycling [350]. Although pathologically multifactorial, sublesional bone demineralization in distal epiphyseal bone sites of patients with spinal cord injury may have a substantial neurogenic component [351]. Studies involving a robust evaluation of post-stroke sensory deficits and bone status will be instrumental in understanding their association and clinical implications.

5.4.6 Limitations

There are several limitations that should be addressed with regards to the scanning procedures analysis and study designed used. The standard micro-finite element analysis with a uniform linear modulus was used for all study participants. With non-linear approaches, cortical and trabecular bone elements are assigned different moduli [107]. These values also differ based on modulus direction [294], with non-linear approaches rendering more direct mechanical bone strength estimations. However, there is also support for the use of linear approaches [107]. Due to the lower vBMD, cortical area, and thickness observed in the present study, a non-linear approach may be useful in assessing bilateral disparity in bone parameters among patients with stroke. Additionally, a standardized fixed offset distance was used for determining the scan region across all participants. Although several studies have used a fixed offset distance method previously [99,104,105,111,276-278], a relative offset distance approach, even with its own inherent limitations, considers individual limb length differences across participants [282]. Regarding the analysis, other confounders which impact bone metabolism were not accounted for as covariates in the regression models due to the limited sample size of the present study. A maximum of six predictors per model (roughly 10 observations per variable) [295] were used under an assumption of minimal variance ($n \geq 8$, with additional degrees of freedom for covariates) [296]. There are also limitations in the generalizability of the findings due to the study design. All participants from the stroke and control groups were recruited through a non-probability sampling method and may unintentionally exclude individuals with diverse clinical presentations. Furthermore, the study was a cross-sectional design and do not provide a causal link between the impairments previously described and fracture risk after stroke. Finally, previous studies have shown sex-specific differences in

tibial bone geometry between males and females after stroke [50]. Further analyses based on gender may be warranted, as there were a larger proportion of males to females in the overall sample. Demographic reports suggest that stroke is more prevalent among females than males [1]. Hence, future studies should aim to recruit larger samples sizes with a representative male to female subject ratio in accordance with stroke prevalence in an effort to enhance the generalizability of the results.

5.5 Conclusion

This study used HR-pQCT, multimodal ultrasound and clinically relevant tests to assess muscle and bone properties as well as functional impairment of the lower limb in individuals with chronic stroke. The paretic distal tibia showed compromised bone density and cortical macrostructure, contributing to a comparatively lower estimated failure load than that of the non-paretic tibia. Bilateral differences in microstructure did not contribute significantly to the side-to-side difference in estimated failure load. Gait speed and spasticity, particularly sustained clonus, emerged as strong correlates of bone strength in the distal tibia. Future intervention strategies with the aim of preserving or improving bone strength should incorporate elements which target these functional limitations.

Table 5.1 Subject characteristics

		Stroke (n=64)	Control (n=64)	p
Demographics	Sex (men/women), n	38/26	39/25	0.858
	Age (years)	60.8 ± 7.7	59.4 ± 7.8	0.306
	Menopause (women), years	12.4 ± 13.1	11.5 ± 9.9	0.787
	Height (cm)	161.06 ± 8.38	163.98 ± 8.86	0.058
	Weight (kg)	62.68 ± 8.88	63.07 ± 9.87	0.814
	BMI (kg/m^2)	24.3 ± 3.1	23.4± 2.8	0.081
	Education (years)	9.8 ± 3.7	11.8 ± 3.7	0.002[b]
	Leg dominance (left/right/equivalent), n	5/56/3	2/62/0	0.101
	AMT (out of 10)	9.3 ± 1.1	9.9 ± 0.4	<0.001[b]
	PASE	114.7 ± 87.4	142.2 ± 79.4	0.065
	Brief BESTest	10.83 ± 5.10	14.75 ± 2.39	<0.001[b]
	10MWT Velocity (m/s)	0.81 ± 0.39	1.87 ± 0.31	<0.001
	Walking aid (none/cane/quadripod/wheelchair), n	14/41/6/3	64/0/0/0	<0.001[b]
	Orthosis (none/ indoor/ outdoor/ both), n	51/1/10/2	64/0/0/0	0.002[b]
	Total number of falls (0/1), n	47/17	59/5	0.005[a]
	Previous surgery (Yes/No), n	33/31	32/32	0.860
Stroke Characteristics	Paretic side (left/right), n	36/28	-	-
	Total number of strokes (1/2), n	63/1	-	-
	Type of stroke (ischemic/hemorrhagic), n	41/23	-	-
	Stroke duration, years	5.8 ± 4.0	-	-
	Stroke location (Oxfordshire classification) (ACS/ PACS/ LS/ PCS/ hemorrhagic)	8/22/10/1/23	-	-
	CSS – Achilles tendon jerk (0-4)	1.69 ± 0.77	-	-
	CSS – Resistance to displacement (0-8)	4.06 ± 2.04	-	-
	CSS – Ankle clonus (1-4)	1.33 ± 0.59	-	-
	CSS – Lower limb total (1-16)	7.08 ± 2.55	-	-
	FMA – Lower limb (0-34)	26.70 ± 4.40	-	-
Comorbidity	Total number of comorbidities per person	1.3 ± 1.3	0.6 ± 0.9	<0.001[b]
	Hypertension, n	37	22	0.006[b]
	Hyperlipidemia, n	21	4	<0.001[b]
	Cardiac arrhythmia, n	1	0	0.315
	Diabetes mellitus, n	14	8	0.150
	Ischemic heart disease, n	1	0	0.315
Medications	Total number of medications per person	4.0 ± 2.7	0.8 ± 1.2	<0.001[b]
	Antihypertensive agents, n	42	16	<0.001[b]
	Hypolipidemic agents, n	41	10	<0.001[b]
	Hypoglycemic agents, n	10	6	0.259
	Anticoagulants, n	23	3	<0.001[b]
	Antispasmodic agents, n	6	0	0.011[a]
	Cardiac medication/ agent, n	4	0	0.039[a]
	PPI/ Gastric agents, n	25	2	**<0.001**
	SSRI/ Antidepressants, n	8	1	**0.016**
Other	Alcohol history (yes/no), n	14/50	24/40	0.053
	Alcohol consumption (drinks/day)	0.2 ± 0.3	0.1 ± 0.3	0.276
	Smoking history (yes/no), n	15/49	14/50	0.833
	Tobacco use (packs/day)	0.7 ± 0.4	0.6 ± 0.3	0.428
	Daily Vitamin D supplementation (yes/no), n	4/60	4/60	1.000
	Daily Calcium supplementation (yes/no), n	3/61	7/57	0.188

[a] $p \leq 0.05$ Statistically significant
[b] $p \leq 0.01$ Statistically significant
AMT = Abbreviated Mental Test, PASE = Physical Activity Scale for the Elderly, CSS = Composite Spasticity Scale, FMA = Fugl-Meyer Assessment, ACS = Anterior Circulation Syndrome, PACS = Partial Anterior Circulation Syndrome, LS = Lacunar Syndrome, PCS = Posterior Circulation Syndrome

Table 5.2 Comparison of HR-pQCT variables

		Stroke Group (n=64)			Control Group (n=64)			Main Effect: Side (Within)		Main Effect: Group (Between)		Side × Group Interaction Effect	
	Parameter	Paretic	Non-Paretic	SSD (%)	Non-Dominant	Dominant	SSD (%)	F	p	F	p	F	p
Volumetric Density	Total vBMD (mg HA/cm^3)	255.42 ± 64.63	277.45 ± 55.77[a]	8.69 ± 8.19[b]	285.12 ± 51.99	286.29 ± 53.32	0.22 ± 5.04	59.51	<0.001*	3.79	0.054	48.07	<0.001*
	Cortical vBMD (mg HA/cm^3)	809.46 ± 82.17	843.20±66.12[a]	4.16 ± 3.81[b]	872.10 ± 57.32	871.76 ± 56.25	-0.05 ± 1.96	61.26	<0.001*	15.67	<0.001*	63.78	<0.001*
	Trabecular vBMD (mg HA/cm^3)	145.40 ± 39.81	151.50 ± 35.10[a]	4.67 ± 10.94[b]	147.30 ± 35.32	147.61 ± 33.60	0.30 ± 6.31	8.59	0.004*	0.03	0.874	6.99	0.009*
Macrostructure	Cortical Area (mm^2)	109.53 ± 32.08	122.56 ± 29.19[a]	11.53 ± 9.21[b]	131.94 ± 24.64	132.42 ± 25.59	-0.05 ± 5.64	75.62	<0.001*	10.87	0.001*	65.33	<0.001*
	Cortical Perimeter (mm)	102.23 ±10.60	102.51 ±10.55	0.30 ± 1.73	103.33 ± 10.40	103.45 ± 10.42	0.16 ± 1.78	1.54	0.216	0.30	0.583	0.27	0.602
	Cortical Thickness (mm)	1.28 ± 0.37	1.43 ± 0.33[a]	10.83 ±10.44[b]	1.50 ± 0.27	1.51 ±0.30	-0.25 ± 6.49	55.97	<0.001*	7.34	0.008*	49.58	<0.001*
Microstructure	Trabecular Area (mm^2)	578.64 ± 138.73	571.38 ± 137.71	-1.31 ± 4.90	576.51 ± 133.86	577.68 ± 135.11	-0.05 ± 4.64	1.75	0.188	0.01	0.931	3.36	0.069
	Trabecular Number (1/mm)	1.12±0.17	1.13±0.15	0.94 ± 6.56	1.10 ± 0.17	1.11 ± 0.16	1.03 ± 4.78	3.30	0.072	0.64	0.426	0.03	0.870
	Trabecular Thickness (mm)	0.25 ±0.02	0.26 ±0.02	0.88 ± 4.52	0.26 ± 0.02	0.25 ± 0.02	-0.17 ± 3.52	0.36	0.550	0.02	0.904	1.83	0.179
	Trabecular Separation (mm)	0.88 ± 0.17	0.86 ± 0.14	-1.72 ± 6.99	0.90 ± 0.17	0.88 ± 0.15	-1.41 ± 5.39	7.10	0.009*	0.37	0.543	0.12	0.728
	Intra-cortical Porosity (%)	0.04± 0.02	0.04±0.01	-12.14 ± 38.04[b]	0.03 ± 0.01	0.03 ± 0.01	-6.55 ±32.52	4.21	0.042*	3.10	0.081	1.13	0.291
μFE	Stiffness (N/mm)	157546.23 ± 48660.51	174974.79 ±46134.29[a]	10.64 ± 10.55[b]	182486.54 ± 45730.71	183164.70 ± 46162.40	-0.05 ± 5.61	53.05	<0.001*	4.11	0.045*	45.40	<0.001*
	Failure Load (N)	-8526.47 ± 2565.85	-9437.76 ± 2405.64[a]	10.33 ± 10.27[b]	-9855.60 ± 2400.04	-9903.59 ± 2425.57	0.05 ± 5.49	55.35	<0.001*	4.39	0.038*	44.82	<0.001*

Value expressed as mean ± SD unless otherwise indicated

* $p < 0.05$ Statistically significant results (two-way ANOVA)

[a] $p < 0.01$ Statistically significant between-sides difference (post hoc paired t-test)

[b] $p < 0.01$ Statistically significant side-to-side difference between two groups (post hoc independent t-test)

vBMD = Volumetric Bone Mineral Density, HA = Hydroxyapatite, N = Newtons, μFE = Finite Element Analysis

Table 5.3 Comparison of ultrasound and functional impairment variables

		Stroke Group (n=64)			Control Group (n=64)			Main Effect: Side (Within)		Main Effect: Group (Between)		Side × Group Interaction Effect	
Measures	Paretic	Non-Paretic	STSD (%)	Non-Dominant	Dominant	STSD (%)	F	p	F	p	F	p
Ultrasound	Fascicle Length											
	4.58 ± 0.74	4.85 ± 0.58[a]	5.38 ±11.85	5.00 ± 0.59	5.07 ± 0.66	0.95 ±7.73	15.52	<0.001*	9.23	0.003*	5.40	0.022*
	Pennation Angle											
	20.09 ± 2.91	19.74 ± 2.93	-3.31 ±17.84	21.40 ± 2.81[a]	20.76 ± 2.96	-3.61 ±9.30	4.27	0.041*	6.57	0.012*	0.39	0.533
	Shear Modulus (kPa)											
	59.74 ± 50.07	47.67 ± 16.81	-37.30 ±114.26	50.46±15.16	51.54±18.46	-0.78 ±16.72	2.84	0.094	0.47	0.495	4.06	0.046*
	Shear Wave Velocity (m/s)											
	4.23 ± 1.24	3.86 ± 0.68	-12.14 ±36.74	4.00 ±0.55	4.00 ±0.69	-0.98 ±8.96	4.37	0.039*	0.10	0.759	4.31	0.040*
	Echo Intensity											
	95.04 ± 20.29[a]	78.09 ± 20.39	-25.58 ±25.37[b]	78.12 ±19.57	81.04 ±21.45	1.32 ±20.22	25.24	<0.001*	4.40	0.038*	50.60	<0.001*
	Peak Systolic Velocity (cm/s)											
	48.10 ± 15.56	47.05 ± 14.13	-4.52 ± 26.79	44.43 ±8.21	44.70 ± 9.83	-1.73 ±19.87	0.17	0.679	2.37	0.126	0.48	0.488
	Blood Flow Volume (mL/min)											
	38.43 ± 23.06	39.04 ± 29.89	-28.64 ±91.85	29.18 ±12.42	32.54 ±16.15	-6.39 ±69.62	1.11	0.295	5.73	0.018*	0.53	0.467
	Arterial Diameter											
	0.53 ± 0.11	0.58 ± 0.11[a]	7.80 ±14.82	0.53 ±0.11	0.55 ±0.10	2.14 ±13.96	19.91	<0.001*	0.77	0.382	5.88	0.017*
Functional Impairment	Isometric Peak Torque (N/m)											
	40.42 ± 15.92	63.93 ± 23.55[a]	30.66 ±34.71[b]	74.83 ± 35.36	74.41 ±37.69	-4.28 ± 22.35	43.05	<0.001*	20.92	<0.001*	46.26	<0.001*
	Pain Pressure Threshold (kg)											
	9.10 ± 4.62	8.92 ± 3.99	-13.16 ± 98.67	7.31 ±3.36	7.39 ±3.15	0.19 ± 23.89	0.06	0.813	6.65	0.011*	0.39	0.531
	Touch Pressure Threshold (gram)											
	31.34 ± 84.86[a]	3.69 ± 22.41	-8722.86 ±53538.08	0.53 ±0.71	0.41 ±0.70	-156.03 ± 444.99	8.03	0.005*	8.04	0.005*	7.89	0.006*

Value expressed as mean ± SD unless otherwise indicated
* $p \leq 0.05$ Statistically significant results (two-way ANOVA);
[a] $p \leq 0.01$ Statistically significant between-sides difference (post hoc paired t-test)
[b] $p < 0.01$ Statistically significant side-to-side difference between two groups (post hoc independent t-test)
kPa = Kilopascals

Table 5.4 Correlates of side-to-side difference in estimated failure load

	Variables	r	p
Stroke Impairment	CSS - Achilles Tendon Jerk	0.177	0.162
	CSS - Resistance to Displacement	0.041	0.745
	CSS - Ankle Clonus	0.293*	0.019
	CSS - Lower Limb Total	0.155	0.223
	FMA - LE	-0.248*	0.048
	Brief BESTest	-0.353**	<0.001
	10MWT	-0.542**	<0.001
Other	Isometric Peak Torque (plantarflexion)	0.386	<0.001**
	Pain Pressure Threshold	0.038	0.673
	Touch Pressure Threshold	-0.131	0.140
	Total Comorbidities	0.187	0.034
	Total Medications	-0.191	0.130
	Alcohol Consumption	0.199	0.230
	Tobacco Usage	0.340	0.071
Ultrasound	Fascicle Length	0.261	0.003**
	Pennation Angle	-0.085	0.339
	Echo Intensity	-0.259	0.003**
	Peak Systolic Velocity	-0.103	0.249
	Blood Flow Volume	-0.044	0.621
	Arterial Diameter	0.091	0.308
	Shear Wave Velocity	-0.053	0.554
	Shear Modulus	-0.112	0.208

*Significant correlation at the 0.05 level (2-tailed)
**Significant correlation at the 0.01 level (2-tailed)
FI = Functional impairment, %SSD = Percent side-to-side difference, CSS = Composite Spasticity Scale, FMA-LE = Fugl-Meyer Assessment-Lower Extremity

Table 5.5 Correlation among predictor variables

	CSS Ankle Clonus	FMA Lower Extremity	Brief BESTest	10 Meter Walk Test	%SSD Peak Torque	%SSD Fascicle Length	%SSD Echo Intensity
CSS - Ankle Clonus	—	-0.260*	-0.76	-0.081	0.199	0.314*	-0.023
FMA-LE		—	0.386**	0.379**	-0.477**	0.060	-0.179
Brief BESTest			—	**0.683****	-0.408**	-0.068	0.072
10MWT				—	-0.498**	0.170	0.389**
%SSD PT					—	0.008	-0.245**
%SSD FL						—	0.073
%SSD EI							—

*Significant correlation at the 0.05 level (2-tailed)
**Significant correlation at the 0.01 level (2-tailed)
CSS = Composite Spasticity Scale, FMA-LE = Fugl-Meyer Assessment - Lower Extremity, 10MWT = 10 Meter Walk Test, IPT = Isometric Peak Torque, FL = Fascicle Length, EI = Echo Intensity

Table 5.6 Regression models

Predictor	F	R^2	B	95% CI		Beta	Sig.
Model 1							
Age	0.996	.079	.046	-.305	.397	.035	.794
Sex			5.347	-.232	10.926	.258	.060
Stroke duration			-.032	-.763	.700	-.012	.931
PASE			-.015	-.048	.019	-.125	.382
BMI			-.0399	-1.297	.499	-.118	.377
Model 2							
Age	1.829	.161	.042	-.296	.381	.032	.804
Sex			5.234	-.139	10.606	.252	.056
Stroke duration			.032	-.675	.738	.012	.929
PASE			-.019	-.051	.014	-.158	.255
BMI			-.309	-1.177	.559	-.092	.479
Ankle clonus			5.039	.774	9.305	.291	.021*
Model 3							
Age	2.388	.230	.044	-.283	.371	.033	.788
Sex			4.157	-1.128	9.443	.200	.121
Stroke duration			-.093	-.785	.600	-.036	.789
PASE			-.003	-.037	.032	-.021	.884
BMI			-.470	-1.322	.382	-.139	.273
Ankle clonus			4.297	.118	8.476	.248	.044*
10MWT			-7.912	-15.018	-.807	-.297	.030*

* $p \leq 0.05$ Statistically significant
B = Unstandardized regression coefficient, Beta = Standardized regression coefficient, 95%CI = 95% confidence interval
PASE = Physical Activity Scale for the Elderly, BMI = Body Mass Index, 10MWT = 10 Meter Walk Test

Supplemental Table 5.1 Differences in %SSD in estimated failure load for subgroups according to alcohol, tobacco and supplement usage (participants with stroke)

	N	Mean Ranks	Sum of Ranks	p
Non-drinker	50	34.38	1719.00	0.126
Drinker	14	25.79	361.00	
Non-smoker	49	33.93	1662.50	0.267
Smoker	15	27.83	417.50	
No supplement usage	61	32.37	1974.50	0.811
Calcium (daily)	3	35.17	105.50	
No supplement usage	60	31.93	1915.50	0.353
Vitamin D (daily)	4	41.13	164.50	

Significant correlation at the 0.05 level (2-tailed)
%SSD = percent side-to-side difference

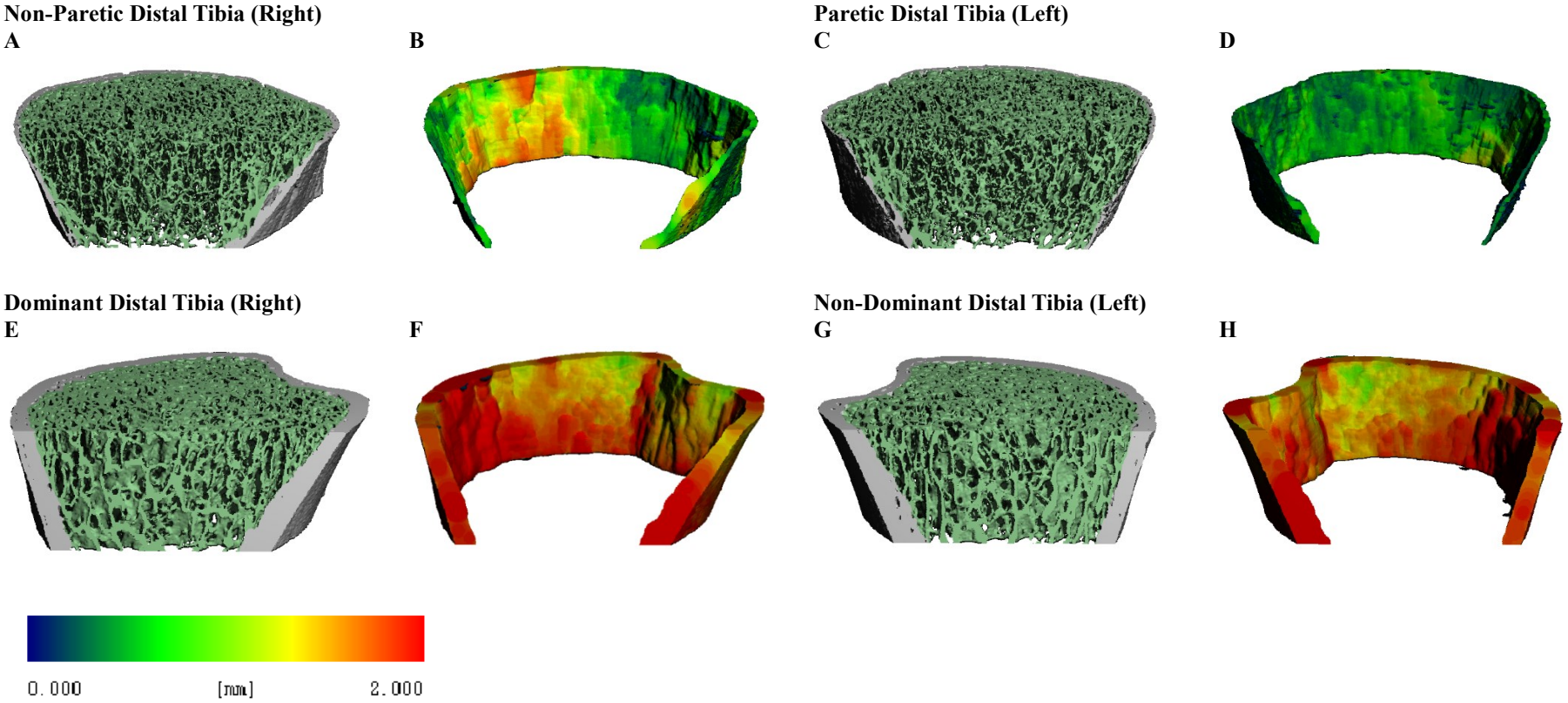

Figure 5.1 Bilateral within and between groups comparison of the distal tibia

HR-pQCT generated 3D rendering of the distal tibia for a representative male participant with chronic stroke and an age-matched male control participant (lower panel). The sagittal cut plane was standardized at a depth of 30% with the wider epiphyseal portion of the tibia oriented superiorly and the diaphyseal portions inferiorly. There are comparatively fewer trabeculae with reduced density and network connectivity between the participant with stroke and control participant. Thinning of the cortical shell is also more pronounced on the paretic side compared to the non-paretic side as indicated by a darker spectral color gradient (standardized range 0-2mm). Bilateral difference in cortical thickness is less pronounced in the control participant. The upper panel shows a bilateral view of the (A) trabecular segment and (B) cortical thickness of the non-paretic tibia compared to the (C) trabecular segment and (D) cortical thickness of the paretic tibia and the lower panel shows the (E) trabecular segment and (F) cortical thickness of the dominant tibia relative to the (G) trabecular segment and (H) cortical thickness of the non-dominant tibia.

Chapter 6. Conclusion

6.1 Project scope

Bone health is compromised after stroke with greater incidence of fall [62] and fracture [63] occurring on the paretic side. Muscle tissue alterations, a common sequela after stroke, also appear to be more pronounced on the paretic side in comparison to non-paretic side [11]. As evidenced by the inherent mechanoresponsivity of musculoskeletal tissues [352], a muscle-bone relationship in people with stroke has been previously postulated [96] with differing clinical implications for the upper [52] and lower extremities [51]. As previously stated, the main objectives of this thesis project were to examine the impact of stroke on muscle and bone properties using diagnostic ultrasound and HR-pQCT, respectively. The data gathered were then used to assess the muscle-bone relationship in individuals with chronic stroke. The main findings for each of the project components and potential implications are summarized in the following section.

6.2 Summary of study findings and future research directions

The systematic review in Chapter 2 demonstrated that ultrasound elastography had moderate to good reliability, excellent discriminative and known-groups validity and good overall responsiveness for the assessment of muscle stiffness in populations with neurological conditions. Variance in reliability estimates were thought to be attributed to differences in reported values [208], muscle sites [202], muscle activity [44], operator experience [203], probe alignment [46], intersystem variance [171,211] and acquisition procedures used [207] and subject age [41]. Future studies should dedicate specific attention to the standardization of measurement protocols, especially those involving more than one operator and visual confirmation of muscle passivity rather than the use of surface EMG. Support for the convergent or criterion validity of ultrasound elastography was lacking. Other methods such as myotonometry may be useful comparators and have been used to examine stiffness after stroke [219] although not concurrently with elastography [221]. Future studies should involve the use of other comparators measuring biomechanical tissue properties.

The study in Chapter 3 showed that multimodal ultrasound had moderate to excellent test-retest reliability for measuring muscle architecture, mechanical and vascular outcomes in a cohort of 20 individuals with chronic stroke. These measures also demonstrated fair to moderate correlation with several relevant clinical measures assessing similar or related measurement constructs. This study builds on the work of previous studies examining

measurement reliability as a primary outcome in individuals with chronic [46] and acute stroke [43]. Future studies involving ICC estimates [269], SEM and %CV [229] should involve larger sample sizes. Additionally, as there is substantial variability throughout the available literature regarding measurement protocols [203], future studies should attempt to incorporate procedural aspects that enhance reliability (i.e., standardized probe orientation, gel layer, ROI size and depth).

Using HR-pQCT enabled us to study bone microstructure in individuals with chronic stroke, which is unexplored in previous research. In the study described in Chapter 4, it was found that compromised trabecular microstructure in addition to lower volumetric bone density may be a significant factor contributing to the side-to-side difference in estimated failure load. The material alterations in paretic muscle (i.e. echo intensity), perceived disuse (i.e., Motor Activity Log) and motor impairment (Fugl-Meyer Motor Assessment) emerged as the predominant determinants of estimated failure load in the distal radius. As the association between motor impairment severity, disuse and reduced bone strength on the paretic side appear to be consistent with relevant associations from previous studies [49,279], these may be important outcomes in future intervention strategies aimed at maintaining or improving bone strength. Additionally, the association between echo intensity and functional impairment [48] as well as other muscle tissue properties (i.e., stiffness) [11] suggests biomechanical muscle parameters may also serve as potential intervention targets for improving functional, and possibly bone, outcomes. Longitudinal studies which involve the assessment of these variables and their association with mechanical bone strength are needed. Furthermore, controlled intervention studies are also required to test the efficacy of these potential methods for increasing bone strength.

The study described in Chapter 5 showed that while significant side-to-side difference in volumetric bone density was also found for the distal tibia, compromised cortical macrostructure (i.e., cortical area) and cortical microstructure (i.e., cortical thickness) may have contributed more to the side-to-side difference in estimated failure load of the tibia. Also, the overall differences in bone microstructure were comparatively less pronounced for the weight bearing tibia than the non-weight bearing radius (Chapter 4). Gait speed (i.e., 10 meter walk test) and spasticity (i.e., ankle clonus subscore of the Composite Spasticity Scale) were the main determinants of estimated failure load in the distal tibia. As less bone loss has been observed following early motor recovery, mobilization, and weight-bearing after stroke in longitudinal studies [70,92], early ambulation and structured group exercise interventions with a walking or mobility component may help in maintaining bone strength after stroke.

However, this hypothesis will need to be tested in future research [6,336]. Previously reported associations (or lack thereof) between spasticity and bone outcomes of the upper and lower limbs are inconsistent [49-52,55,80,85] indicating the need for future studies with greater measurement specificity and precision for understanding the magnitude of association between these parameters in the lower extremities after stroke.

6.3 Concluding remarks

In summary, the evidence put forth by the aforementioned studies reveal important insights with regards to the impact of stroke on muscle and bone properties in the chronic stages of stroke recovery. It also highlights the interrelated nature of muscle and bone tissues post-stroke and their clinical correlates. These may serve as potential targets for therapeutic intervention strategies aimed at improving muscle function and bone strength after stroke.

References

1. Yu R, Chau P, McGhee S, Chau J, Lee C, Chan C, et al. Trends of disease burden consequent to stroke in older persons in Hong Kong: Implications of population ageing. The Hong Kong Jockey Club; 2012.
2. Feigin VL, Lawes CM, Bennett DA, Barker-Collo SL, Parag V. Worldwide stroke incidence and early case fatality reported in 56 population-based studies: a systematic review. The Lancet Neurology. 2009;8(4):355-69.
3. Pang MYC, Ashe MC, Eng JJ, McKay HA, Dawson AS. A 19-week exercise program for people with chronic stroke enhances bone geometry at the tibia: a peripheral quantitative computed tomography study. Osteoporos Int. 2006;17(11):1615-25. Epub 2006/07/29.
4. van der Lee JH, Beckerman H, Knol DL, de Vet HC, Bouter LM. Clinimetric properties of the motor activity log for the assessment of arm use in hemiparetic patients. Stroke. Jun 2004;35(6):1410-4. Epub 2004/04/17.
5. Poole KES, Reeve J, Warburton EA. Falls, fractures, and osteoporosis after stroke. Time to think about protection? Stroke. 2002;33(5):1432-6.
6. Eng JJ. Balance, falls, and bone health: Role of exercise in reducing fracture risk after stroke. The Journal of Rehabilitation Research and Development. 2008;45(2):297-314.
7. McCrea PH, Eng JJ, Hodgson AJ. Time and magnitude of torque generation is impaired in both arms following stroke. Muscle Nerve. Jul 2003;28(1):46-53. Epub 2003/06/18.
8. Duncan PW, Goldstein LB, Horner RD, Landsman PB, Samsa GP, Matchar DB. Similar motor recovery of upper and lower extremities after stroke. Stroke. 1994;25(6):1181-8.
9. Nelson CM, Murray WM, Dewald JPA. Motor Impairment-Related Alterations in Biceps and Triceps Brachii Fascicle Lengths in Chronic Hemiparetic Stroke. Neurorehabil Neural Repair. Sep 2018;32(9):799-809. Epub 2018/08/24.
10. Gao J, He W, Du LJ, Chen J, Park D, Wells M, et al. Quantitative Ultrasound Imaging to Assess the Biceps Brachii Muscle in Chronic Post-Stroke Spasticity: Preliminary Observation. Ultrasound Med Biol. Feb 2 2018. Epub 2018/02/06.
11. Lee SS, Spear S, Rymer WZ. Quantifying changes in material properties of stroke-impaired muscle. Clin Biomech (Bristol, Avon). Mar 2015;30(3):269-75. Epub 2015/02/02.
12. English C, McLennan H, Thoirs K, Coates A, Bernhardt J. Loss of skeletal muscle mass after stroke: a systematic review. Int J Stroke. Oct 2010;5(5):395-402. Epub 2010/09/22.
13. Kallenberg LA, Hermens HJ. Motor unit properties of biceps brachii in chronic stroke patients assessed with high-density surface EMG. Muscle Nerve. Feb 2009;39(2):177-85. Epub 2008/11/27.
14. Dietz V, Ketelsen UP, Berger W, Quintern J. Motor unit involvement in spastic paresis: Relationship between leg muscle activation and histochemistry. J Neurol Sci. 1986/08/01/ 1986;75(1):89-103.
15. Ryan AS, Dobrovolny CL, Smith GV, Silver KH, Macko RF. Hemiparetic muscle atrophy and increased intramuscular fat in stroke patients. Arch Phys Med Rehabil. Dec 2002;83(12):1703-7. Epub 2002/12/11.
16. Sommerfeld DK, Eek EU, Svensson AK, Holmqvist LW, von Arbin MH. Spasticity after stroke: its occurrence and association with motor impairments and activity

limitations. Stroke. Jan 2004;35(1):134-9. Epub 2003/12/20.
17. Sanchez GN, Sinha S, Liske H, Chen X, Nguyen V, Delp SL, et al. In Vivo Imaging of Human Sarcomere Twitch Dynamics in Individual Motor Units. Neuron. Dec 16 2015;88(6):1109-20. Epub 2015/12/22.
18. Booth CM, Cortina-Borja MJF, Theologis TN. Collagen accumulation in muscles of children with cerebral palsy and correlation with severity of spasticity. Dev Med Child Neurol. 2001;43(05).
19. Fridén J, Lieber RL. Spastic muscle cells are shorter and stiffer than normal cells. Muscle Nerve. 2003;27(2):157-64.
20. Yang Y-B, Zhang J, Leng Z-P, Chen X, Song W-Q. Evaluation of spasticity after stroke by using ultrasound to measure the muscle architecture parameters: a clinical study. Int J Clin Exp Med. 09/15 07/08/received 08/16/accepted 2014;7(9):2712-7.
21. O'Dwyer NJ, Ada L, Neilson PD. Spasticity and muscle contracture following stroke. Brain. 1996;119(5):1737-49.
22. Bockbrader MA, Thompson RD, Way DP, Colachis SC, Siddiqui IJ, Luz J, et al. Toward a Consensus for Musculoskeletal Ultrasonography Education in Physical Medicine and Rehabilitation: A National Poll of Residency Directors. Am J Phys Med Rehabil. 2019;98(8):715-24.
23. Kooijman MK, Swinkels ICS, Koes BW, de Bakker D, Veenhof C. One in six physiotherapy practices in primary care offer musculoskeletal ultrasound - an explorative survey. BMC Health Serv Res. Mar 24 2020;20(1):246. Epub 2020/03/27.
24. Eby SF, Zhao H, Song P, Vareberg BJ, Kinnick RR, Greenleaf JF, et al. Quantifying spasticity in individual muscles using shear wave elastography. Radiol Case Rep. Jun 2017;12(2):348-52. Epub 2017/05/12.
25. Park GY, Kwon DR. Application of real-time sonoelastography in musculoskeletal diseases related to physical medicine and rehabilitation. Am J Phys Med Rehabil. Nov 2011;90(11):875-86. Epub 2011/05/10.
26. Seynnes OR, Bojsen-Moller J, Albracht K, Arndt A, Cronin NJ, Finni T, et al. Ultrasound-based testing of tendon mechanical properties: a critical evaluation. J Appl Physiol. Jan 15 2015;118(2):133-41. Epub 2014/11/22.
27. Barber L, Barrett R, Lichtwark G. Passive muscle mechanical properties of the medial gastrocnemius in young adults with spastic cerebral palsy. J Biomech. 2011/09/02/ 2011;44(13):2496-500.
28. Brandenburg JE, Eby SF, Song P, Zhao H, Brault JS, Chen S, et al. Ultrasound elastography: the new frontier in direct measurement of muscle stiffness. Arch Phys Med Rehabil. 2014;95(11):2207-19.
29. Bercoff J, Tanter M, Fink M. Supersonic shear imaging: a new technique for soft tissue elasticity mapping. IEEE Transactions on Ultrasonics, Ferroelectrics, and Frequency Control. 2004;51(4):396-409.
30. Lacourpaille L, Hug F, Bouillard K, Hogrel JY, Nordez A. Supersonic shear imaging provides a reliable measurement of resting muscle shear elastic modulus. Physiol Meas. Mar 2012;33(3):N19-28. Epub 2012/03/01.
31. Lee SS, Gaebler-Spira D, Zhang LQ, Rymer WZ, Steele KM. Use of shear wave ultrasound elastography to quantify muscle properties in cerebral palsy. Clin Biomech (Bristol, Avon). Jan 2016;31:20-8. Epub 2015/10/23.
32. Alhusaini AA, Crosbie J, Shepherd RB, Dean CM, Scheinberg A. No change in calf muscle passive stiffness after botulinum toxin injection in children with cerebral palsy. Dev Med Child Neurol. Jun 2011;53(6):553-8. Epub 2011/05/18.
33. Bar-On L, Slane LC. Shear wave elastography for the assessment of muscle stiffness in children with CP: insights and challenges. Dev Med Child Neurol. Dec

2016;58(12):1209-10. Epub 2016/07/21.
34. Brandenburg JE, Eby SF, Song P, Bamlet WR, Sieck GC, An KN. Quantifying Effect of Onabotulinum Toxin A on Passive Muscle Stiffness in Children with Cerebral Palsy Using Ultrasound Shear Wave Elastography. Am J Phys Med Rehabil. Jul 2018;97(7):500-6. Epub 2018/02/07.
35. Brandenburg JE, Eby SF, Song P, Kingsley-Berg S, Bamlet W, Sieck GC, et al. Quantifying passive muscle stiffness in children with and without cerebral palsy using ultrasound shear wave elastography. Dev Med Child Neurol. Dec 2016;58(12):1288-94. Epub 2016/07/05.
36. Kwon DR, Park GY, Lee SU, Chung I. Spastic Cerebral Palsy in Children: Dynamic Sonoelastographic Findings of Medial Gastrocnemius. Radiology. 2012;263(3):794-801.
37. Vasilescu D, Vasilescu D, Dudea SM, Sfringeu S, Cosma D. Sonoelastography contribution in cerebral palsy spasticity treatment assessment, preliminary report: a systematic review of the literature apropos of seven patients. Med Ultrason. 2010;12(4):306-10.
38. Du LJ, He W, Cheng LG, Li S, Pan YS, Gao J. Ultrasound shear wave elastography in assessment of muscle stiffness in patients with Parkinson's disease: a primary observation. Clin Imaging. Evaluation Studies Nov - Dec 2016;40(6):1075-80.
39. Gao J, He W, Du L-J, Li S, Cheng L-G, Shih G, et al. Ultrasound strain elastography in assessment of resting biceps brachii muscle stiffness in patients with Parkinson's disease: a primary observation. Clin Imaging. 2016;40(3):440-4.
40. Carpenter EL, Lau HA, Kolodny EH, Adler RS. Skeletal muscle in healthy subjects versus those with GNE-related myopathy: evaluation with shear-wave US—a pilot study. Radiology. 2015;277(2):546-54.
41. Lacourpaille L, Hug F, Guevel A, Pereon Y, Magot A, Hogrel JY, et al. Non-invasive assessment of muscle stiffness in patients with Duchenne muscular dystrophy. Muscle Nerve. Feb 2015;51(2):284-6. Epub 2014/09/05.
42. Drakonaki EE, Allen GM. Magnetic resonance imaging, ultrasound and real-time ultrasound elastography of the thigh muscles in congenital muscle dystrophy. Skeletal Radiol. 2010;39(4):391-6.
43. Wu CH, Ho YC, Hsiao MY, Chen WS, Wang TG. Evaluation of Post-Stroke Spastic Muscle Stiffness Using Shear Wave Ultrasound Elastography. Ultrasound Med Biol. 2017;43(6):1105-11.
44. Eby S, Zhao H, Song P, Vareberg BJ, Kinnick R, Greenleaf JF, et al. Quantitative Evaluation of Passive Muscle Stiffness in Chronic Stroke. Am J Phys Med Rehabil. Dec 2016;95(12):899-910. Epub 2016/05/06.
45. Jakubowski KL, Terman A, Santana RVC, Lee SSM. Passive material properties of stroke-impaired plantarflexor and dorsiflexor muscles. Clin Biomech (Bristol, Avon). Nov 2017;49:48-55. Epub 2017/09/04.
46. Mathevon L, Michel F, Aubry S, Testa R, Lapole T, Arnaudeau LF, et al. Two-dimensional and shear wave elastography ultrasound: A reliable method to analyse spastic muscles? Muscle Nerve. Feb 2018;57(2):222-8. Epub 2017/06/01.
47. Rasool G, Wang AB, Rymer WZ, Lee SS. Altered viscoelastic properties of stroke-affected muscles estimated using ultrasound shear waves—Preliminary data. Engineering in Medicine and Biology Society (EMBC), 2016 IEEE 38th Annual International Conference of the: IEEE; 2016. p. 2869-72.
48. Berenpas F, Martens AM, Weerdesteyn V, Geurts AC, van Alfen N. Bilateral changes in muscle architecture of physically active people with chronic stroke: A quantitative muscle ultrasound study. Clin Neurophysiol. Jan 2017;128(1):115-22. Epub

2016/11/27.
49. Pang MY, Ashe MC, Eng JJ. Muscle weakness, spasticity and disuse contribute to demineralization and geometric changes in the radius following chronic stroke. Osteoporos Int. Sep 2007;18(9):1243-52. Epub 2007/04/03.
50. Pang MY, Ashe MC, Eng JJ. Tibial bone geometry in chronic stroke patients: influence of sex, cardiovascular health, and muscle mass. J Bone Miner Res. Jul 2008;23(7):1023-30. Epub 2008/02/28.
51. Pang MY, Ashe MC, Eng JJ. Compromised bone strength index in the hemiparetic distal tibia epiphysis among chronic stroke patients: the association with cardiovascular function, muscle atrophy, mobility, and spasticity. Osteoporos Int. Jun 2010;21(6):997-1007. Epub 2009/11/03.
52. Pang MY, Cheng AQ, Warburton DE, Jones AY. Relative impact of neuromuscular and cardiovascular factors on bone strength index of the hemiparetic distal radius epiphysis among individuals with chronic stroke. Osteoporos Int. Sep 2012;23(9):2369-79. Epub 2012/02/09.
53. Pang MYC, Yang FZH, Jones AYM. Vascular Elasticity and Grip Strength Are Associated With Bone Health of the Hemiparetic Radius in People With Chronic Stroke: Implications for Rehabilitation. Phys Ther. 2013;93(6):774-85.
54. Pang M, Zhang M, Li L, Jones A. Changes in bone density and geometry of the radius in chronic stroke and related factors: A one-year prospective study. J Musculoskelet Neuronal Interact. 2013;13(1):77-88.
55. Yang FZ, Pang MY. Influence of chronic stroke impairments on bone strength index of the tibial distal epiphysis and diaphysis. Osteoporos Int. Feb 2015;26(2):469-80. Epub 2014/09/06.
56. Lam FM, Bui M, Yang FZ, Pang MY. Chronic effects of stroke on hip bone density and tibial morphology: a longitudinal study. Osteoporos Int. Feb 2016;27(2):591-603. Epub 2015/09/04.
57. Dickenson R, Hutton W, Stott J. The mechanical properties of bone in osteoporosis. The Journal of bone and joint surgery British volume. 1981;63(2):233-8.
58. Dennis MS, Lo KM, McDowall M, West T. Fractures After Stroke: Frequency, Types, and Associations. Stroke. 2002;33(3):728-34.
59. Ramnemark A, Nyberg L, Lorentzon R, Englund U, Gustafson Y. Progressive Hemiosteoporosis on the Paretic Side and Increased Bone Mineral Density in the Nonparetic Arm the First Year after Severe Stroke. Osteoporos Int. 1999/03/01 1999;9(3):269-75.
60. Di Monaco M, Vallero F, Di Monaco R, Mautino F, Cavanna A. Functional recovery and length of stay after hip fracture in patients with neurologic impairment. Am J Phys Med Rehabil. Feb 2003;82(2):143-8; quiz 9-51, 57. Epub 2003/01/25.
61. Ramnemark A, Nilsson M, Borssén B, Gustafson Y. Stroke, a major and increasing risk factor for femoral neck fracture. Stroke. 2000;31(7):1572-7.
62. Hyndman D, Ashburn A, Stack E. Fall events among people with stroke living in the community: Circumstances of falls and characteristics of fallers. Arch Phys Med Rehabil. 2002;83(2):165-70.
63. Dennis MS, Lo KM, McDowall M, West T. Fractures After Stroke. Frequency, Types, and Associations. 2002;33(3):728-34.
64. Ramnemark A, Nyberg L, Lorentzon R, Olsson T, Gustafson Y. Hemiosteoporosis After Severe Stroke, Independent of Changes in Body Composition and Weight. Stroke. 1999;30(4):755-60.
65. Jørgensen L, Jacobsen BK. Functional status of the paretic arm affects the loss of bone mineral in the proximal humerus after stroke: A 1-year prospective study. Calcif

Tissue Int. 2001/01/01 2001;68(1):11-5.
66. Jørgensen L, Crabtree NJ, Reeve J, Jacobsen BK. Ambulatory level and asymmetrical weight bearing after stroke affects bone loss in the upper and lower part of the femoral neck differently: bone adaptation after decreased mechanical loading. Bone. 2000/11/01/ 2000;27(5):701-7.
67. Chang K-H, Liou T-H, Sung J-Y, Wang C-Y, Genant HK, Chan WP. Femoral Neck Bone Mineral Density Change Is Associated with Shift in Standing Weight in Hemiparetic Stroke Patients. Am J Phys Med Rehabil. 2014;93(6):477-85.
68. Sherk KA, Sherk VD, Anderson MA, Bemben DA, Bemben MG. Differences in Tibia Morphology Between the Sound and Affected Sides in Ankle-Foot Orthosis-Using Survivors of Stroke. Arch Phys Med Rehabil. 2013/03/01/ 2013;94(3):510-5.
69. Yang FZ, Jehu DAM, Ouyang H, Lam FMH, Pang MYC. The impact of stroke on bone properties and muscle-bone relationship: a systematic review and meta-analysis. Osteoporos Int. 2020/02/01 2020;31(2):211-24.
70. Borschmann K, Iuliano S, Ghasem-Zadeh A, Churilov L, Pang MYC, Bernhardt J. Upright activity and higher motor function may preserve bone mineral density within 6 months of stroke: a longitudinal study. Arch Osteoporos. Jan 8 2018;13(1):5. Epub 2018/01/10.
71. Hamdy RC, Moore SW, Cancellaro VA, Harvill LM. Long-term effects of strokes on bone mass. LWW; 1995.
72. Jørgensen L, Engstad T, Jacobsen BK. Bone Mineral Density in Acute Stroke Patients. Low Bone Mineral Density May Predict First Stroke in Women. Stroke. 2001;32(1):47-51.
73. Jørgensen L, Jacobsen BK. Changes in muscle mass, fat mass, and bone mineral content in the legs after stroke: a 1 year prospective study. Bone. 2001/06/01/ 2001;28(6):655-9.
74. Kim HW, Kang E, Im S, Ko YJ, Im SA, Lee JI. Prevalence of pre-stroke low bone mineral density and vertebral fracture in first stroke patients. Bone. 2008/07/01/ 2008;43(1):183-6.
75. Kim SN, Lee HS, Nam HS, Lee HR, Kim JM, Han SW, et al. Carotid Intima-Media Thickness is Inversely Related to Bone Density in Female but not in Male Patients with Acute Stroke. J Neuroimaging. Jan-Feb 2016;26(1):83-8. Epub 2015/09/12.
76. Lee SB, Cho AH, Butcher KS, Kim TW, Ryu SY, Kim YI. Low bone mineral density is associated with poor clinical outcome in acute ischemic stroke. Int J Stroke. Feb 2013;8(2):68-72. Epub 2011/12/14.
77. Poole KES, Loveridge N, Rose CM, Warburton EA, Reeve J. A Single Infusion of Zoledronate Prevents Bone Loss After Stroke. Stroke. 2007;38(5):1519-25.
78. Ikai T, Uematsu M, Eun SS, Kimura C, Hasegawa C, Miyano S. Prevention of Secondary Osteoporosis Postmenopause in Hemiplegia. Am J Phys Med Rehabil. 2001;80(3):169-74.
79. Kumar V, Kalita J, Gujral RB, Sharma VP, Misra UK. A study of bone densitometry in patients with complex regional pain syndrome after stroke. Postgrad Med J. 2001;77(910):519-22.
80. Lazoura O, Groumas N, Antoniadou E, Papadaki PJ, Papadimitriou A, Thriskos P, et al. Bone mineral density alterations in upper and lower extremities 12 months after stroke measured by peripheral quantitative computed tomography and DXA. J Clin Densitom. Oct-Dec 2008;11(4):511-7. Epub 2008/07/22.
81. Lazoura O, Papadaki PJ, Antoniadou E, Groumas N, Papadimitriou A, Thriskos P, et al. Skeletal and Body Composition Changes in Hemiplegic Patients. J Clin Densitom. 2010/04/01/ 2010;13(2):175-80.

82. Liu M, Tsuji T, Higuchi Y, Domen K, Tsujiuchi K, Chino N. Osteoporosis in hemiplegic stroke patients as studied with dual-energy x-ray absorptiometry. Arch Phys Med Rehabil. 1999/10/01/ 1999;80(10):1219-26.
83. Watanabe Y. An assessment of osteoporosis in stroke patients on rehabilitation admission. Int J Rehabil Res. 2004;27(2):163-6.
84. Marzolini S, McIlroy W, Tang A, Corbett D, Craven BC, Oh PI, et al. Predictors of low bone mineral density of the stroke-affected hip among ambulatory individuals with chronic stroke. Osteoporos Int. 2014/11/01 2014;25(11):2631-8.
85. Pang MY, Eng JJ. Muscle strength is a determinant of bone mineral content in the hemiparetic upper extremity: implications for stroke rehabilitation. Bone. Jul 2005;37(1):103-11. Epub 2005/05/05.
86. Pang MY, Eng JJ, McKay HA, Dawson AS. Reduced hip bone mineral density is related to physical fitness and leg lean mass in ambulatory individuals with chronic stroke. Osteoporos Int. Dec 2005;16(12):1769-79. Epub 2005/05/20.
87. Tomasević-Todorović S, Simić-Panić D, Knežević A, Demeši-Drljan Č, Marić D, Hanna F. Osteoporosis in patients with stroke: A cross-sectional study. Annals of Indian Academy of Neurology. Apr-Jun 2016;19(2):286-8.
88. Celik B, Ones K, Ince N. Body composition after stroke. Int J Rehabil Res. 2008;31(1):93-6.
89. Lam FMH, Pang MYC. Correlation between tibial measurements using peripheral quantitative computed tomography and hip areal bone density measurements in ambulatory chronic stroke patients. Brain Inj. 2016/01/28 2016;30(2):199-207.
90. Hamdy RC, Krishnaswamy G, Cancellaro V, Whalen K, Harvill L. Changes in bone mineral content and density after stroke. Am J Phys Med Rehabil. 1993;72(4):188-91.
91. Pang MYC, Eng JJ, Dawson AS, McKay HA, Harris JE. A community-based fitness and mobility exercise program for older adults with chronic stroke: A randomized, controlled trial. J Am Geriatr Soc. 2005;53(10):1667-74.
92. Jørgensen L, Jacobsen BK, Wilsgaard T, Magnus JH. Walking after Stroke: Does It Matter? Changes in Bone Mineral Density Within the First 12 Months after Stroke. A Longitudinal Study. Osteoporos Int. 2000/05/01 2000;11(5):381-7.
93. Souzanchi MF, Palacio-Mancheno P, Borisov YA, Cardoso L, Cowin SC. Microarchitecture and bone quality in the human calcaneus: local variations of fabric anisotropy. J Bone Miner Res. 2012;27(12):2562-72.
94. Turner CH, Burr DB. Basic biomechanical measurements of bone: A tutorial. Bone. 1993/07/01/ 1993;14(4):595-608.
95. Pang MYC, Lau RWK. The Effects of Treadmill Exercise Training on Hip Bone Density and Tibial Bone Geometry in Stroke Survivors: A Pilot Study. Neurorehabil Neural Repair. 2010;24(4):368-76.
96. Talla R, Galea M, Lythgo N, Eser T, Talla P, Angeli P, et al. Contralateral comparison of bone geometry, BMD and muscle function in the lower leg and forearm after stroke. Journal of Musculoskeletal Neuronal Interactions. 2011;11(4):306-13.
97. Jørgensen HS, Nakayama H, Raaschou HO, Olsen TS. Recovery of walking function in stroke patients: The copenhagen stroke study. Arch Phys Med Rehabil. 1995/01/01/ 1995;76(1):27-32.
98. Liu XS, Stein EM, Zhou B, Zhang CA, Nickolas TL, Cohen A, et al. Individual trabecula segmentation (ITS)-based morphological analyses and microfinite element analysis of HR-pQCT images discriminate postmenopausal fragility fractures independent of DXA measurements. J Bone Miner Res. Feb 2012;27(2):263-72. Epub 2011/11/11.
99. Patsch JM, Burghardt AJ, Yap SP, Baum T, Schwartz AV, Joseph GB, et al. Increased

cortical porosity in type 2 diabetic postmenopausal women with fragility fractures. J Bone Miner Res. Feb 2013;28(2):313-24. Epub 2012/09/20.
100. Pistoia W, van Rietbergen B, Lochmüller EM, Lill CA, Eckstein F, Rüegsegger P. Estimation of distal radius failure load with micro-finite element analysis models based on three-dimensional peripheral quantitative computed tomography images. Bone. 2002/06/01/ 2002;30(6):842-8.
101. Boutroy S, Bouxsein ML, Munoz F, Delmas PD. In vivo assessment of trabecular bone microarchitecture by high-resolution peripheral quantitative computed tomography. J Clin Endocrinol Metab. Dec 2005;90(12):6508-15. Epub 2005/09/29.
102. Cheung AM, Adachi JD, Hanley DA, Kendler DL, Davison KS, Josse R, et al. High-resolution peripheral quantitative computed tomography for the assessment of bone strength and structure: a review by the Canadian Bone Strength Working Group. Curr Osteoporos Rep. Jun 2013;11(2):136-46. Epub 2013/03/26.
103. Biver E, Durosier-Izart C, Chevalley T, van Rietbergen B, Rizzoli R, Ferrari S. Evaluation of Radius Microstructure and Areal Bone Mineral Density Improves Fracture Prediction in Postmenopausal Women. J Bone Miner Res. Feb 2018;33(2):328-37. Epub 2017/09/30.
104. Burt LA, Manske SL, Hanley DA, Boyd SK. Lower Bone Density, Impaired Microarchitecture, and Strength Predict Future Fragility Fracture in Postmenopausal Women: 5-Year Follow-up of the Calgary CaMos Cohort. J Bone Miner Res. Apr 2018;33(4):589-97. Epub 2018/01/25.
105. Sornay-Rendu E, Boutroy S, Duboeuf F, Chapurlat RD. Bone Microarchitecture Assessed by HR-pQCT as Predictor of Fracture Risk in Postmenopausal Women: The OFELY Study. J Bone Miner Res. Jun 2017;32(6):1243-51. Epub 2017/03/10.
106. Arias-Moreno AJ, Hosseini HS, Bevers M, Ito K, Zysset P, van Rietbergen B. Validation of distal radius failure load predictions by homogenized- and micro-finite element analyses based on second-generation high-resolution peripheral quantitative CT images. Osteoporos Int. Jul 2019;30(7):1433-43. Epub 2019/04/19.
107. Macneil JA, Boyd SK. Bone strength at the distal radius can be estimated from high-resolution peripheral quantitative computed tomography and the finite element method. Bone. Jun 2008;42(6):1203-13. Epub 2008/03/25.
108. Zhou B, Wang J, Yu YE, Zhang Z, Nawathe S, Nishiyama KK, et al. High-resolution peripheral quantitative computed tomography (HR-pQCT) can assess microstructural and biomechanical properties of both human distal radius and tibia: Ex vivo computational and experimental validations. Bone. May 2016;86:58-67. Epub 2016/03/01.
109. Mikolajewicz N, Bishop N, Burghardt AJ, Folkestad L, Hall A, Kozloff KM, et al. HR-pQCT Measures of Bone Microarchitecture Predict Fracture: Systematic Review and Meta-Analysis. J Bone Miner Res. Oct 23 2019. Epub 2019/10/24.
110. Wong AK. A comparison of peripheral imaging technologies for bone and muscle quantification: a technical review of image acquisition. J Musculoskelet Neuronal Interact. 2016;16(4):265-82.
111. Szulc P, Boutroy S, Chapurlat R. Prediction of Fractures in Men Using Bone Microarchitectural Parameters Assessed by High-Resolution Peripheral Quantitative Computed Tomography-The Prospective STRAMBO Study. J Bone Miner Res. Aug 2018;33(8):1470-9. Epub 2018/04/26.
112. Burghardt AJ, Kazakia GJ, Ramachandran S, Link TM, Majumdar S. Age- and gender-related differences in the geometric properties and biomechanical significance of intracortical porosity in the distal radius and tibia. J Bone Miner Res. May 2010;25(5):983-93. Epub 2009/11/06.

113. Samelson EJ, Broe KE, Xu H, Yang L, Boyd S, Biver E, et al. Cortical and trabecular bone microarchitecture as an independent predictor of incident fracture risk in older women and men in the Bone Microarchitecture International Consortium (BoMIC): a prospective study. The Lancet Diabetes & Endocrinology. 2019/01/01/ 2019;7(1):34-43.
114. Seeman E, Delmas PD, Hanley DA, Sellmeyer D, Cheung AM, Shane E, et al. Microarchitectural deterioration of cortical and trabecular bone: differing effects of denosumab and alendronate. J Bone Miner Res. Aug 2010;25(8):1886-94. Epub 2010/03/12.
115. Pearson OM, Lieberman DE. The aging of Wolff's "law": ontogeny and responses to mechanical loading in cortical bone. Am J Phys Anthropol. 2004;Suppl 39:63-99. Epub 2004/12/18.
116. Rubin CT, Lanyon LE. Kappa Delta Award paper. Osteoregulatory nature of mechanical stimuli: function as a determinant for adaptive remodeling in bone. J Orthop Res. 1987;5(2):300-10. Epub 1987/01/01.
117. Mosley JR, Lanyon LE. Strain rate as a controlling influence on adaptive modeling in response to dynamic loading of the ulna in growing male rats. Bone. 1998/10/01/ 1998;23(4):313-8.
118. Mosley JR, March BM, Lynch J, Lanyon LE. Strain magnitude related changes in whole bone architecture in growing rats. Bone. 1997/03/01/ 1997;20(3):191-8.
119. Schoenau E. From mechanostat theory to development of the" Functional Muscle-Bone-Unit". Journal of Musculoskeletal and Neuronal Interactions. 2005;5(3):232.
120. Ashe MC, Liu-Ambrose TY, Cooper DM, Khan KM, McKay HA. Muscle power is related to tibial bone strength in older women. Osteoporos Int. Dec 2008;19(12):1725-32. Epub 2008/07/17.
121. Rantalainen T, Nikander R, Kukuljan S, Daly R. Mid-femoral and mid-tibial muscle cross-sectional area as predictors of tibial bone strength in middle-aged and older men. Journal of Musculoskeletal and Neuronal Interactions. 2013;13(3):273-82.
122. MacIntyre N, Rombough R, Brouwer B. Relationships between calf muscle density and muscle strength, mobility and bone status in the stroke survivors with subacute and chronic lower limb hemiparesis. J Musculoskelet Neuronal Interact. 2010;10(4):249-55.
123. Anliker E, Toigo M. Functional assessment of the muscle-bone unit in the lower leg. J Musculoskelet Neuronal Interact. 2012;12(2):46-55.
124. Duran I, Schutz F, Hamacher S, Semler O, Stark C, Schulze J, et al. The functional muscle-bone unit in children with cerebral palsy. Osteoporos Int. Jul 2017;28(7):2081-93. Epub 2017/04/04.
125. Pang MY, Ashe MC, Eng JJ, McKay HA, Dawson AS. A 19-week exercise program for people with chronic stroke enhances bone geometry at the tibia: a peripheral quantitative computed tomography study. Osteoporosis international. 2006;17(11):1615-25.
126. Gao F, Grant TH, Roth EJ, Zhang LQ. Changes in passive mechanical properties of the gastrocnemius muscle at the muscle fascicle and joint levels in stroke survivors. Arch Phys Med Rehabil. May 2009;90(5):819-26. Epub 2009/05/02.
127. Rittweger J, Ferretti J-L. Imaging Mechanical Muscle–Bone Relationships: How to See the Invisible. Clin Rev Bone Miner Metab. 2014;12(2):66-76.
128. Fukunaga T, Miyatani M, Tachi M, Kouzaki M, Kawakami Y, Kanehisa H. Muscle volume is a major determinant of joint torque in humans. Acta Physiol Scand. 2001;172(4):249-55.
129. English CK, Thoirs KA, Fisher L, McLennan H, Bernhardt J. Ultrasound is a reliable

measure of muscle thickness in acute stroke patients, for some, but not all anatomical sites: a study of the intra-rater reliability of muscle thickness measures in acute stroke patients. Ultrasound Med Biol. 2012;38(3):368-76.
130. Nozoe M, Kubo H, Furuichi A, Kanai M, Takashima S, Shimada S, et al. Validity of Quadriceps Muscle Thickness Measurement in Patients with Subacute Stroke during Hospitalization for Assessment of Muscle Wasting and Physical Function. J Stroke Cerebrovasc Dis. Feb 2017;26(2):438-41. Epub 2016/11/08.
131. Sions JM, Tyrell CM, Knarr BA, Jancosko A, Binder-Macleod SA. Age- and stroke-related skeletal muscle changes: a review for the geriatric clinician. J Geriatr Phys Ther. Jul-Sep 2012;35(3):155-61. Epub 2011/11/24.
132. Scherbakov N, von Haehling S, Anker SD, Dirnagl U, Doehner W. Stroke induced Sarcopenia: muscle wasting and disability after stroke. Int J Cardiol. Dec 10 2013;170(2):89-94. Epub 2013/11/16.
133. Fini NA, Holland AE, Keating J, Simek J, Bernhardt J. How Physically Active Are People Following Stroke? Systematic Review and Quantitative Synthesis. Phys Ther. 2017;97(7):707-17.
134. Lewis BA, Napolitano MA, Buman MP, Williams DM, Nigg CR. Future directions in physical activity intervention research: expanding our focus to sedentary behaviors, technology, and dissemination. J Behav Med. Feb 2017;40(1):112-26. Epub 2016/10/11.
135. Weerdesteyn V, de Niet M, van Duijnhoven HJ, Geurts AC. Falls in individuals with stroke. J Rehabil Res Dev. 2008;45(8):1195-213.
136. E. D. Lamb S, M. Ferrucci L, Volpato S, Fried L, M. M. Guralnik J. Risk Factors for Falling in Home-Dwelling Older Women With Stroke The Women's Health and Aging Study2003. 494-501 p.
137. Jørgensen L, Engstad T, Jacobsen BK. Higher incidence of falls in long-term stroke survivors than in population controls: depressive symptoms predict falls after stroke. Stroke. 2002;33(2):542-7.
138. Soyuer F, Ozturk A. The effect of spasticity, sense and walking aids in falls of people after chronic stroke. Disabil Rehabil. May 15 2007;29(9):679-87. Epub 2007/04/25.
139. Forster A, Young J. Incidence and consequences offalls due to stroke: a systematic inquiry. BMJ. 1995;311(6997):83-6.
140. Belgen B, Beninato M, Sullivan PE, Narielwalla K. The association of balance capacity and falls self-efficacy with history of falling in community-dwelling people with chronic stroke. Arch Phys Med Rehabil. Apr 2006;87(4):554-61. Epub 2006/03/31.
141. Kanis JA, Glüer C-C. An Update on the Diagnosis and Assessment of Osteoporosis with Densitometry. Osteoporos Int. journal article March 01 2000;11(3):192-202.
142. Whitson HE, Pieper CF, Sanders L, Horner RD, Duncan PW, Lyles KW. Adding Injury to Insult: Fracture Risk After Stroke in Veterans. J Am Geriatr Soc. 2006;54(7):1082-8.
143. Ramnemark A, Nyberg L, Borssén B, Olsson T, Gustafson Y. Fractures after stroke. Osteoporosis International. 1998;8(1):92-5.
144. Kanis J, Oden A, Johnell O. Acute and Long-Term Increase in Fracture Risk After Hospitalization for Stroke. Stroke. 2001;32(3):702-6.
145. Scott BR, F. CN, B. WJ. Estimating Hip Fracture Morbidity, Mortality and Costs. J Am Geriatr Soc. 2003;51(3):364-70.
146. Jellema S, van Hees S, Zajec J, van der Sande R, Nijhuis-van der Sanden MW, Steultjens EM. What environmental factors influence resumption of valued activities post stroke: a systematic review of qualitative and quantitative findings. Clin Rehabil.

Jul 2017;31(7):936-47. Epub 2016/09/30.
147. Foran JR, Steinman S, Barash I, Chambers HG, Lieber RL. Structural and mechanical alterations in spastic skeletal muscle. Dev Med Child Neurol. 2007;47(10):713-7.
148. Lieber RL, Ward SR. Cellular Mechanisms of Tissue Fibrosis. 4. Structural and functional consequences of skeletal muscle fibrosis. American Journal of Physiology-Cell Physiology. 2013;305(3):C241-C52.
149. Ito J-I, Araki A, Tanaka H, Tasaki T, Cho K, Yamazaki R. Muscle histopathology in spastic cerebral palsy. Brain Dev. 1996;18(4):299-303.
150. Pontén EM, Stål PS. Decreased capillarization and a shift to fast myosin heavy chain IIx in the biceps brachii muscle from young adults with spastic paresis. J Neurol Sci. 2007;253(1-2):25-33.
151. Smith LR, Lee KS, Ward SR, Chambers HG, Lieber RL. Hamstring contractures in children with spastic cerebral palsy result from a stiffer extracellular matrix and increased in vivo sarcomere length. J Physiol. May 15 2011;589(Pt 10):2625-39. Epub 2011/04/14.
152. Lieber RL, Fridén J. Spasticity causes a fundamental rearrangement of muscle-joint interaction. Muscle Nerve. 2002;25(2):265-70.
153. Lee SSM, Jakubowski KL, Spear SC, Rymer WZ. Muscle material properties in passive and active stroke-impaired muscle. J Biomech. Dec 5 2018. Epub 2018/12/16.
154. Haus JM, Carrithers JA, Trappe SW, Trappe TA. Collagen, cross-linking, and advanced glycation end products in aging human skeletal muscle. J Appl Physiol. 2007;103(6):2068-76.
155. Kjær M. Role of Extracellular Matrix in Adaptation of Tendon and Skeletal Muscle to Mechanical Loading. Physiol Rev. 2004;84(2):649-98.
156. Neagoe C, Opitz CA, Makarenko I, Linke WA. Gigantic variety: expression patterns of titin isoforms in striated muscles and consequences for myofibrillar passive stiffness. J Muscle Res Cell Motil. journal article February 01 2003;24(2):175-89.
157. Miscio G, Del Conte C, Pianca D, Colombo R, Panizza M, Schieppati M, et al. Botulinum toxin in post-stroke patients: stiffness modifications and clinical implications. J Neurol. 2004;251(2):189-96.
158. Escolar DM, Henricson EK, Mayhew J, Florence J, Leshner R, Patel KM, et al. Clinical evaluator reliability for quantitative and manual muscle testing measures of strength in children. Muscle Nerve. 2001;24(6):787-93.
159. Alhusaini AAA, Dean CM, Crosbie J, Shepherd RB, Lewis J. Evaluation of Spasticity in Children With Cerebral Palsy Using Ashworth and Tardieu Scales Compared With Laboratory Measures. J Child Neurol. 2010;25(10):1242-7.
160. Boyaci A, Tutoglu A, Boyaci N, Koca I, Calik M, Sakalar A, et al. Changes in spastic muscle stiffness after botulinum toxin A injections as part of rehabilitation therapy in patients with spastic cerebral palsy. NeuroRehabilitation. 2014;35(1):123-9. Epub 2014/07/06.
161. Ceyhan Bilgici M, Bekci T, Ulus Y, Bilgici A, Tomak L, Selcuk MB. Quantitative assessment of muscle stiffness with acoustic radiation force impulse elastography after botulinum toxin A injection in children with cerebral palsy. J Med Ultrason (2001). Jan 2018;45(1):137-41. Epub 2017/03/09.
162. Kwon DR, Park GY, Kwon JG. The change of intrinsic stiffness in gastrocnemius after intensive rehabilitation with botulinum toxin a injection in spastic diplegic cerebral palsy. Ann Rehabil Med. Jun 2012;36(3):400-3. Epub 2012/07/28.
163. Park GY, Kwon DR. Sonoelastographic evaluation of medial gastrocnemius muscles intrinsic stiffness after rehabilitation therapy with botulinum toxin a injection in spastic cerebral palsy. Arch Phys Med Rehabil. 2012;93(11):2085-9.

164. Shao Y-H, Peng Z, Kong X, Wang B, Zhang H. Real-time ultrasound elastography evaluation of achilles tendon properties in patients with mild hemiplegic stroke after rehabilitation training. J Ultrasound Med. 2019;38(3):713-23.
165. Lerner RM, Huang SR, Parker KJ. "Sonoelasticity" images derived from ultrasound signals in mechanically vibrated tissues. Ultrasound Med Biol. 1990/01/01/ 1990;16(3):231-9.
166. Ophir J, Céspedes I, Ponnekanti H, Yazdi Y, Li X. Elastography: A Quantitative Method for Imaging the Elasticity of Biological Tissues. Ultrason Imaging. 1991;13(2):111-34.
167. Lima K, Costa Junior JFS, Pereira WCA, Oliveira LF. Assessment of the mechanical properties of the muscle-tendon unit by supersonic shear wave imaging elastography: a review. Ultrasonography. Jan 2018;37(1):3-15. Epub 2017/06/14.
168. Pedersen M, Fredberg U, Langberg H. Sonoelastography as a Diagnostic Tool in the Assessment of Musculoskeletal Alterations: A Systematic Review. Ultraschall in Med. //
15.10.2012 2012;33(05):441-6. Epub 28.06.2012.
169. Ryu J, Jeong WK. Current status of musculoskeletal application of shear wave elastography. Ultrasonography. Jul 2017;36(3):185-97. Epub 2017/03/16.
170. Wu C-H, Chen W-S, Park G-Y, Wang T-G, Lew HL. Musculoskeletal Sonoelastography: A Focused Review of its Diagnostic Applications for Evaluating Tendons and Fascia. J Med Ultrasound. 2012;20(2):79-86.
171. Sarvazyan A, J Hall T, W Urban M, Fatemi M, R Aglyamov S, S Garra B. An overview of elastography-an emerging branch of medical imaging. Curr Med Imaging Rev. 2011;7(4):255-82.
172. Sigrist RMS, Liau J, Kaffas AE, Chammas MC, Willmann JK. Ultrasound Elastography: Review of Techniques and Clinical Applications. Theranostics. 2017;7(5):1303-29. Epub 2017/04/25.
173. Barr RG. Elastography in clinical practice. Radiol Clin North Am. 2014;52(6):1145-62.
174. Brum J, Bernal M, Gennisson JL, Tanter M. In vivo evaluation of the elastic anisotropy of the human Achilles tendon using shear wave dispersion analysis. Phys Med Biol. Feb 7 2014;59(3):505-23. Epub 2014/01/18.
175. Aubry S, Nueffer J-P, Tanter M, Becce F, Vidal C, Michel F. Viscoelasticity in Achilles Tendonopathy: Quantitative Assessment by Using Real-time Shear-Wave Elastography. Radiology. 2015;274(3):821-9.
176. Ooi CC, Malliaras P, Schneider ME, Connell DA. "Soft, hard, or just right?" Applications and limitations of axial-strain sonoelastography and shear-wave elastography in the assessment of tendon injuries. Skeletal Radiol. 2014;43(1):1-12.
177. Koo TK, Hug F. Factors that influence muscle shear modulus during passive stretch. J Biomech. Sep 18 2015;48(12):3539-42. Epub 2015/06/27.
178. Mulabecirovic A, Vesterhus M, Gilja OH, Havre RF. In Vitro Comparison of Five Different Elastography Systems for Clinical Applications, Using Strain and Shear Wave Technology. Ultrasound Med Biol. Nov 2016;42(11):2572-88. Epub 2016/08/30.
179. Alfuraih AM, O'Connor P, Tan AL, Hensor E, Emery P, Wakefield RJ. An investigation into the variability between different shear wave elastography systems in muscle. Med Ultrason. Nov 29 2017;19(4):392-400. Epub 2017/12/05.
180. Helfenstein-Didier C, Andrade RJ, Brum J, Hug F, Tanter M, Nordez A, et al. In vivo quantification of the shear modulus of the human Achilles tendon during passive loading using shear wave dispersion analysis. Phys Med Biol. Research Support, Non-

U.S. Gov't Mar 21 2016;61(6):2485-96.
181. Kelly JP, Koppenhaver SL, Michener LA, Proulx L, Bisagni F, Cleland JA. Characterization of tissue stiffness of the infraspinatus, erector spinae, and gastrocnemius muscle using ultrasound shear wave elastography and superficial mechanical deformation. J Electromyogr Kinesiol. Feb 2018;38:73-80. Epub 2017/11/28.
182. Andonian P, Viallon M, Le Goff C, de Bourguignon C, Tourel C, Morel J, et al. Shear-Wave Elastography Assessments of Quadriceps Stiffness Changes prior to, during and after Prolonged Exercise: A Longitudinal Study during an Extreme Mountain Ultra-Marathon. PLoS One. 2016;11(8):e0161855. Epub 2016/09/01.
183. Gilbert F, Klein D, Weng AM, Kostler H, Schmitz B, Schmalzl J, et al. Supraspinatus muscle elasticity measured with real time shear wave ultrasound elastography correlates with MRI spectroscopic measured amount of fatty degeneration. BMC Musculoskelet Disord. Dec 28 2017;18(1):549. Epub 2017/12/29.
184. Zhang ZJ, Ng GY, Lee WC, Fu SN. Changes in morphological and elastic properties of patellar tendon in athletes with unilateral patellar tendinopathy and their relationships with pain and functional disability. PLoS One. 2014;9(10):e108337. Epub 2014/10/11.
185. Masaki M, Aoyama T, Murakami T, Yanase K, Ji X, Tateuchi H, et al. Association of low back pain with muscle stiffness and muscle mass of the lumbar back muscles, and sagittal spinal alignment in young and middle-aged medical workers. Clin Biomech (Bristol, Avon). Nov 2017;49:128-33. Epub 2017/09/22.
186. Liberati A, Altman DG, Tetzlaff J, Mulrow C, Gotzsche PC, Ioannidis JP, et al. The PRISMA statement for reporting systematic reviews and meta-analyses of studies that evaluate healthcare interventions: explanation and elaboration. BMJ. Jul 21 2009;339:b2700. Epub 2009/07/23.
187. Mokkink LB, Terwee CB, Patrick DL, Alonso J, Stratford PW, Knol DL, et al. The COSMIN checklist for assessing the methodological quality of studies on measurement properties of health status measurement instruments: an international Delphi study. Qual Life Res. May 2010;19(4):539-49. Epub 2010/02/20.
188. Yang L, Liao LR, Lam FM, He CQ, Pang MY. Psychometric properties of dual-task balance assessments for older adults: a systematic review. Maturitas. Apr 2015;80(4):359-69. Epub 2015/01/27.
189. Oftedal S, Bell KL, Mitchell LE, Davies PS, Ware RS, Boyd RN. A systematic review of the clinimetric properties of habitual physical activity measures in young children with a motor disability. Int J Pediatr. 2012;2012:976425. Epub 2012/08/29.
190. Mokkink LB, de Vet HCW, Prinsen CAC, Patrick DL, Alonso J, Bouter LM, et al. COSMIN Risk of Bias checklist for systematic reviews of Patient-Reported Outcome Measures. Qual Life Res. May 2018;27(5):1171-9. Epub 2017/12/21.
191. Terwee CB, Mokkink LB, Knol DL, Ostelo RW, Bouter LM, de Vet HC. Rating the methodological quality in systematic reviews of studies on measurement properties: a scoring system for the COSMIN checklist. Qual Life Res. May 2012;21(4):651-7. Epub 2011/07/07.
192. Vet HCWd. Measurement in medicine : a practical guide. Cambridge New York: Cambridge University Press; 2011.
193. Jakobsson M, Gutke A, Mokkink LB, Smeets R, Lundberg M. Level of Evidence for Reliability, Validity, and Responsiveness of Physical Capacity Tasks Designed to Assess Functioning in Patients With Low Back Pain: A Systematic Review Using the COSMIN Standards. Phys Ther. 2018;99(4):457-77.
194. Prinsen CA, Vohra S, Rose MR, Boers M, Tugwell P, Clarke M, et al. How to select

outcome measurement instruments for outcomes included in a "Core Outcome Set" - a practical guideline. Trials. Sep 13 2016;17(1):449. Epub 2016/09/14.
195. Borenstein M. Introduction to meta-analysis. Chichester: John Wiley & Sons; 2009.
196. Borenstein M, Higgins JP, Hedges LV, Rothstein HR. Basics of meta-analysis: I(2) is not an absolute measure of heterogeneity. Res Synth Methods. Mar 2017;8(1):5-18. Epub 2017/01/07.
197. Borenstein M, Hedges LV, Higgins JP, Rothstein HR. A basic introduction to fixed-effect and random-effects models for meta-analysis. Res Synth Methods. Apr 2010;1(2):97-111. Epub 2010/04/01.
198. Bilgici MC, Bekci T, Ulus Y, Ozyurek H, Aydin OF, Tomak L, et al. Quantitative assessment of muscular stiffness in children with cerebral palsy using acoustic radiation force impulse (ARFI) ultrasound elastography. J Med Ultrason (2001). Apr 2018;45(2):295-300. Epub 2017/09/14.
199. Lacourpaille L, Gross R, Hug F, Guevel A, Pereon Y, Magot A, et al. Effects of Duchenne muscular dystrophy on muscle stiffness and response to electrically-induced muscle contraction: A 12-month follow-up. Neuromuscul Disord. Mar 2017;27(3):214-20. Epub 2017/02/06.
200. Pichiecchio A, Alessandrino F, Bortolotto C, Cerica A, Rosti C, Raciti MV, et al. Muscle ultrasound elastography and MRI in preschool children with Duchenne muscular dystrophy. Neuromuscul Disord. Jun 2018;28(6):476-83. Epub 2018/04/18.
201. Crosby RD, Kolotkin RL, Williams GR. Defining clinically meaningful change in health-related quality of life. J Clin Epidemiol. 2003;56(5):395-407.
202. Blain M, Bedretdinova D, Bellin MF, Rocher L, Gagey O, Soubeyrand M, et al. Influence of thoracolumbar fascia stretching on lumbar back muscle stiffness: A supersonic shear wave elastography approach. Clin Anat. Article Jan 2019;32(1):73-80.
203. Alfuraih AM, O'Connor P, Hensor E, Tan AL, Emery P, Wakefield RJ. The effect of unit, depth, and probe load on the reliability of muscle shear wave elastography: Variables affecting reliability of SWE. J Clin Ultrasound. Feb 2018;46(2):108-15. Epub 2017/10/11.
204. Goertz RS, Amann K, Heide R, Bernatik T, Neurath MF, Strobel D. An abdominal and thyroid status with Acoustic Radiation Force Impulse Elastometry – A feasibility study. Eur J Radiol. 2011;80(3):e226-e30.
205. Gennisson J-L, Deffieux T, Macé E, Montaldo G, Fink M, Tanter M. Viscoelastic and Anisotropic Mechanical Properties of in vivo Muscle Tissue Assessed by Supersonic Shear Imaging. Ultrasound Med Biol. 2010/05/01/ 2010;36(5):789-801.
206. Deffieux T, Montaldo G, Tanter M, Fink M. Shear wave spectroscopy for in vivo quantification of human soft tissues visco-elasticity. IEEE Trans Med Imaging. Mar 2009;28(3):313-22. Epub 2009/02/27.
207. Le Sant G, Nordez A, Andrade R, Hug F, Freitas S, Gross R. Stiffness mapping of lower leg muscles during passive dorsiflexion. J Anat. 2017;230(5):639-50.
208. Urban MW, Nenadic IZ, Chen S, Greenleaf JF. Discrepancies in reporting tissue material properties. J Ultrasound Med. May 2013;32(5):886-8. Epub 2013/04/27.
209. Ferraioli G, Filice C, Castera L, Choi BI, Sporea I, Wilson SR, et al. WFUMB guidelines and recommendations for clinical use of ultrasound elastography: Part 3: liver. Ultrasound Med Biol. May 2015;41(5):1161-79. Epub 2015/03/25.
210. Hoyt K, Kneezel T, Castaneda B, Parker KJ. Quantitative sonoelastography for the in vivo assessment of skeletal muscle viscoelasticity. Phys Med Biol. 07/08 2008;53(15):4063-80.
211. Prado-Costa R, Rebelo J, Monteiro-Barroso J, Preto AS. Ultrasound elastography:

compression elastography and shear-wave elastography in the assessment of tendon injury. Insights Imaging. Oct 2018;9(5):791-814. Epub 2018/08/19.
212. Cosgrove D, Piscaglia F, Bamber J, Bojunga J, Correas JM, Gilja OH, et al. EFSUMB guidelines and recommendations on the clinical use of ultrasound elastography. Part 2: Clinical applications. Ultraschall in der Medizin (Stuttgart, Germany : 1980). 2013;34(3):238-53.
213. Gennisson JL, Deffieux T, Fink M, Tanter M. Ultrasound elastography: principles and techniques. Diagn Interv Imaging. May 2013;94(5):487-95. Epub 2013/04/27.
214. Bamber J, Cosgrove D, Dietrich CF, Fromageau J, Bojunga J, Calliada F, et al. EFSUMB guidelines and recommendations on the clinical use of ultrasound elastography. Part 1: Basic principles and technology. Ultraschall Med. Apr 2013;34(2):169-84. Epub 2013/04/06.
215. Drakonaki EE, Allen GM, Wilson DJ. Ultrasound elastography for musculoskeletal applications. Br J Radiol. Nov 2012;85(1019):1435-45. Epub 2012/10/24.
216. Ariji Y, Nakayama M, Nishiyama W, Nozawa M, Ariji E. Shear-wave sonoelastography for assessing masseter muscle hardness in comparison with strain sonoelastography: study with phantoms and healthy volunteers. Dentomaxillofac Radiol. Comparative Study Research Support, Non-U.S. Gov't 2016;45(2):20150251.
217. Ewertsen C, Carlsen JF, Christiansen IR, Jensen JA, Nielsen MB. Evaluation of healthy muscle tissue by strain and shear wave elastography - Dependency on depth and ROI position in relation to underlying bone. Ultrasonics. Sep 2016;71:127-33. Epub 2016/06/24.
218. Whittaker JL, Stokes M. Ultrasound imaging and muscle function. The Journal Of Orthopaedic And Sports Physical Therapy. 2011;41(8):572-80.
219. Chuang LL, Wu CY, Lin KC. Reliability, validity, and responsiveness of myotonometric measurement of muscle tone, elasticity, and stiffness in patients with stroke. Arch Phys Med Rehabil. Mar 2012;93(3):532-40. Epub 2012/01/10.
220. Marusiak J, Jaskólska A, Budrewicz S, Koszewicz M, Jaskólski A. Increased muscle belly and tendon stiffness in patients with Parkinson's disease, as measured by myotonometry. Mov Disord. 2011;26(11):2119-22.
221. Feng YN, Li YP, Liu CL, Zhang ZJ. Assessing the elastic properties of skeletal muscle and tendon using shearwave ultrasound elastography and MyotonPRO. Sci Rep. 2018/11/20 2018;8(1):17064.
222. Lorentzen J, Grey MJ, Crone C, Mazevet D, Biering-Sorensen F, Nielsen JB. Distinguishing active from passive components of ankle plantar flexor stiffness in stroke, spinal cord injury and multiple sclerosis. Clin Neurophysiol. Nov 2010;121(11):1939-51. Epub 2010/05/12.
223. Huang M, Miller T, Ying M, Pang MYC. Whole-body vibration modulates leg muscle reflex and blood perfusion among people with chronic stroke: a randomized controlled crossover trial. Sci Rep. Jan 30 2020;10(1):1473. Epub 2020/02/01.
224. Adkins AN, Dewald JPA, Garmirian L, Nelson CM, Murray WM. Serial sarcomere number is substantially decreased within the paretic biceps brachii in individuals with chronic hemiparetic stroke. bioRxiv. 2020:2020.03.12.989525.
225. Olsson MC, Krüger M, Meyer L-H, Ahnlund L, Gransberg L, Linke WA, et al. Fibre type-specific increase in passive muscle tension in spinal cord-injured subjects with spasticity. The Journal of Physiology. 2006/11/15 2006;577(1):339-52.
226. Gao F, Zhang LQ. Altered contractile properties of the gastrocnemius muscle poststroke. J Appl Physiol (1985). Dec 2008;105(6):1802-8. Epub 2008/10/25.
227. Kwah LK, Herbert RD, Harvey LA, Diong J, Clarke JL, Martin JH, et al. Passive mechanical properties of gastrocnemius muscles of people with ankle contracture

after stroke. Arch Phys Med Rehabil. Jul 2012;93(7):1185-90. Epub 2012/04/17.
228. Zhao H, Ren Y, Roth EJ, Harvey RL, Zhang LQ. Concurrent deficits of soleus and gastrocnemius muscle fascicles and Achilles tendon post stroke. J Appl Physiol (1985). Apr 1 2015;118(7):863-71. Epub 2015/02/11.
229. Hopkins WG. Measures of Reliability in Sports Medicine and Science. Sports Med. journal article July 01 2000;30(1):1-15.
230. Chuang L-L, Wu C-Y, Lin K-C. Myotonometric measurement of muscular properties of hemiparetic arms in stroke patients. Rehabilitation Medicine: InTech; 2012.
231. Fröhlich-Zwahlen AK, Casartelli NC, Item-Glatthorn JF, Maffiuletti NA. Validity of resting myotonometric assessment of lower extremity muscles in chronic stroke patients with limited hypertonia: A preliminary study. J Electromyogr Kinesiol. 2014;24(5):762-9.
232. Rydahl SJ, Brouwer BJ. Ankle stiffness and tissue compliance in stroke survivors: A validation of Myotonometer measurements. Arch Phys Med Rehabil. 2004;85(10):1631-7.
233. Akagi R, Kusama S. Comparison Between Neck and Shoulder Stiffness Determined by Shear Wave Ultrasound Elastography and a Muscle Hardness Meter. Ultrasound Med Biol. Comparative Study Research Support, Non-U.S. Gov't Aug 2015;41(8):2266-71.
234. Kuo W-H, Jian D-W, Wang T-G, Wang Y-C. Neck muscle stiffness quantified by sonoelastography is correlated with body mass index and chronic neck pain symptoms. Ultrasound Med Biol. 2013;39(8):1356-61.
235. Strasser EM, Draskovits T, Praschak M, Quittan M, Graf A. Association between ultrasound measurements of muscle thickness, pennation angle, echogenicity and skeletal muscle strength in the elderly. Age (Dordr). Dec 2013;35(6):2377-88. Epub 2013/03/05.
236. Jenkins ND, Miller JM, Buckner SL, Cochrane KC, Bergstrom HC, Hill EC, et al. Test-Retest Reliability of Single Transverse versus Panoramic Ultrasound Imaging for Muscle Size and Echo Intensity of the Biceps Brachii. Ultrasound Med Biol. Jun 2015;41(6):1584-91. Epub 2015/03/10.
237. Rosenberg JG, Ryan ED, Sobolewski EJ, Scharville MJ, Thompson BJ, King GE. Reliability of panoramic ultrasound imaging to simultaneously examine muscle size and quality of the medial gastrocnemius. Muscle Nerve. 2014;49(5):736-40.
238. Pang MY, Eng JJ, Dawson AS, Gylfadóttir S. The use of aerobic exercise training in improving aerobic capacity in individuals with stroke: a meta-analysis. Clin Rehabil. 2006;20(2):97-111.
239. Ivey FM, Gardner AW, Dobrovolny CL, Macko RF. Unilateral Impairment of Leg Blood Flow in Chronic Stroke Patients. Cerebrovasc Dis. 2004;18(4):283-9.
240. Billinger SA, Kluding PM. Use of Doppler Ultrasound to Assess Femoral Artery Adaptations in the Hemiparetic Limb in People with Stroke. Cerebrovasc Dis. 2009;27(6):552-8.
241. Billinger SA, Gajewski BJ, Guo LX, Kluding PM. Single limb exercise induces femoral artery remodeling and improves blood flow in the hemiparetic leg poststroke. Stroke. Sep 2009;40(9):3086-90. Epub 2009/06/13.
242. Aboyans V, Criqui MH, Abraham P, Allison MA, Creager MA, Diehm C, et al. Measurement and interpretation of the ankle-brachial index: a scientific statement from the American Heart Association. Circulation. Dec 11 2012;126(24):2890-909. Epub 2012/11/20.
243. Lam SC, Wong Y-y, Woo J. Reliability and validity of the abbreviated mental test (Hong Kong version) in residential care homes. J Am Geriatr Soc. 2010;58(11):2255-

7.
244. Shiina T, Nightingale KR, Palmeri ML, Hall TJ, Bamber JC, Barr RG, et al. WFUMB guidelines and recommendations for clinical use of ultrasound elastography: Part 1: basic principles and terminology. Ultrasound Med Biol. May 2015;41(5):1126-47. Epub 2015/03/26.
245. Dubois G, Kheireddine W, Vergari C, Bonneau D, Thoreux P, Rouch P, et al. Reliable protocol for shear wave elastography of lower limb muscles at rest and during passive stretching. Ultrasound Med Biol. Research Support, Non-U.S. Gov't Sep 2015;41(9):2284-91.
246. Caresio C, Molinari F, Emanuel G, Minetto MA. Muscle echo intensity: reliability and conditioning factors. Clin Physiol Funct Imaging. Sep 2015;35(5):393-403. Epub 2014/06/07.
247. Aggeloussis N, Giannakou E, Albracht K, Arampatzis A. Reproducibility of fascicle length and pennation angle of gastrocnemius medialis in human gait in vivo. Gait Posture. 2010/01/01/ 2010;31(1):73-7.
248. Langenderfer J, Jerabek SA, Thangamani VB, Kuhn JE, Hughes RE. Musculoskeletal parameters of muscles crossing the shoulder and elbow and the effect of sarcomere length sample size on estimation of optimal muscle length. Clin Biomech (Bristol, Avon). Aug 2004;19(7):664-70. Epub 2004/08/04.
249. McMahon JJ, Turner A, Comfort P. Within- and between-session reliability of medial gastrocnemius architectural properties. Biol Sport. 2016;33(2):185-8.
250. Duclay J, Martin A, Duclay A, Cometti G, Pousson M. Behavior of fascicles and the myotendinous junction of human medial gastrocnemius following eccentric strength training. Muscle Nerve. Jun 2009;39(6):819-27. Epub 2009/03/21.
251. Chino K, Akagi R, Dohi M, Takahashi H. Measurement of muscle architecture concurrently with muscle hardness using ultrasound strain elastography. Acta Radiol. Research Support, Non-U.S. Gov't Sep 2014;55(7):833-9.
252. Nelson CM, Dewald JPA, Murray WM. In vivo measurements of biceps brachii and triceps brachii fascicle lengths using extended field-of-view ultrasound. J Biomech. Jun 14 2016;49(9):1948-52. Epub 2016/04/17.
253. Newman JS, Adler RS, Rubin JM. Power Doppler sonography: use in measuring alterations in muscle blood volume after exercise. American Journal of Roentgenology. 1997/06/01 1997;168(6):1525-30.
254. Ying M, Ng DKS, Yung DMC, Lee EST. A semi-quantitative approach to compare high-sensitivity power Doppler sonography and conventional power Doppler sonography in the assessment of thyroid vascularity. Thyroid. 2009;19(11):1265-9.
255. Chen H, Ho HM, Ying M, Fu SN. Correlation between computerised findings and Newman's scaling on vascularity using power Doppler ultrasonography imaging and its predictive value in patients with plantar fasciitis. The British Journal of Radiology. 04/12/ 2012;85(1015):925-9.
256. Agyapong-Badu S, Warner M, Samuel D, Stokes M. Measurement of ageing effects on muscle tone and mechanical properties of rectus femoris and biceps brachii in healthy males and females using a novel hand-held myometric device. Arch Gerontol Geriatr. Jan-Feb 2016;62:59-67. Epub 2015/10/20.
257. Ko CY, Choi HJ, Ryu J, Kim G. Between-day reliability of MyotonPRO for the non-invasive measurement of muscle material properties in the lower extremities of patients with a chronic spinal cord injury. J Biomech. May 17 2018;73:60-5. Epub 2018/03/31.
258. Dewald JPA, Beer RF. Abnormal joint torque patterns in the paretic upper limb of subjects with hemiparesis. Muscle Nerve. 2001;24(2):273-83.

259. Ekstrand E, Lexell J, Brogardh C. Isometric and isokinetic muscle strength in the upper extremity can be reliably measured in persons with chronic stroke. J Rehabil Med. Sep 2015;47(8):706-13. Epub 2015/07/17.
260. Yang J, Lee J, Lee B, Kim S, Shin D, Lee Y, et al. The Effects of Elbow Joint Angle Changes on Elbow Flexor and Extensor Muscle Strength and Activation. Journal of Physical Therapy Science. 2014;26(7):1079-82.
261. Ada L. Stroke patients have selective muscle weakness in shortened range. Brain. 2003;126(3):724-31.
262. Garcia SC, Dueweke JJ, Mendias CL. Optimal joint positions for manual isometric muscle testing. J Sport Rehabil. 02/24/ 2016;25(4):jsr.2015-0118.
263. MacDougall AM, Tandon V, Wilson MP, Wilson TW. Oscillometric measurement of the ankle-brachial index. The Canadian Journal of Cardiology. 03/04/ 2008;24(1):49-51.
264. Hirsch AT, Haskal ZJ, Hertzer NR, Bakal CW, Creager MA, Halperin JL, et al. ACC/AHA 2005 Practice Guidelines for the management of patients with peripheral arterial disease (lower extremity, renal, mesenteric, and abdominal aortic): a collaborative report from the American Association for Vascular Surgery/Society for Vascular Surgery, Society for Cardiovascular Angiography and Interventions, Society for Vascular Medicine and Biology, Society of Interventional Radiology, and the ACC/AHA Task Force on Practice Guidelines (Writing Committee to Develop Guidelines for the Management of Patients With Peripheral Arterial Disease): endorsed by the American Association of Cardiovascular and Pulmonary Rehabilitation; National Heart, Lung, and Blood Institute; Society for Vascular Nursing; TransAtlantic Inter-Society Consensus; and Vascular Disease Foundation. Circulation. Mar 21 2006;113(11):e463-654. Epub 2006/03/22.
265. Włodek A, Sarzyńska-Długosz I, Sandercock PAG, Członkowska A. Agreement between the clinical Oxfordshire Community Stroke Project classification and CT findings in Poland. Eur J Neurol. 2004;11(2):91-6.
266. Platz T, Pinkowski C, Wijck Fv, Kim I-H, Bella Pd, Johnson G. Reliability and validity of arm function assessment with standardized guidelines for the Fugl-Meyer Test, Action Research Arm Test and Box and Block Test: a multicentre study. Clin Rehabil. 2005;19(4):404-11.
267. Chan C. Motor and sensory deficits following stroke: Relevance to a comprehensive evaluation. Physiother Can. 1986;38:29-34.
268. Ng SS, Hui-Chan CW. The timed up & go test: its reliability and association with lower-limb impairments and locomotor capacities in people with chronic stroke. Arch Phys Med Rehabil. Aug 2005;86(8):1641-7. Epub 2005/08/09.
269. Koo TK, Li MY. A Guideline of Selecting and Reporting Intraclass Correlation Coefficients for Reliability Research. J Chiropr Med. Jun 2016;15(2):155-63. Epub 2016/06/23.
270. Ng SS, Hui-Chan CW. Contribution of ankle dorsiflexor strength to walking endurance in people with spastic hemiplegia after stroke. Arch Phys Med Rehabil. Jun 2012;93(6):1046-51. Epub 2012/03/24.
271. Son J, Rymer WZ, Lee SSM. Limited fascicle shortening and fascicle rotation may be associated with impaired voluntary force-generating capacity in pennate muscles of chronic stroke survivors. Clin Biomech (Bristol, Avon). May 2020;75:105007. Epub 2020/04/28.
272. Billinger S. Cardiovascular Regulation after Stroke: Evidence of Impairment, Trainability, and Implications for Rehabilitation. Cardiopulm Phys Ther J. 2010;21(1):22-4.

273. Demaerschalk BM, Hwang H-M, Leung G. US cost burden of ischemic stroke: a systematic literature review. The American journal of managed care. 2010/07// 2010;16(7):525-33.
274. Beaupre GS, Lew HL. Bone-Density Changes After Stroke. Am J Phys Med Rehabil. 2006;85(5):464-72.
275. Sievänen H, Koskue V, Rauhio A, Kannus P, Heinonen A, Vuori I. Peripheral Quantitative Computed Tomography in Human Long Bones: Evaluation of In Vitro and In Vivo Precision. J Bone Miner Res. 1998;13(5):871-82.
276. Cheuk KY, Hu Y, Tam EMS, Shi L, Yu FWP, Hung VWY, et al. Bone measurements at multiple skeletal sites in adolescent idiopathic scoliosis-an in vivo correlation study using DXA, HR-pQCT and QCT. Arch Osteoporos. Jun 27 2019;14(1):70. Epub 2019/06/30.
277. Wu D, Griffith JF, Lam SHM, Wong PCH, Shi L, Li EK, et al. Progressive structural bone changes and their relationship with treatment in patients with psoriatic arthritis: a longitudinal HR-pQCT study. Arthritis Res Ther. Dec 4 2019;21(1):265. Epub 2019/12/06.
278. Zhu TY, Hung VW, Cheung WH, Cheng JC, Qin L, Leung KS. Value of Measuring Bone Microarchitecture in Fracture Discrimination in Older Women with Recent Hip Fracture: A Case-control Study with HR-pQCT. Sci Rep. Sep 27 2016;6:34185. Epub 2016/09/28.
279. Ashe MC, Fehling P, Eng JJ, Khan KM, McKay HA. Bone geometric response to chronic disuse following stroke: a pQCT study. Journal of Musculoskeletal and Neuronal Interactions. 2006;6(3):226.
280. MacNeil JA, Boyd SK. Accuracy of high-resolution peripheral quantitative computed tomography for measurement of bone quality. Med Eng Phys. 2007/12/01/ 2007;29(10):1096-105.
281. Faul F, Erdfelder E, Lang A-G, Buchner A. G*Power 3: A flexible statistical power analysis program for the social, behavioral, and biomedical sciences. Behav Res Methods. journal article May 01 2007;39(2):175-91.
282. Whittier DE, Boyd SK, Burghardt AJ, Paccou J, Ghasem-Zadeh A, Chapurlat R, et al. Guidelines for the assessment of bone density and microarchitecture in vivo using high-resolution peripheral quantitative computed tomography. Osteoporos Int. May 26 2020. Epub 2020/05/28.
283. Sode M, Burghardt AJ, Pialat J-B, Link TM, Majumdar S. Quantitative characterization of subject motion in HR-pQCT images of the distal radius and tibia. Bone. 2011/06/01/ 2011;48(6):1291-7.
284. Chiba K, Okazaki N, Kurogi A, Isobe Y, Yonekura A, Tomita M, et al. Precision of Second-Generation High-Resolution Peripheral Quantitative Computed Tomography: Intra- and Intertester Reproducibilities and Factors Involved in the Reproducibility of Cortical Porosity. J Clin Densitom. 2018/04/01/ 2018;21(2):295-302.
285. Agarwal S, Rosete F, Zhang C, McMahon DJ, Guo XE, Shane E, et al. In vivo assessment of bone structure and estimated bone strength by first- and second-generation HR-pQCT. Osteoporos Int. Oct 2016;27(10):2955-66. Epub 2016/05/09.
286. Sanford J, Moreland J, Swanson LR, Stratford PW, Gowland C. Reliability of the Fugl-Meyer assessment for testing motor performance in patients following stroke. Phys Ther. 1993;73(7):447-54.
287. Ngai SP, Cheung RT, Lam PL, Chiu JK, Fung EY. Validation and reliability of the Physical Activity Scale for the Elderly in Chinese population. J Rehabil Med. May 2012;44(5):462-5. Epub 2012/05/03.
288. Portney LG. Foundations of clinical research : applications to practice. Third edition.

ed. Watkins MP, editor. Philadelphia, PA: F.A. Davis Company; 2015.
289. van Rietbergen B, Ito K. A survey of micro-finite element analysis for clinical assessment of bone strength: The first decade. J Biomech. 2015/03/18/ 2015;48(5):832-41.
290. Whittaker JL, Teyhen DS, Elliott JM, Cook K, Langevin HM, Dahl HH, et al. Rehabilitative Ultrasound Imaging: Understanding the Technology and Its Applications. J Orthop Sports Phys Ther. 2007;37(8):434-49.
291. Berenpas F, Weerdesteyn V, Geurts AC, van Alfen N. Long-term use of implanted peroneal functional electrical stimulation for stroke-affected gait: the effects on muscle and motor nerve. J Neuroeng Rehabil. journal article July 10 2019;16(1):86.
292. Vilayphiou N, Boutroy S, Sornay-Rendu E, Van Rietbergen B, Munoz F, Delmas PD, et al. Finite element analysis performed on radius and tibia HR-pQCT images and fragility fractures at all sites in postmenopausal women. Bone. Apr 2010;46(4):1030-7. Epub 2010/01/02.
293. Zhu TY, Griffith JF, Qin L, Hung VW, Fong TN, Au SK, et al. Structure and strength of the distal radius in female patients with rheumatoid arthritis: a case-control study. J Bone Miner Res. Apr 2013;28(4):794-806. Epub 2012/10/24.
294. Turner CH, Rho J, Takano Y, Tsui TY, Pharr GM. The elastic properties of trabecular and cortical bone tissues are similar: results from two microscopic measurement techniques. J Biomech. 1999/04/01/ 1999;32(4):437-41.
295. Nunnally JC. Psychometric theory. 3rd ed.. ed. Bernstein IH, editor. New York: McGraw-Hill; 1994.
296. Jenkins DG, Quintana-Ascencio PF. A solution to minimum sample size for regressions. PLoS One. 2020;15(2):e0229345. Epub 2020/02/23.
297. Poole KE, Reeve J, Warburton EA. Falls, fractures, and osteoporosis after stroke: time to think about protection? Stroke. 2002;33(5):1432-6.
298. Dennis M, Lo K, McDowall M, West T. Fractures after stroke: frequency, types, and associations. Stroke. 2002;33(3):728-34.
299. Di Monaco M, Vallero F, Di Monaco R, Mautino F, Cavanna A. Functional recovery and length of stay after hip fracture in patients with neurologic impairment. American journal of physical medicine & rehabilitation. 2003;82(2):143-8.
300. Langsetmo L, Peters KW, Burghardt AJ, Ensrud KE, Fink HA, Cawthon PM, et al. Volumetric Bone Mineral Density and Failure Load of Distal Limbs Predict Incident Clinical Fracture Independent of FRAX and Clinical Risk Factors Among Older Men. J Bone Miner Res. 2018;33(7):1302-11.
301. Fink HA, Langsetmo L, Vo TN, Orwoll ES, Schousboe JT, Ensrud KE, et al. Association of High-resolution Peripheral Quantitative Computed Tomography (HR-pQCT) bone microarchitectural parameters with previous clinical fracture in older men: The Osteoporotic Fractures in Men (MrOS) study. Bone. Aug 2018;113:49-56. Epub 2018/05/12.
302. Burghardt AJ, Buie HR, Laib A, Majumdar S, Boyd SK. Reproducibility of direct quantitative measures of cortical bone microarchitecture of the distal radius and tibia by HR-pQCT. Bone. Sep 2010;47(3):519-28. Epub 2010/06/22.
303. Velotta J, Weyer J, Ramirez A, Winstead J, Bahamonde R. Relationship between leg dominance tests and type of task. 2011.
304. Asdaghi N, Jeerakathil T, Hameed B, Saini M, McCombe JA, Shuaib A, et al. Oxfordshire community stroke project classification poorly differentiates small cortical and subcortical infarcts. Stroke. Aug 2011;42(8):2143-8. Epub 2011/06/28.
305. Duncan PW, Propst M, Nelson SG. Reliability of the Fugl-Meyer Assessment of Sensorimotor Recovery Following Cerebrovascular Accident. Phys Ther.

1983;63(10):1606-10.
306. Chu L, Pei C, Ho M, Chan P. Validation of the Abbreviated Mental Test (Hong Kong version) in the elderly medical patient. 1995.
307. Washburn RA, Ficker JL. Physical Activity Scale for the Elderly (PASE): the relationship with activity measured by a portable accelerometer. Journal of sports medicine and physical fitness. 1999;39(4):336.
308. Dinger MK, Oman F, Taylor EL, Vesely SK, Able J. Stability and convergent validity of the Physical Activity Scale for the Elderly (PASE). Journal of Sports Medicine and Physical Fitness. 2004;44(2):186.
309. Flansbjer UB, Holmback AM, Downham D, Patten C, Lexell J. Reliability of gait performance tests in men and women with hemiparesis after stroke. J Rehabil Med. Mar 2005;37(2):75-82. Epub 2005/03/25.
310. Severinsen K, Jakobsen JK, Overgaard K, Andersen H. Normalized muscle strength, aerobic capacity, and walking performance in chronic stroke: a population-based study on the potential for endurance and resistance training. Arch Phys Med Rehabil. Oct 2011;92(10):1663-8. Epub 2011/08/30.
311. Mehrholz J, Wagner K, Rutte K, Meissner D, Pohl M. Predictive validity and responsiveness of the functional ambulation category in hemiparetic patients after stroke. Arch Phys Med Rehabil. Oct 2007;88(10):1314-9. Epub 2007/10/03.
312. Kollen B, Kwakkel G, Lindeman E. Time Dependency of Walking Classification in Stroke. Phys Ther. 2006;86(5):618-25.
313. Jácome C, Cruz J, Oliveira A, Marques A. Validity, Reliability, and Ability to Identify Fall Status of the Berg Balance Scale, BESTest, Mini-BESTest, and Brief-BESTest in Patients With COPD. Phys Ther. 2016;96(11):1807-15.
314. Duncan RP, Leddy AL, Cavanaugh JT, Dibble LE, Ellis TD, Ford MP, et al. Comparative Utility of the BESTest, Mini-BESTest, and Brief-BESTest for Predicting Falls in Individuals With Parkinson Disease: A Cohort Study. Phys Ther. 2013;93(4):542-50.
315. Huang M, Pang MY. Psychometric properties of Brief-Balance Evaluation Systems Test (Brief-BESTest) in evaluating balance performance in individuals with chronic stroke. Brain Behav. Mar 2017;7(3):e00649. Epub 2017/03/16.
316. Eng JJ, Kim CM, MacIntyre DL. Reliability of lower extremity strength measures in persons with chronic stroke. Arch Phys Med Rehabil. 2002;83(3):322-8.
317. Juodzbaliene V, Darbutas T, Skurvydas A, Brazaitis M. Does the Length of Elbow Flexors and Visual Feedback Have Effect on Accuracy of Isometric Muscle Contraction in Men after Stroke? Biomed Res Int. 2016;2016:7641705. Epub 2016/04/05.
318. Koo TKK, Mak AFT, Hung LK. In vivo determination of subject-specific musculotendon parameters: applications to the prime elbow flexors in normal and hemiparetic subjects. Clinical Biomechanics. 2002;17(5):390-9.
319. Nishiyasu T, Nagashima K, Nadel ER, Mack GW. Effects of posture on cardiovascular responses to lower body positive pressure at rest and during dynamic exercise. J Appl Physiol. 1998;85(1):160-7.
320. Rabelo M, Nunes GS, da Costa Amante NM, de Noronha M, Fachin-Martins E. Reliability of muscle strength assessment in chronic post-stroke hemiparesis: a systematic review and meta-analysis. Top Stroke Rehabil. Feb 2016;23(1):26-36. Epub 2015/08/06.
321. Ricardo Viana M, John Chae M, Richard Wilson M, Tom Miller M, Teasell R. Hemiplegic Shoulder Pain & Complex Regional Pain Syndrome. 2018.
322. Akyuz G, Kuru P. Systematic Review of Central Post Stroke Pain: What Is Happening

in the Central Nervous System? Am J Phys Med Rehabil. Aug 2016;95(8):618-27. Epub 2016/05/14.
323. Andersen G, Vestergaard K, Ingeman-Nielsen M, Jensen TS. Incidence of central post-stroke pain. Pain. 1995/05/01/ 1995;61(2):187-93.
324. Leijon G, Boivie J, Johansson I. Central post-stroke pain — neurological symptoms and pain characteristics. Pain. 1989/01/01/ 1989;36(1):13-25.
325. Lindgren I, Jonsson AC, Norrving B, Lindgren A. Shoulder pain after stroke: a prospective population-based study. Stroke. Feb 2007;38(2):343-8. Epub 2006/12/23.
326. Bowden JL, Lin GG, McNulty PA. The prevalence and magnitude of impaired cutaneous sensation across the hand in the chronic period post-stroke. PLoS One. 2014;9(8):e104153. Epub 2014/08/15.
327. Yuen-Chi Lau R, Qian X, Po K-T, Li L-M, Guo X. Response of Rat Tibia to Prolonged Unloading Under the Influence of Electrical Stimulation at the Dorsal Root Ganglion. Neuromodulation: Technology at the Neural Interface. 2017;20(3):284-9.
328. Menz HB, Morris ME, Lord SR. Foot and Ankle Characteristics Associated With Impaired Balance and Functional Ability in Older People. The Journals of Gerontology: Series A. 2005;60(12):1546-52.
329. Ducic I, Short KW, Dellon AL. Relationship Between Loss of Pedal Sensibility, Balance, and Falls in Patients With Peripheral Neuropathy. Ann Plast Surg. 2004;52(6):535-40.
330. Lin CH, Chen KH, Chang CH, Chen CM, Huang YC, Hsu HC, et al. Muscle pain intensity and pressure pain threshold changes in different periods of stroke patients. Am J Phys Med Rehabil. Apr 2014;93(4):299-309. Epub 2013/11/20.
331. Salom-Moreno J, Sanchez-Mila Z, Ortega-Santiago R, Palacios-Cena M, Truyol-Dominguez S, Fernandez-de-las-Penas C. Changes in spasticity, widespread pressure pain sensitivity, and baropodometry after the application of dry needling in patients who have had a stroke: a randomized controlled trial. J Manipulative Physiol Ther. Oct 2014;37(8):569-79. Epub 2014/09/10.
332. Kinser AM, Sands WA, Stone MH. Reliability and validity of a pressure algometer. The Journal of Strength & Conditioning Research. 2009;23(1):312-4.
333. Fischer AA. Pressure algometry over normal muscles. Standard values, validity and reproducibility of pressure threshold. Pain. 1987;30(1):115-26.
334. Fulk GD, He Y, Boyne P, Dunning K. Predicting Home and Community Walking Activity Poststroke. Stroke. Feb 2017;48(2):406-11. Epub 2017/01/07.
335. Raja B, Neptune RR, Kautz SA. Quantifiable patterns of limb loading and unloading during hemiparetic gait: Relation to kinetic and kinematic parameters. J Rehabil Res Dev. 2012;49(9):1293-304.
336. Eng JJ. Fitness and Mobility Exercise (FAME) Program for stroke. Topics in Geriatric Rehabilitation. 2010;26(4):310-23.
337. Burr D, Robling AG, Turner CH. Effects of biomechanical stress on bones in animals. Bone. 2002;30(5):781-6.
338. Turner CH, Robling AG. Designing exercise regimens to increase bone strength. Exercise and sport sciences reviews. 2003;31(1):45-50.
339. Omisore AD, Ayoola OO, Ibitoye BO, Fawale MB, Adetiloye VA. Sonographic Evaluation of Endothelial Function in Brachial Arteries of Adult Stroke Patients. J Ultrasound Med. Feb 2017;36(2):345-51. Epub 2016/12/13.
340. Tiftik T, Kara M, Ozcan HN, Turkkan C, Ural FG, Ekiz T, et al. Doppler ultrasonographic evaluation of the radial and ulnar arteries in hemiparetic patients after stroke. J Clin Ultrasound. Jun 2014;42(5):277-82. Epub 2014/01/18.
341. Cardoso L, Fritton SP, Gailani G, Benalla M, Cowin SC. Advances in assessment of

bone porosity, permeability and interstitial fluid flow. J Biomech. Jan 18 2013;46(2):253-65. Epub 2012/11/24.
342. Cowin SC, Cardoso L. Blood and interstitial flow in the hierarchical pore space architecture of bone tissue. J Biomech. Mar 18 2015;48(5):842-54. Epub 2015/02/11.
343. Warburton DER, Nicol CW, Gatto SN, Bredin SSD. Cardiovascular disease and osteoporosis: balancing risk management. Vasc Health Risk Manag. 2007;3(5):673-89.
344. Hamerman D. Osteoporosis and atherosclerosis: biological linkages and the emergence of dual-purpose therapies. QJM. Jul 2005;98(7):467-84. Epub 2005/06/16.
345. Whitney C, Warburton DER, Frohlich J, Chan SY, McKay H, Khan K. Are Cardiovascular Disease and Osteoporosis Directly Linked? Sports Med. 2004/10/01 2004;34(12):779-807.
346. Gassner M, Killu K, Bauman Z, Coba V, Rosso K, Blyden D. Feasibility of common carotid artery point of care ultrasound in cardiac output measurements compared to invasive methods. J Ultrasound. Jun 2015;18(2):127-33. Epub 2015/07/21.
347. Ioakeimidis N, Vlachopoulos C, Rokkas K, Kratiras Z, Angelis A, Samentzas A, et al. Dynamic penile peak systolic velocity predicts major adverse cardiovascular events in hypertensive patients with erectile dysfunction. J Hypertens. 2016;34(5).
348. Steinvil A, Sadeh B, Arbel Y, Justo D, Belei A, Borenstein N, et al. Prevalence and Predictors of Concomitant Carotid and Coronary Artery Atherosclerotic Disease. J Am Coll Cardiol. 2011/02/15/ 2011;57(7):779-83.
349. Alexandrov AV, Brodie DS, McLean A, Hamilton P, Murphy J, Burns PN. Correlation of Peak Systolic Velocity and Angiographic Measurement of Carotid Stenosis Revisited. Stroke. 1997;28(2):339-42.
350. Frotzler A, Coupaud S, Perret C, Kakebeeke TH, Hunt KJ, Donaldson NN, et al. High-volume FES-cycling partially reverses bone loss in people with chronic spinal cord injury. Bone. Jul 2008;43(1):169-76. Epub 2008/04/29.
351. Dolbow DR, Gorgey AS, Daniels JA, Adler RA, Moore JR, Gater Jr DR. The effects of spinal cord injury and exercise on bone mass: A literature review. NeuroRehabilitation. 2011;29:261-9.
352. Hamrick MW, McGee-Lawrence ME, Frechette DM. Fatty Infiltration of Skeletal Muscle: Mechanisms and Comparisons with Bone Marrow Adiposity. Front Endocrinol (Lausanne). 2016;7:69. Epub 2016/07/06.